Synthesis and Properties of Novel Iodonium Salts

Dissertation
towards the academic degree
Doctor rerum naturalium (Dr. rer. nat.)

submitted to the
Faculty of Biology and Chemistry
at the University of Bremen

by

Julian Spils

Bremen, March 2024

The herein described work was carried out under the supervision of Prof. Dr. Boris J. Nachtsheim from February 2020 until February 2024 at the Institute of Organic and Analytical Chemistry, Faculty of Biology and Chemistry at the University of Bremen.

1. Reviewer: Prof. Dr. Boris J. Nachtsheim (University of Bremen)
2. Reviewer: Prof. Dr. Peter Spiteller (University of Bremen)

Date of the Colloquium: 26th of April 2024

Versicherung an Eides Statt

Ich, Julian Spils, geb. am 27.02.1996 in Vechta,

versichere an Eides Statt durch meine Unterschrift, dass ich die vorliegende Arbeit selbstständig und ohne fremde Hilfe angefertigt und alle Stellen, die ich wörtlich dem Sinne nach aus Veröffentlichungen entnommen habe, als solche kenntlich gemacht habe, mich auch keiner anderen als der angegebenen Literatur oder sonstiger Hilfsmittel bedient habe.

Ich versichere an Eides Statt, dass ich die vorgenannten Angaben nach bestem Wissen und Gewissen gemacht habe und dass die Angaben der Wahrheit entsprechen und ich nichts verschwiegen habe.

Die Strafbarkeit einer falschen eidesstattlichen Versicherung ist mir bekannt, namentlich die Strafandrohung gemäß §156 StGB bis zu drei Jahren Freiheitsstrafe oder Geldstrafe bei vorsätzlicher Begehung der Tat bzw. gemäß §161 Abs. 1 StGB bis zu einem Jahr Freiheitsstrafe oder Geldstrafe bei fahrlässiger Begehung.

Bremen, den 18. März 2024 Julian Spils

Erklärung zur elektronischen Version und zur Überprüfung einer Dissertation

Hiermit bestätige ich gemäß §7 Abs. 7 Punkt 4 der Promotionsordnung (Dr. rer. nat.) der Universität Bremen für den Fachbereich 2 (Biologie/Chemie), dass die zu Prüfungszwecken beigelegte elektronische Version meiner Dissertation identisch ist mit der abgegebenen, gedruckten Version.

Ich bin mit der Überprüfung meiner Dissertation gemäß §6 Abs. 2 Punkt 5 mit qualifizierter Software im Rahmen der Untersuchung von Plagiatsvorwürfen einverstanden.

Bremen, den 18. März 2024 Julian Spils

Declaration on the contribution of the candidate to a multi-author article/manuscript which is included as a chapter in the submitted doctoral thesis

Chapter 3.2: Two-Step Continuous-Flow Synthesis of Cyclic Iodonium Salts
Beilstein J. Org. Chem. **2023**, *19*, 27–32.

Experimental concept and design:	ca. 90%
Experimental work and/or acquisition of (experimental) data:	ca. 100%
Data analysis and interpretation:	ca. 100%
Preparation of Figures and Tables:	ca. 100%
Drafting of the manuscript:	ca. 90%

Chapter 3.3: Oxidative Cyclization and Enzyme-free Deiodination of Thyroid Hormones
Org. Chem. Front. **2024**, Advance Article

Experimental concept and design:	ca. 90%
Experimental work and/or acquisition of (experimental) data:	ca. 90%
Data analysis and interpretation:	ca. 100%
Preparation of Figures and Tables:	ca. 95%
Drafting of the manuscript:	ca. 90%

Some results described in this thesis were presented on the following conferences:

1. HalChem X - The 10th International Meeting on Halogen Chemistry
   Łódź, Poland, Sept. 2022
   Poster: *Continuous-flow synthesis of cyclic iodonium salts via anodic oxidation* (Poster Award)

2. ICHIC 7 - 7th International Conference on Hypervalent Iodine Chemistry
   Stockholm, Sweden, June 2023
   Poster: *Advances in the Synthesis of Cyclic Diaryliodonium Salts via a Flow-Procedure and from Naturally Derived Iodoarenes*

Bremen, the 18th of March 2024 Julian Spils

Danksagung

Mein besonderer Dank gilt Prof. Dr. Boris J. Nachtsheim für die die Aufnahme in seine Arbeitsgruppe und die Betreuung während der Doktorarbeit. Vorallem für die Freiheiten und Anregungen beim Erstellen dieser Arbeit sowie die Ermöglichung von Forschungsaufenthalte und Koferenzreisen ins Ausland.

Weiterhin danke ich Prof. Dr. Peter Spiteller für die Übernahme des Zweitgutachtens sowie allen weiteren Mitgliedern der Prüfungskommission: Prof. Dr. Jens Beckmann, Prof. Dr. Ralf Dringen, Jan Rick Koch und Marcel Sancken.

Auch möchte ich Prof. Dr. Thomas Wirth für die Möglichkeit eines Forschungsaufenthalts in seiner Arbeitsgruppe in Cardiff danken. Die gewonnen Erfahrungen haben mein Interesse an neuen Synthesemethoden geweckt.

Den ehemaligen sowie aktuellen Mitgliedern der AG Nachtsheim danke ich für die zahlreichen lustigen Momente, Diskussionen und Gespräche in den letzten Jahren.

Ebenso danke ich den Mitarbeitern, ohne die diese Arbeit nicht möglich gewesen wäre. Mein Dank gilt Dr. Enno Lork, Dr. Pim Puylaert und Dr. Daniel Duvinage für ihre Unterstützung bei zahlreichen Kristallstrukturen. Johannes Stelten und Dr. Wieland Wilker danke ich für ihre Hilfe bei NMR-Problemen, sowie Thomas Dülcks und Dorit Kempen für die massenspektrometrische Analyse verschiedenster Proben und Probleme. Ebenso möchte ich allen Bachelorstudenten und Forschungspraktikanten Philip Diephaus, Matthis Kohröde und Marcel Sancken, welche ich über die Jahre betreuen durfte, für die Unterstützung im Labor danken.

Herzlichster Dank gilt meiner Familie die mich trotz allem, so anstrengend es auch war, immer unterstützt hat und mir diesen Weg ermöglichte. Besonders Julia, Danke, dass du immer für mich da bist!

Vielen Dank!

Abstract

Diaryliodonium salts are versatile reagents used for various applications that include electrophilic arylations, building larger cyclic scaffolds, benzyne precursors, and organocatalysis.

This thesis presents the synthesis and structural elucidation of novel structures containing two iodonium units in *peri*-substitution, where a rather repulsive interaction was observed via X-ray crystallography. Furthermore, mixed iodo-iodonium salts were obtained by oxidising only one iodine atom. These were also investigated via X-ray crystallography showing an interaction between the two iodine atoms by coordination of the iodide into the sigma hole of the iodonium salt, resulting in a significantly lowered interatomic distance.

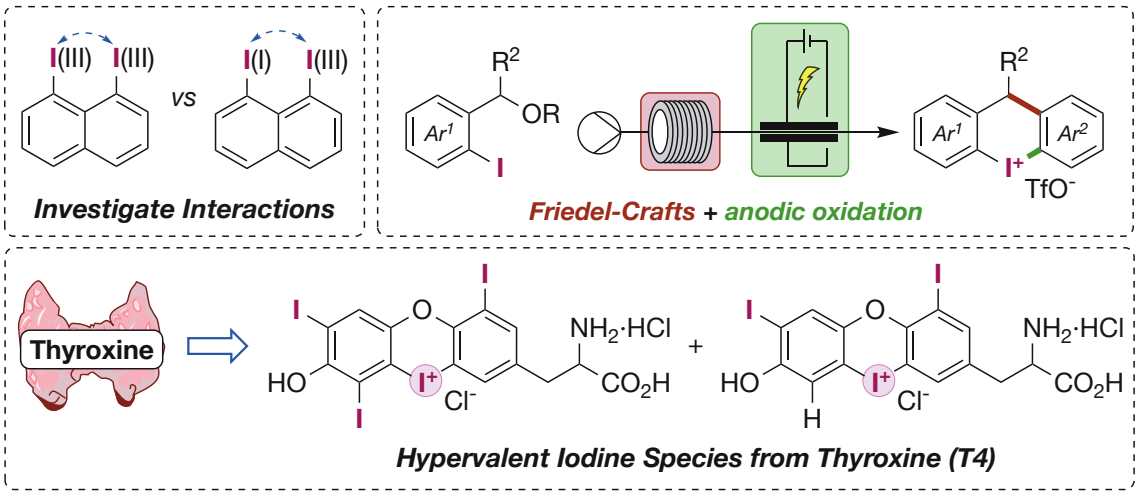

In a second project, a continuous multi-step flow procedure was developed for the generation of cyclic diaryliodonium salts from readily available benzyl acetates and alcohols. Combining a Friedel-Crafts step with an anodic oxidation resulted in a method offering a better atom economy combined with a scalable setup.

In a third project, cyclic diaryliodonium salts were generated from protected thyroxine. It was possible to generate the corresponding oxidised free thyroxine as well as triiodothyronine. The latter by selective deiodination. The mechanism of this deiodination was investigated via DFT calculations showing resemblance with enzymatic processes with involved halogen bonding. This was also confirmed experimentally as selective coordination to one iodine(I) atom was observed.

Kurzfassung

Diaryliodoniumsalze sind vielseitige Reagenzien mit verschiedenen Anwendungen, wie der elektrophilen Arylierung, dem Aufbau größerer zyklischer Gerüste, als Arinpräkursor und zuletzt in der Organokatalyse.

Diese Arbeit präsentiert zunächst die Synthese und Strukturaufklärung neuartiger Strukturen, welche zwei Iodoniumeinheiten in *peri*-Substitution enthalten, wobei mittels Röntgenstrukturanalyse eine eher abstoßende Wechselwirkung beobachtet wurde. Darüber hinaus wurden gemischte Iod-Iodoniumsalze durch Oxidation nur eines Jods erhalten. Diese wurden ebenfalls mittels Röntgenstrukturanalyse untersucht und zeigten eine Wechselwirkung zwischen den beiden Iodatomen durch Koordination des Iodids in das Sigma-Loch des Iodoniumsalzes, was in einem signifikant verringerten interatomaren Abstand resultierte.

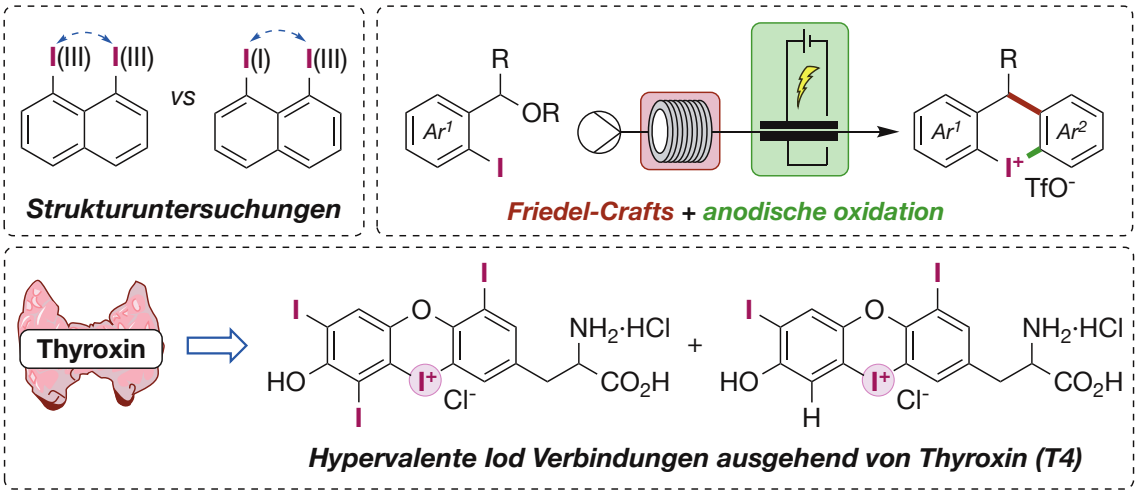

In einem zweiten Projekt wurde ein kontinuierlicher mehrstufiger Fluss-Prozess zur Erzeugung zyklischer Diaryliodoniumsalze aus leicht verfügbaren Benzylacetaten und -alkoholen entwickelt. Die Kombination eines Friedel-Crafts-Schritts mit einer anodischen Oxidation ergab einen Aufbau, welche eine geringere Atomökonomie kombiniert mit Skalierbarkeit bietet.

In einem dritten Projekt wurden zyklische Diaryliodoniumsalze aus geschütztem Thyroxin erzeugt. Es gelang, sowohl das entsprechende oxidierte freie Thyroxin als auch Triiodthyronin zu erzeugen. Letzteres durch selektive Deiodierung. Der Mechanismus dieser Deiodierung wurde mittels DFT-Rechnungen untersucht und zeigte Ähnlichkeit mit enzymatischen Prozessen unter beteiligter Halogenbindung. Dies wurde auch experimentell bestätigt, da eine selektive Koordination an ein Iod(I)atom beobachtet werden konnte.

Table of Contents

1 Introduction

Iodine in its pure form is a violet to black solid which sublimes at room temperature. This observation was first made by the French saltpetre manufacturer Bernard Courtois and published in the year 1813.[1] He sent his samples to J. L. Gay-Lussac and H. Davy who quickly verified the discovery of the new element and named it „Iodine“.[2, 3]

Iodine has found applications in numerous fields of science and industry. It has a vast oxidation chemistry existing in oxidation states from -1 (iodide) to +7 (periodate) owing to its high polarisability sitting in the fifth period of the periodic table as the heaviest stable halogen.

Nowadays as a result, elemental iodine is broadly used for oxidative transformations be it stoichiometric or in combination with other oxidants catalytically,[4, 5] or for the preparation of organoiodine reagents.[6] The latter can be oxidised to generate hypervalent iodine compounds. These have been extensively used for oxidative transformations, as electrophilic transfer reagents and more, as highlighted by various review articles and books.[7–16]

1.1 Hypervalent Iodine Compounds

Following IUPAC nomenclature hypervalent organoiodine compounds can be generally divided into the trivalent λ^3-iodanes (+3) and pentavalent λ^5-iodanes (+5). Alternatively, the Martin-Arduengo notation (N-X-L) can be used. This notation uses besides the number of ligands L, also the number of valence electrons N around the central atom X. In this notation λ^3-iodanes are described as 10-I-3. The λ^5-iodanes are described accordingly as 12-I-5 (Fig. 1.1).

The structure of hypervalent compounds was first explained by J. I. Musher in 1969 and later further applied to organohalogen derivatives by J. C. Martin.[17, 18] λ^3-iodanes (RIL_2) bearing ten valence electrons and the iodine formally in the oxidation state +3 feature three ligands arranged in a T-shape. Their geometry can be described as a trigonal bipyramid where one ligand R is in the equatorial position (usually an arene) and two electronegative ligands L are in the orthogonal apical positions. Together with the 5p orbital of the iodine, these two ligands form a three-centre four-electron bond ($3c-4e^-$), resulting in three new molecular orbitals of which the bonding and non-bonding one are occupied. The non-bonding orbital having a knot where the iodine sits causes a partial positive charge on this and a partial negative on the ligands, explaining their electrophilic character.[19, 20]

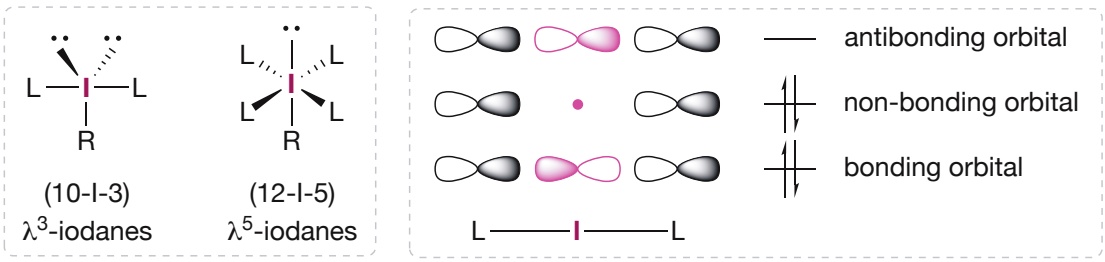

Figure 1.1. General structure of λ^3- and λ^5-iodanes and the molecular orbitals involved in the $3c-4e^-$ bond.

λ^5-iodanes (RIL_4) in contrast bear twelve valence electrons with the iodine being formally in the oxidation state +5 coordinated by five ligands. Their geometry is best described as square bipyramidal with the least electronegative ligand R (usually an arene) in an apical position and

the residual more electronegative ligands L in one plane on the equatorial positions, establishing two $3c-4e^-$ bonds.[19, 20]

The reactivity of hypervalent iodine compounds is often compared to the cross-coupling chemistry of transition metals. Generally, there are multiple different pathways, but most start from the exchange of one ligand (L) for a nucleophile (Nu^-) on the iodine (Scheme 1.1). Exchange can happen by either dissociation of one ligand, going through an unstable iodonium (8-I-2) species, followed by coordination of the nucleophile to produce the newly formed iodane or via association, where the nucleophile coordinates first forming an anionic 12-I-4 species, which then liberates one ligand.[19, 20]

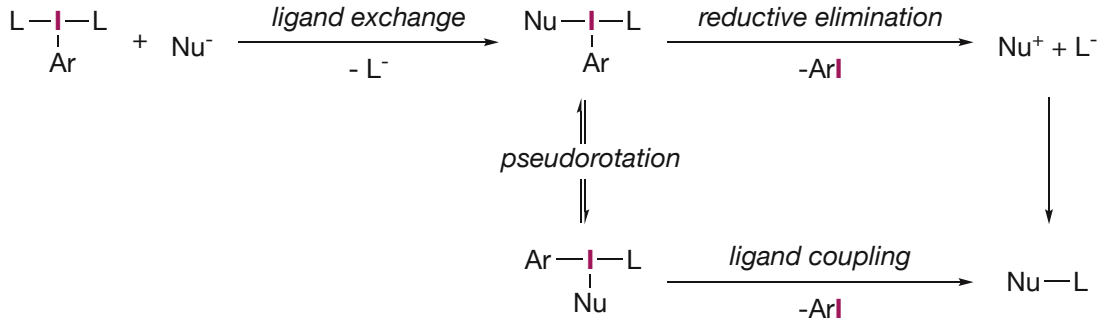

Scheme 1.1. General mechanism for the reaction of nucleophiles with λ^3-iodanes.

The iodane formed this way can then collapse under multiple pathways. One option is the reductive elimination by which the reduced iodoarene and the coupling product, through recombination of the ligands, are formed. Another way would be the direct ligand coupling by initial pseudorotation of the ligands to yield the desired product and iodoarene. This exceptional reactivity leads to these compounds being regarded as hypernucleofuges. This is undermined by the reduced iodoarene having a leaving group ability up to six orders of magnitude higher when compared to a triflate anion. Specific types of iodanes display a manifold of various additional reactivities like radical type, homolytic or single-electron transfer reactions. [14, 19, 20]

Iodanes (Fig. 1.2) have found widespread application in organic synthesis since their first discovery in 1886 by Willgerodt in the form of dichloroiodobenzene **1**, which can be used for mild oxidations or chlorinations.[21–24] The corresponding difluoride **2** has found extensive usage as a source of electrophilic fluorine.[25–27] By treatment of such iodanes with base the insoluble iodosylbenzene (**3**) can be obtained which was already demonstrated by Willgerodt and is still being used for oxidative transformations.[28–32] By exchanging the ligands, the broadly utilised oxidants phenyliodine(III) diacetate (**4**, PIDA) and phenyliodine(III) trifluoroacetate (**5**, PIFA) can be obtained.[33–39] By exchange with stronger acids like *para*-toluenesulfonic acid the unsymmetric Koser's reagent **6** is obtained.[40–42] As previously mentioned iodanes can also be used for electrophilic group transfer reactions. In this field notable examples are acyclic or cyclic iodonium salts **7** for arylation,[43, 44] ethynylbenziodoxolones **8** for alkynylations[45] or the Togni reagent **9** to realise electrophilic trifluoromethylation.[46] Furthermore, iodonium ylides **10** can for example be used similar to metallocarbenes in insertions but also for arylations.[47]

The λ^5-iodanes are generally not used for electrophilic transformations as the necessary structures are not stable enough. They find their application as a class of highly thought-after oxidants. Similar to **3**, the λ^5-iodane iodylbenzene (**11**) has a very low solubility and as a result an accordingly low reactivity. This can be improved by *ortho*-stabilising groups like benzoic acids as in the case of iodoxybenzoic acid (**12**, IBX) or the well-known Dess-Martin-Periodinan **13** (DMP).

Their solubility is in a usable range with **13** being soluble in most organic solvents, although it tends to hydrolyse forming the much less soluble **12**. They are established reagents for the selective oxidation of alcohols to ketones under mild conditions, tolerating various functional groups.[14, 48]

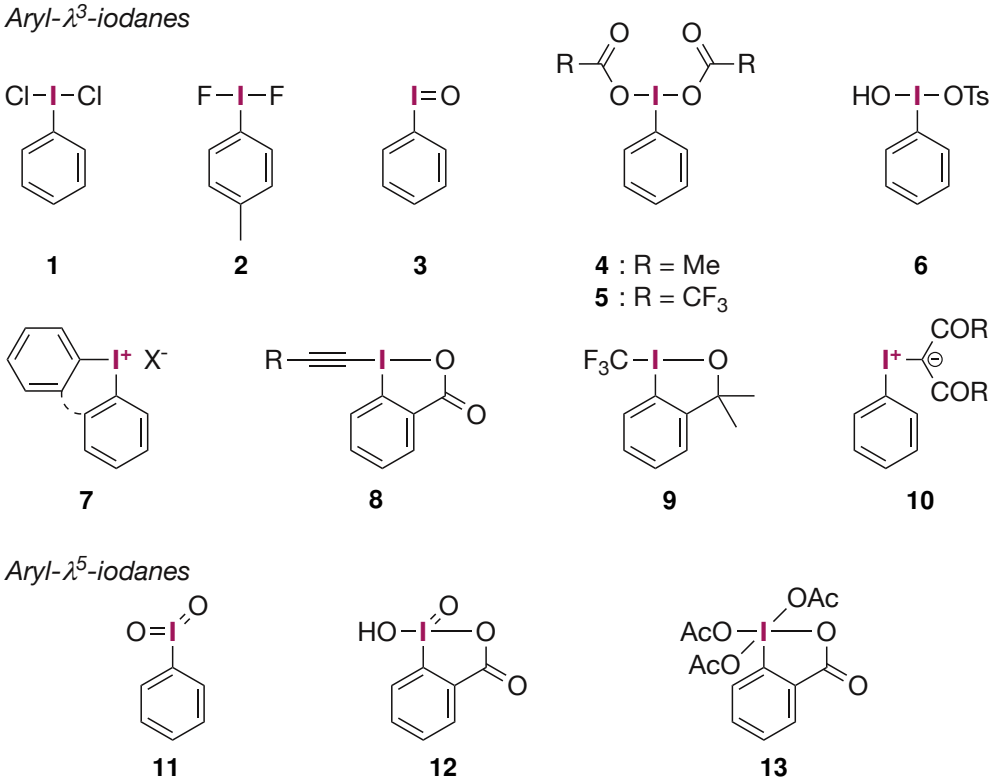

Figure 1.2. Selection of commonly used λ^3- and λ^5-iodanes.

1.2 Diaryliodonium Salts

Diaryliodonium salts were one of the first iodanes to be discovered.[49, 50] Nowadays they found their place as a general tool for electrophilic arylations,[44, 51, 52] initiators for polymerisations[53, 54] and recently also in the field of organocatalysis due to them being strong halogen bond donors.[10] They also benefit from the previously described hypernucleofugality and their reaction usually proceeds analogously to other λ^3-iodanes. This section will focus on the preparation (section 1.2.1) and synthetic applications (section 1.2.2) of the more popular acyclic varieties, cyclic diaryliodonium salts are to be discussed in section 1.3.

The term "diaryliodonium salts" suggests a tetrahedral ionic structure (Fig. 1.3, **A**) that would not be hypervalent as discussed before since the iodine (8-I-2), coordinated by only two ligands, has eight valence electrons, which fits the octet rule. So far there is no crystal structure suggesting such a tetrahedral geometry, but rather a distorted T-shape with the anion or other molecules (solvents, etc.) coordinating.[19] Especially for more coordinating anions like halides the expected structure of λ^3-iodanes is more fitting (Fig. 1.3, **B**), which is also reflected in their properties and reactivity. Nonetheless, diaryliodonium salts with weak coordinating ions dissociate in solution, showing an increased solubility and for example high conductivity comparable to standard electrolytes.[55] Recent studies by Legault and Huber criticise the conventional display of the two lone pairs in the case of diaryliodonium salts as DFT calculations suggest majorly a 5s and 5p orbital, still in a T-shape geometry (Fig. 1.3, C).[56]

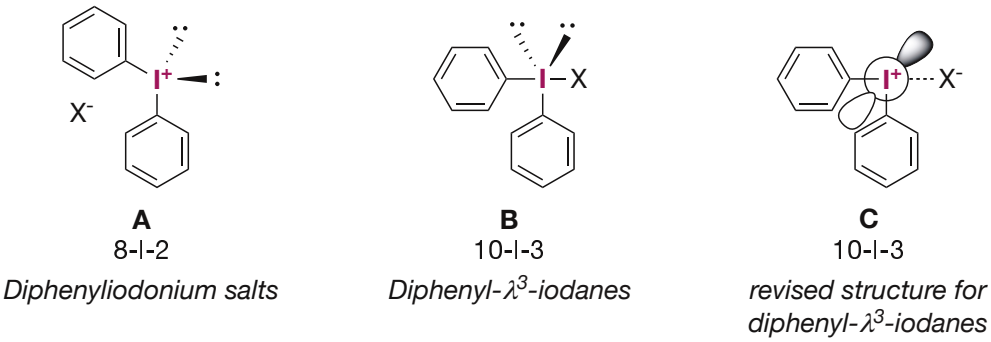

Figure 1.3. Structure of diaryliodonium salts. Diphenyliodonium salts (**A**) or diphenyl-λ^3-iodanes (**B**) and the recently revised structure bearing an 5s and 5p orbital **C**.

However, in the subsequent text, all structures where iodine is coordinated by two aryl ligands will be referred to as "diaryliodonium salts". This is to maintain consistency with existing literature and avoid any confusion with other λ^3-iodanes.

1.2.1 Preparation

The general preparation for diaryliodonium salts goes through a hypervalent oxidised iodoarene which is coupled with another arene by an electrophilic substitution. During recent years four different strategies have emerged of which two are the prevailing ones. The desired iodane can be either generated in situ and coupled directly with a corresponding arene (Scheme 1.2, **A**) via an electrophilic substitution or if oxidants have to be avoided the iodane can be generated and isolated prior to synthesis and then reacted in a similar fashion with another arene (Scheme 1.2, **B**). If necessary, these arenes can be modified by *ipso*-directing groups to increase their reactivity and selectivity during the coupling. Typical directing groups are boronic

acids, trifluoroborates, stannanes and silyl groups. These two pathways have the advantage of furnishing unsymmetric salts, which can lower cost and reduce waste if complex arenes are supposed to be employed. Alternatively, a less selective but also inexpensive way is the usage of elemental iodine (Scheme 1.2, **C**). Under oxidative and acidic conditions iodine gets coupled with arenes to yield symmetric diaryliodonium salts in a one-pot manner. Likewise, the iodine can be oxidised to an inorganic I(III)-species and afterwards reacted with arenes.[44, 52, 57]

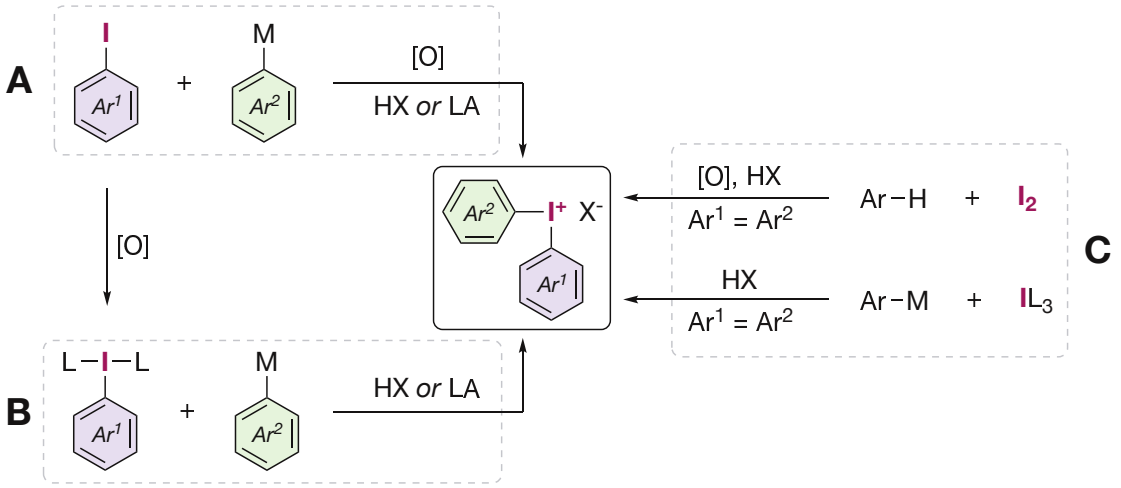

Scheme 1.2. Exemplative pathways for the generation of diaryliodonium salts. **A**: A one-pot procedure starting from iodoarenes. **B**: Coupling of iodanes with different arenes. **C**: Procedure starting from elemental iodine or inorganic λ^3-iodanes. M = H, $B(OH)_2$, BF_3K, TMS, $SnBu_3$.

More recent approaches try to improve existing methodologies with new technologies like for example flow chemistry. The preparation of diaryliodonium salts via oxidation of an iodoarene with *m*CPBA followed by activation with TfOH to couple with another arene is a well-documented procedure that has widespread application.[57] In 2017, Noël et al. realised such a process in a flow setup, where they were also able to monitor reaction enthalpies highlighting the highly exothermic nature of the synthesis (Scheme 1.3).[51] They split the components into three separate reservoirs. One for the iodoarene **14** and to-be-coupled arene **15** and one for the *m*CPBA and TfOH each. By this any side-reaction taking place before the actual reaction is avoided. It was possible to apply this procedure to a broad scope of substrates yielding up to

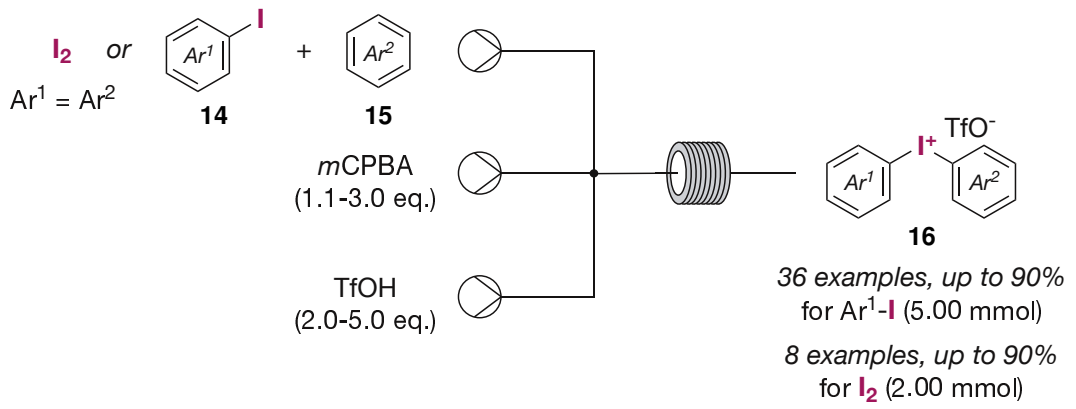

Scheme 1.3. Flow procedure for the synthesis of symmetric and unsymmetric diaryliodonium salts **16** from iodoarenes **14** or iodine.

92% (~8.3 mmol h^{-1}) of the desired iodonium salts **16**. In the case of electron-poor iodoarenes **14**, they had to increase the reaction time and the amount of TfOH due to their lower reactivity. Additionally, they were able to realise the coupling of arenes **15** with iodine in this setup as well, furnishing symmetric diaryliodonium salts (up to 90%).

A few years later, Wirth and Yusubov et al. presented a flow procedure with Oxone as an immobile oxidant.[58] The oxidation of iodoarenes with Oxone in trifluoroacetic acid was already well known and adaption was straightforward. By passing a solution of iodoarene **17** with trifluoroacetic acid through a cartridge, filled with Oxone, oxidation to the corresponding bistrifluoroacetates **18** was possible. Mixing with another solution containing arene **19** then gave the unsymmetric diaryliodonium salts **20** in excellent yields (up to 96%, ~1.1 mmol h^{-1}). Due to the low solubility of Oxone in the chosen solvents, it is possible to either reuse the cartridge or let it run for extended amounts without the need for replacement.

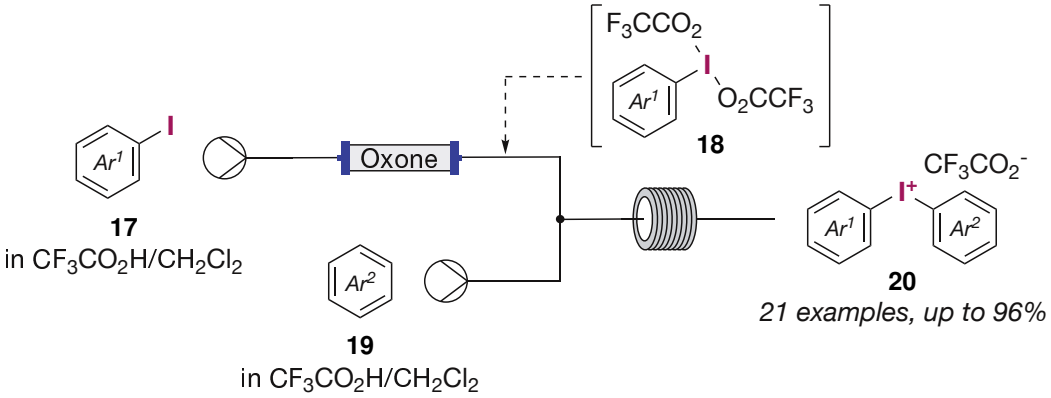

Scheme 1.4. Application of Oxone as a stationary oxidant for the synthesis of unsymmetric diaryliodonium salts **20**.

Yoshikai et al. took a different approach. Normally unactivated or activated arenes are reacted with a λ^3-iodane as an electrophile exchanging one ligand, forming a diaryliodane. They however used arynes, which usually also react in an electrophilic manner, together with λ^3-iodanes **21** to form new diaryliodanes **22** (Scheme 1.5).[59] The necessary arynes were generated from the precursor **23** with caesium fluoride. Reacting these with differently substituted iodanes **21**, that feature two carbon ligands, they were able to isolate a wide range of *ortho*-substituted diaryliodanes **22**. Namely alkyne-substituted iodanes **22a** in 40-83% yield, the alkene-substituted iodanes **22b** with up to 78% yield and aryl-substituted iodanes **22c** with up to 77% yield. In regards to the latter ones it was only possible to use electron-rich arenes. The insertion of the aryne into the polarised iodine-carbon bond is proposed to happen via the addition of the in situ formed aryne to the iodine-carbon bond, forming two new bonds and breaking the bond to the old ligand. Similar reactivity was also recently described for stabilised amino- and alkoxyiodanes in a preprint.[60]

1.2.2 Synthetic Applications

Diaryliodonium salts have been extensively used as electrophilic arylating reagents. In such instances, symmetric salts usually give the best results, due to no selectivity issues towards the iodonium salt. Nonetheless, unsymmetric salts are frequently being used since they provide a better atom economy and fewer steps preparation. In such cases, one aryl-ligand usually

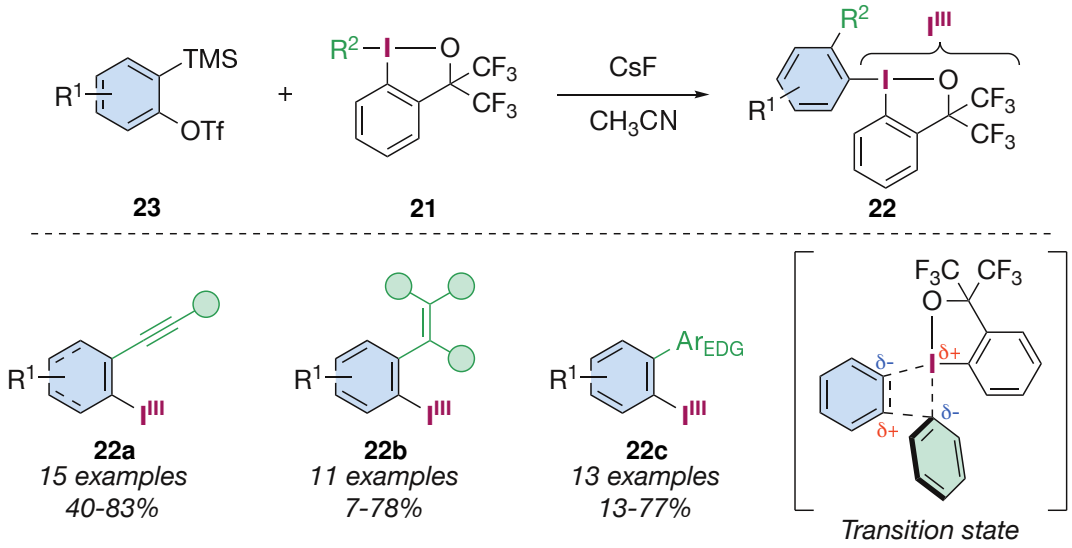

Scheme 1.5. Synthesis of stabilised *ortho*-substituted diaryliodanes **22** by addition of arynes to iodanes **21**.

functions as a dummy ligand being more electron-rich to favour substitution on the desired ligand. An exception to this can be observed with *ortho*-substituted aryl-ligands, e.g. mesityl, where the *ortho*-substituted ligand reacts even in the presence of a more electron-poor ligand.[61] Various procedures for the α-arylation of carbonyls,[61–66] the arylation of anilines,[61, 67–70] aliphatic amines,[69–73] phenols,[74–78] alcohols,[78–81], carboxylic acids[75, 82–84] and halides[85–88], especially fluorides[89–92] have been described. Following are some recent applications.

Atom economy is one major drawback of acyclic diaryliodonium salts since the iodoarene is usually a waste product. Olofsson et al. managed to improve this by using *ortho*-fluorinated electron-poor iodonium salts **24**. This allowed them to first substitute the fluorine, forming the intermediate **25**, and via subsequent arylation of the nucleophile obtain the iodinated, double-arylated substrates **26** (Scheme 1.6).[69] They were able to apply the method to various nucleophiles. Alkylamines yielded the corresponding *N*-aryl-*N*-alkyl-anilines with up to 99% and (hetero)arylamines gave triarylamines with up to 93% yield. Ammonia and water were also employed as nucleophiles giving the corresponding diarylamines and diarylethers in good to excellent yields (70-85% and 55-98%). In general, the method tolerates a large number of functional groups as seen in substrate **26a**. The electronics of the migrating aryl group have an influence as a low electron density could result in competing initial substitution as may be seen in substrate **26b**. Further, they observed that the electron-withdrawing group has to be *para* to the fluoride as otherwise substitution of the iodonium centre occurs.

Diaryliodonium salts are suitable precursors for the generation of arynes. Due to them being highly reactive nucleofuges they readily β-eliminate under the right conditions.[13] So far four different types of diaryliodanes have been successfully used for the generation of arynes **27** (Scheme 1.7). Generation happens for example via heating as seen in the case of carboxylic acid stabilised iodanes **28**, which undergo anionic decarboxylation with subsequent elimination of an iodoarene.[93, 94] Alternatively, *ortho*-unfunctionalised salts **29** that can be deprotonated by sterically hindered bases,[95–97] *ortho*-TMS iodonium salts **30** that get desilylated by a fluoride source[98, 99] or *ortho*-boronic acid substituted iodonium salts **31** that get activated by only water can also be used.[100] Notably, it was so far not possible to utilise *ortho*-trifluoroborate

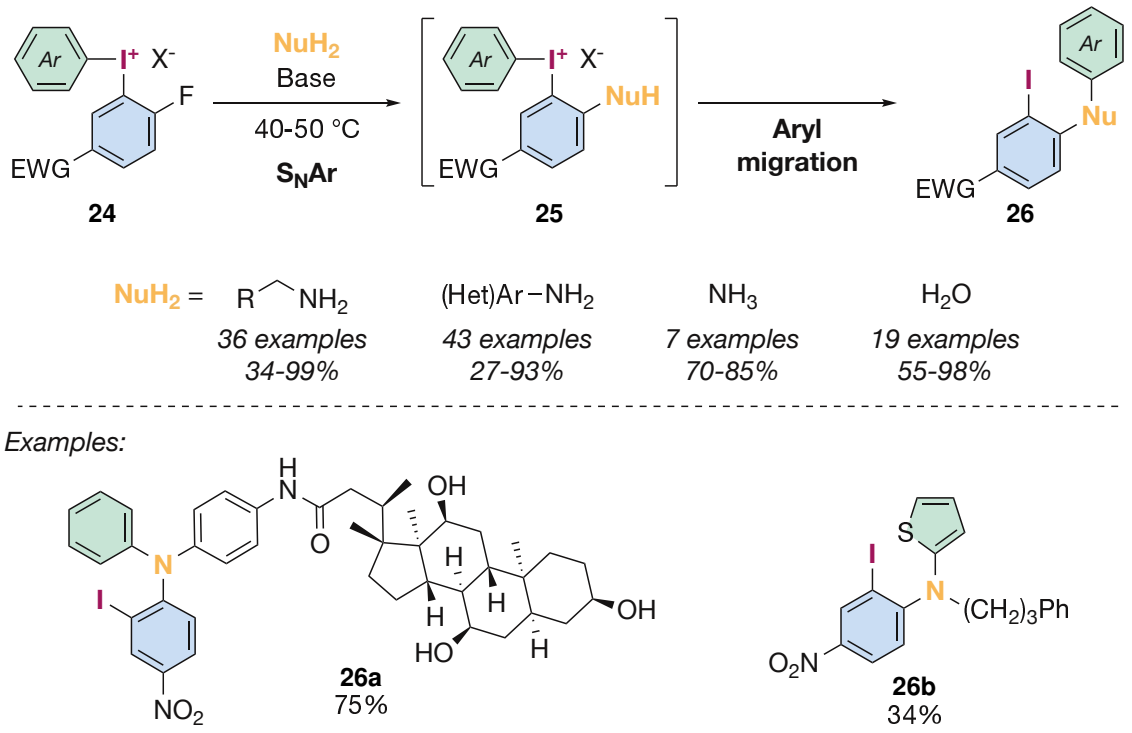

Scheme 1.6. Application of *ortho*-fluoroiodonium salts **24** to diarylate various *N*- and *O*-nucleophiles forming the double arylated products **26** via the intermediate **25**

substituted iodonium salts in such a manner.[101] Further, for salts of type **29**, the β-elimination pathway represents one possible side reactivity for the usually observed electrophilic arylation chemistry these salts are known for.[96]

One example of this type of application is the procedure presented by Stuart et al. in 2023. They were able to generate arynes under relatively mild conditions from iodonium salts **32** and react them with a range of different arynophiles **33** while also tolerating a wide range of functional groups (Scheme 1.8).[95] The method needed only potassium phosphate in contrast to usually employed stronger bases like *tert*-butoxides. This can be explained by the even higher nucleofugality of the trimethoxy-iodobenzene group, due to this they were also able to use electron-rich iodonium salts that usually show low or no reactivity. They employed furan to obtain the product **34a** in 64% yield, similarly, the addition of phenylpyrrole gave the product **34b** with 55% yield and by addition of a nitrone they were able to obtain **34c** with 89% yield. Further, simple nucleophiles like tert-butylamine or *N*-methyl-*N*-phenylamine also worked with high selectivity giving the products **34d** (70%) and **34e** (87%).

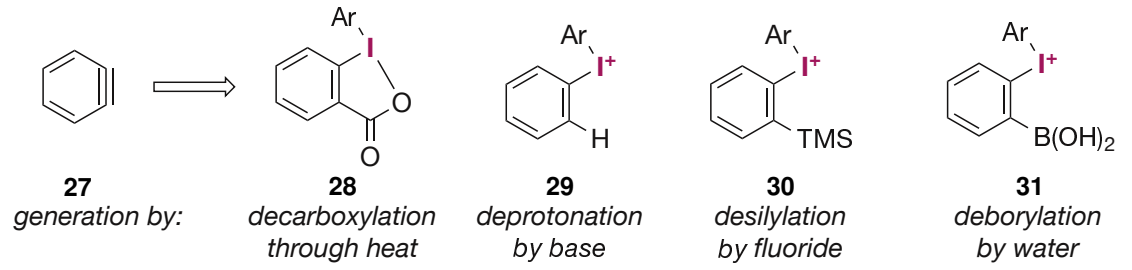

Scheme 1.7. Various types of aryne precursors **27**, **28**, **29** and **30** with iodonium salts as a nucleofuge.

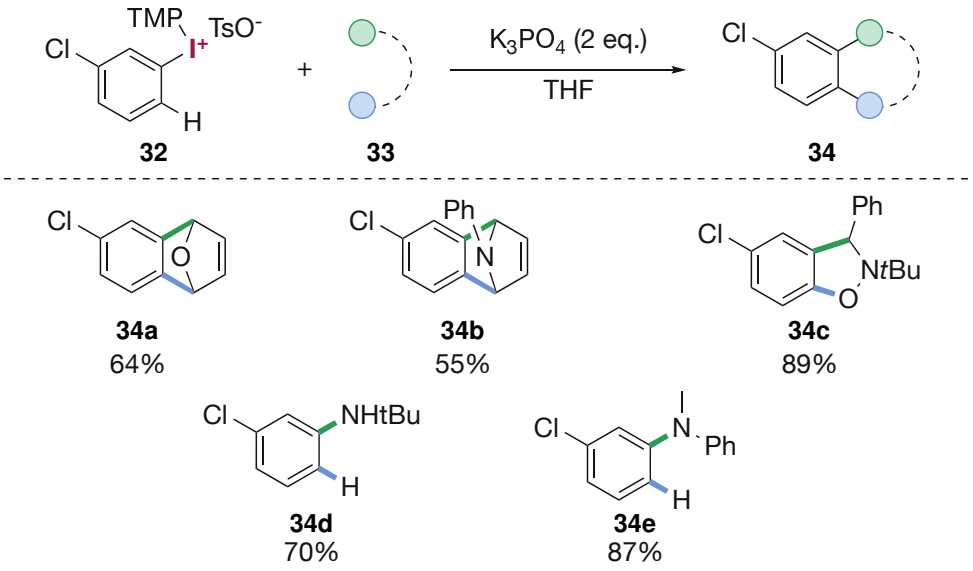

Scheme 1.8. Mild generation of arynes from diaryliodonium tosylate **32** and reaction with different arynophiles **33**.

Their high nucleofugality causes diaryliodonium salts to be valuable electrophiles in the field of transition metal catalysis, although the produced iodoarene can be a problem as it in itself can act as an electrophile under such conditions. One recent example is the four-component cyclisation by Wu et al. (Scheme 1.9).[102] In a first step, condensation of the fluorinated acetimidoyl chloride **35** with propargylamine (**36**) occurs followed by amino palladation and cyclisation to form the imidazole motive. Next carbon monoxide, generated from acetic anhydride and formic

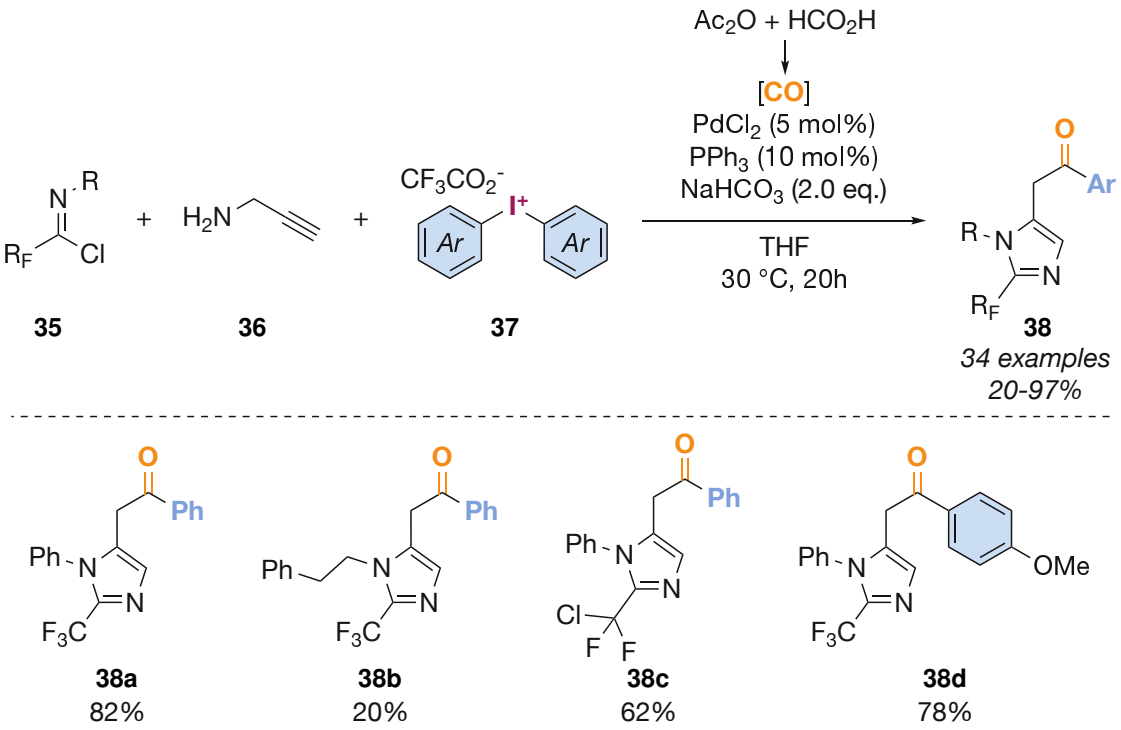

Scheme 1.9. Four component cascade cyclisation utilising diaryliodonium salts **37** as electrophiles towards imidazoles **38**.

acid, inserts followed by an oxidative addition of the symmetric diaryliodonium salt **37**. After reductive elimination, the product **38** is then formed. The method was applicable to a wide range of substrates (20-97%), like the unsubstituted derivative **38a** giving an 82% yield. When using imidoyl chlorides with an aliphatic rest a lower yield was obtained as can be seen for **38b** (20%). On the other hand derivatisation of the fluorocarbon chain or the utilised diaryliodonium salt was very well tolerated as can be seen for the substrates **38c** and **38d** (62% and 78%).

1.3 Cyclic Diaryliodonium Salts

Cyclic diaryl iodonium salts differ from their acyclic counterparts as the two aryl moieties are not just bridged (typically by the *ortho*-positions) but they also feature a great difference in reactivity. As their acyclic counterparts have been employed for numerous types of reactions, cyclic iodonium salts remain comparatively underdeveloped, although new procedures for their generation and newly popularised fields of application, like halogen bond catalysis, might change this soon.[9, 43, 103–105] Besides their applications for organic chemistry, they have been found to have biological activity notably as NADPH and flavoprotein inhibitors.[106–109]

1.3.1 Preparation

The general preparation for cyclic diaryliodonium species goes analogously to the one for acyclic derivatives with the slight difference that the bridging backbone has to be installed first. This also transforms the intermolecular iodonium formation into an intramolecular one with the resulting change in reactivity and selectivity. On the other hand, this can also result in a more tedious preparation as multiple steps are necessary to build the backbone, install the iodine and cyclise to the desired iodonium salt. An example is the preparation of iodolium salts **39** (Scheme 1.10). They can be built by Suzuki-coupling of an *ortho*-iodoaniline **40** with a boronic acid **41** generating **42**, followed by a Sandmeyer iodination towards iodoarene **43**. Oxidation of **43** and cyclisation then furnish the five-membered iodolium salt **39**.[110]

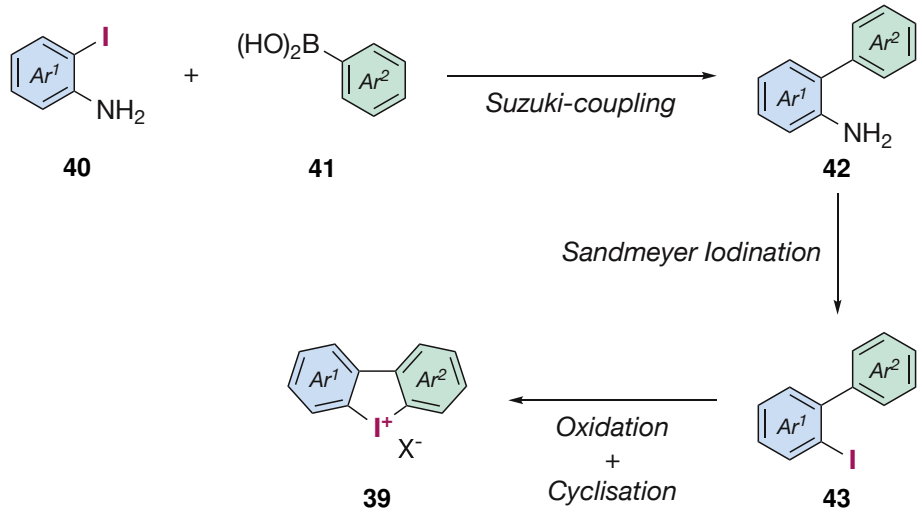

Scheme 1.10. Conventional pathway for the generation of five-membered cyclic iodonium salts **39** from iodoanilines **40** and boronic acids **41**.

Postnikov et al. described recently the preparation of imidazole containing five-membered iodonium salts **44** from readily available reagents (Scheme 1.11).[111] Reaction of diacetoxyio-

danes **45** with 1*H*-imidazole gave the acyclic iodonium salts **46** which rearranged copper catalysed to the *N*-aryl-2-iodoimidazoles **47**.[112] Oxidation and cyclisation were performed under green albeit harsh conditions with Oxone in sulfuric acid yielding the imidazole-bearing iodonium hydrogensulfates **44** in up to 95%. Interestingly, the combination of Oxone in sulfuric acid was the only one that produced **44**, other oxidants like commonly used *m*CPBA did not yield any product. This new type of iodonium salt was then investigated in regards to its reactivity by reaction with sulfur under basic conditions yielding the corresponding imidazothiazoles in good yields.

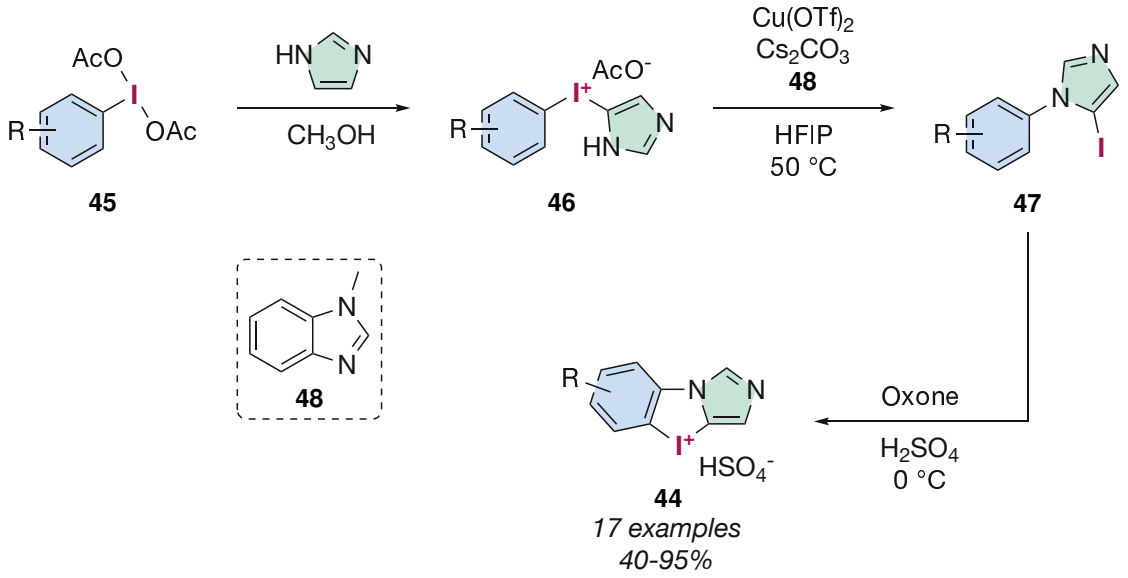

Scheme 1.11. Formation of cyclic *N*-heterocyclic iodonium salts **44** from diacetoxyiodanes **45**.

Electrochemistry recently gained great attention in the field of hypervalent iodine chemistry. As a result, multiple procedures for the generation of iodonium salts by anodic oxidation were developed by different groups.[113–116] Moran et al. were able to synthesise a wide range of five-membered iodonium salts **49**. Although they did not improve the overall steps necessary, they demonstrated a more atom-economic method by avoiding chemical oxidants which contribute to the generated waste (Scheme 1.12).[113] By oxidation of iodoarene **50** in the presence of TfOH under constant current electrolysis it was possible to efficiently obtain the desired iodolium triflates **49** in yields of up to 98%. 1,1,1,3,3,3-Hexafluoroisopropanol was chosen as a solvent by optimisation, fluorinated solvents are typical for the electrochemical generation of hypervalent iodine species as they stabilise the intermediary-generated radical cations and further function as ligands during the oxidation.[117, 118] Further they were able to utilise tosylic acid and trifluoroacetic acid yielding the corresponding tosylates and trifluoroacetates. Acyclic salts from iodoarenes and arenes were also possible to obtain under these conditions.

For the generation of six-membered iodonium salts, the group of Nachtsheim developed several one-pot procedures. First were two similar methods for the preparation of carbon-bridged iodininium salts **51** from benzyl alcohols **52** (Scheme 1.13).[119] In the case of primary benzyl alcohols or secondary diphenylmethanols, they employed TfOH to couple the *ortho*-iodobenzyl alcohols **52** with an additional arene **53** in a Friedel-Crafts-like reaction generating the intermediary iodoarene **54**. This was followed by the addition of Oxone in combination with sulfuric acid to oxidise the iodine and cyclise under the acidic conditions towards the

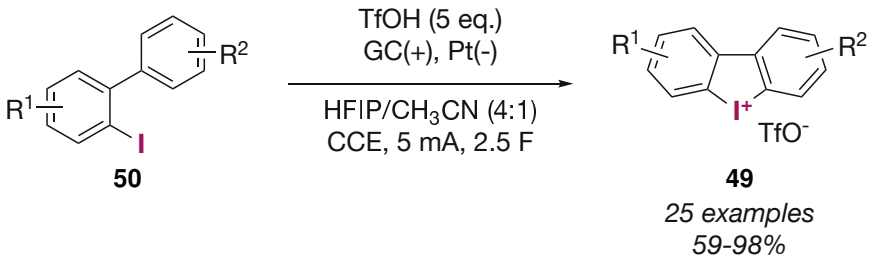

Scheme 1.12. Electrochemical preparation of iodolium salts **49**.

product **51** in excellent yields with up to 93%. For aliphatic secondary benzyl alcohols, on the other hand, slightly milder conditions were necessary as decomposition was observed under the previous conditions. To prevent this tetrafluoroboric acid (HBF_4) was chosen for the initial coupling, followed by the addition of *m*CPBA furnishing **51** in good yields of up to 83%. In their studies, they were also able to show a conformational isomerism for the iodonium salts with a substituent in the methylene bridge, as the substituent would switch between an equatorial and axial orientation.

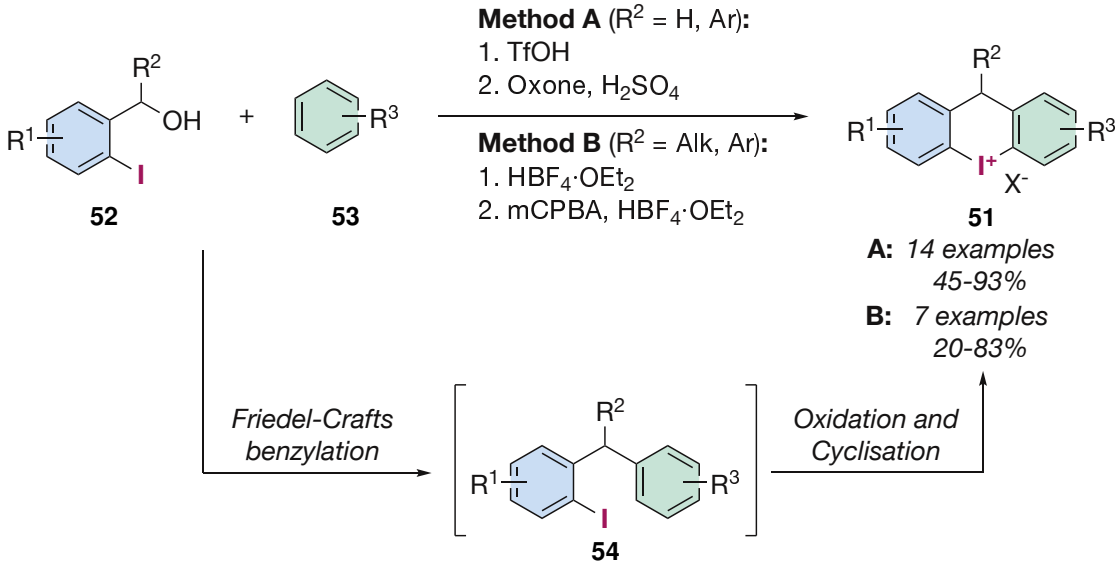

Scheme 1.13. One-pot procedure for the generation of carbon-bridged iodininium salts **51**.

In a second one-pot procedure novel six-membered iodaoxinium and iodazinium salts **55** and **56** were prepared from the *ortho*-iodophenols **57** and *ortho*-iodophenylsulphonamides **58** (Scheme 1.14).[120] Initially, the phenols or sulphonamides were arylated by in situ generated arynes from **59** through the addition of caesium fluoride. After the formation of iodoarene **60** Selectfluor and acetic acid were added to form the diacetate **61** which then cyclises by the addition of TfOH generating the iodaoxinium triflates **55** in yields of up to 91% and the iodazinium triflates **56** with up to 96%. They also demonstrated their applicability by various methods of derivatisation with reactivities comparable to already literature-known substrates.

1.3.2 Synthetic Applications

The applications for cyclic diaryliodonium salts cover a range of different fields, as they can be utilised like their acyclic counterparts for electrophilic transformations either under metal-

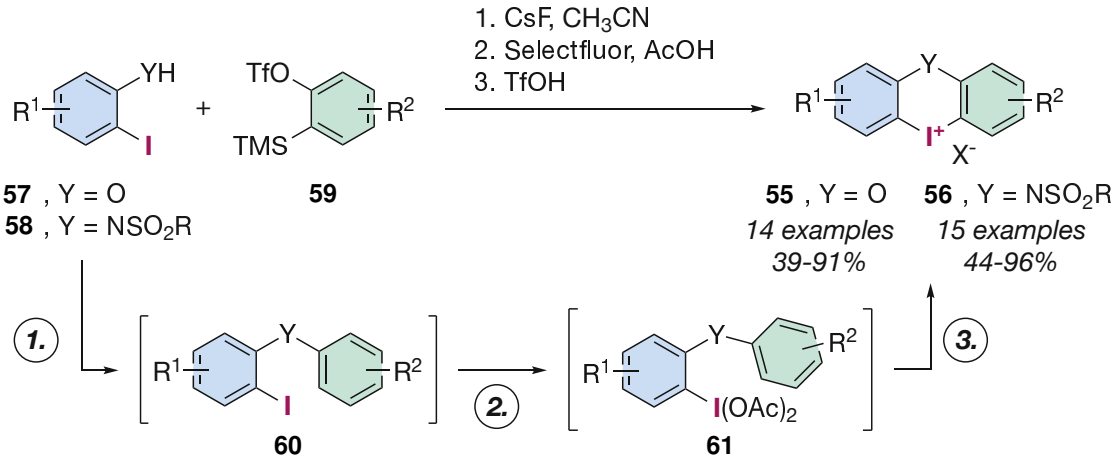

Scheme 1.14. One-pot procedure for the generation of the oxygen-bridged iodaoxinium salts **55** and iodazinium salts **56**.

free or metal catalysed conditions. In comparison to some previously described examples (Section 1.2.2), they intrinsically offer a better atom economy since the leaving iodoarene is covalently bonded and can be further utilised in a multi-step procedure or metal-catalysed transformation (Scheme 1.15). A field that recently gained a lot of attention is their usage as Lewis acids since they are strong halogen bond donors. In this regard, they represent a mild and metal-free alternative to conventional Lewis acids.[9, 10]

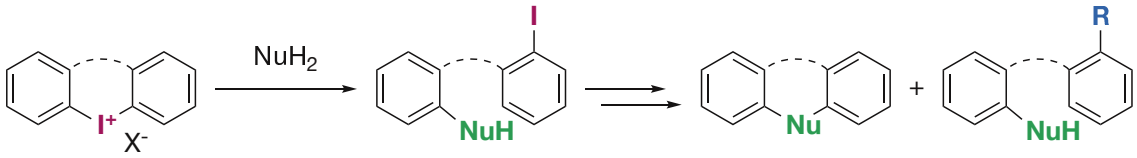

Scheme 1.15. General reactivity of cyclic iodonium salts towards nucleophiles, retaining the iodoarene in the product for further transformations.

Jiang et al. described a metal-free substitution of the iodine by either a sulfur or selenium atom under basic conditions and high temperatures (Scheme 1.16).[121] For the reaction with sulfur, they were able to apply it to a broad scope of substrates **62** with varying ring sizes of the iodacycle ($n = 0 - 3$) as can for example be seen with the sulfide **63a** (69%). It was further possible to react iodonium salts containing two iodonium centres under these conditions furnishing thioxanthene **63b** in still 41% yield. For the substitution by selenium, they needed the sterically hindered base KO*t*Bu although temperatures could be lowered. When comparing the insertion of sulfur with selenium they obtained the products in slightly lower yields as can be seen with the thiophenes and selenophenes **63c** and **64a** as well as **63d** and **64b**. This was not dependent on the electronic nature of the starting material. The reaction mechanism for the sulfur insertion is proposed to undergo via the formation of $S_3^{\cdot -}$ radicals that attach to the iodine, causing a homolytic cleavage of the C-I bond, binding to another $S_3^{\cdot -}$ and elimination of the iodine, giving the cyclised product **63**.

When reacting cyclic diaryliodonium salts with nucleophiles aryne formation can be observed, contrasting the reactivity of acyclic salts (Scheme 1.17). Wu and Zhang et al. investigated the reaction of five-membered iodonium triflates **65** with phenols **66** under basic conditions finding that the major product **67** bears the phenol group attached in the *meta*-position suggesting

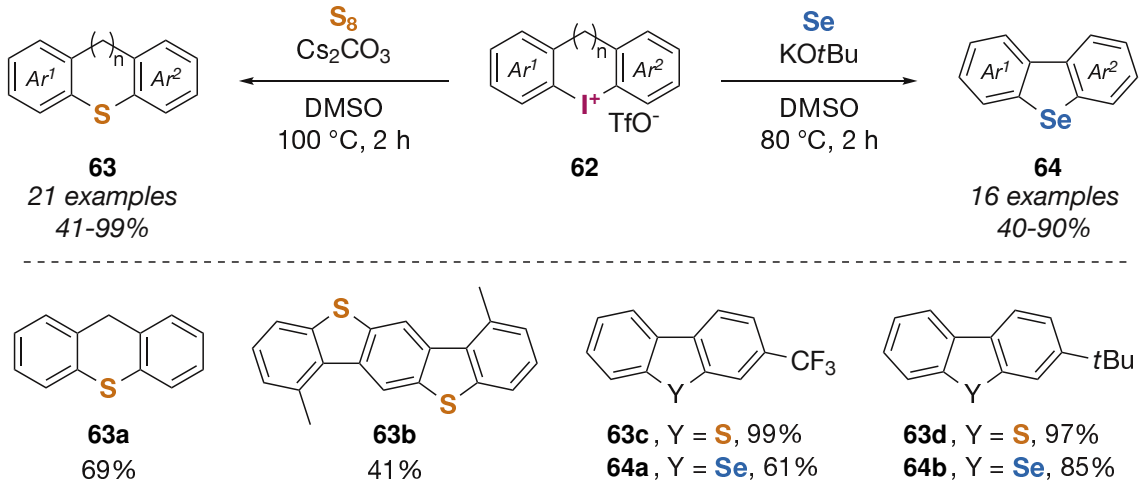

Scheme 1.16. Substitution with sulfur and selenium in cyclic diaryliodonium salts **62** generating sulfides **63** and selenides **64**.

an intermediary aryne formation opposed to an electrophilic arylation of the phenol **66**.[110] They applied these conditions to a range of substrates observing mostly *meta*/*ortho* ratios higher than 90:10, suggesting a predominant aryne mechanism, as can be seen in the reaction of phenol and pyridin-2-one forming the *meta*-substituted ethers **67a** and **67b** in 67% and 54% yield. When using substituted iodonium salts **65**, a higher selectivity for the *ortho* position could be observed in certain cases. This resulted in a significantly shifted ratio for ether **67c** and an exclusive *ortho* substitution for ether **67d**. To prove the existence of in situ generated arynes, they successfully trapped these by the addition of furan.

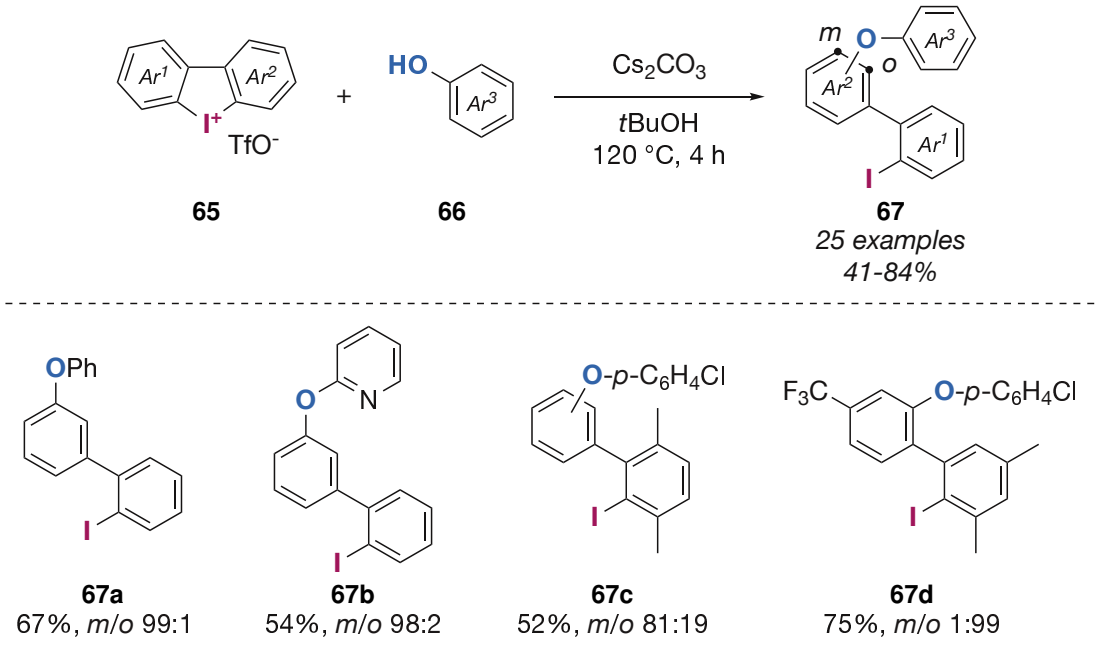

Scheme 1.17. Aryne formation vs. nucleophilic substitution in the reaction of cyclic diaryliodonium salts **65** with phenols.

Five-membered iodonium salts gained special attention due to them being precursors for chiral biphenyl systems by enantioselective opening of the iodonium centre. This is usually done

under copper catalysis with a chiral ligand. Zhang et al. were able to utilise this in an asymmetric acyloxylation of the iodonium salts **68** with various carboxylic acids **69** (Scheme 1.18).[122] The best results were obtained with the bisoxazolin ligand **L** needing only 5 mol% of the catalyst and ligand each. The substitution then proceeded under mild conditions only slightly above room temperature to furnish the asymmetric biphenylester **70** in high yields and high enantiomeric excess. The method tolerated various functional groups like the free phenol **70a** which could be obtained in 99% yield (95% *ee*) or the terminal alkyne **70b** which was obtained with 99% yield (99% *ee*). One exception to this was the binaphtyl derivative **70c** which could only be obtained in 52% (99% *ee*) with no influence on the enantiomeric excess.

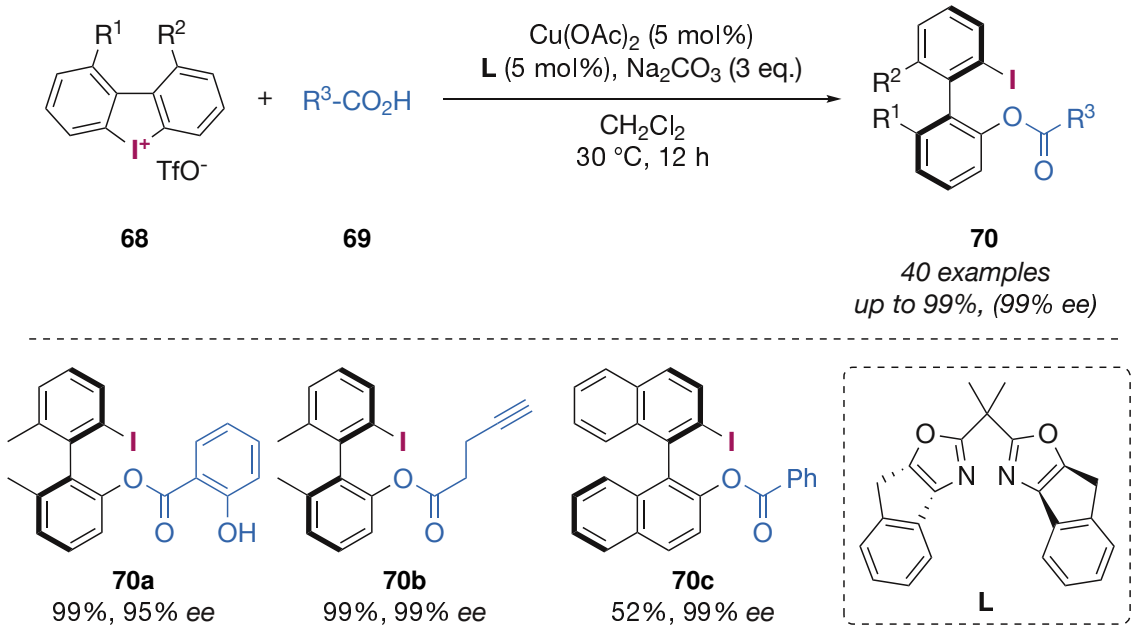

Scheme 1.18. Copper catalysed preparation of chiral iodobiphenyls **70** from iodonium salts **68**.

Organoiodine compounds feature a so-called sigma hole, an electropositive region, opposite to the sigma bond. Iodonium salts, due to having two covalently bounded ligands, feature two of these and further due to their positive charge they can be more pronounced. This results in iodonium salts recently gaining attraction as Lewis acid catalysts. Cyclic iodonium salts in this regard also benefit from their higher stability towards nucleophilic substitution and even stronger sigma holes due to their restricted geometry.[10, 56] So far there have already been a few successful applications in various types of reactions as they were able to catalyse halogen abstractions, Diels-Alder reactions, Michael additions or reductions with Hantzsch ester or cyanoborohydride.[9, 123, 124] Their reactivity can be altered to rival strong Lewis acids like BF_3 as can be seen in Scheme 3.5 (Section 3.1.2).

2 Objectives

In this thesis, structurally different diaryliodonium salts were supposed to be investigated in regard to their preparation and properties. This includes structural analysis as well as chemical characteristics.

Examples of hypervalent iodine compounds featuring multiple iodonium centres remain scarce. To fill this gap, iodine-iodine interactions, specifically I(III)-I(III) and I(I)-I(III) interactions, were supposed to be studied (Fig. 2.1). For this purpose, the *peri*-substitution was chosen to bring the iodine atoms in close proximity and stimulate new modes of interaction. The *peri*-substitution was not studied until recently, although in a sterically hindered way. It still lacks general protocols for the synthesis of the necessary compounds. Finally, these iodonium salts are supposed to be investigated towards possible applications to evaluate the influence of the two iodine atoms on each other.

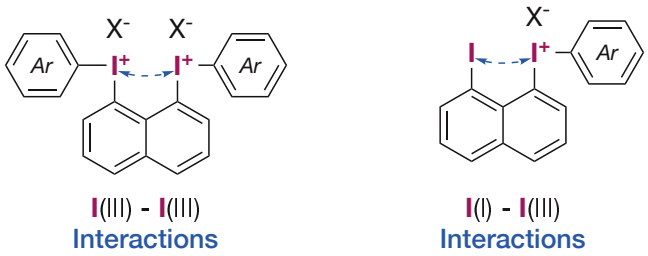

Figure 2.1. Structures to be investigated towards iodine-iodine interactions by bisiodonium salts in *peri*-position.

In a second topic, the focus was on the synthesis of diaryliodonium salts with the aim of enhancing the atom economy and scalability of existing protocols. An already existing multi-step procedure was supposed to be taken as the starting point. One major drawback when using chemical oxidants is the inevitably generated waste. There are different strategies for minimising such waste, like low molecular weight oxidants or using no chemical oxidants at all. Anodic oxidation recently gained popularity in the field of hypervalent iodine compounds but there are so far only a few examples for the generation of iodonium salts. Additionally, since the scalability should be studied electrochemical procedures pose the benefit of being easily transferable into a flow setup, from which they usually also benefit. By realising such a procedure it should also be investigated whether it is possible to combine it with different steps to create a continuous multi-step procedure for the generation of diaryliodonium salts.

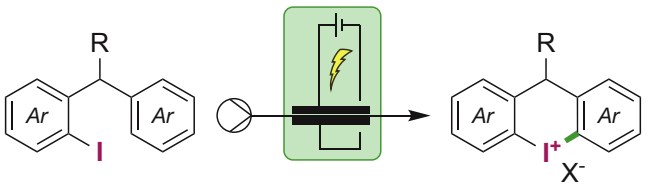

Scheme 2.1. General scheme for the electrochemical oxidation of iodoarenes towards cyclic diaryliodonium salts.

Lastly, a structurally more complex target for investigations was chosen. Thyroxine **T4** and the deiodinated triiodothyronine **T3** are one of the few naturally occurring iodoarenes. They play a crucial role in the regulation of the metabolism of various vertebrates. Due to this, the

question arises whether hypervalent iodine compounds derived from **T4** or **T3** have a biological relevance. If so, they should be isolated and investigated towards their role in the biosynthesis of thyroid hormones. Isolation would also make it possible to investigate these compounds in biological systems. To reach this goal the structures are supposed to be first simplified to develop an initial synthetic strategy that can afterwards be applied to the thyroid hormones.

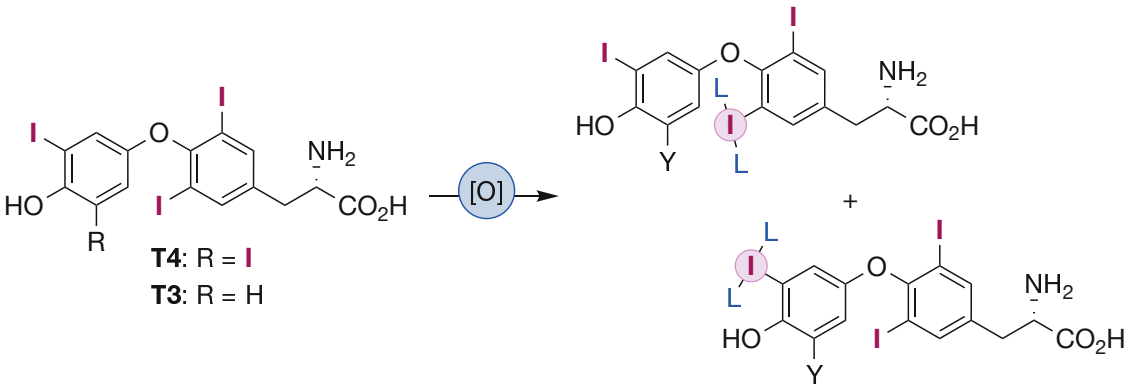

Scheme 2.2. Potential products from the oxidation of the thyroid hormones **T4** and **T3**.

3 Results and Discussion

3.1 Structural Investigation of *peri*-Bisiodonium Salts

3.1.1 Preliminary Remarks

All syntheses in chapter 3.1 were conducted by me including their analytics. Crystals were prepared by me. The measurement of these was done by P. Puylaert, who also refined them together with E. Lork.

3.1.2 Introduction into Bisiodonium Salts

Compounds with multiple oxidised iodine centres are interesting synthetic targets. In comparison to traditional reagents, they offer possibly new structural motives, new reactivities and a higher atom economy when used as a group-transfer reagent. They are generally investigated less than their monocationic relatives due to their more tedious and less straightforward synthesis as well as lower stability due to the higher amount of reactive positions. In recent literature examples, they mostly show up as scope substrates for new synthetic procedures,[117, 125–127] as side products,[76] but also for the synthesis of natural products[128] and in the preparation of metal complexes.[129–131]

The first example was provided by Willgerodt and Hilgenberg, where they showed for the first time the possibility of generating iodoso-species from polyiodinated aromatics and transforming these into bisiodonium salts via a Meyer-Hartmann reaction.[132] Over 60 years later examples from Olah et al. [133, 134] and Okawara et al. [135] also demonstrated the possibility of benzenes substituted with multiple halonium centres even though not stable at room temperature due to using aliphatic substituents. It took another fifteen years until Kitamura et al. took an interest in such compounds (Scheme 3.1).[136] They showed that activated forms

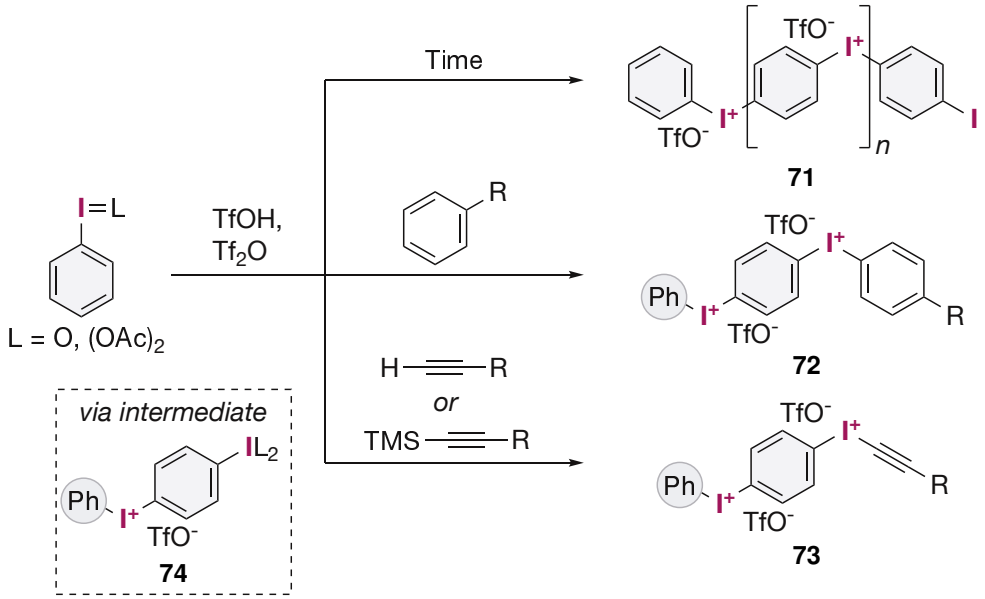

Scheme 3.1. Early reports on the reaction of oxidised iodobenzenes towards oligomers **71**, arylbisiodonium salts **72** and alkynylbisiodonium salts **73**.

of iodosobenzene or PIDA react, in the absence of nucleophiles, intermolecular with another equivalent of themselves to form the intermediate **74**. This self-reaction continues to form polymeric polycations **71** (chain lengths of 3-4 units are usually obtained)[137] or can be stopped with an arene[136, 138] or alkyne[139, 140] to form the dicationic salts **72** and **73**.

The phenylene bisarylbisiodonium **72** can be used like the monocationic counterparts for the arylation of nucleophiles especially to form the corresponding dicationic ammonium, phosphonium and sulfonium salts.[131, 138]

In comparison the alkyne-substituted salts have found applications comparable and distinct to their monocationic counterparts, their synthesis is well documented and multiple pathways are described. The same behaviour towards triflic acid can be observed as it adds to the triple bond in the β-position furnishing vinyl iodonium salts. This behaviour is also displayed in their reactivity (Scheme 3.2) as the nucleophile usually attacks in the β-position which initially after reduction of the iodine results in a terminal carbene. This carbene can rearrange furnishing α-substituted alkynes as seen in the reaction with thiocyanate (87-97%).[139] When employing phenolate as a nucleophile it can be observed that after initial addition the carbene does not immediately rearrange but, due to its electrophilic character, inserts into the aromatic C-H bond to build the benzofuranes **75** in good yields of 49-62%.[141] Furthermore, similar behaviour can be seen in the reaction of 1,3-dicarbonyls with **73**, here the intermediary carbene rearranges to give the expected alkynes **76** (39-86%) or inserts, if present, into the aliphatic C-H bond giving the cyclopentenes **77** in high yields of 70-75%.[142]

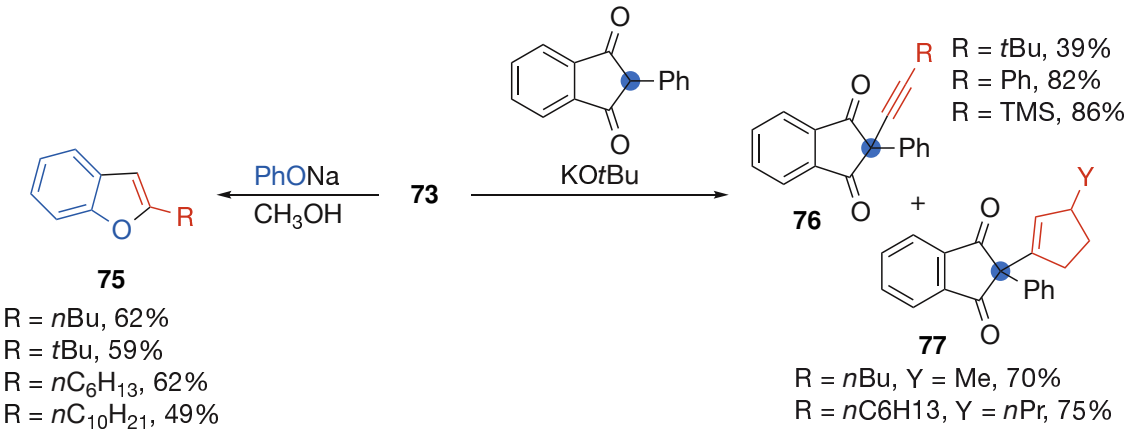

Scheme 3.2. Applications for the alkynylbisiodonium salt **73**.

Bisiodonium salts have also been used for asymmetric transformations. One early example is the phenylation of β-ketoesters by Ochiai et al. (Scheme 3.3).[143] They started from bis(diacetoxyiodo)-binaphthyl **79**, reacting it with tetraphenylstannane, to obtain the chiral salt **80** with a good yield of 90%. **80** performed quite well in the studied arylation of **81a** furnishing **82** with a yield of 51% and 37% *ee*. Although it should be noted that **80** did not perform best, this turned out to be the corresponding monocationic species ([1,1'-binaphthalen]-2-yl(phenyl)iodonium tetrafluoroborate).

Accordingly, Quideau et al. developed an asymmetric alkynylation of β-ketoesters and *O*-silyl-α-naphthols without the need for chiral additives or catalysts (Scheme 3.4).[144] By using the chiral dicationic biphenyl bisalkynyliodonium tosylate **83**, which they prepared by activation of the diacetate **84** with *p*TsOH and coupling with an alkynylboronate, they were able to transform a wide variety of substrates giving up to 99% yield and 68% *ee* in the case of β-ketoesters **81**

and 99% yield and 84% *ee* for the investigated naphthols **85**.

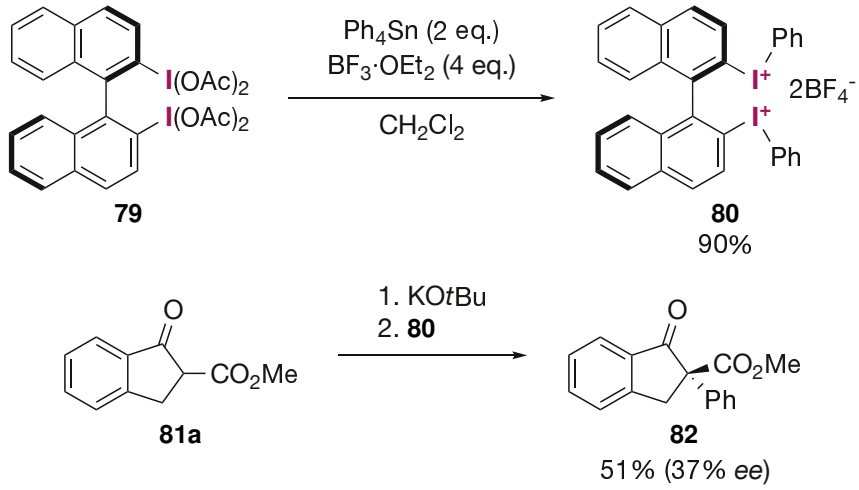

Scheme 3.3. Synthesis of the asymmetric arylbisiodonium salt **80** and application in the arylation of indanone **81a**.

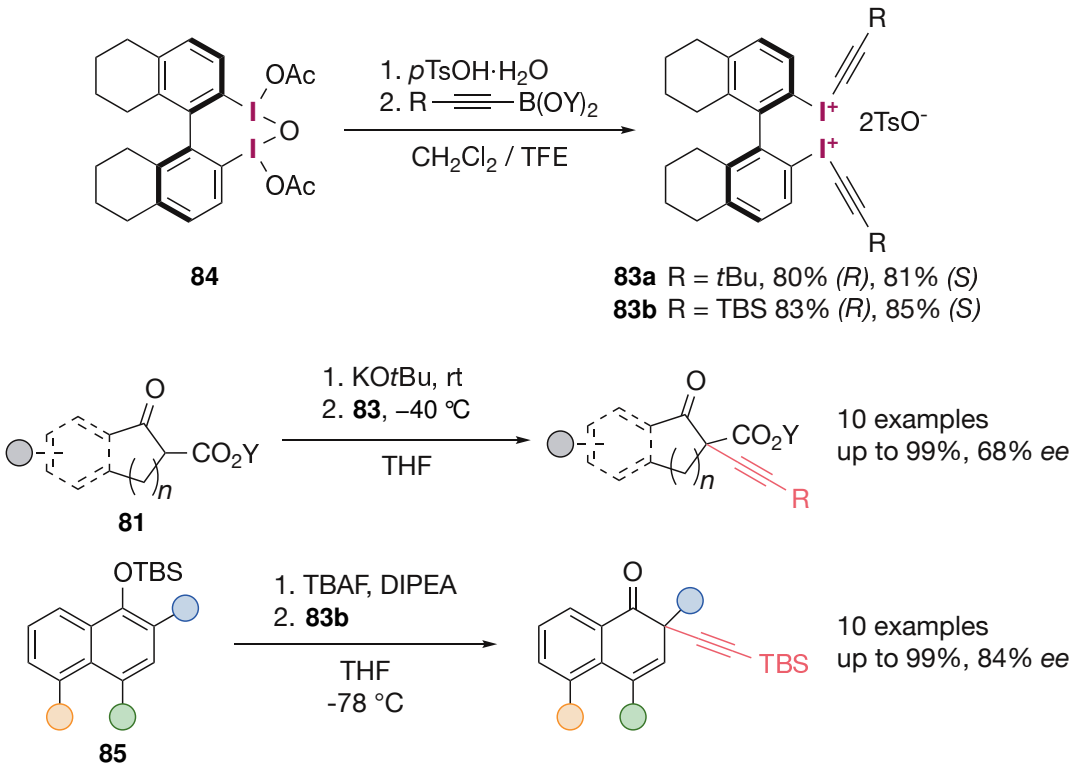

Scheme 3.4. Synthesis of the asymmetric alkynylbisiodonium salt **83** and application in the arylation of indanones **81** and naphthols **85**.

Regarding cyclic structures, Xu and Tan with coworkers presented a trisiodonium triflate similar to sumanene, but bearing iodines instead of methylene groups. The preparation was done with *m*CPBA/TfOH and they were able to substitute the iodonium centres under basic conditions with various p-Block elements like sulfur, selenium and iodide.[145]

By bringing the iodonium centers into closer proximity they can be utilised as strong halogen bond donors. Due to the higher charge and the naturally lower electron density binding in dica-

tionic iodonium salts increases significantly.[146] In the case of two iodonium centres it additionally bears the advantage of more coordination sites for more target-specific activations. This was for example demonstrated with the bisiodonium salt **86**, which was first prepared as a triflate salt **86a** by Yoshikai and Wu by oxidation with *m*CPBA and cyclisation with TfOH,[147] and later utilised as the first bidentate catalyst with two iodonium centres for halogen bonding catalysis by Huber et al. (Scheme 3.5). They employed the tetrakis(3,5-bis(trifluoromethyl)phenyl)borate ($BArF_4^-$) salt **86b** and were able to demonstrate a reactivity surpassing all at the time described catalysts, that are based on halogen bonding.[123] They employed the catalyst in the Michael addition of *N*-methylindole (**87**) to the crotonophenone **88** with a 74% formation of product **89** after 1 h (full conv. after 9 h). They were further able to drop the catalyst loading to 1 mol% (before 10 mol%) still yielding **89** with 62% after 12 h. They then investigated the nitro-Michael addition of methoxyindole **90** to the nitrostyrene **91**, where the product **92** could be observed in 83% yield after 1 h at 10 mol% catalyst loading (full conv. after 3 h) and when lowering the amount of catalyst to 1 mol% they were still able to obtain **92** with 55% after 8 h. Lastly, they looked at the Diels-Alder reaction of diene **93** and dienophile **94**. Here, higher catalyst loadings were necessary (30 mol%), nevertheless, they were able to obtain the product **95** in 73% yield after 12 h rivalling the activity of the strong Lewis acid BF_3. These results are especially remarkable when comparing them to monodentate iodonium catalysts which showed no product formation at all.

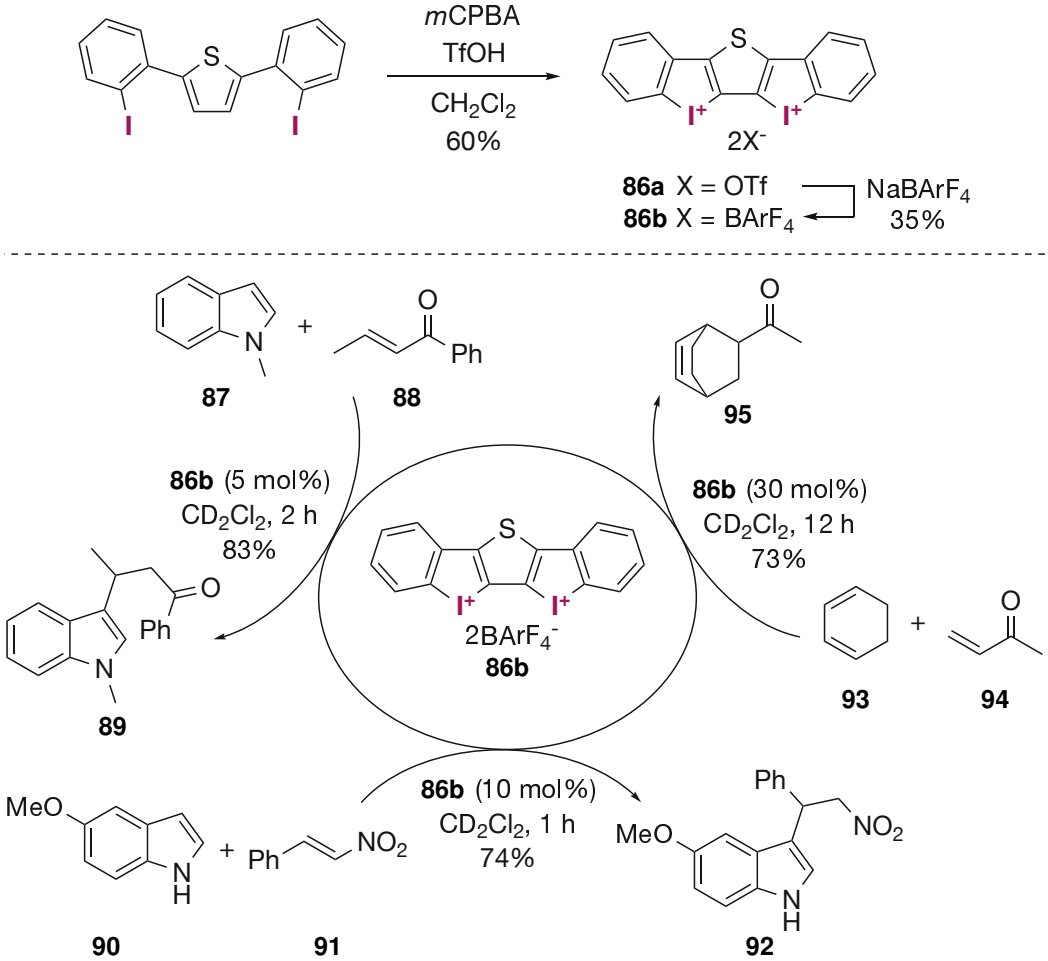

Scheme 3.5. Synthesis of the dicationic bisiodonium salt **86** and application in various halogen bond catalysed reactions.

Stang et al. prepared different-sized macrocycles with up to four iodonium centres (Scheme 3.6 and 3.7).[148, 149] The goal was to create a new type of cationic host for anions based on already existing structures, which utilised mainly ammonium salts. They prepared these macrocycles in a very similar fashion, where they reacted a diaryl system with an oxidised iodine on each arene with a similar system but with TMS groups instead, which acts as an *ipso*-directing group. The iodanes were usually activated with TMSOTf. This way they could directly, in the case of the diphenylmethane bisiodane **96** and bistrimethylsilyl diphenylmethanes **97**, obtain the two bisiodonium salt **98** and **99** in 71% and 55% yield (Scheme 3.6). Structures with higher

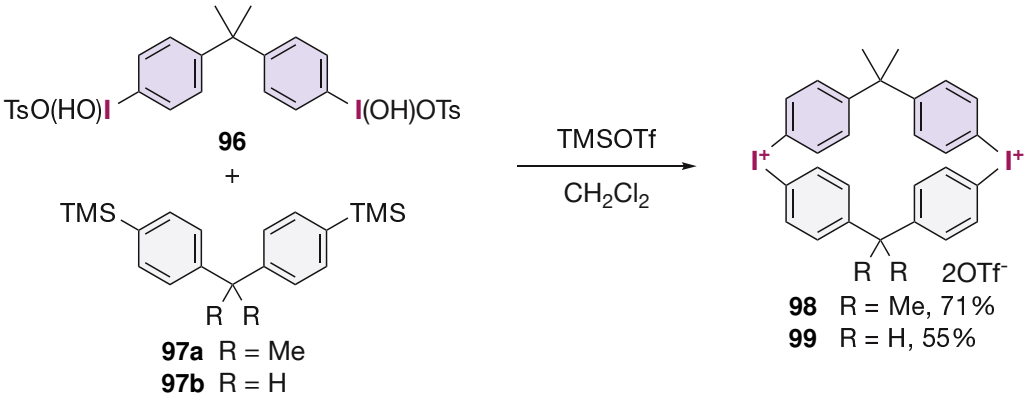

Scheme 3.6. Synthesis of the macrocyclic bisiodonium salts **98** and **99**.

numbers of iodonium centres, needed a stepwise approach (Scheme 3.7). They first reacted the biphenyl bisiodane **100** with two equivalents of the bistrimethylsilyl biphenyl **101** to obtain the bisiodonium salt **102** in a high yield of 90%. Intermediate **102** was then further reacted with another equivalent of bisiodane **96** or **100** to yield either the quadratic tetraiodonium salt **103** (70%) or the pentagonal tetraiodonium salt **104** (60%). In comparison when reacted in a one-pot procedure with equivalent amounts of iodane **100** and TMS-arene **101** the compound **103** yielded only 15%.

Twenty years later the groups of Shafir and Cuenca published three new types of cyclic bisiodonium salts.[150] In growing distance between the iodines, namely the dibenzo bisiodonium salt **105**, the dinaphtho bisiodonium salt **106** and the xanthene-derived macrocycle **107** (Schemes 3.8 to 3.10). All these substrates were synthesised by utilising a similar strategy which starts with a bifunctionalised arene, bearing a to-be-oxidised iodine and an *ipso*-directing group (−TMS, $-BF_3K$). By oxidising the iodine, coupling it with another equivalent of iodoarene and repeating this the desired cyclic bisiodonium salts could be generated. Starting with the smallest ring size they initially looked at the already known preparation of intermediate **108** from iodophenyltrifluoroborate **109** with Selectfluor,[101] but realised that full closure to the desired structure could only be observed in HFIP at elevated temperatures as other conditions lead to substitution or decomposition of the intermediate **108** or maybe even target compound **105** yielding only 1,2-diiodobenzene. Purification was possible by precipitation as the tosylate **105** with a yield of 71%. By exchange to iodide and further exchange via silver salts, the corresponding triflate, tetrafluoroborate and tetrakis(3,5-bis(trifluoromethyl)phenyl)borate were obtained. They were also able to prepare analogous mixed halonium species (I(III)/Br(III) and I(III)/Cl(III)) by a slightly different approach using a diazonium salt as the *ipso*-directing group and "oxidant".

In a similar fashion to **105**, it was possible to cyclise the iodonaphthyltrifluoroborate **110** to either obtain the tetrafluoroborate **106a** (73%) via reverse phase column chromatography or the

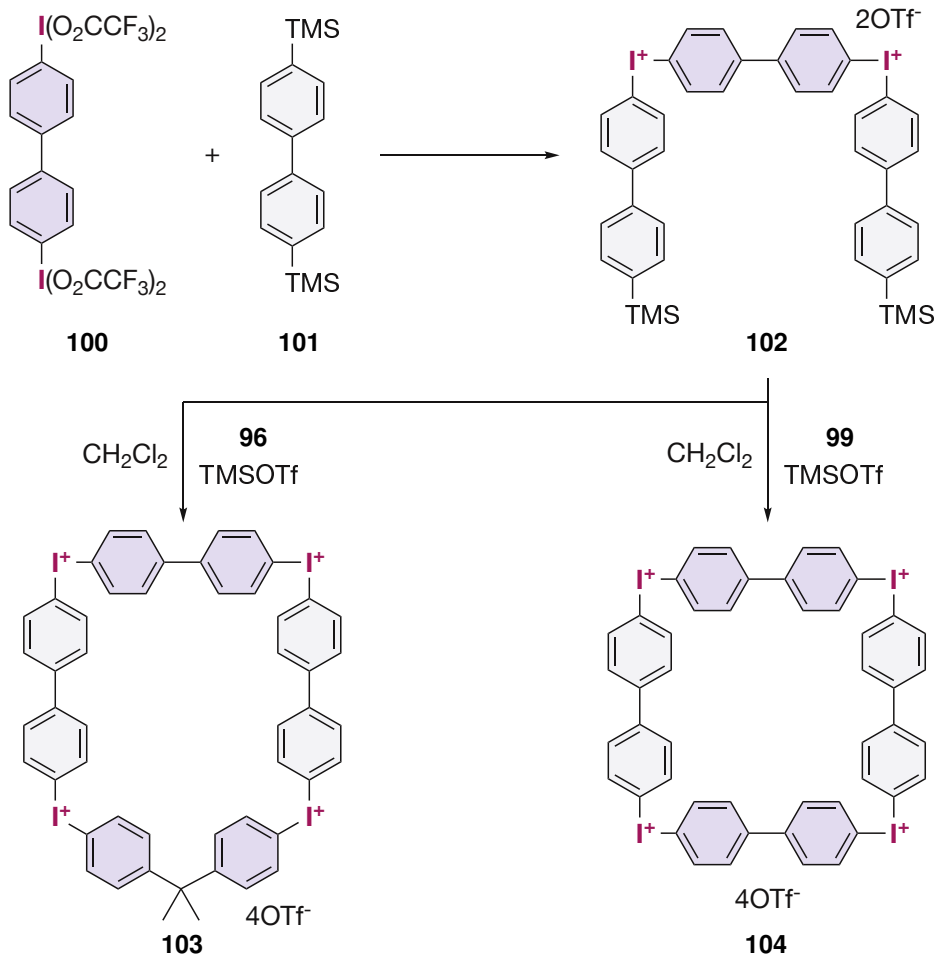

Scheme 3.7. Synthesis of the macrocyclic tetraiodonium salts **103** and **104**

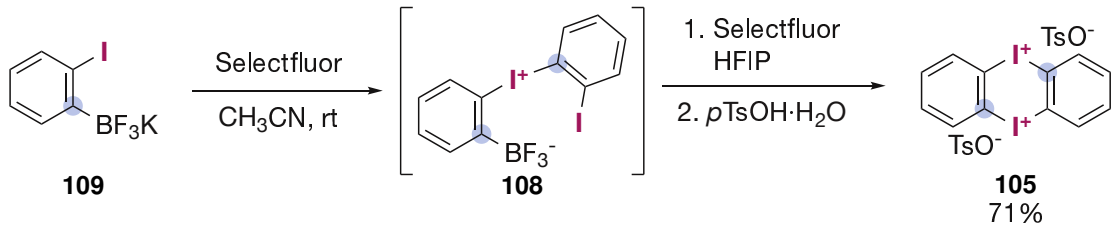

Scheme 3.8. Synthesis of the dibenzobisiodonium salt **105** by oxidation and subsequent self-reaction of **109**.

tosylate **106b** (86%) via precipitation with tosylic acid. Again, conversion to the iodide and from there to the triflate, hexafluorophosphate and tetrakis(3,5-bis(trifluoromethyl)phenyl)borate via silver salts was possible.

The next bigger system would be based on anthracene, but to their disappointment, their attempts towards such a macrocycle did not succeed. Nonetheless, they overcame this by using a dimethylxanthene backbone **111**. Preparation of **111** was done from 9,9-dimethylxanthene via instalment of two TMS-groups in positions four and five, followed by mono-iodination with iodine and Selectfluor. They then oxidised **111** with Selectfluor, but needed $BF_3 \cdot OEt_2$ and higher temperatures to induce cyclisation and obtain the tetrafluoroborate **107** (40%). Also in this case, it was possible to exchange the anion to iodide and from there to triflate.

Overall these structures present a very interesting study as they gradually move the iodine

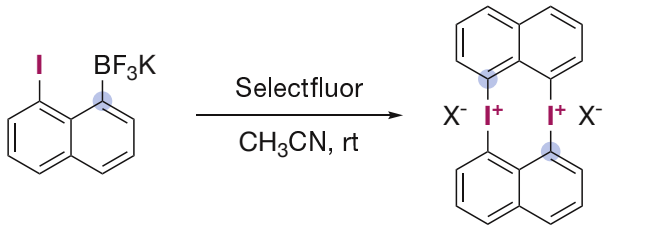

110

106a, X = BF_4^-, 73%
106b, X = TsO^-, 86%

Scheme 3.9. Synthesis of the dinaphthobisiodonium salts **106**.

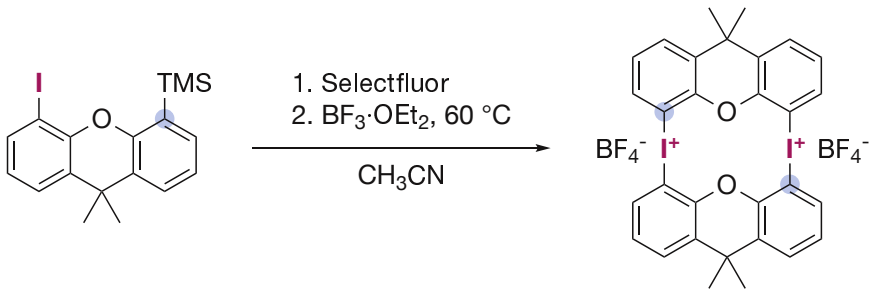

111

107
40%

Scheme 3.10. Synthesis of the xanthene derived bisiodonium salt **107**.

further apart. Data obtained from crystal structures proves this with distances of 3.38 Å for the dinaphtho bisiodonium **106**, 3.52 Å for the dibenzo bisiodonium **105** and ~4.2 Å for the xanthene derivative **107**.

3.1.3 Synthesis of Symmetrical *peri*-Bisiodonium Salts 114

Since most examples of bisiodonium species in literature are based on benzene or biphenyl motives (section 3.1.2), in various substitution patterns (*para*, *ortho*, *meta*), *peri*-substituted naphthalenes were investigated as a new target. Since this should allow for unique and so far not described interactions between the two iodine(III) atoms. During previous investigations towards such iodonium salts where the initial goal was a more symmetric salt analogous to recently published works by Shafir and Cuenca (Schemes 3.8 and 3.9),[150, 151] test reactions were conducted to prove the possibility of a 1,8-substituted naphthalene with two oxidised iodine centres. Following literature-known procedures, diiodonaphthalene **112** was oxidised and coupled with phenylboronic acid (**113a**) by activation with boron trifluoride etherate ($BF_3 \cdot OEt_2$) to obtain the bisiodonium salt **114a** in a satisfactory yield of 32% (Scheme 3.11).[57] Initially, the activity as a halogen bond donor was investigated in a Ritter-type halogen abstraction, resulting in an observable but not significantly higher activity compared to a simple diphenyl iodonium salt.

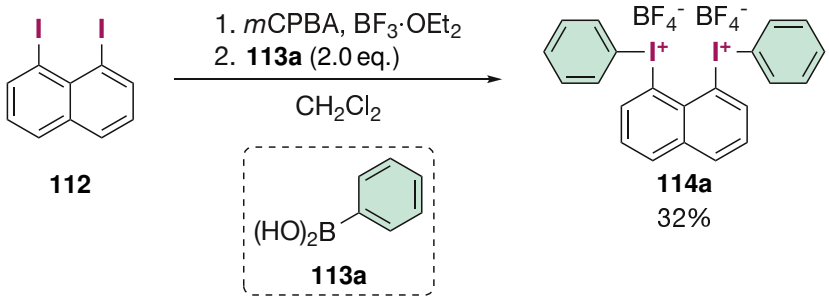

Scheme 3.11. Previous synthesis of **114a**.

Nonetheless, in this thesis this type of salts were supposed to be investigated structurally and for this, a small scope of five symmetric substrates was conducted (Scheme 3.12). Besides the original substrate **114a**, two more electron-rich (**114b**,**c**) and two more electron-poor substrates (**114d**,**e**) were chosen. Derivatisation was only done in the *para*-position of the attached phenyl moieties. By slight adjustments to the procedure and improved workup the substrate **114a** could now be obtained in a 48% yield. A similar yield of 45% was also possible for the highly electron-rich substrate **114b**, although the addition of the boronic acid had to be done at −80 °C, caused by the higher reactivity of the boronic acid, to prevent side reactions as well as decomposition from this. The *para*-methyl derivative **114c** could also be obtained in a sufficient yield of 39%. Only the electron-poor *para*-bromo and *para*-fluoro substituted derivatives **114d** and **114e** could be isolated in merely 19% each, owing to the low reactivity and by this not full reaction to the double oxidised bisiodonium salt. Major side products that were observed during these reactions were besides the iodoarene **112** and deiodination of this, various forms of mono-oxidised salts, mostly comprising of the iodide **112** coupled with only one boronic acid **113**. Although symmetrically substituted diphenyl iodonium salts and coupling between two iodoarenes **112** were observed.

To investigate these new compounds structurally, suitable crystals for X-ray crystallography were grown of all substrates **114a**–**e**. Additionally, **114a** was crystallised in the presence of TfOH to obtain the corresponding triflate salt **114f**. Selected bond lengths, interatomic distances and angles are presented in Tab. 3.1. Three basic conformations were obtained. In all cases, the aryl ligands are perpendicular to the naphthalene plane as can be seen by the C11-I1-I2 and C17-I2-I1 angles that vary between 74° to 80°. Typically an angle of 90° would be expected as

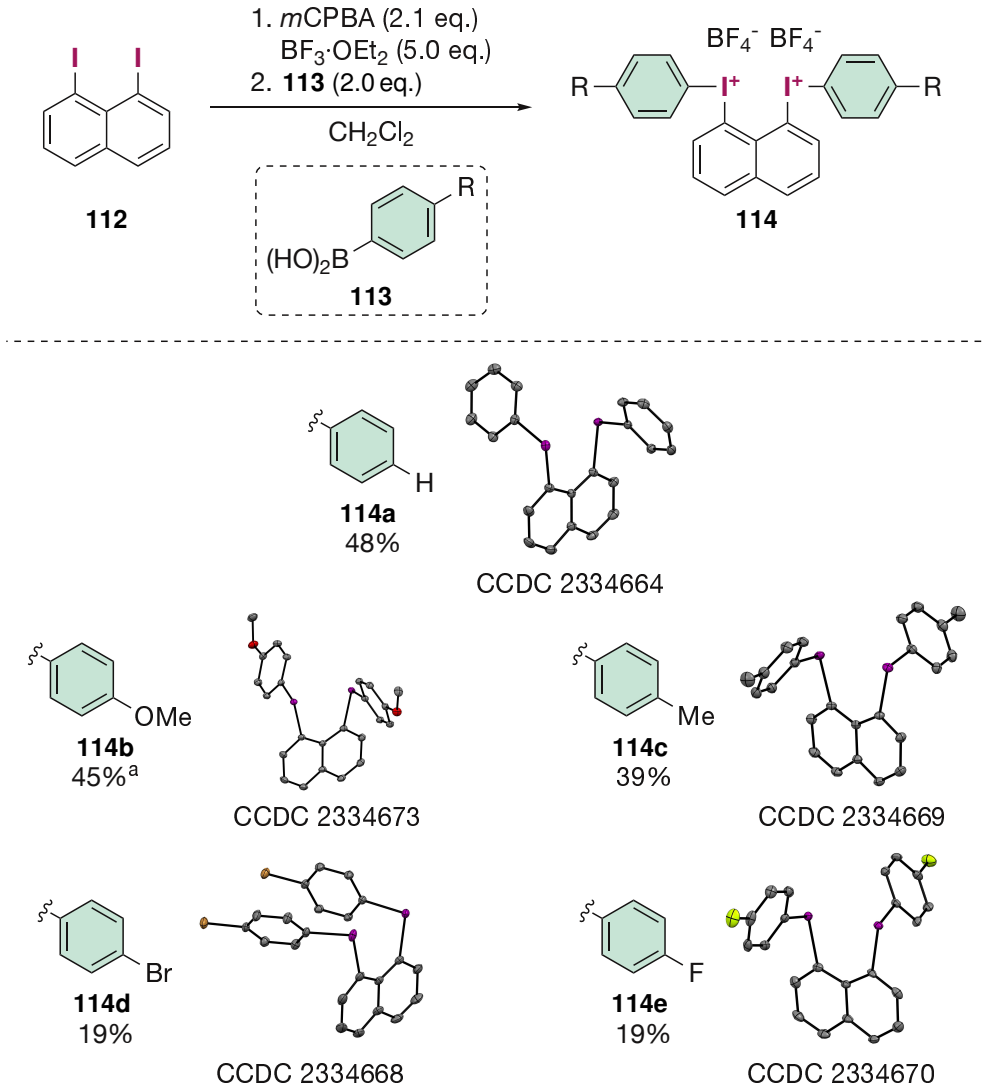

Scheme 3.12. Substrate scope for the preparation of symmetric bisiodonium salts **114** from **112**. Single crystal structures (ORTEP drawing; hydrogen atoms, anions and solvent molecules were omitted) of **114a–e**. Thermal ellipsoids are displayed with 50% probability. *a*. Addition of the boronic acid **113b** at –80 °C.

can be seen for the naphthyl(phenyl)iodonium tetrafluoroborate.[152] The compounds **114a**,**b**,**f** crystallised in an "Anti"-conformation with the aryl ligands pointing in opposite directions. The derivatives **114c**,**e** were obtained in the opposite conformation. Only for the substrate **114d**, a "Syn"-conformation was observed where both aryl ligands are on the same side of the naphthalene plane. When looking at the ligand sphere of each iodine, the C-I bond lengths for each aryl ligand as well as the naphthalene are well in agreement with literature data of monocationic and dicationic naphthyliodonium salts.[150, 152] The I-F (I-O for **114f**) distances towards the anion are slightly shortened in comparison to similar monocationic examples[152] with roughly 80-87% of the van der Waals radii,[152, 153] although in agreement with the dicationic bisiodonium salt **106** (Scheme 3.9).[150] Interaction between the two oxidised iodine atoms seems to be mostly of a repulsive nature as the I-I distances are close to the literature-described distances for the 1,8-diiodonaphthalene (**112**) ranging between 3.526 Å to 3.572 Å (equivalent to ~90% of the vdW radii),[154] although longer than for the bisiodonium salt **106**, which could be explained by a lower strain on the *peri*-region due to their acyclic structure. Furthermore, the iodine atoms in all

structures show displacement out of the naphthalene plane comparable to structure **106**, which can be explained by the two positively charged iodonium centres close to each other causing charge repulsion. This strain in the *peri*-region is also visible in the splay angle of roughly 25° to 29° for all structures **114**.

Table 3.1. Experimental interatomic distances [Å] and angles [°] of compounds **114a–f**

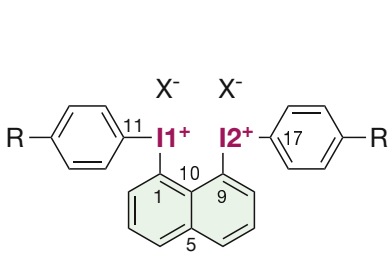

114

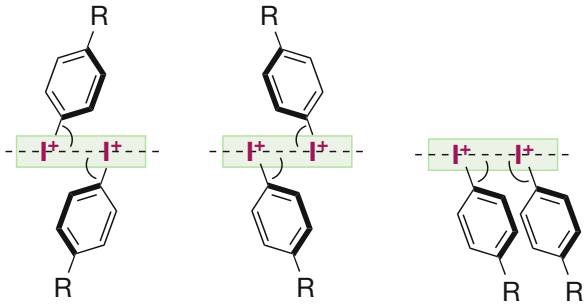

Anti-1 Anti-2 Syn

	114a	**114f**[a]	**114b**	**114c**[a]	**114d**	**114e**[b]
R =	H	H	OMe	Me	Br	F
X =	BF_4	TfO	BF_4	BF_4	BF_4	BF_4
Conformation	Anti-1	Anti-1	Anti-1	Anti-2	Syn	Anti-2
I1 · · · I2	3.534(1)	3.572(1)	3.526(1)	3.554(1)	3.537(1)	3.550(1)
I1 – C1	2.109(2)	2.109(2)	2.109(1)	2.107(1)	2.111(2)	2.113(5)
I2 – C9	2.102(2)		2.105(1)		2.108(2)	2.108(5)
I1 – C11	2.117(3)	2.110(2)	2.101(1)	2.103(1)	2.112(2)	2.105(5)
I2 – C17	2.121(3)		2.103(1)		2.112(2)	2.113(5)
I1 · · · F[c]	2.762(2)	2.827(2)[e]	2.805(1)	2.993(1)	3.004(5)	2.838(4)
I2 · · · F[c]	2.794(2)		2.754(1)		2.835(1)	2.879(4)
C1 – I1 – C11	96.4(1)	97.19(7)	96.16(5)	95.64(5)	94.81(8)	96.0(2)
C9 – I2 – C17	97.3(1)		97.69(5)		95.93(8)	96.3(2)
C11 – I1 – I2	74.82(7)	76.43(5)	78.76(4)	78.84(3)	116.98(5)	74.1(1)
C17 – I2 – I1	76.65(8)		78.03(4)		73.67(5)	79.6(1)
Out-of-plane displacement						
I1	0.193	0.032	0.118	0.143	0.108	0.069
I2	0.260		0.071		0.208	0.146
peri region angles						
I1 – C1 – C10	127.1(2)	127.9(2)	126.6(1)	127.5(1)	125.7(2)	127.4(4)
C1 – C10 – C9	131.2(2)	131.0	130.9(1)	130.9	131.5(2)	132.1(5)
C10 – C9 – I2	126.5(2)		127.7(1)		128.0(2)	125.7(4)
Sum of bay angles	384.8(6)	368.8(4)	385.2(3)	385.9(2)	385.2(6)	385.2(13)
Splay angle[d]	24.8(6)	28.8(4)	25.2(3)	25.9(2)	25.2(6)	25.2(13)

a. Some values were omitted due to the structures being C_2-symmetric along the C5-C10 bond, *b*. Chosen values from one of two nearly identical molecules **114e** in one unit cell, *c*. Closest fluorine from the BF_4^- anion was chosen, *d*. Splay angle: sum of three bay region angles −360°, *e*. I1 · · · O distance to the triflate.

3.1.4 Synthesis of Unsymmetrical *peri*-Bisiodonium Salts 115

Besides the symmetric bisiodonium salts **114** described in section 3.1.3, it seemed more interesting how unsymmetric versions of these would differ structurally and chemically. Initially, an analogous one-pot approach based on the synthesis for the symmetric salts **114** was attempted where instead of adding only one boronic acid after the oxidation two different boronic acids were added, to furnish an unsymmetric salt. In the case of phenylboronic acid (**113a**) and *para*-bromophenylboronic acid (**113c**), this approach was successful, although symmetric salt **114a** (Ph-Ph) was the major product. Initial conditions yielded a mixture of roughly 31% **115** and 34% **114** (based on ratios determined by NMR). An optimisation of these conditions was attempted but with no success. Changing the solvent (entry 2) and raising the amount of **113c** (entry 3) did not result in any observable product formation. Since entry 1 uses an excess of boronic acid it was also attempted to keep the ratios the same but lower the overall amount to the theoretical minimum with (entry 4). Lastly the use of the, in comparison, more reactive *para*-methylboronic acid (**113d**) was also attempted but with no avail (entry 5 and 6).

Table 3.2. Preliminary Screening of different boronic acids **113** for the generation of unsymmetric bisiodonium salts **115** in a one-pot reaction.

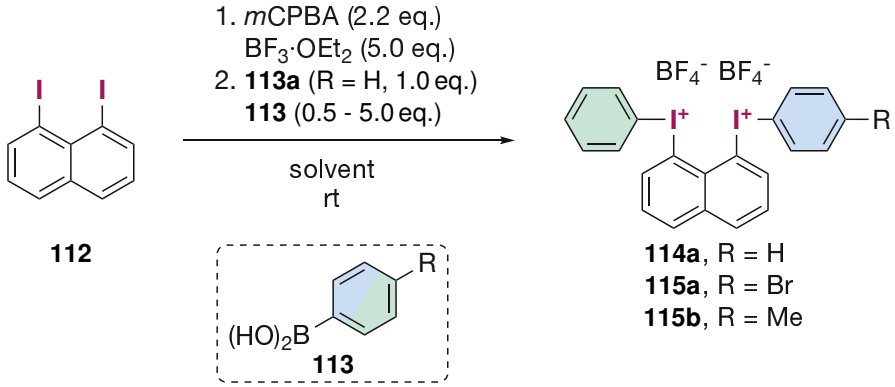

#[a]	**113** (R, eq.)	Solvent	Yield **115** [%] and Notes
1	**113c** (Br, 1.0)	CH_2Cl_2	31% **115a** + 34% **114a** (68% **114a** based on **113a**)
2	**113c** (Br, 1.0)	CH_3CN	**114** and **115a** ND
3	**113c** (Br, 5.0)	CH_2Cl_2	**114** and **115a** ND
4[b]	**113c** (Br, 0.5)	CH_2Cl_2	**114** and **115a** ND
5	**113d** (Me, 1.0)	CH_2Cl_2	**114** and **115b** ND
6	**113d** (Me, 1.0)	CH_3CN	**114** and **115b** ND

a. To a solution of **112** (0.100 mmol, 50.0 mM) and *m*CPBA (2.2 eq.) was added $BF_3 \cdot OEt_2$ (5.0 eq.) and after 15 min simultaneously $PhB(OH)_2$ (**113a**, 1 eq.) and the corresponding boronic acid **113**. *b*. **113a** (0.5 eq.). ND = not detected

It was not possible to purify the obtained mixture of **114a** and **115a**, due to their high similarity, but it was possible to verify the presence of **115a** besides **114a** via HRMS. Attempts to crystallise **115a** were unsuccessful. The NMR of the mixture clearly shows the signals corresponding to **114a** and an additional set that varies especially in regards to the signals corresponding to the phenyl rings (Fig. 3.1). When comparing the spectrum of the mixture to the one of **114a**, most

signals show a underlying second signal, this is true for all signals corresponding to protons of the naphthalene and the phenyl moiety. Additionally, there is one striking difference in that the mixture shows two new doublets, these can be attributed to the protons on the *para*-bromophenyl moiety of **115a**, which gets further confirmed when comparing the very similar shifts of the symmetric compound **114d**.

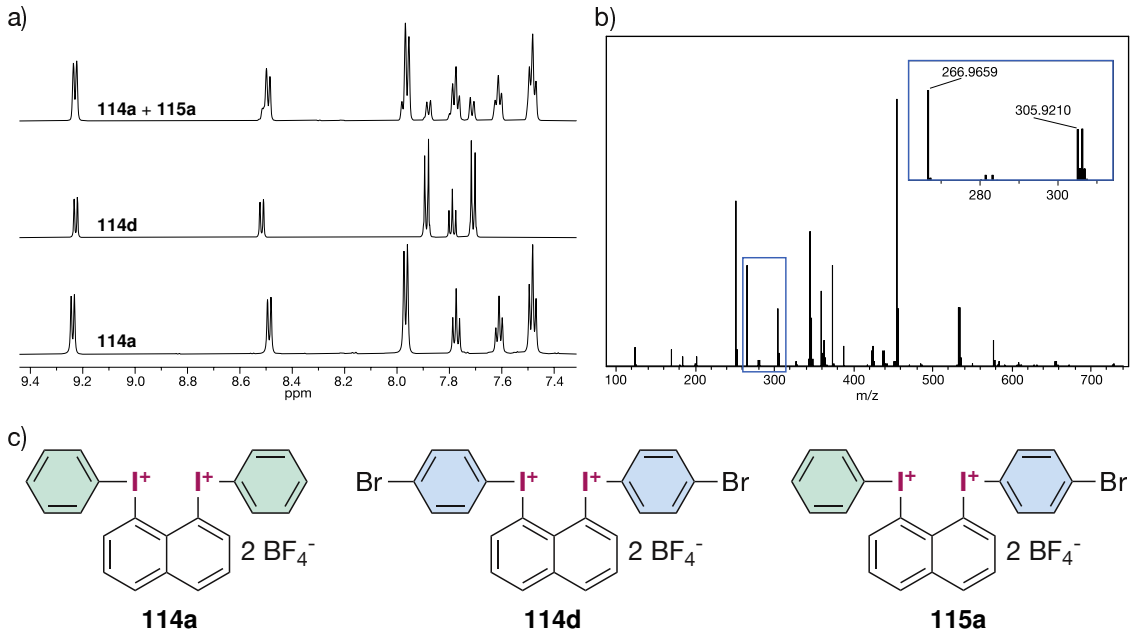

Figure 3.1. Analysis of the one-pot reaction with two different boronic acids forming unsymmetric bisiodonium salt **115a**. a) ^{1}H NMR spectrum showing the obtained product mixture of **114a** and **115a** and the spectra of the compounds **114a**,**d** for reference. b) HRMS (ESI) spectrum of the obtained product mixture showing signals for the symmetric **114a** (calc. *m/z* = 266.9665) and the unsymmetric **115a** (calc. *m/z* = 305.9218). c) Compounds **114a**,**d** and **115a**.

With these preliminary results in hand, knowing that unsymmetric salts are stable, but a more selective route is needed, two general pathways opened up. First, a stepwise approach where only one iodine is oxidised, then coupled with an arene yielding a mono-oxidised intermediate **116** followed by the same sequence again with a different arene furnishing an unsymmetric bisiodonium salt **115** (Scheme 3.13, A). This could be challenging due to the tendency of diiodoarenes to easily over oxidise and by this, produce impurities of similar polarity which would be difficult to separate. Alternatively, a "reversed" approach is possible by installing an *ipso*-directing group (−TMS, −B(OR)$_2$) *peri* to an iodonium salt **117** (Scheme 3.13, B) and reacting such species with an activated iodane in the form of ArIL$_2$.

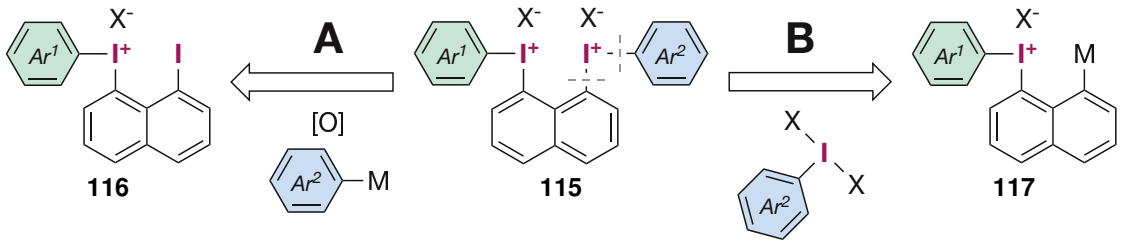

Scheme 3.13. Synthetic strategies towards unsymmetric *peri*-bisiodonium salts **115**. A: Stepwise oxidation and coupling with activated arenes ArM. B: Instalment of activating and directing group *peri* to a iodonium centre two facilitate coupling with another iodane ArIL$_2$. M = TMS, B(OR)$_2$

3.1.4.1 Stepwise Oxidation

For the stepwise approach, the necessary mono-oxidised iodonium salts **116** had to be prepared selectively. Attempts to utilise conditions similar to the symmetric salts **114** (Scheme 3.12) by adjusting the equivalents of oxidant and boronic acid were not successful as the salts **114** still formed in a significant amount. Further, it was observed that in chlorinated solvents the I(III)-I(I)-species derived from the reaction with one equivalent of *m*CPBA was significantly less stable than the I(III)-I(III)-species resulting from two equivalents of *m*CPBA. To circumvent this, different strategies were investigated.

Initially, based on literature examples,[155] an oxidised I(III)-I(III)-species derived from **112** was supposed to be isolated and investigated in regards to the more selective formation of desired mono-oxidised salts **116**. As seen in scheme 3.14 it was possible to isolate the diacetate **118** by oxidation with Selectfluor in a mixture of acetonitrile and acetic acid in a satisfying yield of 74%. So far attempts to investigate **118** structurally by X-ray-crystallography, did not succeed, due to its decomposition in solution over time.

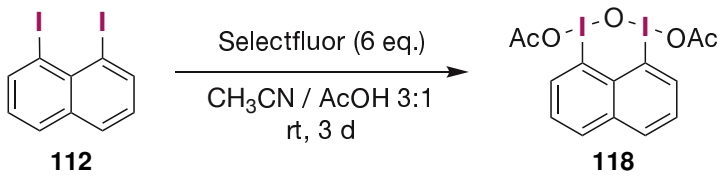

Scheme 3.14. Preparation of the diacetate **118** by oxidation with Selectfluor.

Diacetate **118** was then reacted analogously to reports for diaryliodonium salts in 2,2,2-trifluoroethanol (TFE) with sodium tetrafluoroborate as an additive (Scheme 3.15).[117, 156] This allowed a very mild and slow ligand exchange to furnish the desired mono-oxidised tetrafluoroborates **116a–d** with no impurities from double arylation. Unfortunately, all substrates were obtained in low yields. The electron-poor *para*-bromophenyl derivative **116a** could be obtained with 13% whereas the slightly more electron-rich phenyliodonium salt **116b** yielded 16%. The tolyl derivative **116c** gave only a 6% yield, which was surprising as the more electron-rich anisyl derivative **116d** could be obtained with a yield of 21%. Regarding the nature of this reaction, it is presumed that first, a ligand exchange on one of the iodine takes place, which

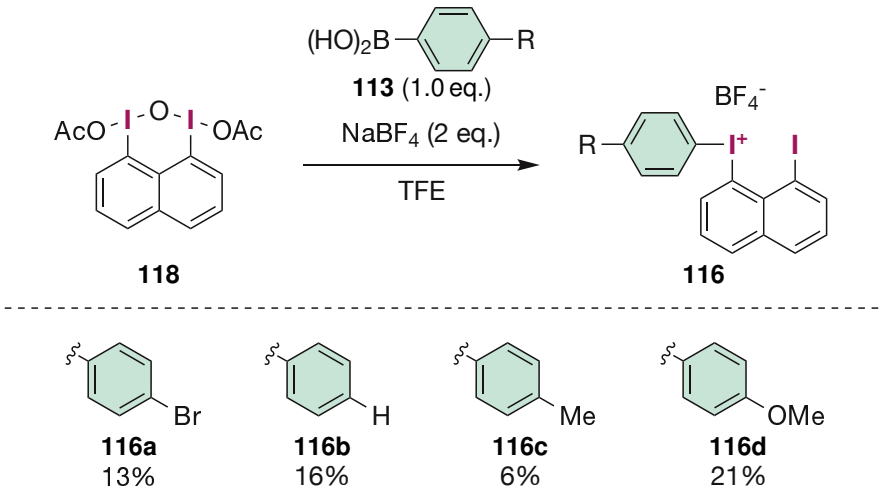

Scheme 3.15. Substrate scope for the preparation of iodonium salts **116a–d** from the diacetate **118**.

destabilises the structure leading to a reduction of the second I(III) centre.

Due to the time-consuming and unreliable preparation of diacetate **118** it was deemed useful to further look into methods for the direct preparation of the iodonium salts **116** from the iodoarene **112**. The unsubstituted (iodonaphthyl)(phenyl)iodonium salt **116b** was chosen as a target for this optimisation (Tab. 3.3). Initially, one equivalent of *m*CPBA was chosen to avoid over-oxidation. Various solvents, including CH_2Cl_2, TFE, CH_3CN, were then screened (entries 1 – 3) with no satisfying results as yields were low and the formation of the symmetric salt **114a** (Ph-Ph) was observed. Based on the synthesis of diacetate **112** a mixture of acetonitrile and acetic acid was tested with either *m*CPBA or Selectfluor as an oxidant (entries 4 and 5) giving similar results or no product formation at all. Since instability of **112** with one equivalent of oxidant in solution was observed, diethyl ether (Et_2O) was tested as a solvent and fortunately showed precipitation of what can presumably be described as a mixed I(III)-I(I) species with full conversion based on analysis by TLC. When adding the phenylboronic acid to this suspension the product **116b** formed after a few hours yielding 20%. To test the scalability of the method the reaction was performed at a ten times higher scale, still yielding the product **116b** in 15%.

Table 3.3. Screening of oxidants and solvents for an one-pot procedure of iodonium salts **116a–e** from iodoarene **112**.

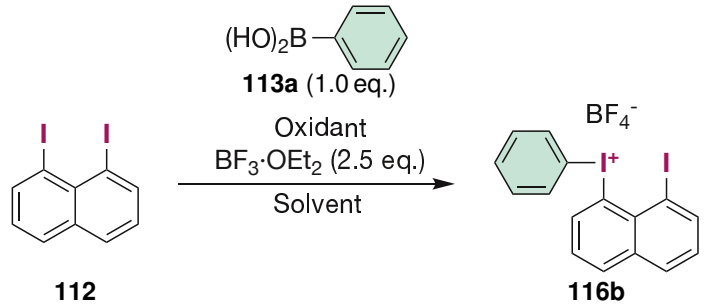

112 **116b**

#[a]	Oxidant (eq.)	Solvent	Yield **116b** [%] and Notes
1	*m*CPBA (1.0)	CH_2Cl_2	<10; **114a** as a major SP
2	*m*CPBA (1.0)	TFE	<10
3	*m*CPBA (1.0)	CH_3CN	<10
4	*m*CPBA (1.0)	CH_3CN/AcOH 3:1	10
5	Selectfluor (2.5)	CH_3CN/AcOH 3:1	—
6	*m*CPBA (1.0)	Et_2O	20
7[b]	*m*CPBA (1)	Et_2O	15 (56 brsm.)

a. **112** (0.1 mmol), $PhB(OH)_2$ (**113a**, 1 eq.), 0.1 M, *b*. 1 mmol scale.

A small scope was performed (Scheme 3.16) to test the general applicability of the procedure, especially in contrast to the one described before (Scheme 3.15). Delightfully the yields did not differ a lot as the *para*-bromo derivative **116a** was obtained in a slightly increased yield of 22%. The substrates **116b** (phenyl) and **116c** (tolyl) were obtained in 15% and 6% respectively, matching previous results. In contrast, the electron-rich anisyl derivative **116d** proved to be challenging, yielding only 13% (compared to the previous 21%). Moreover, the addition of the boronic acid had to be at −80 °C. Furthermore, 2,4,6-trimethoxyphenyl derivative **116e** could

also obtained by this method (18%).

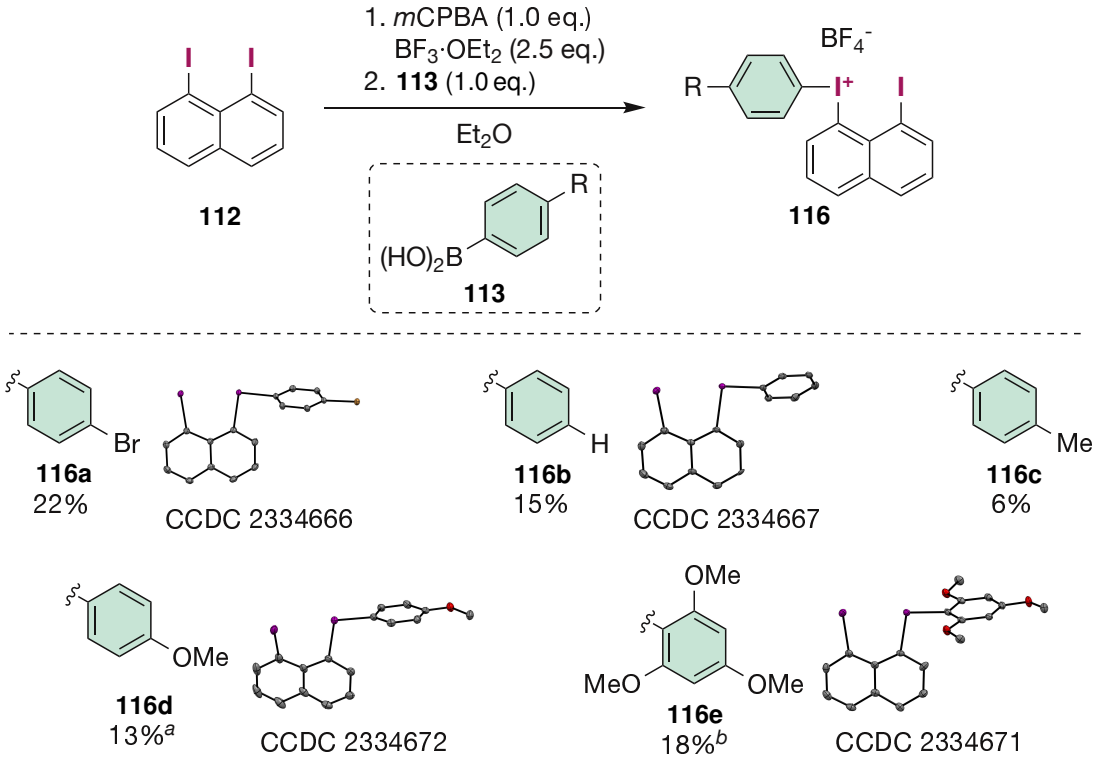

Scheme 3.16. Substrate scope of the one-pot procedure for iodonium salts **116a–e** from the iodoarene **112**. Single crystal structures (ORTEP drawing; hydrogen atoms, anions and solvent molecules were omitted) of **116a**,**b**,**d**,**e**. Thermal ellipsoids are displayed with 50% probability. *a*. Addition of the boronic acid **113b** at −80 °C, *b*. 1,3,5-Trimethoxybenzene (1.0 eq.) was used instead of **113**.

It was possible to obtain crystals suitable for X-ray crystallography of all substrates except the tolyliodonium salt **116c**. Selected bond lengths, interatomic distances and angles are presented in Tab. 3.4. The major difference when comparing these structures to previous symmetric **114** is, besides the oxidation state of the second iodine, that the aryl substituent lies almost in the plane of the naphthalene system. Visible by the dihedral angle C8-C9-I2-C11 which ranges between 1° to 24°. This is especially striking in comparison to the literature known naphthyl(phenyl)iodonium tetrafluoroborate where the ligand is coordinated perpendicular to the naphthalene plane.[152] As a result, the C11-I1-I2 angle ranges between 168° to 175° indicating that the I(III) acts as a halogen bond donor with the I(I) coordinating into the sigma-hole of the I(III) atom. Because of this, the I1-I2 distance (3.24 Å to 3.27 Å) is significantly shortened in comparison to either the previously mentioned dicationic structures **114** (3.53 Å to 3.57 Å) or the 1,8-diiodonaphthalene[154] (**112**, 3.51 Å to 3.54 Å). Consequently, the splay angle is reduced by more than 10° in comparison to structures **114**. The ligand sphere of the I(III) atom is otherwise in agreement with literature data[150, 152] although the I2-C9 bond is overall slightly elongated by 0.030 Å to 0.094 Å in comparison to the I2-C11 bond. This could be caused by the previously described iodine-iodine interaction. Interactions between the iodine and the counterion (BF_4^-) are mostly as expected reflecting I-F distances similar to literature-known structures.[152] Peculiarly, in the case of substrate **116a** the tetrafluoroborate is closer to the reduced I(I) than the I(III) (I1-F<I2-F). An explanation could be the stronger electron-withdrawing effect due to the bromide substitution, leading to an induced partial positive

Table 3.4. Experimental interatomic distances [Å] and angles [°] of compounds **116a**,**b**,**d**,**e**

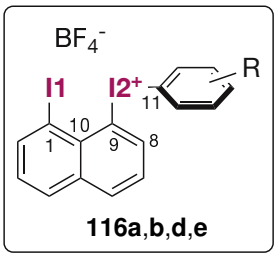

116a,**b**,**d**,**e**

	116a	**116b**	**116d**	**116e**
R =	4-Br	4-H	4-OMe	2,4,6–$(OMe)_3$
I1 ··· I2	3.251(1)	3.270(1)	3.272(1)	3.241(1)
I1 – C1	2.094(2)	2.094(4)	2.108(3)	2.095(3)
I2 – C9	2.169(2)	2.146(2)	2.150(3)	2.162(3)
I2 – C11	2.104(2)	2.116(3)	2.089(3)	2.068(3)
I1 ··· F[a]	3.092(3)	3.282(2)	3.542(2)	3.180(2)
I2 ··· F[a]	3.225(2)	2.906(2)	2.982(2)	2.937(2)
C9 – I2 – C11	95.29(8)	95.4(1)	98.4(1)	99.3(1)
I1 – I2 – C11	172.00(6)	168.01(9)	175.34(7)	175.14(7)
C8 – C9 – I2 – C11	-13.4(2)	23.6(2)	11.7(2)	-0.8(2)
Out-of-plane displacement				
I1	0.204	0.366	0.574	0.240
I2	0.290	0.461	0.521	0.158
peri region angles				
I1 – C1 – C10	123.3(1)	123.5(2)	122.9(2)	123.3(2)
C1 – C10 – C9	129.7(2)	129.2(3)	128.8(3)	130.1(2)
C10 – C9 – I2	123.9(1)	123.5(2)	122.2(2)	123.7(2)
Sum of bay angles	376.9(4)	376.2(7)	373.9(7)	377.1(6)
Splay angle[b]	16.9(4)	16.2(7)	13.9(7)	17.1(6)

a. Closest fluorine from the BF_4^- anion was chosen, *b*. Splay angle: sum of three bay region angles −360°.

charge on the I(I) atom. Additionally, in comparison to previous dicationic structures **114**, the monocationic structures **116** display a greater displacement of the iodine atoms out of the naphthalene plane.

Having these intermediary structures in hand, the next step was the oxidation of the second iodine and the subsequent coupling with an arene to form the desired unsymmetric bisiodonium salts **115**. Various conditions were tested. Different oxidants and activated arenes were screened (Scheme 3.17). Unfortunately, no condition produced any product in isolable quantities. Further, does the dicationic nature result in these compounds being comparably fragile for analysis via mass spectrometry, which made it additionally difficult to detect small quantities in product mixtures. As an example, inspired by the procedures from Shafir and Cuenca (Scheme 3.9),[150] when trying to oxidise the methoxy derivative **116d** in the presence of potassium trifluoro(phenyl)borate (**119**) almost no conversion was observed except for the sideproducts **120** and **121**, which could be detected by HPLC-MS. These can be explained by the formation of the desired salt **115** and subsequent substitution of an iodoarene by HFIP. The liberated iodoarene then gets oxidised again followed by coupling to **119** furnishing the diaryliodonium salts **121**. Due to the unselictivity of the process, different substitution patterns were detected.

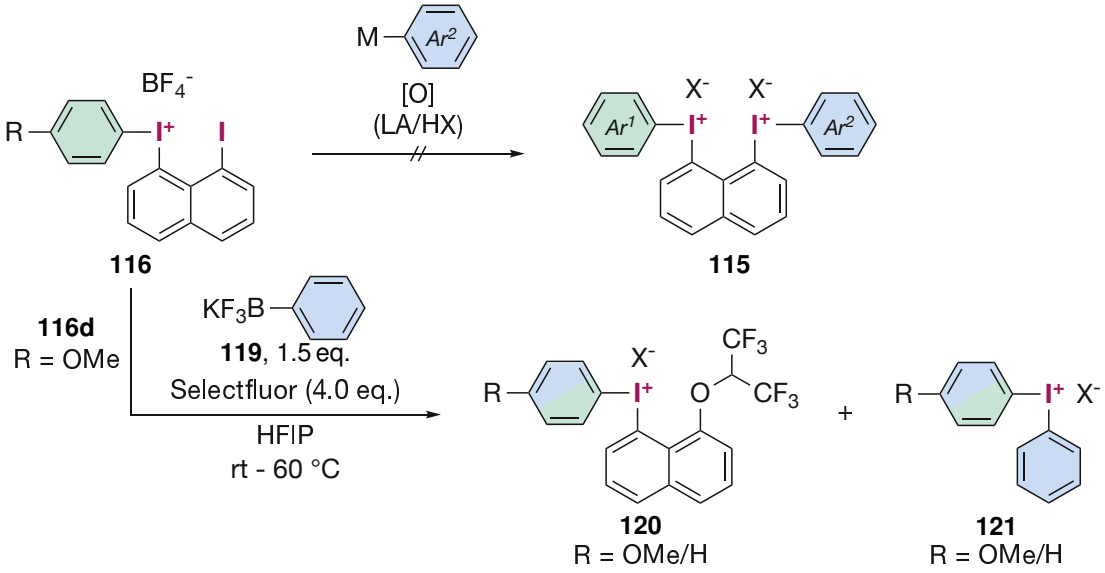

Scheme 3.17. Unsuccessful attempts in the synthesis of unsymmetric bisiodonium salts **115** and observation of exemplary side products **120** and **121**.

3.1.4.2 Electrophilic Substitution on the Naphthalene

A "reversed" approach was explored as an alternative route to unsymmetric bisiodonium salts. Instead of oxidising an I(I) next to an already oxidised I(III) installing a directing group could facilitate the coupling of the iodonium-substituted naphthalene with another I(III) species (Scheme 3.13).

Boronic acids are viable *ipso*-directing groups in the synthesis of diaryliodonium salts.[57] Additionally, mixed benzene-based iodonium-boronic acid species are known to be stable (Scheme 1.7),[100, 157] therefore boronic acids were chosen as a directing group. The iodonaphthylboronic acid **122** could be prepared from the diiodide **112** in 59% yield (Scheme 3.18). Analogously to the literature as well as using various other procedures the oxidation of **122** was investigated, for further transformation into a *peri*-boronic acid substituted iodane **123**. All attempts were unsuccessful. Oxidation of the boronic acid or decomposition of the substrate was observed. One-pot approaches did not yield any isolable product either.

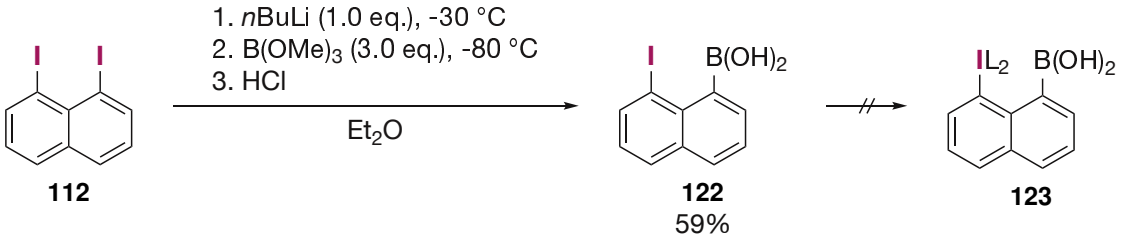

Scheme 3.18. Synthesis of boronic acid **122**.

Not let down, attention was directed at another directing group, namely the trimethylsilyl group (-TMS). The literature suggests also in this case that mixed iodonium-TMS species should be stable (Scheme 1.7).[98, 99] The TMS substituted iodoarene **124** was therefore prepared (Scheme 3.19). Since acid induces a shift of the TMS group,[158] TFE was selected as a solvent since it aids in the activation of hypervalent iodine species, especially when no further Lewis acid can be employed (Scheme 3.15).[117, 156] It was possible to oxidise the iodoarene **124** with Selectfluor in TFE and immediately couple it in a one-pot manner with a boronic acid to obtain the TMS-substituted iodonium salts **117**. The lack of activating additives is noticeable as the tolyl derivative **117a** yielded only 19% in comparison to the highly activated anisyl derivative **117b** which gave a yield of 58%.

The reaction of various iodanes ($ArIL_2$) with compounds **117a**,**b** was then investigated resulting in no observable product formation and little conversion of **117** in general (Scheme 3.19). This is not surprising since TMS is usually not the first choice due to its comparably low reactivity and electron-donating character which in the case of S_EAr-type reactions can lead to undesirable side reactions.

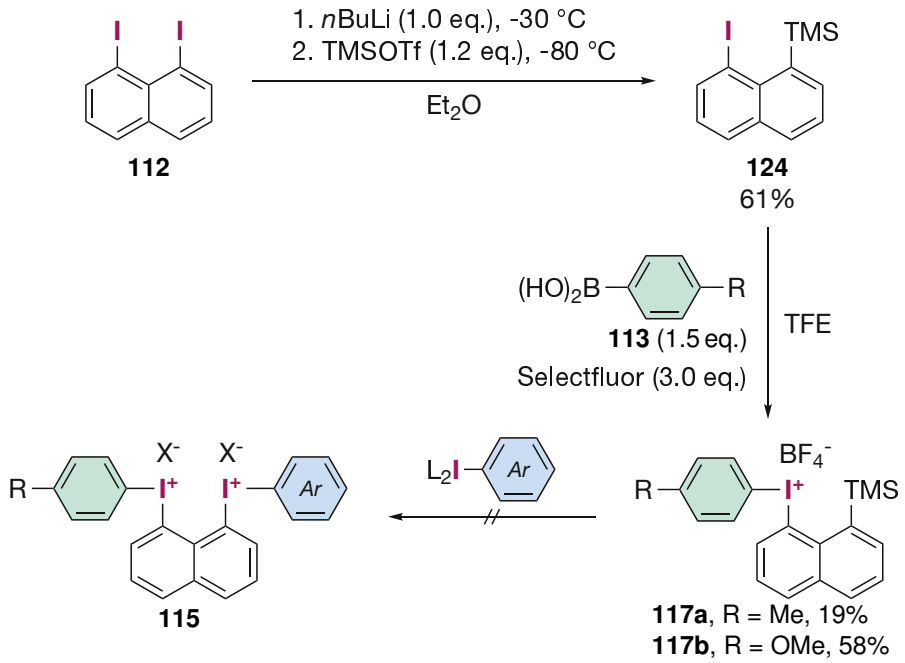

Scheme 3.19. Synthesis of *peri*-TMS-iodonium salts **117** by a one-port reaction of **124** with boronic acids **113**.

3.1.5 Application of Novel Iodonium Salts 116 as organocatalysts

Even though it was not possible to isolate products from the oxidation of novel iodonium salts **116** that were prepared in Section 3.1.4.1, these salts could function as an organocatalyst. Especially if oxidation is possible, but the resulting product is not stable, e.g. too reactive. This would make them perfect candidates for such an application. So far there is no description of a catalytically employed iodoarene bearing an additional iodonium substitution in the literature. To test this hypothesis the tosyloxylation of propiophenone (**125**) was investigated (Scheme 3.20).

*m*CPBA and *p*TsOH were chosen so that the conditions are comparable with literature, and the screening was done at catalyst loading of 10 mol%.[159] Diiodonaphthalene **112** and the iodonaphthalene **126** were chosen as a control and gave under these conditions 50% and 42% respectively. When using the previously prepared iodanes **116a**,**b**,**d** a trend was observable as the bromide substituted iodane **116a** yielded 37%, the unsubstituted **116b** yielded 31% and the methoxy substituted **116d** yielded 24%. All substrates performed worse than the iodoarenes **112** and **126**, which could be explained by some stabilising effect of the neighbouring iodonium centre, which would be unexpected as Lewis bases are usually used for this purpose.[159] More likely is a higher oxidation potential for the derivatives **116** as the neighbouring iodonium centre could lower the electron density by coordination as described in Section 3.1.4.1. Although decomposition was not observed, this reactivity could also be explained by the decomposition of the catalysts forming either **112** or **126**, which were both shown to be more active.

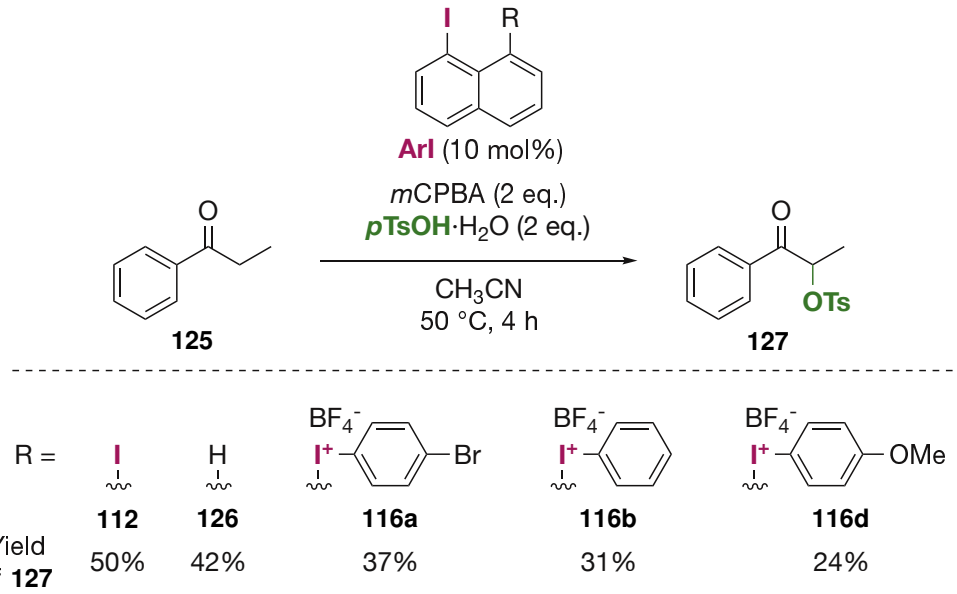

Scheme 3.20. Application of iodonium salts **116** in the tosyloxylation of propiophenone (**125**) and comparison to the iodoarenes **112** and **126**.

In summary, this section uncovered intriguing interactions between nearby iodine atoms that are in different oxidation states. Building on these insights, Section 3.2 is dedicated to developing more efficient methods for preparing diaryliodonium salts. Furthermore, Section 3.3 delves into the synthesis of structurally complex and naturally derived iodonium salts.

3.2 Two-Step Continuous-Flow Synthesis of Cyclic Iodonium Salts

Aim: Based on pre-existing batch results, a procedure for carbon-bridged cyclic diaryliodonium salts with improved scalability and efficiency was to be developed. Flow-chemistry and electrochemistry were chosen to address these goals, as these should allow for more mild and precise reaction conditions.

Title of the publication: Two-step continuous-flow synthesis of 6-membered cyclic iodonium salts via anodic oxidation

Julian Spils, Thomas Wirth, Boris J. Nachtsheim, *Beilstein J. Org. Chem.* **2023**, *19*, 27–32.
DOI: 10.3762/bjoc.19.2

The manuscript and the Supporting Information including detailed experimental procedures, characterisation data, copies of NMR spectra are available free of charge on the journal's website.

A non-peer-reviewed version of this article has been published as a preprint.

Julian Spils, Thomas Wirth, Boris J. Nachtsheim, *ChemRXiv* **2022**.
DOI: 10.26434/chemrxiv-2022-9q4px

Abstract: We describe a multi-step continuous-flow procedure for the generation of six-membered diaryliodonium salts. The accompanying scalability and atom economy are significant improvements to existing batch methods. Benzyl acetates are submitted to this two-step procedure as highly available and cheap starting materials. An acid-catalyzed Friedel–Crafts alkylation followed by an anodic oxidative cyclization yielded a defined set of cyclic iodonium salts in a highly substrate-dependent yield.

Author Contribution to this Publication: The idea for this project and the general setup were developed by me. Synthesis of all precursors was done by me. I conducted the optimisation of the anodic oxidation in batch and in flow as well as the optimisation for the combined two-step flow setup. The substrate scope was prepared by me. All characterisation and analysis was done by me. The manuscript and the Supporting Information were written by me. B. J. Nachtsheim and T. Wirth were the principal investigators and edited the article.

BEILSTEIN JOURNAL OF ORGANIC CHEMISTRY

Two-step continuous-flow synthesis of 6-membered cyclic iodonium salts via anodic oxidation

Julian Spils[1], Thomas Wirth[2] and Boris J. Nachtsheim[*1]

Letter

Open Access

Address:
[1]Institute for Organic and Analytical Chemistry, University of Bremen, Leobener Straße 7, 28359 Bremen, Germany and [2]School of Chemistry, Cardiff University, Park Place, Main Building, Cardiff CF10 3AT, UK

Email:
Boris J. Nachtsheim[*] - nachtsheim@uni-bremen.de

* Corresponding author

Keywords:
electrochemistry; flow chemistry; hypervalent compounds; iodine; oxidation

Beilstein J. Org. Chem. **2023,** *19,* 27–32.
https://doi.org/10.3762/bjoc.19.2

Received: 21 October 2022
Accepted: 07 December 2022
Published: 03 January 2023

Associate Editor: J. G. Hernández

Abstract

We describe a multi-step continuous-flow procedure for the generation of six-membered diaryliodonium salts. The accompanying scalability and atom economy are significant improvements to existing batch methods. Benzyl acetates are submitted to this two-step procedure as highly available and cheap starting materials. An acid-catalyzed Friedel–Crafts alkylation followed by an anodic oxidative cyclization yielded a defined set of cyclic iodonium salts in a highly substrate-dependent yield.

Introduction

Hypervalent iodine compounds (HVI) are well-established reagents for synthetic chemists. They are portrayed as an alternative to otherwise hazardous transition metals. This is due to their great reactivity in electrophilic group transfers [1-4], photo- or organocatalysis [5-15], and their utility as building blocks for the synthesis of natural products [16-21]. One subclass of HVIs is diaryliodonium salts (DIS), which have been used as versatile electrophilic arylation reagents in metal-catalyzed and metal-free reactions [22,23]. The corresponding cyclic diaryliodonium salts (CDIS) have also been investigated as useful building blocks for the synthesis of larger diaryl-based molecules, (hetero)aromatic tricyclic systems, or new aryl-moieties [24,25]. Most methods that generate DIS utilize iodoarenes as starting materials [26,27]. In these one-pot procedures, iodoarenes react with nucleophilic arenes under oxidative acidic conditions.The synthesis of CDIS is more challenging since the arene moiety must be covalently connected to the iodoarene prior to cyclization. Recently, we published two new methods that describe the generation of carbon- and heteroatom-bridged CDIS [28,29]. Herein, we improved the formation of iodoarenes through a Brønsted acid-mediated Friedel–Crafts reaction followed by an oxidative cyclization to form the desired CDIS **1** (Scheme 1A). This one-pot approach is based on *ortho*-iodinated benzyl alcohols as starting materials. It allows access to a variety of otherwise tedious to synthesize CDIS robustly in short reaction times. A significant draw-

Beilstein J. Org. Chem. **2023,** *19,* 27–32.

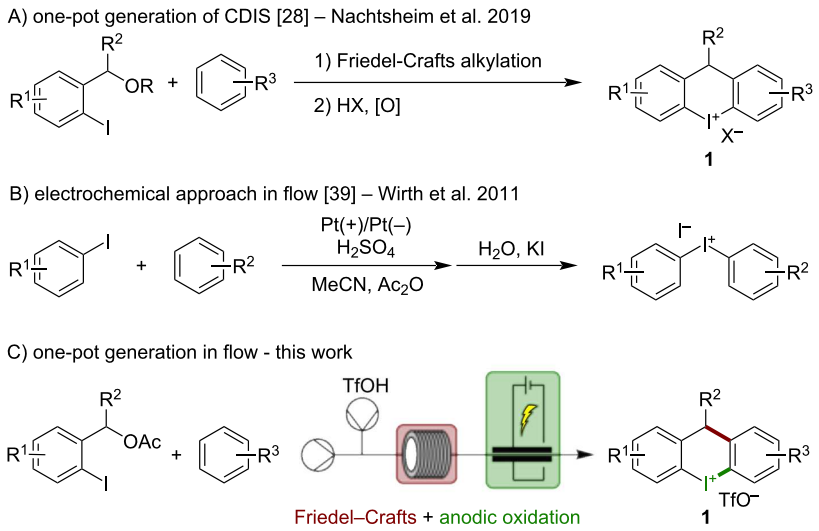

Scheme 1: Synthesis of acyclic (DIS) and cyclic (CDIS) diaryliodonium salts.

back still is the use of stoichiometric amounts of chemical oxidants, which decreases the atom economy and necessitates additional workup procedures. A possible solution is the anodic oxidation of iodoarenes as electrochemistry is a highly economical tool that avoids chemical oxidants for synthesizing hypervalent iodine reagents [30]. Iodoarenes are suitable and well-established mediators in either in- or ex-cell electrochemical processes [31-36].

Nonetheless, HVIs, DIS and CDIS have been generated by anodic oxidation [37-40]. Due to the apparent advantages of electrochemical processes, their implementation in flow is simple and straightforward since further dilution or additives are unnecessary [41,42]. One early example of this combination in the field of HVI chemistry is the anodic oxidation of iodoarenes to form DIS by Wirth et al. (Scheme 1B) [39]. Herein, established conditions for synthesizing DIS were transferred into flow chemistry utilizing a model flow reactor with two platinum electrodes. Other recent examples include the generation of five-membered CDIS utilizing fluorinated alcohols as a solvent [37,38]. Therefore, we attempt to transfer our already established one-pot procedure towards CDIS **1** into a multi-step electrochemical flow process, improving reaction times, atom economy, and scalability (Scheme 1C).

Results and Discussion

We initially investigated the second step of the proposed multi-step procedure since we assumed it to be the more challenging. We initially intended to oxidize and cyclize the intermediate iodoarene **2** electrochemically under batch conditions (Table 1). Through preliminary observations (see Supporting Information File 1, Table S1), triflic acid was established to be suitable for cyclization and as a counterion. 2,2,2-Trifluoroethanol (TFE) as a solvent already resulted in a yield of 45% of compound **1a** (Table 1, entry 1). It was possible to reduce its amount to 20 vol % by replacement with MeCN or CH_2Cl_2 without any significant drop in the yields (40–46%, Table 1, entries 2 and 3). By exchanging TFE for the more stabilizing 1,1,1,3,3,3-hexafluoropropan-2-ol (HFIP) it was possible to increase the yield even further to 78% (Table 1, entry 4) [43,44]. Finally, we decreased the amount of TfOH to 2 equiv still yielding product **1a** in 76% yield (Table 1, entry 5).

After establishing the optimized reaction conditions for batch, we wanted to find conditions for a flow procedure. It was observed that plastic parts made out of PEEK did not tolerate the acidic conditions in HFIP, and the solvent was changed back to TFE. This worked surprisingly well with only two equivalents of TfOH forming product **1a** in 74% yield (Table 2, entry 1). We found that these reaction conditions cannot be applied in the proposed multi-step procedure since the added benzene clogs the flow reactor through precipitation of a black solid.

We could overcome this issue by employing $MeNO_2$ as a solvent, which leads to a 48% yield of **1a** (Table 2, entry 2). This yield could be increased further by a combination with TFE to 63% (Table 2, entry 3). We could also omit the additional electrolyte $TBABF_4$ with no product loss (Table 2, entry 4), while the yield could not be improved further by increasing the charge (Table 2, entry 5).

Beilstein J. Org. Chem. **2023,** *19,* 27–32.

Table 1: Optimization of the oxidation and cyclization in batch.

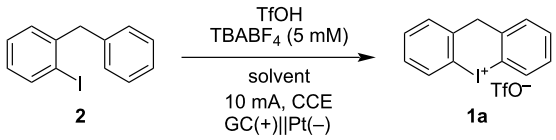

Entry[a]	TfOH [equiv]	Solvent	Charge [F]	**1a** Yield [%]
1	5	TFE	2.1	45
2	5	**MeCN**/TFE (4:1)	2.0	40
3	5	**CH_2Cl_2**/TFE (4:1)	2.2	46
4	**5**	**CH_2Cl_2/HFIP (4:1)**	**2.0**	**78**
5	**2**	CH_2Cl_2/HFIP (4:1)	2.0	76

[a]Electrolysis was carried out with an ElectraSyn 2.0 in an undivided cell. Vials were equipped with a glassy carbon (GC) anode and a Pt cathode. Immersed area: 2.4 cm^2. General reaction conditions: **2** (0.200 mmol), TfOH, $TBABF_4$ (0.005 M), solvent (40.0 mM, 5 mL), 10 mA, CCE.

Table 2: Optimization of the oxidation and cyclization in flow.

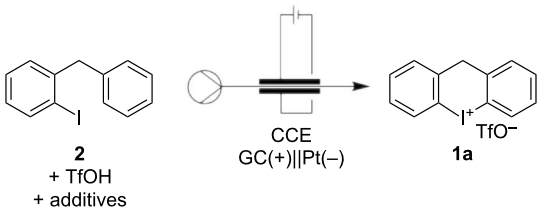

Entry[a]	TfOH [equiv]	Additives	Solvent	Current [mA]	**1a** Yield [%]
1	2	$TBABF_4$	CH_2Cl_2/TFE	32 (2.0 F)	74
2	2	$TBABF_4$ PhH (9 equiv)	**$MeNO_2$**	32 (2.0 F)	48
3	2	$TBABF_4$ PhH (9 equiv)	$MeNO_2$/**TFE**	32 (2.0 F)	63
4	**2**	**PhH (9 equiv)**	**$MeNO_2$/TFE**	**32 (2.0 F)**	**62**
5	2	PhH (9 equiv)	$MeNO_2$/TFE	**48 (3.0 F)**	62

[a]Reaction was performed in a Vapourtec Ion electrochemical flow reactor with a glassy carbon (GC) anode and a Pt cathode. General reaction conditions: **1** (0.1 M), $TBABF_4$ (0.005 M). Flowrate: 0.1 mL·min^{-1}. Yield is based on collecting for 20 min (0.200 mmol) after two reactor volumes had passed at the respective conditions.

For a final combination of the two reaction steps, benzyl acetate **3a** was chosen as a model substrate due to its high solubility and good reactivity as was previously demonstrated by us (Table 3) [28]. We determined an optimal reaction time of 20 min for the Friedel–Crafts reaction via GC analysis. Both steps in series resulted in successful product formation with an albeit slightly diminished yield of 49% (Table 3, entry 3).

We increased the yield to 54% by introducing an electrolyte (Table 3, entry 2). A further current increase had no beneficial effect (Table 3, entry 3). We then investigated longer reaction times (4 × 50 min, 4 × 0.500 mmol), but without additional electrolyte the overall yield of 38% was significantly lower. It was possible to compensate for this to some degree by using $TBABF_4$ as shown in Table 3, entry 2. This adjustment improved the overall yield to 43%.

Finally, we investigated a variety of substituted benzyl acetates **3** (Figure 1). Substitutions *para* to the iodine led with F- and Cl-derivatives **1b** and **1c** to strongly diminished yields of 15% and 26%, respectively, due to expected lower yields in the Friedel–Crafts step. It was impossible to improve this signifi-

Beilstein J. Org. Chem. **2023,** *19,* 27–32.

Table 3: Optimization of the two-step flow process in series.

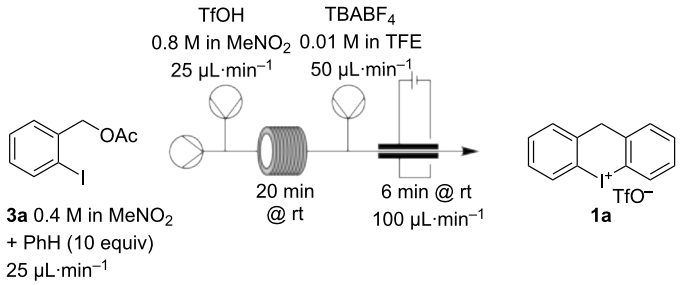

Entry[a]	Electrolyte	Current [mA]	**1a** Yield [%]
1	–	32 (2.0 F)	49
2	**$TBABF_4$**	**32 (2.0 F)**	**54**
3	$TBABF_4$	**48 (3.0 F)**	54

[a]Reaction was performed in a Vapourtec Ion electrochemical flow reactor with a glassy carbon (GC) anode and a Pt cathode. Yield is based on collecting for 20 min (0.200 mmol) after two reactor volumes had passed at the respective conditions.

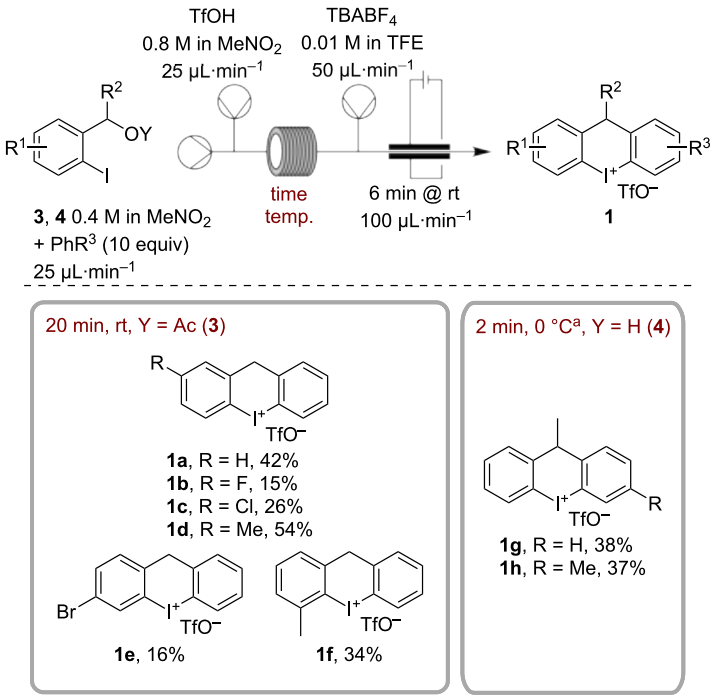

Figure 1: Substrate scope using the optimized conditions of Table 3. Yield is based on collecting for 3 h 20 min (2.00 mmol) after two reactor volumes had passed at the respective conditions. [a]Solutions of benzyl alocohol and TfOH were precooled in flow before mixing (see Supporting Information File 1).

cantly by increasing the time or temperature. In case of the more electron-rich derivative **1d**, we increased the yield to 54%. Other electron-withdrawing substituents show the same trend as in the Br-substituted **1e** yielding only 16%. Methylated substrate **1f** was isolated in 34% yield indicating that steric effects play a role during the oxidation step. We further wanted to in-

Beilstein J. Org. Chem. **2023,** *19,* 27–32.

vestigate different arenes, but due to the lack of selectivity of the primary benzyl acetates in the Friedel–Crafts step, we were limited to *para*-substituted arenes, which unfortunately all resulted in the formation of insoluble intermediary iodoarenes. Derivatizing the benzylic position was done by employing secondary benzyl alcohols. These are well soluble and lead to an about 10-times shortened Friedel–Crafts step at 0 °C for the conversion of **3g**. Longer times only resulted in the decomposition of the intermediary iodoarene. Here it was possible to perform the procedure with either benzene or toluene, leading to a moderate yield of 38% and 37%. We could not use derivatives with any other substituents with secondary benzyl acetates since those led only to inseparable product mixtures.

Conclusion

In summary, we have developed the first multi-step continuous-flow procedure for the generation of cyclic six-membered diaryliodonium salts. Starting from easily accessible benzyl acetates we were able to combine a Friedel–Crafts alkylation with a subsequent anodic oxidative cyclization in flow. The method is currently limited by the narrow starting materials being used due to the rather harsh conditions of those reactions. By addressing this issue, other substrates and higher yields could be realized in future.

Supporting Information

Supporting Information File 1

Experimental, analytical data and copies of NMR spectra.
[https://www.beilstein-journals.org/bjoc/content/supplementary/1860-5397-19-2-S1.pdf]

Acknowledgements

We thank the School of Chemistry, Cardiff University, for support.

Funding

We thank the Bremen Cardiff Alliance Collaborative Fund for financial support.

ORCID® iDs

Julian Spils - https://orcid.org/0000-0003-2895-5610
Thomas Wirth - https://orcid.org/0000-0002-8990-0667
Boris J. Nachtsheim - https://orcid.org/0000-0002-3759-2770

Preprint

A non-peer-reviewed version of this article has been previously published as a preprint: https://doi.org/10.26434/chemrxiv-2022-9q4px

References

1. Charpentier, J.; Früh, N.; Togni, A. *Chem. Rev.* **2015,** *115,* 650–682. doi:10.1021/cr500223h
2. Li, Y.; Hari, D. P.; Vita, M. V.; Waser, J. *Angew. Chem., Int. Ed.* **2016,** *55,* 4436–4454. doi:10.1002/anie.201509073
3. Yoshimura, A.; Zhdankin, V. V. *Chem. Rev.* **2016,** *116,* 3328–3435. doi:10.1021/acs.chemrev.5b00547
4. Caspers, L. D.; Nachtsheim, B. J. *Chem. – Asian J.* **2018,** *13,* 1231–1247. doi:10.1002/asia.201800102
5. Baralle, A.; Fensterbank, L.; Goddard, J.-P.; Ollivier, C. *Chem. – Eur. J.* **2013,** *19,* 10809–10813. doi:10.1002/chem.201301449
6. Flores, A.; Cots, E.; Bergès, J.; Muñiz, K. *Adv. Synth. Catal.* **2019,** *361,* 2–25. doi:10.1002/adsc.201800521
7. Le Vaillant, F.; Garreau, M.; Nicolai, S.; Gryn'ova, G.; Corminboeuf, C.; Waser, J. *Chem. Sci.* **2018,** *9,* 5883–5889. doi:10.1039/c8sc01818a
8. Wang, D.; Mao, J.; Zhu, C. *Chem. Sci.* **2018,** *9,* 5805–5809. doi:10.1039/c8sc01763h
9. Boelke, A.; Nachtsheim, B. J. *Adv. Synth. Catal.* **2019,** *362,* 184–191. doi:10.1002/adsc.201901356
10. Cots, E.; Flores, A.; Romero, R. M.; Muñiz, K. *ChemSusChem* **2019,** *12,* 3028–3031. doi:10.1002/cssc.201900360
11. Declas, N.; Le Vaillant, F.; Waser, J. *Org. Lett.* **2019,** *21,* 524–528. doi:10.1021/acs.orglett.8b03843
12. Li, L.; Guo, S.; Wang, Q.; Zhu, J. *Org. Lett.* **2019,** *21,* 5462–5466. doi:10.1021/acs.orglett.9b01717
13. Abazid, A. H.; Clamor, N.; Nachtsheim, B. J. *ACS Catal.* **2020,** *10,* 8042–8048. doi:10.1021/acscatal.0c02321
14. Abazid, A. H.; Nachtsheim, B. J. *Angew. Chem., Int. Ed.* **2020,** *59,* 1479–1484. doi:10.1002/anie.201912023
15. Massignan, L.; Tan, X.; Meyer, T. H.; Kuniyil, R.; Messinis, A. M.; Ackermann, L. *Angew. Chem., Int. Ed.* **2020,** *59,* 3184–3189. doi:10.1002/anie.201914226
16. Ghosh, S.; Pradhan, S.; Chatterjee, I. *Beilstein J. Org. Chem.* **2018,** *14,* 1244–1262. doi:10.3762/bjoc.14.107
17. Jacquemot, G.; Maertens, G.; Canesi, S. *Chem. – Eur. J.* **2015,** *21,* 7713–7715. doi:10.1002/chem.201500185
18. Maertens, G.; L'Homme, C.; Canesi, S. *Front. Chem. (Lausanne, Switz.)* **2015,** *2*. doi:10.3389/fchem.2014.00115
19. Silva, L. F., Jr.; Olofsson, B. *Nat. Prod. Rep.* **2011,** *28,* 1722–1754. doi:10.1039/c1np00028d
20. Ciufolini, M.; Braun, N.; Canesi, S.; Ousmer, M.; Chang, J.; Chai, D. *Synthesis* **2007,** 3759–3772. doi:10.1055/s-2007-990906
21. Hamamoto, H.; Shiozaki, Y.; Nambu, H.; Hata, K.; Tohma, H.; Kita, Y. *Chem. – Eur. J.* **2004,** *10,* 4977–4982. doi:10.1002/chem.200400358
22. Novák, Z.; Aradi, K.; Tóth, B.; Tolnai, G. *Synlett* **2016,** *27,* 1456–1485. doi:10.1055/s-0035-1561369
23. Merritt, E. A.; Olofsson, B. *Angew. Chem., Int. Ed.* **2009,** *48,* 9052–9070. doi:10.1002/anie.200904689
24. Chatterjee, N.; Goswami, A. *Eur. J. Org. Chem.* **2017,** 3023–3032. doi:10.1002/ejoc.201601651
25. Grushin, V. V. *Chem. Soc. Rev.* **2000,** *29,* 315–324. doi:10.1039/a909041j
26. Bielawski, M.; Zhu, M.; Olofsson, B. *Adv. Synth. Catal.* **2007,** *349,* 2610–2618. doi:10.1002/adsc.200700373
27. Bielawski, M.; Aili, D.; Olofsson, B. *J. Org. Chem.* **2008,** *73,* 4602–4607. doi:10.1021/jo8004974
28. Caspers, L. D.; Spils, J.; Damrath, M.; Lork, E.; Nachtsheim, B. J. *J. Org. Chem.* **2020,** *85,* 9161–9178. doi:10.1021/acs.joc.0c01125

29. Damrath, M.; Caspers, L. D.; Duvinage, D.; Nachtsheim, B. J. *Org. Lett.* **2022,** *24,* 2562–2566. doi:10.1021/acs.orglett.2c00691
30. Elsherbini, M.; Wirth, T. *Chem. – Eur. J.* **2018,** *24,* 13399–13407. doi:10.1002/chem.201801232
31. Francke, R. *Curr. Opin. Electrochem.* **2019,** *15,* 83–88. doi:10.1016/j.coelec.2019.03.012
32. Doobary, S.; Sedikides, A. T.; Caldora, H. P.; Poole, D. L.; Lennox, A. J. J. *Angew. Chem., Int. Ed.* **2020,** *59,* 1155–1160. doi:10.1002/anie.201912119
33. Elsherbini, M.; Winterson, B.; Alharbi, H.; Folgueiras-Amador, A. A.; Génot, C.; Wirth, T. *Angew. Chem., Int. Ed.* **2019,** *58,* 9811–9815. doi:10.1002/anie.201904379
34. Maity, A.; Frey, B. L.; Hoskinson, N. D.; Powers, D. C. *J. Am. Chem. Soc.* **2020,** *142,* 4990–4995. doi:10.1021/jacs.9b13918
35. Wirth, T. *Curr. Opin. Electrochem.* **2021,** *28,* 100701. doi:10.1016/j.coelec.2021.100701
36. Winterson, B.; Rennigholtz, T.; Wirth, T. *Chem. Sci.* **2021,** *12,* 9053–9059. doi:10.1039/d1sc02123k
37. Zu, B.; Ke, J.; Guo, Y.; He, C. *Chin. J. Chem.* **2021,** *39,* 627–632. doi:10.1002/cjoc.202000501
38. Elsherbini, M.; Moran, W. J. *Org. Biomol. Chem.* **2021,** *19,* 4706–4711. doi:10.1039/d1ob00457c
39. Watts, K.; Gattrell, W.; Wirth, T. *Beilstein J. Org. Chem.* **2011,** *7,* 1108–1114. doi:10.3762/bjoc.7.127
40. Peacock, M. J.; Pletcher, D. *J. Electrochem. Soc.* **2001,** *148,* D37. doi:10.1149/1.1353574
41. Elsherbini, M.; Wirth, T. *Acc. Chem. Res.* **2019,** *52,* 3287–3296. doi:10.1021/acs.accounts.9b00497
42. Pletcher, D.; Green, R. A.; Brown, R. C. D. *Chem. Rev.* **2018,** *118,* 4573–4591. doi:10.1021/acs.chemrev.7b00360
43. Dohi, T.; Yamaoka, N.; Kita, Y. *Tetrahedron* **2010,** *66,* 5775–5785. doi:10.1016/j.tet.2010.04.116
44. Eberson, L.; Hartshorn, M. P.; Persson, O.; Radner, F. *Chem. Commun.* **1996,** 2105–2112. doi:10.1039/cc9960002105

3.3 Oxidative Cyclization and Enzyme-free Deiodination of Thyroid Hormones

Aim: Thyroid hormones are highly interesting as there are not many naturally occurring organoiodides, especially with this degree of complexity and amount of molecular bound iodine. The question is whether literature described reactivities of iodoarenes with oxidants yielding hypervalent organoiodides have any relevance in the biosynthesis or mode of action of these hormones. To answer this question such hypervalent derivatives of thyroid hormones have to be prepared and further investigated in regards to their reactivity and general properties.

Title of the publication: Oxidative Cyclization and Enzyme-free Deiodination of Thyroid Hormones

Julian Spils, Lucien D. Caspers, Pim Puylaert, Boris J. Nachtsheim, *Org. Chem. Front.* **2024**, Advance Article
DOI: 10.1039/D4QO00220B

A non-peer-reviewed version of this article has been published as a preprint.

Julian Spils, Lucien D. Caspers, Pim Puylaert, Boris J. Nachtsheim, *ChemRXiv* **2024**.
DOI: 10.26434/chemrxiv-2024-lqg5k

Abstract: We introduce the first non-enzymatic deiodination of thyroid hormones from a so far unknown hypervalent iodaoxinium state. After developing oxidative processes for thyroxine(T4)-derived model cyclic diaryliodonium salts, we successfully produced an iodaoxinium salt through the direct oxidation of *O*- and *N*-protected T4. DFT calculations revealed a novel halogen bonding-based deiodination mechanism, circumventing the traditional selenium-dependent pathways. Our findings open new avenues in thyroid hormone chemistry, suggesting alternative mechanisms for their involvement in metabolic processes, regulation of oxidative stress, and gene expression.

Author Contribution to this Publication: The initial idea for this project was conceived by B. J. Nachtsheim. The synthesis and optimisation for the preparation of the iodonium salts and the protected thyroxine as well as their characterisation was conducted by me. Lucien D. Caspers developed the synthesis of the model iodoarenes and characterised these. I grew the crystals suitable for X-ray crystallography. The measurement as well as the refinement was done by Pim Puylaert. The manuscript was written by me and B. J. Nachtsheim who was the principal investigator. All schemes and figures were created by me. The Supporting information was written by me.

ORGANIC CHEMISTRY FRONTIERS

RESEARCH ARTICLE

View Article Online
View Journal

Cite this: DOI: 10.1039/d4qo00220b

Oxidative cyclization and enzyme-free deiodination of thyroid hormones†

Julian Spils, [a] Lucien D. Caspers,[a] Pim Puylaert [b] and Boris J. Nachtsheim *[a]

We introduce the first non-enzymatic deiodination of thyroid hormones from a so far unknown hypervalent iodoaxinium state. After developing oxidative processes for thyroxine (**T4**)-derived model cyclic diaryliodonium salts, we successfully produced an iodoaxinium salt through the direct oxidation of *O*- and *N*-protected **T4**. DFT calculations revealed a novel halogen bonding-based deiodination mechanism, circumventing the traditional selenium-dependent pathways. Our findings open new avenues in thyroid hormone chemistry, suggesting alternative mechanisms for their involvement in metabolic processes, regulation of oxidative stress, and gene expression.

Received 1st February 2024,
Accepted 14th March 2024

DOI: 10.1039/d4qo00220b

rsc.li/frontiers-organic

Introduction

Thyroid hormones (TH) play a vital role in regulating metabolic processes and are crucial for the development and metabolic homeostasis of higher organisms.[1] They are in particular capable of modulating gene expression through binding to TH-specific transcription factors, which are present in almost all vertebrate tissues.[1–3] From thyroxine (**T4**) as the main TH initially secreted by the mammalian thyroid gland, other THs such as 3,5,3′-triiodothyronine (**T3**) or 3,3′,5′-triiodothyronine (**rT3**) are formed *via* selective deiodination by one of three selenoenzymes DIO1, DIO2 and DIO3 (Scheme 1).[4–6] Of all THs, **T3** is the most active derivative with up to 40 times higher affinity to thyroid receptors than its parent compound **T4**.[7,8]

The exact mechanism of the reductive deiodination is still under investigation, but it is evident that selenocysteines are present in all related enzymes and recent literature has shown that halogen bond activation plays an important role in this process.[9–12] Nobody described a selenium-independent deiodination mechanism so far in biological systems that results in a regioselective deiodination.

We found such a potential pathway by serendipity as part of an ongoing research program that is intended to elaborate and understand a potential biologically relevant non-enzymatic oxidation of thyroxines to hypervalent iodine reagents **ox-T3/T4** or cyclic iodoaxinium salts **1** (**cyclo-ox-T3/T4**) derived from them (Scheme 2).[13–18] In the future these substrates could also enable diverse further derivations based on previous work by Chen and co-workers.[19,20]

Results and discussion

In our initial experiments, we oxidized commercially available thyroxine (**T4**) using common oxidants such as peracids, hypochlorite solutions, SelectFluor®, and Oxone®. However, these attempts only led to the decomposition of the starting material.

Notably, the solubility issues and cleavage of the central diaryl ether, due to quinone formation, posed significant challenges.

Consequently, we shifted our focus from THs to simplified structures, where the α-amino acid is replaced with a simple methyl group and the free phenol group is protected as a

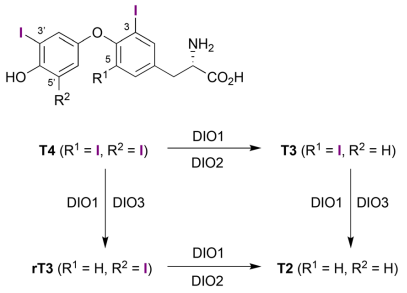

Scheme 1 Formation of different THs *via* deiodination of thyroxine (**T4**).

[a]*Institute for Organic and Analytical Chemistry, University of Bremen, Leobener Straße 7, 28359 Bremen, Germany. E-mail: nachtsheim@uni-bremen.de*
[b]*Institute for Inorganic Chemistry and Crystallography, University of Bremen, Leobener Straße 7, 28359 Bremen, Germany*

† Electronic supplementary information (ESI) available. CCDC 2291802. For ESI and crystallographic data in CIF or other electronic format see DOI: https://doi.org/10.1039/d4qo00220b

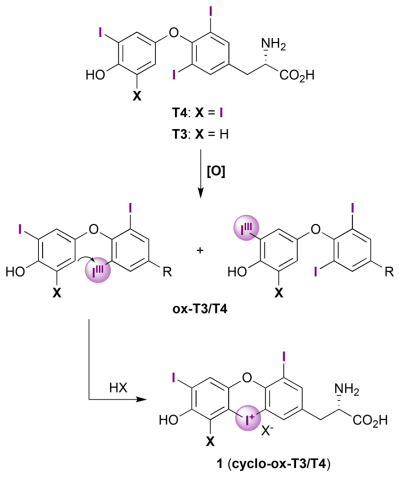

Scheme 2 Proposed oxidation of THs to hypervalent iodine reagents and their cyclization to iodaoxinium salts **1**.

methyl ether. We employed a straightforward reaction sequence, beginning with a nucleophilic aromatic substitution followed by a Sandmeyer iodination. This approach enabled us to isolate the desired simplified TH analogues **2a–c** in yields of 50–61%, starting from 4-methoxyphenol and the corresponding nitroarenes, as shown in Scheme 3. We then investigated their oxidation using literature-known conditions.[18,21,22]

In our initial oxidation experiments, as outlined in Scheme 2, we aimed to isolate an acyclic aryl-λ^3-iodane derivative from either **ox-T3** or **ox-T4**. However, these attempts were unsuccessful. Instead, when using SelectFluor® as the oxidant and subsequently treating the reaction with TfOH, we successfully isolated the desired cyclic diaryliodonium salts, **3a** and **3c**. These compounds were obtained in yields of 73% and 23%, respectively.

Treating compound **2b** under similar oxidative conditions proved more challenging, as we only detected trace amounts of product **3b** and its isomers *via* HPLC-MS. Attempts with other polyiodinated diaryl ethers did not yield any products, as detailed in the ESI, Table 1.† Our subsequent objective was to synthesize the free phenol of type **4**, as depicted in Scheme 4. A recently published one-step method has demonstrated the stability of similar acyclic iodonium salts,[23] yet only one *meta*-hydroxy-substituted derivative closely related to our target structure has been described.[24]

For the deprotection of the methyl ether, we found that typical conditions using BBr_3 were effective. However, due to the low solubility of **3a** and its bromide salt, we had to employ elevated temperatures. Ultimately, we successfully obtained the unprotected bromide salt **4a** in 82% yield. We then

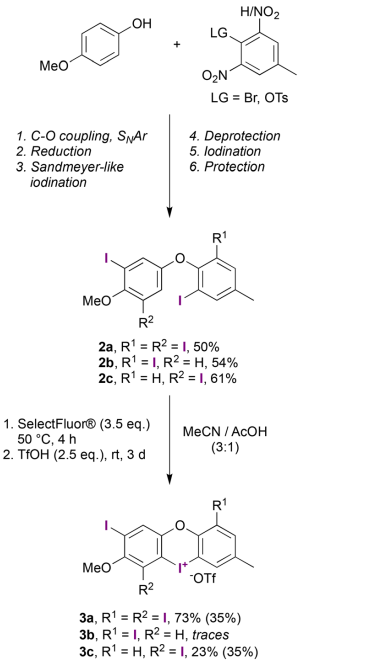

Scheme 3 Synthesis of iodoarenes **2** and their oxidative cyclization to iodaoxinium salts **3** (50 μmol scale). Yields in brackets are upscaled (500 μmol). A detailed synthetic procedure is shown in the ESI.†

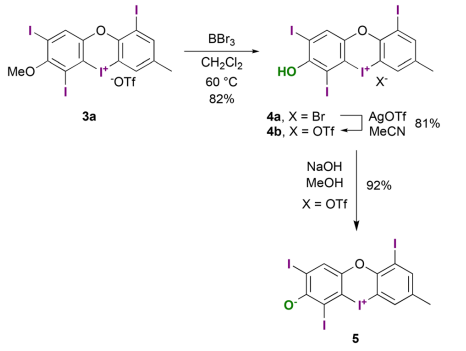

Scheme 4 Deprotection of **3a** towards **4a** and subsequent anion exchange to the triflate salt **4b**, followed by deprotonation to the zwitterion **5**.

achieved anion exchange to the triflate salt **4b** using AgOTf with an 81% yield. Further deprotonation with NaOH gave the orange-coloured zwitterion **5** with a 92% yield.

After confirming the stability of cyclic iodaoxinium salts **4**, we confidently proceeded to work with thyroid hormones (THs) directly. We began with thyroxine, converting its carboxylic acid into a methyl ester and acylating both the amino and phenol groups. However, using our previously developed method, we only observed trace amounts of the desired product. Switching to well-established oxidative conditions with *m*CPBA and TfOH proved successful. This approach enabled the direct synthesis of the iodaoxinium salt **6a** through *in situ* deprotection of the phenol group, yielding a moderate efficiency with an isolated yield of 53% (as shown in Scheme 5). We also noted that phenol **6** could be deprotonated to produce the zwitterion **7**, which was stable at room temperature in its solid form achieving a yield of 72%, although decomposition was observed in highly polar solvents such as DMSO, DMF, and NMP.

The solid state structure of the iodaoxinium salt **6a** was determined by X-ray diffraction analysis, revealing it had crystallised as a hydrogen-bridged dimer (Fig. 1). The geometry around the iodonium centre is as expected in a T-shape with C–I–C angles of 90.0° and 89.7° and triflates coordinating at angles of 175.2° and 172.69°. The I–O bond between triflate and iodine is at 2.757 Å and 2.752 Å, comparable to known iodaoxinium salts.[22] Interestingly the dimer shows hydrogen bonding between the phenol and the amide carbonyl indicated by O–O distances of 2.563 Å and 2.606 Å. We also observed significant π–π-interactions between the two phenol-bearing aromatic rings with a centroid-to-centroid distance of 3.650 Å.

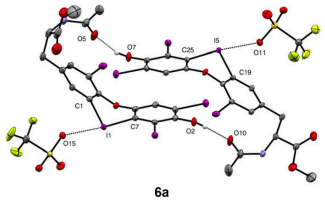

6a

Fig. 1 Single crystal structure (ORTEP drawing; hydrogen atoms, except those participating in hydrogen bonding, were omitted) of **6a** as a dimer (CCDC 2291802†) with aromatic ring interaction and hydrogen bonding visible inside the dimer. Thermal ellipsoids displayed with 50% probability. Selected parameters [Å, °]: I1–O15: 2.757(2); I5–O11: 2.752 (2); O5–O7: 2.563(4); O2–O10: 2.606(4); C1–I1–C7: 90.0(1); C19–I5–C25: 89.7(1); C7–I1–O15: 175.2(1); C25–I5–O11: 172.69(9).

Our objective was to create a thyroid hormone (TH)-derived substrate, with the sole modification being a cyclized iodonium centre. To achieve this, we needed to deprotect the amino acid. Treating **6a** with aqueous HCl at 120 °C led to the formation of the desired **T4**-derived iodaoxinium salt **1a**, with a yield of 57% (Scheme 6). However, during a side-product analysis of this reaction using HPLC-MS, we unexpectedly discovered a deiodination product. On lowering the reaction temperature and increasing the reaction time, this side product was formed exclusively. We identified this compound as the **T3**-derived iodaoxinium salt **1b**, which was isolated in 65% yield.

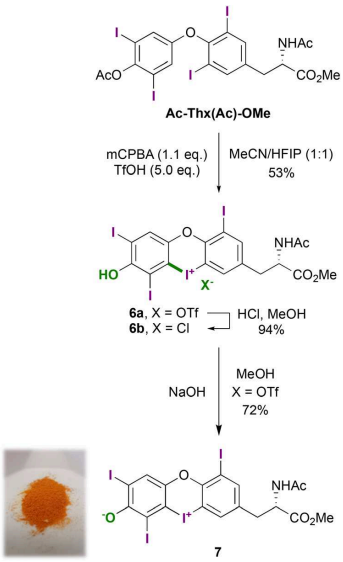

Scheme 5 Synthesis of TH-derived iodaoxinium salts **6** and **7** from protected thyroxine **T4**.

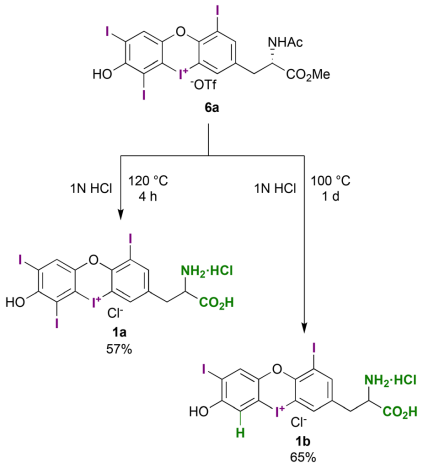

Scheme 6 Deprotection of the amino acid functionality of salt **7a** to generate the salt **1a** and *via* selective protic deiodination **1b**.

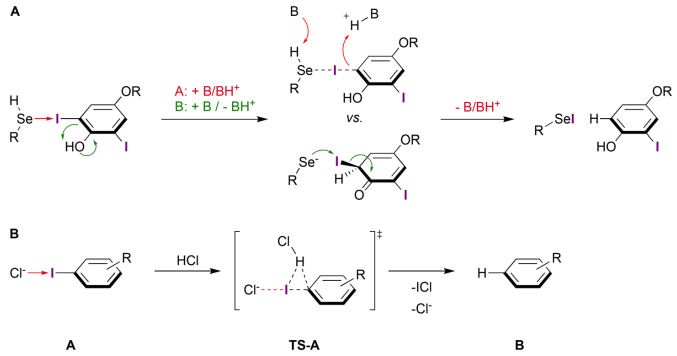

Scheme 7 A: Selenocysteine-mediated deiodination mechanism as proposed by Rafferty (red) *vs.* the mechanism *via* enolization (green). B: Corresponding chloride/HCl-mediated deiodination mechanism.

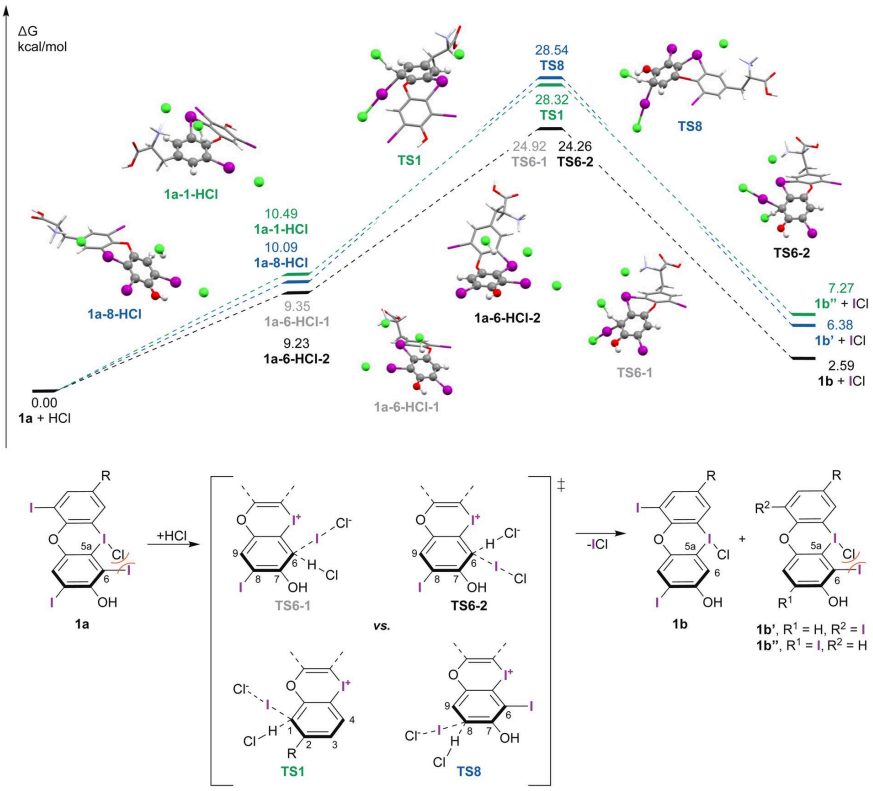

Scheme 8 Energy profile for the deiodination of **1a** *via* the addition of HCl to generate **1b**, **1b'** and **1b''**. And a simplified schematic representation of the mechanism.

View Article Online
Organic Chemistry Frontiers Research Article

To gain a deeper understanding of the unexpected deiodination, especially its high selectivity for the C6 position *ortho* to the iodonium centre, we conducted Density Functional Theory (DFT) calculations. These were performed at the PBE0-D3(BJ)/def2-TZVP+CPCM level of theory, using geometries optimized at the PBE0-D3(BJ)/def2-SVP+CPCM level. For guidance in elucidating the correct reaction pathway, we referred to a study by Rafferty and co-workers. This research explored the deiodination of thyroid hormones by selenols, employing a simplified catalytic triad.[9] Following this path, in the presence of HCl as a Brønsted-acid, a trimolecular reaction through **TS-A** should be induced to generate ICl and the deiodinated arene **B** (Scheme 7).

Building on this mechanism, we explored three separate pathways, each beginning with an XB interaction between a chloride ion and one of the three monovalent iodine atoms located at positions C1, C6, and C8. These calculated reaction pathways are depicted in Scheme 8. Initially, the addition of HCl led to the formation of XB adducts **1a-6-HCl** (with an energy of +9.23 kcal mol^{-1}), **1a-8-HCl** (+10.09 kcal mol^{-1}), and **1a-1-HCl** (+10.49 kcal mol^{-1}). In our notation, the middle index (1a-X-HCl) specifies the position of the coordinated iodine. These XB complexes then transitioned into the states **TS6-1**, **TS6-2**, **TS8**, and **TS1**. The difference between **TS6-1** and **TS6-2** lies in the varying attack sites of the chloride anion. A comparison of the relative energies of these transition states revealed that **TS6-1** and **TS6-2**, leading to the formation of the **T3**-derived iodaoxinium salt, possessed the lowest activation barriers at 24.92 kcal mol^{-1} and 24.26 kcal mol^{-1}, respectively. In contrast, **TS8** and **TS1** exhibited significantly higher barriers, at 28.32 kcal mol^{-1} and 28.54 kcal mol^{-1}, respectively. Moreover, deiodination at C6 uniquely resulted in the transformation of the bent iodaoxinium **1a** into a less bent geometry **1b**, accompanied by a notable twist angle change of +6.7° between the two phenyl rings. Additionally, the dihedral angle between C6–C5a–I–Cl relaxed by −23.8° during the transition from **1a** to **1b**. Transitions to other deiodinated iodaoxinium salts **1b′** and **1b″**, did not exhibit such significant changes in ground state geometry.

To gain further insight into this reaction and to verify the proposed halogen bond interaction, we looked at the binding of compound **6a** with tetra-*n*-butylammonium chloride (TBACl). The initial addition of one equivalent of TBACl resulted in a general downfield shift, caused by anion exchange from triflate to chloride, matching spectral data for **6b**. Upon further addition of TBACl (5 eq.) only for one carbon a shift (downfield) is observed (Fig. 2). This signal likely corresponds to position C6 as there is no correpsonding ^{13}C-signal in the NMR of C6-deiodinated **1b**. When we added a huge excess of TBACl (50 eq.), further downfield shifts are observed for C6 as well as for the other two iodinated carbons (C1 and C8).

As previously mentioned, the iodaoxinium salt **1a** possesses an asymmetric bent geometry, allowing it to be protonated by HCl from either a convex or a concave face. In Scheme 9, we present a direct comparison of both pathways. Protonation through the convex face, *via* **TS6-1**, reveals a weak XB-interaction between the chlorine atom of the HCl molecule and the iodonium ion, measured at a distance of 3.22 Å and an angle of 158.49°. On the other hand, protonation from the concave face leads to a slightly more favourable transition state, **TS6-2**, with an energy difference of −0.66 kcal mol^{-1}. In this state, a shorter than van der Waals distance between the iodine atom at C6 and the iodonium ion still suggests a weak XB-bond, however with an even more distorted angle of 146.83°. This interaction appears to be energetically slightly more favourable compared to the Cl–I interaction observed in **TS6-1**. Given the minimal energy difference between the two transition states, it's likely that both pathways will occur under the applied elevated reaction temperature of 100 °C.

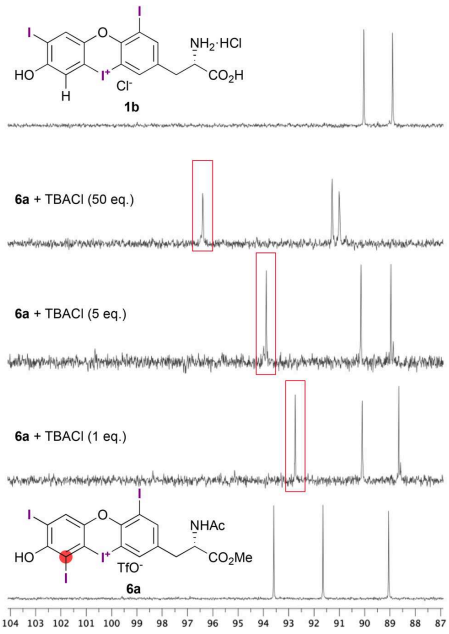

Fig. 2 NMR observations upon addition of different amounts of tetra-*n*-butylammonium chloride (TBACl) to iodaoxinium salt **6a** and comparison to **1b**.

However, both transition states represent a unique selenoenzyme-free deiodination mechanism of thyroxines based on intrinsic XB interactions. This discovery not only broadens the understanding of thyroid hormone chemistry but also challenges the conventional belief that enzymatic pathways are the sole mediators for the selective deiodination of THs. These XB interactions, driving the deiodination process, highlight a novel aspect of thyroxine's molecular behaviour, potentially reshaping our approach to thyroid hormone-related (bio) chemistry.

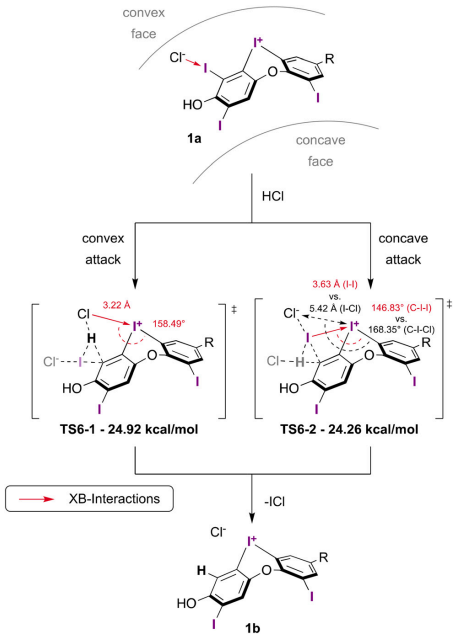

Scheme 9 Distinct transition states from a convex and concave protonation of **1a**, both leading to **1b**.

Conclusions

In summary, our research demonstrates that oxidized thyroxine (**T4**), in the form of a hypervalent iodoaxinium salt (**1a**), is a stable entity that can be directly synthesized from *O*-acylated thyroxine under oxidative and acidic conditions. Interestingly, we discovered that **1a** can undergo selective deiodination at the C6 position, resulting in an oxidized **T3**-derivative. This deiodination process, which occurs without the involvement of selenoenzymes, is not only unprecedented but also features a unique activation mechanism driven by XB interactions with the central iodonium ion. To further explore the possibility of these thyroxine-derived iodoaxinium salts acting as reactive intermediates under oxidative stress in biological systems, it is essential to confirm their presence *in vivo*. Additionally, we aim to investigate their potential reduction to T3 or reverse T3 (rT3) by natural reducing agents, such as flavins or dihydropyridines.

Conflicts of interest

There are no conflicts to declare.

Acknowledgements

P. P. acknowledges the Central Research Development Fund of the University of Bremen for the postdoctoral fellowship.

References

1 R. Mullur, Y. Y. Liu and G. A. Brent, Thyroid hormone regulation of metabolism, *Physiol. Rev.*, 2014, **94**, 355–382.
2 A. C. Bianco and B. W. Kim, Deiodinases: implications of the local control of thyroid hormone action, *J. Clin. Invest.*, 2006, **116**, 2571–2579.
3 G. A. Brent, Mechanisms of thyroid hormone action, *J. Clin. Invest.*, 2012, **122**, 3035–3043.
4 J. Köhrle, Iodothyronine deiodinases, *Methods Enzymol.*, 2002, **347**, 125–167.
5 A. C. Bianco, D. Salvatore, B. Gereben, M. J. Berry and P. R. Larsen, Biochemistry, cellular and molecular biology, and physiological roles of the iodothyronine selenodeiodinases, *Endocr. Rev.*, 2002, **23**, 38–89.
6 G. G. Kuiper, M. H. Kester, R. P. Peeters and T. J. Visser, Biochemical mechanisms of thyroid hormone deiodination, *Thyroid*, 2005, **15**, 787–798.
7 H. H. Samuels, J. S. Tsai, J. Casanova and F. Stanley, Thyroid hormone action: in vitro characterization of solubilized nuclear receptors from rat liver and cultured GH1 cells, *J. Clin. Invest.*, 1974, **54**, 853–865.
8 J. W. Apriletti, N. L. Eberhardt, K. R. Latham and J. D. Baxter, Affinity chromatography of thyroid hormone receptors. Biospecific elution from support matrices, characterization of the partially purified receptor, *J. Biol. Chem.*, 1981, **256**, 12094–12101.
9 C. A. Bayse and E. R. Rafferty, Is halogen bonding the basis for iodothyronine deiodinase activity?, *Inorg. Chem.*, 2010, **49**, 5365–5367.
10 D. Manna, S. Mondal and G. Mugesh, Halogen bonding controls the regioselectivity of the deiodination of thyroid hormones and their sulfate analogues, *Chemistry*, 2015, **21**, 2409–2416.
11 C. A. Bayse, Halogen Bonding from the Bonding Perspective with Considerations for Mechanisms of Thyroid Hormone Activation and Inhibition, *New J. Chem.*, 2018, **42**, 10623–10632.
12 S. Mondal, D. Manna, K. Raja and G. Mugesh, Halogen Bonding in Biomimetic Deiodination of Thyroid Hormones and their Metabolites and Dehalogenation of Halogenated Nucleosides, *ChemBioChem*, 2020, **21**, 911–923.
13 B. Olofsson, in *Hypervalent Iodine Chemistry*, ed. T. Wirth, Springer International Publishing, Cham, 2015/10/27 edn, 2016, pp. 135–166.
14 A. Yoshimura and V. V. Zhdankin, Advances in Synthetic Applications of Hypervalent Iodine Compounds, *Chem. Rev.*, 2016, **116**, 3328–3435.

15 R. Robidas, D. L. Reinhard, C. Y. Legault and S. M. Huber, Iodine(III)-Based Halogen Bond Donors: Properties and Applications, *Chem. Rec.*, 2021, **21**, 1912–1927.
16 N. Chatterjee and A. Goswami, Synthesis and Application of Cyclic Diaryliodonium Salts: A Platform for Bifunctionalization in a Single Step, *Eur. J. Org. Chem.*, 2017, 3023–3032.
17 H. C. Cheng, J. L. Ma and P. H. Guo, Cyclic Diaryliodonium Salts: Eco–Friendly and Versatile Building Blocks for Organic Synthesis, *Adv. Synth. Catal.*, 2023, **365**, 1112–1139.
18 X. Peng, A. Rahim, W. Peng, F. Jiang, Z. Gu and S. Wen, Recent Progress in Cyclic Aryliodonium Chemistry: Syntheses and Applications, *Chem. Rev.*, 2023, **123**, 1364–1416.
19 C. Chen, P. Wu, J. Zhou and Z. Bao, The Preparation and Application of Diaryliodonium Salts Derived from Gemfibrozil and Gemfibrozil Methyl Ester, *Synthesis*, 2021, 1388–1394.
20 J. Zhou, Z. Bao, P. Wu and C. Chen, Preparation and Synthetic Application of Naproxen-Containing Diaryliodonium Salts, *Molecules*, 2021, **26**, 3240.
21 D. L. Reinhard, F. Heinen, J. Stoesser, E. Engelage and S. M. Huber, Tuning the Halogen Bonding Strength of Cyclic Diaryliodonium Salts, *Helv. Chim. Acta*, 2021, **104**, e2000221.
22 M. Damrath, L. D. Caspers, D. Duvinage and B. J. Nachtsheim, One-Pot Synthesis of Heteroatom-Bridged Cyclic Diaryliodonium Salts, *Org. Lett.*, 2022, **24**, 2562–2566.
23 A. Yoshimura, M. T. Shea, O. Guselnikova, P. S. Postnikov, G. T. Rohde, A. Saito, M. S. Yusubov, V. N. Nemykin and V. V. Zhdankin, Preparation and structure of phenolic aryliodonium salts, *Chem. Commun.*, 2018, **54**, 10363–10366.
24 K. Zhu, K. Xu, Q. Fang, Y. Wang, B. Tang and F. Zhang, Enantioselective Synthesis of Axially Chiral Biaryls via Cu-Catalyzed Acyloxylation of Cyclic Diaryliodonium Salts, *ACS Catal.*, 2019, **9**, 4951–4957.

3.3.1 Additional Experiments

The described novel iodaoxinium salts **128** and **129** were further investigated towards their reduction back to the corresponding amino acids **T4** and **T3**. To test this the Hantzsch ester **130** was chosen as a reducing agent as dihydropyridines are analogues of NADH (Scheme 3.21). When reacting **128** in the presence of **130** in methanol no reaction could be observed. Contrary, when conducting the same experiment but with **129** the product could be detected by HPLC-MS, although by isolation and NMR analysis it became clear that the reaction did not progress stereoselective. The ^{1}H NMR clearly shows signals corresponding to formed **T3** (**131**) mixed with a second set of signals representing a second stereoisomer **132** in a ~1:2.5 ratio.[160] So far It was not possible to separate these two isomers.

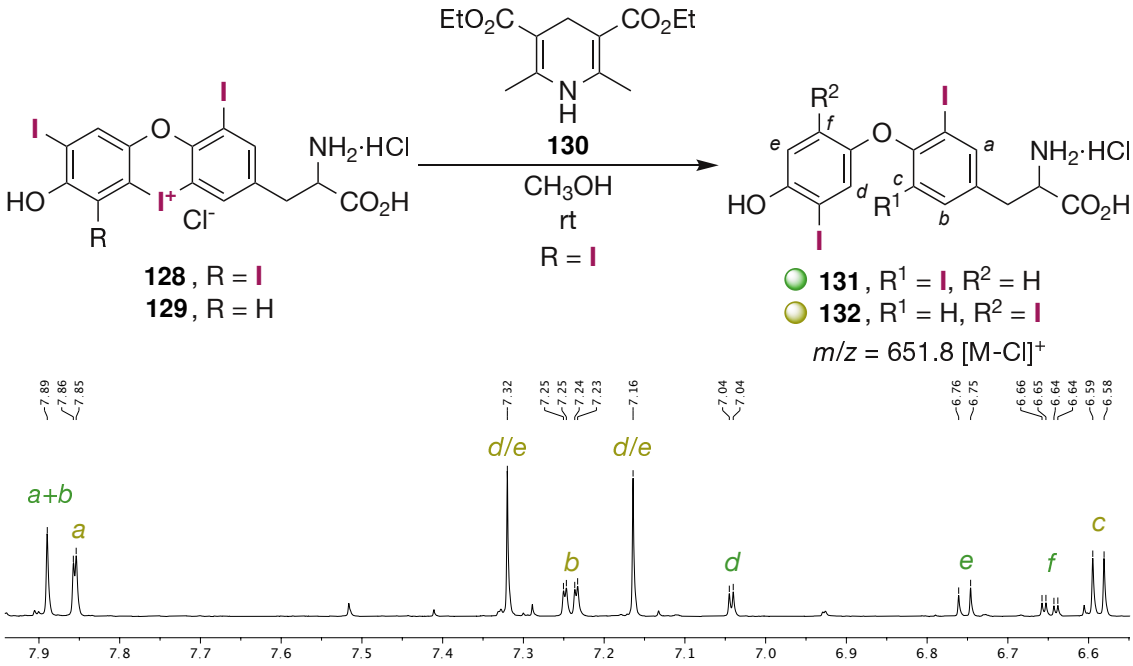

Scheme 3.21. Attempted reduction of **T4** and **T3** derived iodaoxinium salts **128** and **129** by **130** and the obtained NMR in CD_3OD indicating an unselective formation of **T3** (**131**) and its isomer **132**.

4 Summary

This thesis examines the structural, synthetic, and theoretical properties of diaryliodonium salts, a subclass of iodanes. To investigate this, a variety of structures was examined.

Structural Investigation of *peri*-Bisiodonium Salts

In the first project, different *peri*-substituted iodonium salts were synthesised and investigated, including mono- and dicationic structures.

A general procedure for synthesising a small scope of five *peri*-bisiodonium tetrafluoroborates was established. Suitable crystals were obtained for all of them and an additional where the anion was exchanged to triflate. These were then structurally investigated. Three different conformers were observed hereby, with general parameters concerning the ligand sphere of the iodine matching known examples. Interatomic I-I distances of 3.53 Å to 3.57 Å were observed, resembling the distance of the unoxidised iodoarene but also being further apart than in one comparable dicationic literature example. This was attributed to the high degree of freedom around the iodonium centres. The interaction of the iodonium cations towards the anions seemed to be stronger than for monocationic structures (shortened I-F bond), which was attributed to the overall lower electron density of the molecule.

While it was not possible to isolate pure unsymmetric bisiodonium salts, it could be demonstrated that these compounds are indeed stable.

Five different iodonium salts with a *peri*-iodine(I) substitution were obtained during the experiments. Four of these structures were investigated by X-ray crystallography. The results showed a significant reduction in the I-I distance (3.24 Å to 3.27 Å) in all cases, suggesting that the iodine(I) is donating into the sigma hole of the iodine(III). Further, undermined by the C11-I2-I1 angle ranging from 168° to 175°, typical for a halogen bond. This resulted in one case, in the anion being more closely coordinated to the iodine(I) than to the iodine(III) centre suggesting an induced positive charge on the iodine(I) atom. Additionally, they all showed a slightly enlarged I2-C9 bond, which was attributed to the coordination of the iodine(I). Apart from these observations, the structural parameters were mostly consistent with known examples.

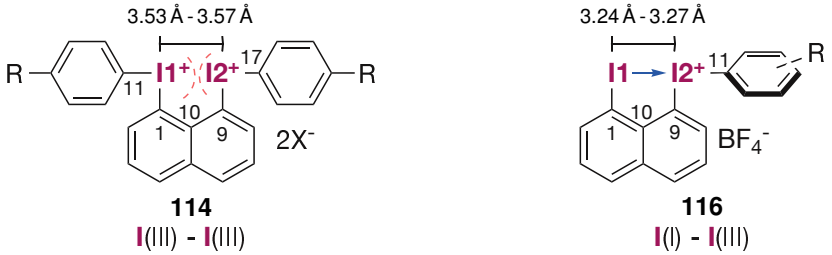

Figure 4.1. Investigated structures in regards to their iodine-iodine interactions. Bisiodonium salts **114** and *peri*-iodo-iodonium salts **116**.

These monocationic structures were also investigated as potential organocatalysts as the iodine(I) could still act in a redox cycle. It could be shown that these types of mixed iodoarene-iodonium salt structures are acting in such a reaction quite well although their activity is still below comparable iodoarenes that don't feature an iodonium substitution in close proximity.

As an additional finding, two examples of novel TMS-substituted iodonium salts were successfully prepared in a general one-pot procedure.

Two-Step Continuous-Flow Synthesis of Cyclic Iodonium Salts

In the second project, the aim was to find a procedure for the synthesis of cyclic diaryliodonium salts under more atom-economical conditions. This was achieved by generating the salts through anodic oxidation. Initially, a batch process was optimised, and after achieving a satisfactory yield, the process was transferred into a flow setup. Here, parameters were further optimised, though the choice of solvents had to be adjusted due to limitations posed by the available reactor-specific materials.

After optimising the anodic oxidation process in flow, it should be coupled with a second step inspired by a previous procedure. This second step would go before the iodonium salt formation by generating the iodoarenes from benzyl acetates and alcohols through a Friedel-Crafts-like reaction. The two steps were successfully combined in a single continuous flow apparatus. After finding optimal conditions, the procedure was tested on a small scale of eight substrates, each at a 2.00 mmol scale, taking 3 hours and 20 minutes. This showcased the applicability of the developed procedure. The setup was particularly useful for more delicate substrates as it allowed for precise control in each step, including time and temperature.

In summary, the first multi-step continuous-flow procedure for the generation of cyclic six-membered diaryliodonium salts was developed, by combining a Friedel–Crafts benzylation with a subsequent anodic oxidative cyclisation in flow.

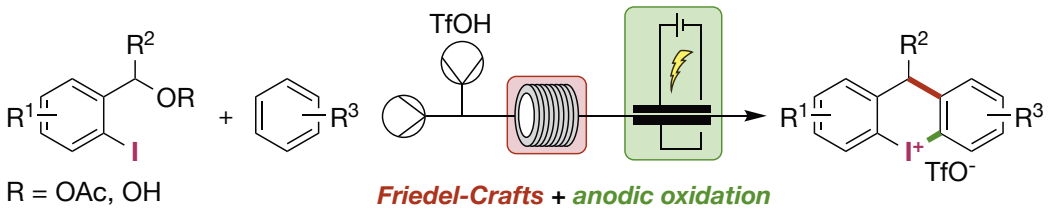

Scheme 4.1. Continuous multi-step flow procedure with initial Fridel-Crafts benzylation followed by an anodic oxidation step to generate cyclic diaryliodonium salts.

Oxidative Cyclization and Enzyme-free Deiodination of Thyroid Hormones

Six-membered diaryliodonium salts became also the relevant structures in the last project of this thesis. Initially, the aim was to investigate the oxidation of thyroxine and related structures. Various model substrates were tested under different conditions with the aim of observing oxidation on one of the aryl iodides. This was successful for **T4**- and **rT3**-derived substrates as the oxidation of an inner ring iodine with subsequent cyclisation towards a six-membered oxygen-bridged iodaoxinium salt was observed. After optimising the conditions for this formation and testing them on different polyiodinated biaryl ethers, the conditions were supposed to be applied to protected thyroid hormones.

Here it became evident that although structures were very similar the oxidation of thyroxine (**T4**) needed further optimisation. After improving conditions, the targeted and cyclised thyroxine derivative could be successfully isolated. Further investigation highlighted different properties as the highly pH-dependent stability. While attempting to fully deprotect the amino

acid, a selective deiodination was noticed that resulted in the formation of an oxidised and cyclised triiodothyronine (**T3**) derivative, which was not accessible by procedures analogous to the oxidation of **T4**.

The mechanism of this deiodination was investigated by DFT calculations, due to its peculiarly high selectivity. Here it became evident that by coordination of a chloride anion to the aryl iodides, substitution of these by a hydrogen was significantly preferred for the experimentally observed position. This preferred coordination to one iodide could also be confirmed experimentally by observing a shift of the related carbon signal in the ^{13}C NMR under varying amounts of an chloride source. The resulting mechanism resembles literature-described DFT calculations on the enzymatic deiodination of **T4** and could give further valuable insight into natural pathways.

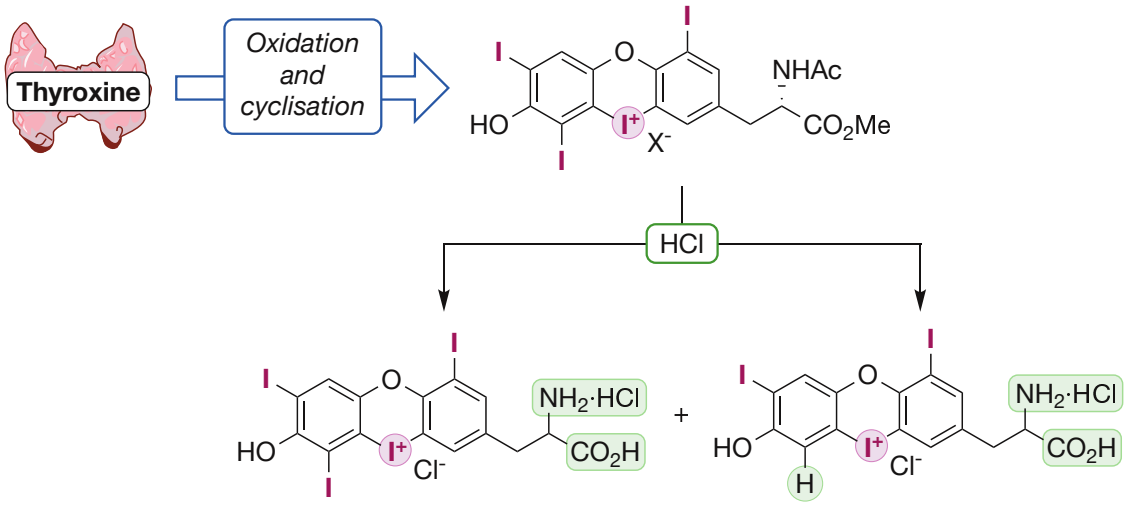

Scheme 4.2. Synthesis of cyclic iodaoxinium salts starting from Thyroxine (**T4**) and further deprotection and post-functionalisation.

5 Zusammenfassung

Diese Arbeit befasst sich mit den strukturellen, synthetischen sowie theoretischen Eigenschaften von Diaryliodoniumsalzen, einer Untergruppe der Iodane. Hierfür wurde eine Vielfalt von Strukturen untersucht.

Strukturelle Untersuchungen von *peri*-Bisiodoniumsalzen

In einem ersten Projekt wurden verschiedene *peri*-substituierte Iodoniumsalze hergestellt und untersucht, dies umfasste mono- als auch dikationische Strukturen. Es wurde ein allgemeines Protokoll an der Synthese von fünf *peri*-Bisiodoniumtetrafluoroboraten demonstriert. Für alle Strukturen wurden geeignete Kristallstrukturen erhalten, sowie zusätzlich eine unter Austausch zum Triflat. Diese wurden im Anschluss ausgewertet und diskutiert. Hierbei wurden drei verschiedene Konformere beobachtet, wobei die allgmeinen Parameter bzgl. der Ligandsphäre der Iod mit bekannten Beispiele in Einklang waren. Es wurden interatomare I-I Abstände von 3.53 Å bis 3.57 Å beobachtet, die dem nichtoxidierten Iodaren ähneln, allerdings weiter entfernt sind als in einem vergleichbaren dikationischen Literaturbeispiel. Dies wurde auf den hohen Freiheitsgrad um die Iodoniumzentren zurückgeführt. Die Wechselwirkung der Iodoniumkationen mit den Anionen erschien stärker, als bei monokationischen Strukturen (verkürzte I-F-Bindung), was auf die insgesamt geringere Elektronendichte des Moleküls zurückgeführt wurde.

Obwohl es nicht möglich war, reine unsymmetrische Bisiodoniumsalze zu isolieren, konnte gezeigt werden, dass diese Verbindungen stabil sind.

Im Rahmen der Experimente wurden fünf verschiedene *peri*-Iod(I)-substituierte Iodoniumsalze erhalten. Vier dieser Strukturen wurden mittels Röntgenstrukturanalyse untersucht. Die Ergebnisse zeigten in allen Fällen eine signifikante Verringerung des I-I-Abstands (3.24 Å bis 3.27 Å), was darauf hindeutet, dass das Iod(I) in das Sigma-Loch des Iod(III) doniert. Dies wird durch den C11-I2-I1-Winkel im Bereich von 168° bis 175° gestützt, der typisch für eine Halogenbindung ist. Dies führte in einem Fall dazu, dass das Anion näher an das Iod(I)- als an das Iod(III)-Zentrum koordiniert ist, was auf eine induzierte positive Ladung am Iod(I)-Atom schließen lässt. Darüber hinaus zeigten alle eine leicht vergrößerte I2-C9-Bindung, was auf die Koordination des Iod(I) zurückgeführt wurde. Ansonsten stimmen die Strukturparameter größtenteils mit bekannten Beispielen überein.

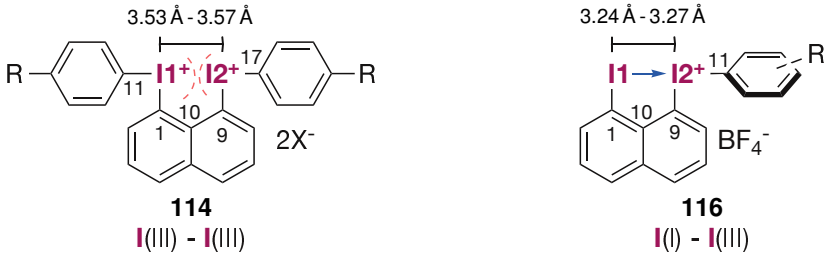

Figure 5.1. Untersuchte Strukturen hinsichtlich ihrer Iod-Iod-Wechselwirkungen. Bisiodoniumsalze **114** und *peri*-Iod-Iodoniumsalze **116**.

Die erhaltenen monokationischen Strukturen wurden auch als potenzielle Organokatalysatoren untersucht, da das Iod(I) immer noch in einem Redoxzyklus reagieren könnte. Es konnte gezeigt werden, dass diese Arten von gemischten Iodaren-Iodoniumsalzstrukturen katalytische

aktivität aufweisen, jedoch liegt ihre Aktivität unter der vergleichbarer Iodarene, welche keine Iodoniumsubstitution in unmittelbarer Nähe aufweisen.

Zusätzliche konnten zwei Beispiele neuartiger TMS-substituierter Iodoniumsalze erfolgreich in einem allgemeinen Eintopfverfahren hergestellt werden.

Zweistufige Kontinuierliche Fluss-Synthese Zyklischer Iodoniumsalze

In einem zweiten Projekt wurde, ein Verfahren zur Synthese zyklischer Diaryliodoniumsalze unter atomökonomischeren Bedingungen erarbeitet. Dies konnte durch die Generierung der Iodoniumsalze mittels anodischer Oxidation erreicht werden. Zunächst wurde die Reaktion in einem diskontinuierlichen Verfahren optimiert und nach Erreichen einer zufriedenstellenden Ausbeute in einen kontinuierlichen Fluss-Prozess überführt. Hier wurden die Parameter erneut optimiert, allerdings musste die Wahl der Lösungsmittel aufgrund von Einschränkungen durch die verfügbaren reaktorspezifischen Materialien angepasst werden.

Nach der Optimierung des anodischen Oxidation im Fluss-Prozess sollte dieser mit einem zweiten Schritt gekoppelt werden, inspiriert durch vorherige Arbeiten. Dieser zweite Schritt würde der Bildung des Iodoniumsalzes vorangehen, indem die Iodoarene aus Benzylacetaten und -alkoholen durch eine Friedel-Crafts-ähnliche Reaktion erzeugt werden. Die beiden Schritte wurden erfolgreich in einer einzigen Fluss-Apparatur kombiniert. Nachdem optimale Bedingungen gefunden wurden, wurde das Verfahren in für acht Substrate, jeweils im 2.00 mmol Maßstab (3 Stunden 20 Minuten), getestet, um die Anwendbarkeit des entwickelten Verfahrens zu demonstrieren. Der Prozess erwies sich besonders bei empfindlicheren Substraten als vorteilhaft, da er eine präzise Steuerung jedes Schritts, einschließlich Zeit und Temperatur, ermöglichte.

Zusammenfassend wurde der erste mehrstufige kontinuierliche Fluss-Prozess zur Erzeugung zyklischer sechsgliedriger Diaryliodoniumsalze entwickelt, indem eine Friedel-Crafts-Benzylierung mit einer anschließenden anodischen oxidativen Zyklisierung im Durchfluss kombiniert wurde.

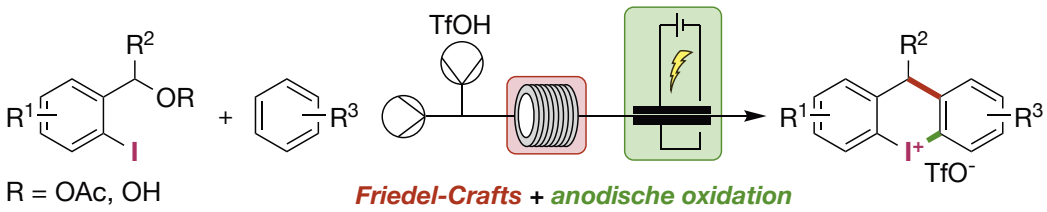

Scheme 5.1. Kontinuierlicher mehrstufiger Fluss-Prozess mit initialer Fridel-Crafts-Benzylierung, gefolgt von einer anodischen Oxidation zur Erzeugung zyklischer Diaryliodoniumsalze.

Oxidative Zyklisierung und Enzymfreie Deiodierung von Schilddrüsenhormonen

Sechsgliedrige Diaryliodoniumsalze waren auch im letzten Projekt dieser Arbeit relevante Strukturen. Ziel war zunächst, die Oxidation von Thyroxin und verwandten Strukturen zu untersuchen. Hierfür wurden Modellsubstrate unter verschiedenen Bedingungen getestet mit dem Ziel, die Oxidation an einem der Aryliodide zu beobachten. Dies war für **T4**- und **rT3**-abgeleitete Substrate erfolgreich, da die Oxidation eines Iods am inneren Ring mit anschließender Cyclisierung zu einem sechsgliedrigen, sauerstoffverbrückten Iodaoxiniumsalz beobachtet

werden konnte. Nachdem die Bedingungen optimiert und an verschiedenen polyiodierten Biarylethern getestet wurden, sollten die Bedingungen auf geschützte Schilddrüsenhormone angewendet werden.

Dabei zeigte sich, dass trotz sehr ähnlicher Strukturen die Oxidation von Thyroxin (**T4**) weitere Optimierung benötigte. Nachdem dies erreicht wurde, konnte das erzielte zyklisierte Thyroxin-Derivat erfolgreich isoliert werden. Weitere Untersuchungen hoben verschiedene Eigenschaften wie die stark pH-abhängige Stabilität hervor. Beim Versuch, die Aminosäure vollständig zu entschützen, wurde eine eine selektive Deiodierung beobachtet, die zur Bildung eines oxidierten cyclisierten Triiodthyronin-Derivats (**T3**) führte, welches durch Verfahren analog zur Oxidation von **T4** nicht zugänglich war.

Der Mechanismus dieser Deiodierung wurde aufgrund ihrer besonders hohen Selektivität durch DFT-Rechnungen untersucht. Hier zeigte sich, dass durch die Koordination eines Chloridanions an die Aryliodide deren Substitution durch ein Proton für die experimentell beobachtete Position deutlich bevorzugt war. Diese bevorzugte Koordination an ein Iodid konnte auch experimentell bestätigt werden, indem eine Verschiebung des zugehörigen Kohlenstoffsignals im ^{13}C-NMR unter variierenden Mengen einer Chloridquelle beobachtet wurde. Der resultierende Mechanismus ähnelt in der Literatur beschriebenen DFT-Rechnungen zur enzymatischen Deiodierung von **T4** und könnte weitere wertvolle Einblicke in natürliche Prozesse liefern.

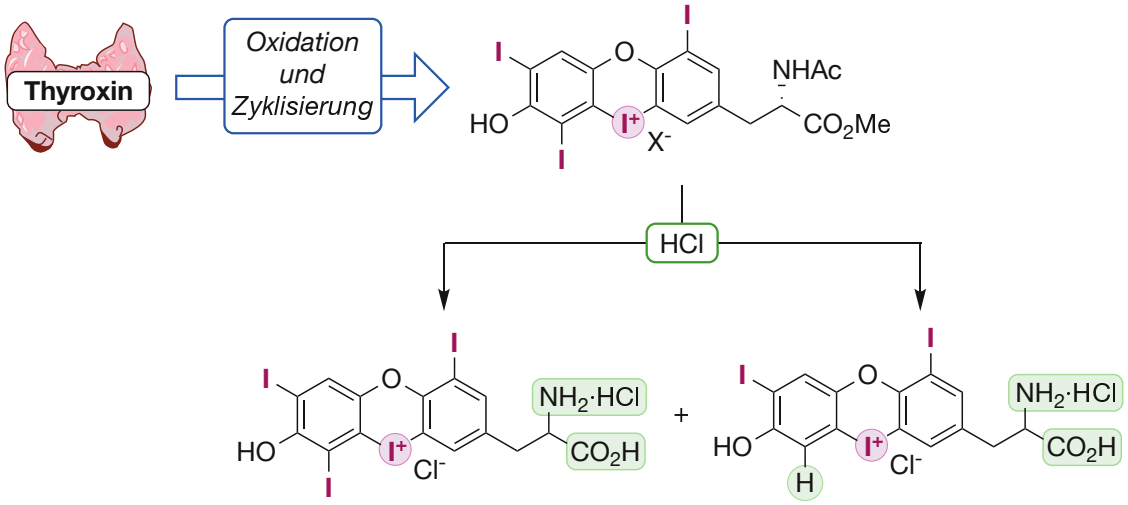

Scheme 5.2. Synthese zyklischer Iodaoxiniumsalze ausgehend von Thyroxin (**T4**) sowie die weitere Entschützung und Funktionalisierung.

6 Outlook

This thesis presents a range of diaryliodonium salts with varying properties and characteristics. The naphthalene motive can be used to provoke interactions between two iodine in the same or different oxidation state. Though the isolation of asymmetric naphthalene-bisiodonium salts is yet to be achieved, further research is required to investigate different halides and halonium species. Similar studies involving the isoelectronic chalcogenes have revealed interesting modes of interaction. Mixed halonium salts **133** could be prepared by generating iodonium salts **134** from bromoiodonaphthalene **135** as described for various substrates in this thesis using oxidants and an activated arene and subsequently reacting these with a diazonium salt.

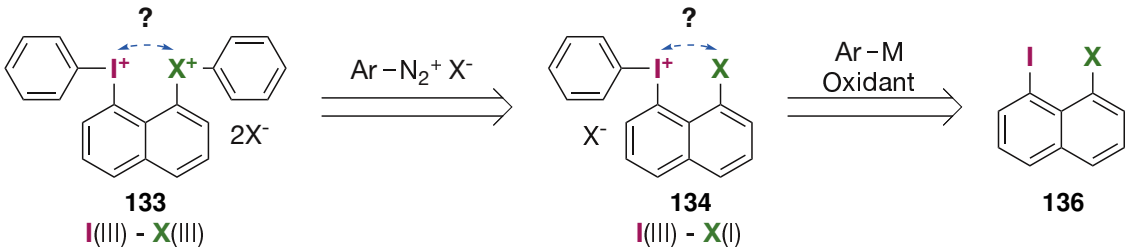

Scheme 6.1. Generation of mixed Iodonium and Halonium/Halide (X = Br, Cl) salts for the structural investigation of the intramolecular interaction of such novel compounds.

After synthesising and demonstrating first reactivities of novel iodaoxinium salts derived from naturally occurring thyroxine (**T4**), there is significant potential for further studies and applications of these compounds. Initially one should think about optimising the procedure to achieve a more simple and scalable preparation. This could be achieved by transferring certain steps into a flow setup where conditions can be controlled very precisely. Especially in the case of the deprotection with optional deiodination, selectivities could potentially be increased this way. Furthermore, these compounds call for investigation into their influence on biological systems, although likely modifications of the functional groups to increase their solubility and bioavailability have to be done first. In this regard, the reduction towards the already observed

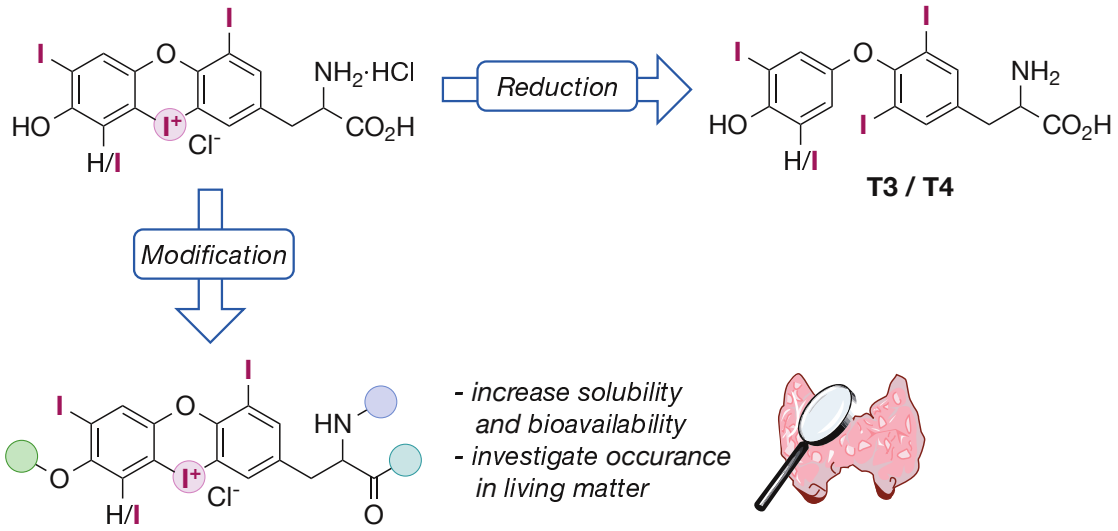

Scheme 6.2. Further applications of novel iodaoxinium salts by reduction back to triiodothyronine (**T3**) or by testing their biological activity.

T3 has to be investigated towards a more selective reduction as this could be a relatively simple mechanism for the initial generation of **T3** from **T4** in vertebrates.

Due to the applicability of cyclic iodonium salts as halogen bond catalysts, future application could be found in asymmetric transformations as the *ortho*-iodo substitution blocks one sigma hole while the other is in close vicinity of an chiral ligand. By increasing the structure of the amino acid moiety, better coordination and influence in asymmetric reactions could be achieved.

Further as **T4** and also **T3** are readily used medications the generation of derivatives could be achieved via acyclic diaryliodonium salts derived from **T4**. This could allow for the synthesis of various potentially active compounds and enable the generation of for example short-lived radio-labelled compounds via late-stage modification.

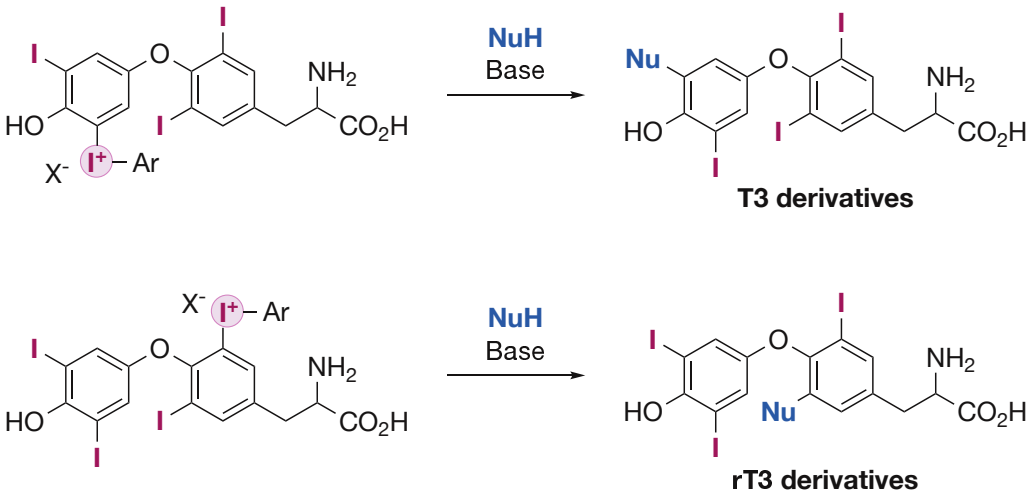

Scheme 6.3. Application of thyroxine derived acyclic iodonium salts to enable the derivatisation of **T3** and **rT3**.

7 Experimental Section

7.1 Supporting Information for Section 3.1

7.1.1 General Information

Unless otherwise noted, all reactions were carried out under air. Reactions with chemicals sensitive to moisture or oxygen were carried out under a nitrogen atmosphere using standard Schlenk techniques. All chemicals were purchased from commercial suppliers and either used as received or purified according to "Purification of Laboratory Chemicals".[161] Anhydrous diethyl ether (Et_2O) was obtained from an Inert PS-MD-6 solvent purification system. All other solvents were dried using standard methods if necessary.

NMR spectroscopy

NMR spectra were recorded on a *Bruker* Avance Neo 600. Chemical shifts for ^{1}H NMR spectra are reported as δ (parts per million) relative to the residual proton signal of $CDCl_3$ at $\delta = 7.26$ ppm (s), DMSO-d_6 at $\delta = 2.50$ ppm (quint) and CD_3OD at $\delta = 3.31$ ppm (quint). Chemical shifts for ^{13}C NMR spectra are reported as δ (parts per million) relative to the signal of $CDCl_3$ at $\delta = 77.0$ ppm, DMSO-d_6 at $\delta = 39.52$ ppm and CD_3OD at $\delta = 49.00$ ppm. Chemical shifts for ^{19}F NMR spectra are reported as δ (parts per million) relative to the signal of $Si(CH_3)_4$ at 0.00 ppm. The following abbreviations are used to describe splitting patterns: br. = broad, s = singlet, d = doublet, t = triplet, q = quartet, quint = quintet, sept = septet, m = multiplet. Coupling constants J are given in Hz.

Chromatography

Thin layer chromatography was performed on fluorescence indicator marked precoated silica gel 60 plates (*Macherey-Nagel*, ALUGRAM Xtra SIL G/UV254) and visualised by UV light (254 nm/366 nm).

Flash column chromatography was performed on silica gel (0.040 mm to 0.063 mm) with the solvents given in the procedures.

Mass spectrometry

Low-resolution ESI mass spectra were recorded on an *Agilent* 6120 Series LC/MSD system. Low-resolution EI mass spectra were recorded on an *Agilent* 5977A Series GC/MSD system. High-resolution (HR) EI mass spectra were recorded on a double-focusing mass spectrometer ThermoQuest MAT 95 XL from *Finnigan MAT*. High resolution (HR) ESI mass spectra were recorded on a *Bruker* Impact II. All Signals are reported with the quotient from mass to charge m/z.

Infrared spectroscopy

IR spectra were recorded on a *Nicolet* Thermo iS10 scientific spectrometer with a diamond ATR unit. The absorption bands ν are reported in cm^{-1}.

Melting Points

Melting points of solids were measured on a *Büchi* M-5600 Melting Point apparatus and are uncorrected. The measurements were performed with a heating rate of $2\,^{\circ}\mathrm{C\,min^{-1}}$ and the melting point temperatures T are reported in °C.

Crystallographic Measurements

Intensity data of suitable single crystals were collected on a *Bruker* Venture D8 diffractometer at 100 K with Mo Kα (0.7107 Å) radiation. All structures were solved by direct methods and refined based on F^2 by the use of the SHELX program package as implemented in Olex2.[162–164] All non-hydrogen atoms were refined using anisotropic displacement parameters. Hydrogen atoms attached to carbon atoms were included in geometrically calculated positions using a rigid model. The ORTEP drawings were made using the program Mercury from the CCDC.[165] Crystallographic data for the structural analyses have been deposited with the Cambridge Crystallographic Data Centre. Copies of this information may be obtained free of charge from The Director, CCDC, 12 Union Road, Cambridge CB2 1EZ, U.K. (Fax: +44- 1223-336033; e-mail: deposit@ccdc.cam.ac.uk or http://www.ccdc.cam.ac.uk/).

7.1.2 Synthetic Procedures

1,8-Diiodonaphthalene (112)

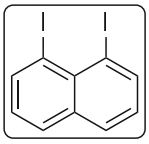

To a suspension of 1,8-diaminonaphtalene (19.0 g, 120 mmol) in a mixture of H_2O/H_2SO_4 (230 mL, 2:1) was added dropwise a solution of $NaNO_2$ (20.7 g, 300 mmol) in H_2O (95 mL) at −20 °C. The solution was stirred for further 30 min and was poured in portions to a solution of KI (120 g, 720 mmol) in H_2O (95 mL) at rt while keeping the first solution at −20 °C. The mixture was stirred over night at rt and afterwards neutralised with 3 M NaOH and sat. $NaHCO_3$. A sat. solution of $Na_2S_2O_3$ was added, stirred for 10 min and the precipitate was filtered off and refluxed in toluene (200 mL) for 1 h. The solution was filtered hot, washed with Et_2O and the organic phase was washed with sat. $Na_2S_2O_3$ and dried over Na_2SO_4. The solvent was removed under reduced pressure and the crude product (24.5 g) was purified by column chromatography (silica, PE→Cy) to obtain the product (21.8 g, 57.2 mmol, 48%) in the form of pale yellow needles.

^{1}H NMR ($CDCl_3$, 601 MHz) $\delta = 8.42$ (dd, J = 7.3, 1.3 Hz, 2H), 7.85 (dd, J = 8.2, 1.2 Hz, 2H), 7.08 (t, J = 7.7 Hz, 2H). **^{13}C NMR** ($CDCl_3$, 151 MHz) $\delta = 144.2, 136.0, 132.3, 131.2, 127.1, 96.2$. **FTIR** (ATR, neat) $\tilde{\nu} = 3051, 1532, 1488, 1417, 1346, 1316, 1177, 1130, 800, 742$. **MS** (EI, 70 eV) m/z = 379.9 $[M]^{\cdot+}$, 252.9 $[M - I]^+$. **Mp** $T = 106 - 107$. Analytical data is in agreement with literature.[166]

(8-Iodonaphthalen-1-yl)boronic acid (122)

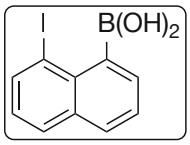

Based on a literature procedure[167] 1,8-diiodonaphthalene (**112**, 1.90 g, 5.00 mmol) was dissolved under argon atmosphere in dry Et_2O (50 mL) and *n*BuLi (2.00 mL, 5.00 mmol, 2.5 M in hexanes) was added dropwise at −30 °C. After 30 min the mixture was cooled to −80 °C and $B(OMe)_3$ (1.67 mL, 15.0 mmol) was added dropwise. The mixture was allowed to warm to rt over night, extracted with CH_2Cl_2 (3×30 mL) and concentrated under reduced pressure. The crude product was dissolved in a minimal amount of CH_3CN, an excess of conc. HCl was added and the mixture was stirred at 40 °C. Solvents were removed and the crude product was precipitated from 1,2-dichloroethane with PE and recrystallised from H_2O to obtain the product (876 mg, 2.94 mmol, 59%) as an off-white powder.

^{1}H NMR (DMSO-d_6, 600 MHz) $\delta = 8.17$ (d, J = 7.2 Hz, 1H), 8.12 (s, 2H), 7.96 (d, J = 8.1 Hz, 1H), 7.86 (d, J = 7.8 Hz, 1H), 7.52 (d, J = 6.6 Hz, 1H), 7.49 (t, J = 7.3 Hz, 1H), 7.22 (t, J = 7.7 Hz, 1H). **^{13}C NMR** (DMSO-d_6, 151 MHz) $\delta = 143.5$ (very weak due to boron coupling), 139.0, 136.4, 134.9, 132.5, 130.0, 129.4, 127.1, 126.1, 100.8. **FTIR** (ATR, neat) $\tilde{\nu} = 3273, 3047, 1488, 1323, 1145, 1060, 1033, 969, 811, 763$. **MS** ($ESI^+$, CH_3CN/H_2O (0.02% TFA) m/z = 281.0 $[M - OH]^+$, 321.0 $[M + Na]^+$, 362.0 $[M + Na + CH_3CN]^+$. **Mp** $T = 150$. Analytical data is in agreement with literature.[167]

(8-Iodonaphthalen-1-yl)trimethylsilane (124)

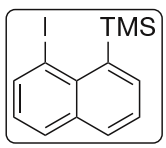

According to a literature procedure[167] 1,8-Diiodonaphthalene (**112**, 950 mg, 2.50 mmol) was dissolved under argon atmosphere in dry Et_2O (25 mL) and *n*BuLi (1.00 mL, 2.50 mmol, 2.5 M in hexanes) was added dropwise at −30 °C. After 30 min the mixture was cooled to −80 °C and TMSOTf (543 µL, 3.00 mmol) was added dropwise. The mixture was allowed to warm to rt over night, neutralised with

sat. $NaHCO_3$ (25 mL) and extracted with Et_2O (3×25 mL). The organic phases were dried over Na_2SO_4 and concentrated under reduced pressure. After column chromatography (silica, Cy) and Kugelrohr distillation (at 0.50 mbar/70.0 °C first fraction, at 0.50 mbar/115 °C Product fraction) the product **124** was obtained as a yellowish oil (0.498 g, 1.53 mmol, 61%).

^{1}H NMR ($CDCl_3$, 600 MHz) δ = 8.26 (d, J = 7.2 Hz, 1H), 7.97 (d, J = 6.9 Hz, 1H), 7.82 (d, J = 8.0 Hz, 1H), 7.73 (d, J = 8.0 Hz, 1H), 7.40 (t, J = 7.5 Hz, 1H), 7.11 (t, J = 7.6 Hz, 1H), 0.64 (s, 9H). **^{13}C NMR** ($CDCl_3$, 151 MHz) δ = 141.2, 140.7, 140.5, 138.1, 135.7, 130.8, 130.2, 126.1, 124.8, 96.7, 5.7. **FTIR** (ATR, neat) $\tilde{\nu}$ = 3051, 2957, 2894, 1488, 1188, 1247, 969, 832, 810, 764, 689. **HRMS** (EI, 70 eV) m/z = 325.9979 $[M]^{\cdot+}$. Calculated for $C_{13}H_{15}ISi^{\cdot+}$: m/z = 325.9982. Analytical data is in agreement with literature.[167]

1,3-Diacetoxy-1*H*,3*H*-naphtho[1,8-*de*][1,3,2]diiodaoxine (118)

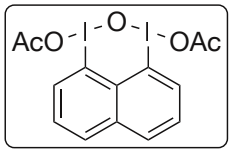

1,8-Diiodonaphthalene (**112**, 1.90 g, 5.00 mmol) and Selectfluor (8.86 g, 25.0 mmol) were dissolved in a mixture of CH_3CN/AcOH (100 mL, 2:1) and stirred for 3 d at rt under exclusion from light. Afterwards, H_2O (100 mL) was added and the aqueous phase was extracted with $CHCl_3$ (3×50 mL). The organic phase was dried over Na_2SO_4 and concentrated under reduced pressure while keeping exposure to light and heat at a minimum. The resulting yellow solid was washed with Et_2O and carefully dried under reduced pressure to obtain the product (**118**, 1.90 g, 3.70 mmol, 74%) as a yellow solid. *Note: The compound should be handled with care and dried carefully as removal of all excess AcOH resulted once in explosive decomposition. Due to this the compound was isolated with varying amounts of acetate ligands (2 - 4).*

^{1}H NMR (CD_3OD, 600 MHz) δ = 8.51 (d, J = 7.7 Hz, 2H), 8.22 (d, J = 7.8 Hz, 2H), 7.64 (t, J = 7.9 Hz, 2H), 1.98 (s, 6H). **^{13}C NMR** (CD_3OD, 151 MHz) δ = 176.2, 139.7, 137.3, 135.7, 129.1, 127.7, 114.8, 21.1. **FTIR** (ATR, neat) $\tilde{\nu}$ = 3051, 2957, 2894, 1488, 1188, 1247, 969, 832, 810, 764, 689. **HRMS** (ESI^+, CH_3CN) m/z = 638.8969 $[M + 2\,AcOH - H_2O + Na]^+$. Calculated for $C_{18}H_{18}I_2Na^+$: m/z = 638.8983. HRMS data corresponds to **118** with four acetate ligands.

7.1.2.1 General Procedure for the Synthesis of Symmetric Bisiodonium Salts 114 (GP1)

1,8-Diiodonaphtalene (**112**, 1.0 eq.) and *m*CPBA (2.1 eq., 85% w/w) were dissolved in CH_2Cl_2 (50 mM) at 0 °C. $BF_3 \cdot OEt_2$ (5.0 eq.) was added slowly and the solution was stirred for 2 h at rt. Afterwards the corresponding boronic acid (**113**, 2.1 eq.) was added at 0 °C and the solution was stirred for 16 h at rt. The solution was decanted and the resulting precipitate washed with CH_2Cl_2 (7 x 7.5 mL mmol^{-1}) and precipitated from HFIP with Et_2O to give the products **114** as a solid.

Naphthalene-1,8-diylbis(phenyliodonium) bistetrafluoroborate (114a)

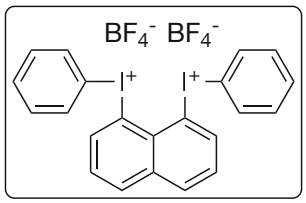

Following **GP1**, 1,8-Diiodonaphtalene (**112**, 760 mg, 2.00 mmol) and *m*CPBA (853 mg, 4.20 mmol) in CH_2Cl_2 (40 mL) with $BF_3 \cdot OEt_2$ (1.25 mL, 10.0 mmol) and phenylboronic acid (**113a**, 512 mg, 4.20 mmol) gave the product (**114b**, 676 mg, 0.955 mmol, 48%) as a beige solid.

^{1}H NMR (DMSO-d_6, 601 MHz) δ = 9.24 (dd, J = 7.5, 1.2 Hz, 2H), 8.48 (d, J = 7.4 Hz, 2H), 7.97 (d, J = 7.6 Hz, 4H), 7.77 (t, J = 7.8 Hz, 2H), 7.61 (t, J = 7.4 Hz, 2H), 7.48 (t, J = 7.9 Hz, 4H). **^{13}C NMR** (DMSO-d_6, 151 MHz) δ = 145.4, 136.2, 136.2, 134.0, 132.3, 131.9, 129.5, 127.7, 119.2, 114.8. **^{19}F NMR** (DMSO-d_6, 565 MHz) δ = -148.1. **FTIR** (ATR, neat) $\tilde{\nu}$ = 3191, 3092, 1492, 1473, 1444, 1004, 982, 821, 735. **HRMS** (ESI$^+$, CH_3OH) m/z = 266.9660 $[M-2\,BF_4]^{2+}$. Calculated for $C_{22}H_{16}I_2^{2+}$: m/z = 266.9665. **Mp** T = 225, with decomposition at 235.

Naphthalene-1,8-diylbis((4-methoxyphenyl)iodonium) bistetrafluoroborate (114b)

Following **GP1**, 1,8-Diiodonaphtalene (**112**, 190 mg, 0.500 mmol) and *m*CPBA (213 mg, 1.05 mmol) in CH_2Cl_2 (10 mL) with $BF_3 \cdot OEt_2$ (314 µL, 2.50 mmol) and (*p*-methoxyphenyl)boronic acid (**113b**, 160 mg, 1.05 mmol, addition at −80 °C) gave the product (**114b**, 174 mg, 0.226 mmol, 45%) as a white solid.

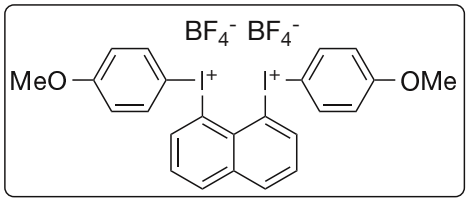

^{1}H NMR (DMSO-d_6, 600 MHz) δ = 9.18 (dd, J = 7.5, 1.2 Hz, 2H), 8.43 (dd, J = 8.2, 1.2 Hz, 2H), 8.02 – 7.96 (m, 4H), 7.74 (t, J = 7.8 Hz, 2H), 7.06 – 7.00 (m, 4H), 3.76 (s, 6H). **^{13}C NMR** (DMSO-d_6, 151 MHz) δ = 162.1, 144.4, 136.2, 136.1, 135.7, 129.3, 127.5, 117.4, 115.5, 108.2, 55.8. **^{19}F NMR** (DMSO-d_6, 565 MHz) δ = -148.2. **FTIR** (ATR, neat) $\tilde{\nu}$ = 3089, 2945, 2844, 1568, 1486, 1304, 1262, 1054, 1015, 820, 744. **HRMS** (ESI$^+$, CH_3CN/H_2O (9:1)) m/z = 296.9768 $[M-2\,BF_4]^{2+}$. Calculated for $C_{24}H_{20}I_2O_2^{2+}$: m/z = 296.9771. **Mp** T = 175 − 180 (decomposition).

Naphthalene-1,8-diylbis(*p*-tolyliodonium bistetrafluoroborate) (114c)

Following **GP1**, 1,8-Diiodonaphtalene (**112**, 190 mg, 0.500 mmol) and *m*CPBA (213 mg, 1.05 mmol) in CH_2Cl_2 (10 mL) with $BF_3 \cdot OEt_2$ (314 µL, 2.50 mmol) and (*p*-methylphenyl)boronic acid (**113d**, 143 mg, 1.05 mmol) gave the product (**114c**, 142 mg, 0.193 mmol, 39%) as a white solid.

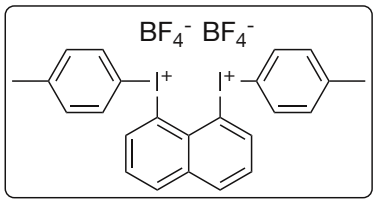

^{1}H NMR (DMSO-d_6, 600 MHz) δ = 9.19 (dd, J = 7.5, 1.2 Hz, 2H), 8.46 (dd, J = 8.3, 1.2 Hz, 2H), 7.85 (d, J = 8.5 Hz, 4H), 7.75 (t, J = 7.8 Hz, 2H), 7.29 (d, J = 8.5 Hz, 4H), 2.31 (s, 6H). **^{13}C NMR** (DMSO-d_6, 151 MHz) δ = 145.0, 142.8, 136.1, 135.9, 133.9, 132.3, 129.3, 127.5, 115.5, 114.8, 20.7. **^{19}F NMR** (DMSO-d_6, 565 MHz) δ = -148.3. **FTIR** (ATR, neat) $\tilde{\nu}$ = 3088, 1478, 1288, 1184, 1054, 1012, 995, 824, 801, 746. **HRMS** (ESI$^+$, CH_3CN/H_2O+HCO_2H (0.1%) (9:1)) m/z = 281.9824 $[M-2\,BF_4]^{2+}$. Calculated for $C_{22}H_{14}F_2I_2^{2+}$: m/z = 280.9822. **Mp** T = 148 − 153 (decomposition).

Naphthalene-1,8-diylbis((4-bromophenyl)iodonium) bistetrafluoroborate (114d)

Following **GP1**, 1,8-Diiodonaphtalene (**112**, 190 mg, 0.500 mmol) and *m*CPBA (213 mg, 1.05 mmol) in CH_2Cl_2 (10 mL) with $BF_3 \cdot OEt_2$ (314 µL, 2.50 mmol) and (*p*-bromophenyl)boronic acid (**113c**, 211 mg, 1.05 mmol) gave the product (**114d**, 83.8 mg, 96.8 µmol, 19%) as a white solid.

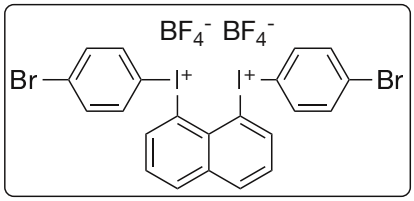

^{1}H NMR (DMSO-d_6, 600 MHz) δ = 9.23 (d, J = 7.4 Hz, 2H), 8.52 (d, J = 8.0 Hz, 2H), 7.89 (d, J = 8.9 Hz, 4H), 7.79 (t, J = 7.8 Hz, 2H), 7.71 (d, J = 8.8 Hz, 4H). **^{13}C NMR** (DMSO-d_6, 151 MHz) δ = 145.4, 136.3, 136.2, 135.6, 134.6, 129.5, 127.4, 126.3, 117.6, 114.7. **^{19}F NMR** (DMSO-d_6, 565 MHz)

δ = -148.2. **FTIR** (ATR, neat) $\tilde{\nu}$ = 3086, 1471, 1383, 1187, 1016, 988, 817, 799, 742. **HRMS** (ESI$^+$, CH_3CN) *m/z* = 344.8768 $[M-2\,BF_4]^{2+}$. Calculated for $C_{22}H_{14}Br_2I_2^{2+}$: *m/z* = 344.8770. **Mp** $T = 185 - 190$ (decomposition).

Naphthalene-1,8-diylbis((4-fluorophenyl)iodonium bistetrafluoroborate) (114e)

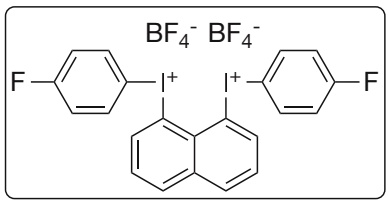

Following **GP1**, 1,8-Diiodonaphtalene (**112**, 190 mg, 0.500 mmol) and *m*CPBA (213 mg, 1.05 mmol) in CH_2Cl_2 (10 mL) with $BF_3 \cdot OEt_2$ (314 µL, 2.50 mmol) and (*p*-fluorohenyl)boronic acid (**113e**, 147 mg, 1.05 mmol) gave the product (**114e**, 70.6 mg, 94.9 µmol, 19%) as a orange solid.

^{1}H NMR (DMSO-d_6, 600 MHz) δ = 9.23 (dd, *J* = 7.5, 1.2 Hz, 2H), 8.49 (dd, *J* = 8.3, 1.2 Hz, 2H), 8.12 – 8.08 (m, 4H), 7.77 (t, *J* = 7.8 Hz, 2H), 7.39 (t, *J* = 8.9 Hz, 4H). **^{13}C NMR** (DMSO-d_6, 151 MHz) δ = 164.8, 163.1, 145.0, 136.8 (d, *J* = 9.0 Hz), 136.2 (d, *J* = 12.3 Hz), 129.5, 127.4, 119.1 (d, *J* = 23.0 Hz), 115.1, 113.3 (d, *J* = 3.1 Hz). **^{19}F NMR** (DMSO-d_6, 565 MHz) δ = = -106.6 (tt, *J* = 9.0, 5.1 Hz, 2H), -148.3 (s, 8H). **FTIR** (ATR, neat) $\tilde{\nu}$ = 3094, 1577, 1482, 1401, 1245, 1162, 997, 821, 745. **HRMS** (ESI$^+$, CH_3CN/H_2O (9:1)) *m/z* = 284.9570 $[M-2\,BF_4]^{2+}$. Calculated for $C_{22}H_{14}F_2I_2^{2+}$: *m/z* = 284.9571. **Mp** $T = 167 - 172$ (decomposition).

7.1.2.2 General Procedure for the Synthesis of Iodonium Salts 116 from Diiodonaphthalene 112 (GP2)

1,8-Diiodonaphtalene (**112**, 380 mg, 1.00 mmol, 1.0 eq.) and *m*CPBA (173 mg, 1.00 mmol, 1.0 eq., 85% w/w) were dissolved in Et_2O (20 mL, 50 mM) and stirred for 20 min at rt. $BF_3 \cdot OEt_2$ (317 µL, 2.50 mmol, 2.5 eq.) was added carefully and the solution was stirred for 10 min at rt. A yellow precipitate was formed. Afterwards the corresponding boronic acid (**113**, 1.00 mmol, 1.0 eq.) was added at rt and the solution was stirred for over night. The resulting precipitate was concentrated and filtered over silica (CH_2Cl_2 → CH_2Cl_2/CH_3OH (10:1) → CH_3OH). Solvent was removed and the crude products were precipitated from CH_2Cl_2/CH_3OH (9:1) with Et_2O to give the products **116** as a solid. During workup heat should be avoided, as the compounds showed decomposition even at rt while concentrating.

7.1.2.3 General Procedure for the Synthesis of Iodonium Salts 116 from 118 (GP3)

118 (257 mg to 308 mg, 0.500 mmol, 1.0 eq., used as obtained from preparation with varying amounts of acetic acid) and $NaBF_4$ (110 mg, 1.00 mmol, 2.0 eq.) were suspended in TFE (2.5 mL, 200 mM) and the corresponding boronic acid (**113**, 0.500 mmol, 1.0 eq.) was added under stirring at rt. After 24 h the mixture was diluted with H_2O (5 mL) and extracted with CH_2Cl_2 (3×5 mL). The organic phases were dried over Na_2SO_4 and concentrated under reduced pressure. The obtained crude product was precipitated multiple from CH_2Cl_2/CH_3OH (9:1) with Et_2O to yield the products **116** as a solid. During workup heat should be avoided, as the compounds showed decomposition even at rt while concentrating.

(4-Bromophenyl)(8-iodonaphthalen-1-yl)iodonium tetrafluoroborate (116a)

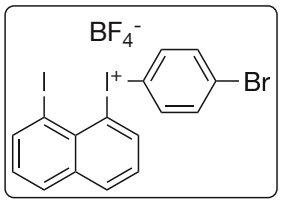

Following **GP2**, using (*p*-bromophenyl)boronic acid (**113c**, (201 mg, 1.00 mmol) yielded the product (**116a**, 134 mg, 0.216 mmol, 22%) as a white solid.

Following **GP3**, using (*p*-bromophenyl)boronic acid (**113c**, (100 mg, 0.500 mmol) yielded the product (**116a**, 39.2 mg, 63.0 µmol, 13%) as a white solid.

^{1}H NMR (DMSO-d_6, 600 MHz) δ = 8.86 (d, J = 7.5 Hz, 1H), 8.55 (d, J = 7.4 Hz, 1H), 8.37 (d, J = 8.1 Hz, 1H), 8.22 (d, J = 8.0 Hz, 1H), 8.05 (d, J = 8.3 Hz, 2H), 7.76 (d, J = 8.2 Hz, 2H), 7.61 (t, J = 7.8 Hz, 1H), 7.39 (t, J = 7.8 Hz, 1H). **^{13}C NMR** (DMSO-d_6, 151 MHz) δ = 144.6, 143.0, 136.2, 136.0, 135.7, 134.7, 131.6, 128.9, 128.6, 128.2, 126.2, 117.7, 117.3, 94.3. **^{19}F NMR** (DMSO-d_6, 565 MHz) δ = = -148.3. **FTIR** (ATR, neat) $\tilde{\nu}$ = 3090, 1529, 1385, 1320, 1183, 1051, 1036, 990, 814, 742. **HRMS** (ESI$^+$, CH_3CN/H_2O (9:1)) m/z = 534.8050 $[M-BF_4]^+$. Calculated for $C_{16}H_{10}BrI_2^+$: m/z = 534.8050. **Mp** T = 173 − 178 (decomposition).

(8-Iodonaphthalen-1-yl)(phenyl)iodonium tetrafluoroborate (116b)

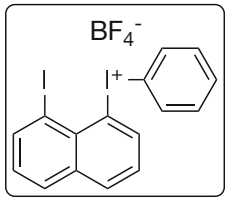

Following **GP2**, using phenylboronic acid (**113a**, 122 mg, 1.00 mmol) yielded the product (**116b**, 83.4 mg, 0.153 mmol, 15%) as a brown solid.

Following **GP3**, using phenylboronic acid (**113a**, 61.0 mg, 0.500 mmol) yielded the product (**116b**, 43.0 mg, 79.1 µmol, 16%) as a brown solid.

^{1}H NMR (DMSO-d_6, 600 MHz) δ = 8.82 (d, J = 7.4 Hz, 1H), 8.55 (d, J = 7.4 Hz, 1H), 8.35 (d, J = 8.0 Hz, 1H), 8.21 (d, J = 8.1 Hz, 1H), 8.15 (d, J = 7.9 Hz, 2H), 7.65 (t, J = 7.5 Hz, 1H), 7.59 (t, J = 7.8 Hz, 1H), 7.53 (t, J = 7.7 Hz, 2H), 7.38 (t, J = 7.8 Hz, 1H). **^{13}C NMR** (DMSO-d_6, 151 MHz) δ = 144.5, 142.7, 136.0, 135.4, 134.4, 132.1, 131.8, 131.6, 129.2, 128.5, 128.2, 119.3, 117.3, 94.4. **^{19}F NMR** (DMSO-d_6, 565 MHz) δ = = -148.3. **FTIR** (ATR, neat) $\tilde{\nu}$ = 3077, 1530, 1442, 1351, 1321, 1181, 1034, 810, 742. **HRMS** (ESI$^+$, CH_3CN/H_2O (9:1)) m/z = 456.8950 $[M-BF_4]^+$. Calculated for $C_{16}H_{11}I_2^+$: m/z = 456.8945. **Mp** T = 164 − 169 (decomposition).

(8-Iodonaphthalen-1-yl)(p-tolyl)iodonium tetrafluoroborate (116c)

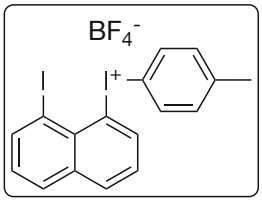

Following **GP2**, using (*p*-methylphenyl)boronic acid (**113d**, 136 mg, 1.00 mmol) yielded the product (**116c**, 34.4 mg, 61.7 µmol, 6%) as a brown solid.

Following **GP3**, using (*p*-methylphenyl)boronic acid (**113d**, 68.0 mg, 0.500 mmol) yielded the product (**116c**, 17.4 mg, 31.2 µmol, 6%) as a brown solid.

^{1}H NMR (DMSO-d_6, 600 MHz) δ = 8.75 (d, J = 7.5 Hz, 1H), 8.54 (d, J = 7.3 Hz, 1H), 8.34 (d, J = 8.0 Hz, 1H), 8.20 (d, J = 8.1 Hz, 1H), 8.05 (d, J = 8.0 Hz, 2H), 7.58 (t, J = 7.8 Hz, 1H), 7.39 (t, J = 7.9 Hz, 1H), 7.35 (d, J = 8.0 Hz, 2H), 2.33 (s, 3H). **^{13}C NMR** (DMSO-d_6, 151 MHz) δ = 144.4, 142.8, 142.1, 136.1, 135.3, 134.5, 132.5, 131.5, 129.2, 128.5, 128.2, 117.1, 115.4, 94.3, 20.8. **^{19}F NMR** (DMSO-d_6, 565 MHz) δ = = -148.3. **FTIR** (ATR, neat) $\tilde{\nu}$ = 3051, 1534, 1435, 1353, 1184, 1012, 813, 795, 763, 744. **HRMS** (ESI$^+$, CH_3CN/H_2O (9:1)) m/z = 470.9101 $[M-BF_4]^+$. Calculated for $C_{17}H_{13}I_2^+$: m/z = 470.9101. **Mp** T = 127 − 132 (decomposition).

(8-Iodonaphthalen-1-yl)(4-methoxyphenyl)iodonium tetrafluoroborate (116d)

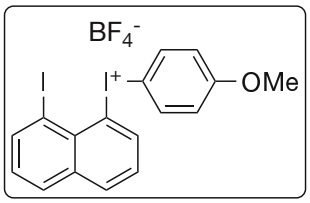

Following **GP2**, using (*p*-methoxyphenyl)boronic acid (**113b**, 152 mg, 1.00 mmol, addition at −80 °C) yielded the product (**116d**, 72.5 mg, 0.126 mmol, 13%) as a brown solid.

Following **GP3**, using (*p*-methoxyphenyl)boronic acid (**113b**, 76.0 mg, 0.500 mmol) yielded the product (**116d**, 61.5 mg, 0.107 mmol, 21%) as a brown solid.

^{1}H NMR (DMSO-d_6, 600 MHz) δ = 8.64 (dd, J = 7.6, 1.2 Hz, 1H), 8.54 (dd, J = 7.4, 1.2 Hz, 1H), 8.32 (dd, J = 8.2, 1.2 Hz, 1H), 8.20 (dd, J = 8.2, 1.3 Hz, 1H), 8.15 – 8.08 (m, 2H), 7.57 (t, J = 7.8 Hz, 1H), 7.39 (t, J = 7.7 Hz, 1H), 7.13 – 7.07 (m, 2H), 3.79 (s, 3H). **^{13}C NMR** (DMSO-d_6, 151 MHz) δ = 162.7, 144.6, 141.7, 137.3, 136.7, 135.5, 131.9, 129.9, 129.0, 128.6, 118.2, 117.9, 108.3, 94.8, 56.2. **^{19}F NMR** (DMSO-d_6, 565 MHz) δ = = -148.3. **FTIR** (ATR, neat) $\tilde{\nu}$ = 3077, 2939, 2840, 1568, 1533, 1485, 1458, 1438, 1304, 1259, 1174, 1051, 1014, 813, 744. **HRMS** (ESI$^+$, CH_3CN/H_2O (9:1)) m/z = 486.9054 $[M-BF_4]^+$. Calculated for $C_{17}H_{13}I_2O^+$: m/z = 486.9050. **Mp** T = 95 − 100 (decomposition).

(8-Iodonaphthalen-1-yl)(2,4,6-trimethoxyphenyl)iodonium tetrafluoroborate (116e)

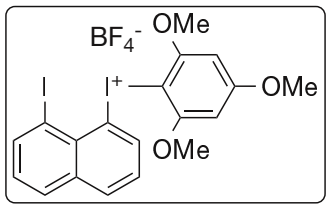

Following **GP2**, using 1,3,5-trimethoxybenzene (168 mg, 1.00 mmol) in place of a boronic acid yielded the product (**116e**, 116 mg, 0.184 mmol, 18%) as a brown solid.

^{1}H NMR (DMSO-d_6, 600 MHz) δ = 8.50 (d, J = 7.3 Hz, 1H), 8.21 (d, J = 8.0 Hz, 1H), 8.17 (d, J = 8.1 Hz, 1H), 7.89 (d, J = 7.6 Hz, 1H), 7.48 (t, J = 7.9 Hz, 1H), 7.42 (t, J = 7.7 Hz, 1H), 6.52 (s, 2H), 3.91 (s, 3H), 3.87 (s, 6H). **^{13}C NMR** (DMSO-d_6, 151 MHz) δ = 167.1, 159.8, 143.0, 137.0, 135.6, 133.8, 131.5, 130.9, 128.6, 128.4, 114.9, 94.0, 92.6, 89.5, 57.4, 56.3. **^{19}F NMR** (DMSO-d_6, 565 MHz) δ = = -148.3. **FTIR** (ATR, neat) $\tilde{\nu}$ = 3078, 2967, 2841, 1569, 1533, 1485, 1456, 1438, 1346, 1305, 1259, 1174, 1053, 1013, 811, 744. **HRMS** (ESI$^+$, CH_3CN/H_2O (9:1)) m/z = 546.9265 $[M-BF_4]^+$. Calculated for $C_{19}H_{17}I_2O_3^+$: m/z = 546.9262. **Mp** T = 150 − 155 (decomposition).

7.1.2.4 General Procedure for the Synthesis of TMS-substituted Iodonium Salts 117 (GP4)

Iodoarene **124** (163 mg, 0.500 mmol, 1.0 eq.) was dissolved in a mixture of CH_2Cl_2/TFE (5 mL, 1:1), Selectfluor (531 mg, 1.50 mmol, 3 eq.) and the corresponding boronic acid (**113**, 0.750 mmol, 1.5 eq.) was added under stirring at rt. After 24 h the mixture was diluted with H_2O (5 mL) and extracted with CH_2Cl_2 (3×5 mL). The organic phases were dried over Na_2SO_4 and concentrated under reduced pressure. The crude product was precipitated multiple times from CH_2Cl_2/CH_3OH (9:1) with Et_2O to yield the products **117** as a white solid.

***p*-Tolyl(8-(trimethylsilyl)naphthalen-1-yl)iodonium tetrafluoroborate (117a)**

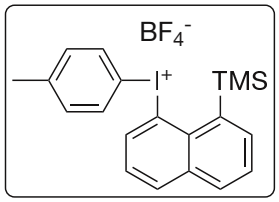

Following **GP4**, using (*p*-methylphenyl)boronic acid (**113d**, 102 mg, 0.750 mmol) yielded the product (**117a**, 47.0 mg, 93.2 µmol, 19%) as a white solid.

^{1}H NMR (DMSO-d_6, 601 MHz) δ = 8.82 (d, J = 7.4 Hz, 1H), 8.32 (d,

J = 8.1 Hz, 1H), 8.14 (d, J = 7.2 Hz, 1H), 8.06 (d, J = 8.0 Hz, 1H),
7.62 (t, J = 7.6 Hz, 2H), 7.48 (d, J = 8.3 Hz, 2H), 7.17 (d, J = 8.3 Hz, 2H), 2.21 (s, 3H), 0.60 (s, 9H) **^{13}C NMR** (DMSO-d_6, 151 MHz) δ = 142.2, 141.9, 140.6, 137.8, 136.4, 136.0, 135.4, 132.5, 132.4, 131.9, 127.3, 126.2, 115.6, 113.7, 20.5, 3.4. **^{19}F NMR** (DMSO-d_6, 565 MHz) δ = = -148.3. **FTIR** (ATR, neat) $\tilde{\nu}$ = 3090, 2951, 1477, 1307, 1259, 1188, 1016, 824, 798, 771. **HRMS** (ESI^+, CH_3CN) m/z = 417.0514 $[M-BF_4]^+$. Calculated for $C_{20}H_{22}ISi^+$: m/z = 417.0530. **Mp** T = 162 (with immediate decomposition).

(4-Methoxyphenyl)(8-(trimethylsilyl)naphthalen-1-yl)iodonium tetrafluoroborate (117b)

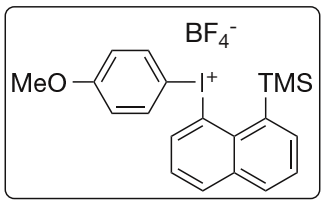

Following **GP4**, using (*p*-methoxyphenyl)boronic acid (**113b**, 114 mg, 0.750 mmol) yielded the product (**117b**, 150 mg, 0.289 mmol, 58%) as a white solid.

^{1}H NMR (DMSO-d_6, 600 MHz) δ = 8.81 (d, J = 6.9 Hz, 1H), 8.30 (d, J = 8.0 Hz, 1H), 8.15 (d, J = 7.0 Hz, 1H), 8.05 (d, J = 8.0 Hz, 1H), 7.63 – 7.59 (m, 2H), 7.59 – 7.56 (m, 2H), 6.94 – 6.90 (m, 2H), 3.69 (s, 3H), 0.61 (s, 9H). **^{13}C NMR** (DMSO-d_6, 151 MHz) δ = 162.1, 142.0, 141.0, 138.2, 136.8, 136.5, 135.8, 135.1, 132.4, 127.8, 126.6, 118.0, 116.7, 106.6, 56.1, 3.9. **^{19}F NMR** (DMSO-d_6, 565 MHz) δ = = -148.2. **FTIR** (ATR, neat) $\tilde{\nu}$ = 3088, 2977, 1568, 1486, 1306, 1255, 1178, 1018, 823, 770. **HRMS** (ESI^+, CH_3CN) m/z = 433.0467 $[M-BF_4]^+$. Calculated for $C_{20}H_{22}IOSi^+$: m/z = 433.0479. **Mp** T = 155 (with immediate decomposition).

7.1.2.5 Yield Determination for the α-Tosyloxylation of Propiophenone by NMR

*m*CPBA (40.8 mg, 0.200 mmol, 2.0 eq., 85% w/w) and *p*TsOH · H_2O (38.0 mg, 0.200 mmol, 2.0 eq.) were dissolved in CH_3CN (1 mL, 0.1 M), propiophenone (**125**, 13.4 mg, 0.100 mmol) and the catalyst (**112**, **116a**,**f**,**d** and **126**, 10 mol%) were added, and the mixture was stirred at 50 °C for 4 h. The reaction was quenched with Me_2S (14.6 µL, 0.200 mmol, 2.0 eq.) and the yield of the crude mixture was determined by ^{1}H NMR in $CDCl_3$ with anisole (10.9 µL, 10.8 mg) as an internal standard. Signals at 5.82 ppm for propiophenone (**125**) and at 3.83 ppm for anisole were compared. For spectra see Fig. 7.51 - 7.55.

7.1.3 Crystallography Data

Crystallographic data and structure refinement for the substrates **114a–f** and **116a**,**b**,**d**,**e** (CCDC 2334664 - 2334673). Selected interatomic distances, bond lengths and angles can be found in Tab. 3.1 and Tab. 3.4.

Naphthalene-1,8-diylbis(phenyliodonium) bistetrafluoroborate (114a)

Single crystals of **114a** were prepared by dissolving the substance in a minimum amount of acetonitrile. Diethyl ether was introduced via gas-phase diffusion to obtain a suitable crystal. (CCDC 2334664)

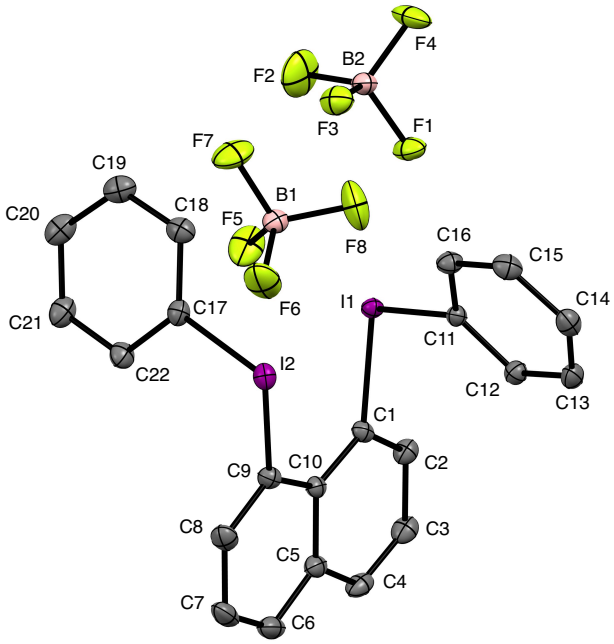

Figure 7.1. Single crystal structure (ORTEP drawing; hydrogen atoms were omitted) of **114a**. Thermal ellipsoids displayed with 50% probability.

Table 7.1. Crystal data and structure refinement for **114a**

Empirical formula	$C_{22}H_{16}B_2F_8I_2$	μ/mm^{-1}	2.821
Formula weight	707.77	F(000)	1344
Temperature/K	101	Crystal size/mm^3	0.17 ×0.13 ×0.12
Crystal system	monoclinic	Radiation	MoKα ($\lambda = 0.71073$)
Space group	$P2_1/n$	2Θ range for data collection/°	4.204 to 75
a/Å	12.1397(16)	Index ranges	$-20 \leq h \leq 20, 0 \leq k \leq 24, 0 \leq l \leq 22$
b/Å	14.4155(18)	Reflections collected	12325
c/Å	13.0915(17)	Independent reflections	12325 [$R_{int} = 0.0521, R_{sigma} = 0.0254$]
α/°	90	Data/restraints/parameters	12325/0/308
β/°	92.109(6)	Goodness-of-fit on F^2	1.245
γ/°	90	Final R indexes [I >= 2σ (I)]	$R_1 = 0.0294, wR_2 = 0.0738$
Volume/$Å^3$	2289.5(5)	Final R indexes [all data]	$R_1 = 0.0350, wR_2 = 0.0799$
Z	4	Largest diff. peak/hole / e $Å^{-3}$	0.93/-1.72
ρ_{calc} g cm^{-3}	2.053		

Naphthalene-1,8-diylbis((4-methoxyphenyl)iodonium) bistetrafluoroborate (114b)

Single crystals of **114b** were prepared by dissolving the substance in a minimum amount of acetonitrile. Diethyl ether was introduced via gas-phase diffusion to obtain a suitable crystal. (CCDC 2334673)

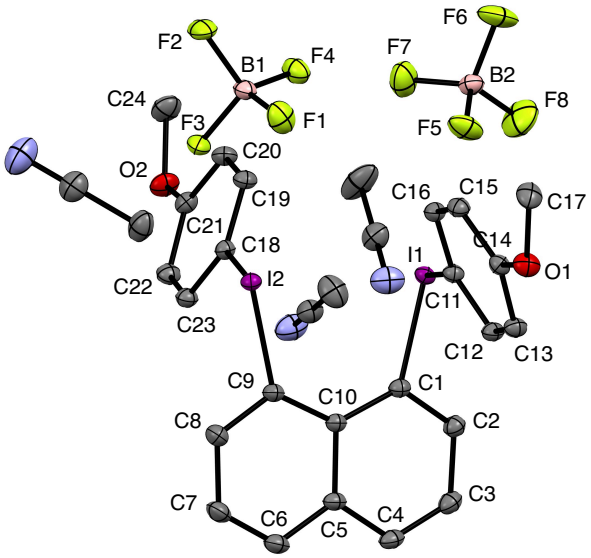

Figure 7.2. Single crystal structure (ORTEP drawing; hydrogen atoms were omitted) of **114b**. Thermal ellipsoids displayed with 50% probability.

Table 7.2. Crystal data and structure refinement for **114b**

Empirical formula	$C_{30}H_{29}B_2F_8I_2N_3O_2$	μ/mm^{-1}	1.95
Formula weight	890.98	F(000)	1736
Temperature/K	100	Crystal size/mm^3	0.22 ×0.12 ×0.11
Crystal system	monoclinic	Radiation	MoKα ($\lambda = 0.71073$)
Space group	$P2_1/n$	2Θ range for data collection/°	3.67 to 72.652
a/Å	12.0487(4)	Index ranges	$-20 \leq h \leq 20, -30 \leq k \leq 35, -21 \leq l \leq 17$
b/Å	21.5226(5)	Reflections collected	79454
c/Å	12.9514(5)	Independent reflections	16259 [$R_{int} = 0.0329, R_{sigma} = 0.0235$]
α/°	90	Data/restraints/parameters	16259/0/429
β/°	91.2140(10)	Goodness-of-fit on F^2	1.114
γ/°	90	Final R indexes [I >= 2σ (I)]	$R_1 = 0.0266, wR_2 = 0.0561$
Volume/$Å^3$	3357.80(19)	Final R indexes [all data]	$R_1 = 0.0308, wR_2 = 0.0576$
Z	4	Largest diff. peak/hole / e $Å^{-3}$	1.09/-1.55
ρ_{calc} g cm^{-3}	1.762		

Naphthalene-1,8-diylbis(*p*-tolyliodonium bistetrafluoroborate) (114c)

Single crystals of **114b** were prepared by dissolving the substance in a minimum amount of methanol. Diethyl ether was introduced via gas-phase diffusion to obtain a suitable crystal. (CCDC 2334669)

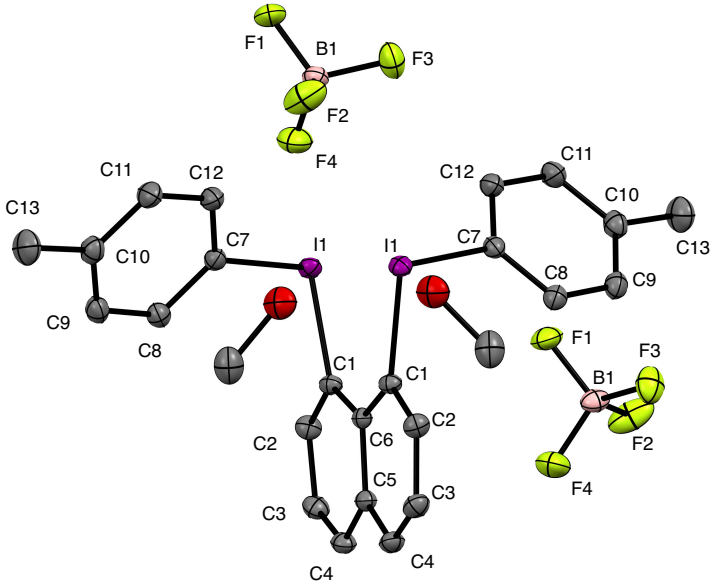

Figure 7.3. Single crystal structure (ORTEP drawing; hydrogen atoms were omitted) of **114c**. Thermal ellipsoids displayed with 50% probability.

Table 7.3. Crystal data and structure refinement for **114c**

Empirical formula	$C_{26}H_{28}B_2F_8I_2O_2$	μ/mm^{-1}	2.237
Formula weight	799.9	F(000)	1552
Temperature/K	100	Crystal size/mm^3	0.214 ×0.184 ×0.102
Crystal system	orthorhombic	Radiation	MoKα ($\lambda = 0.71073$)
Space group	Pbcn	2Θ range for data collection/°	5.15 to 72.638
a/Å	13.2043(4)	Index ranges	$-22 \leq h \leq 21, -19 \leq k \leq 19, -31 \leq l \leq 31$
b/Å	11.5514(4)	Reflections collected	97888
c/Å	19.0684(7)	Independent reflections	7057 [$R_{int} = 0.0329, R_{sigma} = 0.0136$]
α/°	90	Data/restraints/parameters	7057/0/188
β/°	90	Goodness-of-fit on F^2	1.117
γ/°	90	Final R indexes [I >= 2σ (I)]	$R_1 = 0.0216, wR_2 = 0.0495$
Volume/$Å^3$	2908.47(17)	Final R indexes [all data]	$R_1 = 0.0242, wR_2 = 0.0505$
Z	4	Largest diff. peak/hole / e $Å^{-3}$	0.87/-1.15
ρ_{calc} g cm^{-3}	1.827		

Naphthalene-1,8-diylbis((4-bromophenyl)iodonium) bistetrafluoroborate (114d)

Single crystals of **114d** were prepared by dissolving the substance in a minimum amount of acetonitrile. Diethyl ether was introduced via gas-phase diffusion to obtain a suitable crystal. (CCDC 2334668)

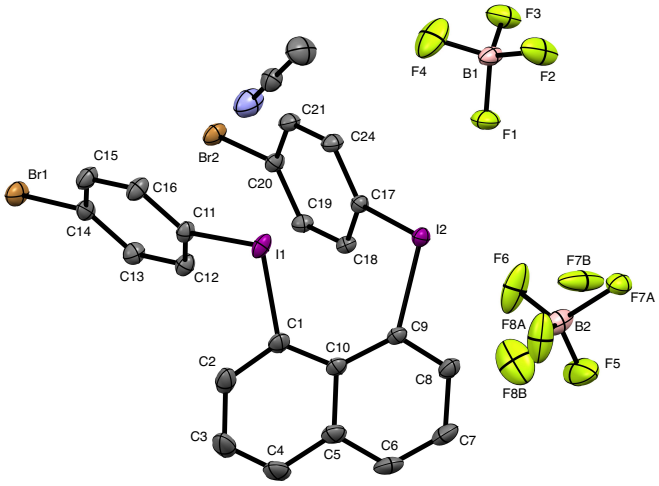

Figure 7.4. Single crystal structure (ORTEP drawing; hydrogen atoms were omitted) of **114d**. Thermal ellipsoids displayed with 50% probability.

Table 7.4. Crystal data and structure refinement for **114d**

Empirical formula	$C_{24}H_{17}B_2Br_2F_8I_2N$	μ/mm^{-1}	5.291
Formula weight	906.62	F(000)	852
Temperature/K	100	Crystal size/mm^3	0.14 ×0.12 ×0.09
Crystal system	triclinic	Radiation	MoKα ($\lambda = 0.71073$)
Space group	P-1	2Θ range for data collection/°	5.028 to 61.01
a/Å	8.5739(4)	Index ranges	$-12 \leq h \leq 12, -13 \leq k \leq 13, -25 \leq l \leq 25$
b/Å	9.4770(4)	Reflections collected	27899
c/Å	17.9550(7)	Independent reflections	8361 [$R_{int} = 0.0265, R_{sigma} = 0.0254$]
α/°	97.068(2)	Data/restraints/parameters	8361/2/372
β/°	99.163(2)	Goodness-of-fit on F^2	1.066
γ/°	105.313(2)	Final R indexes [I >= 2σ (I)]	$R_1 = 0.0218, wR_2 = 0.0503$
Volume/$Å^3$	1368.14(10)	Final R indexes [all data]	$R_1 = 0.0250, wR_2 = 0.0516$
Z	2	Largest diff. peak/hole / e $Å^{-3}$	1.26/-1.16
ρ_{calc} g cm^{-3}	2.201		

Naphthalene-1,8-diylbis((4-fluorophenyl)iodonium bistetrafluoroborate) (114e)

Single crystals of **114e** were prepared by dissolving the substance in a minimum amount of acetonitrile. Diethyl ether was introduced via gas-phase diffusion to obtain a suitable crystal. (CCDC 2334670)

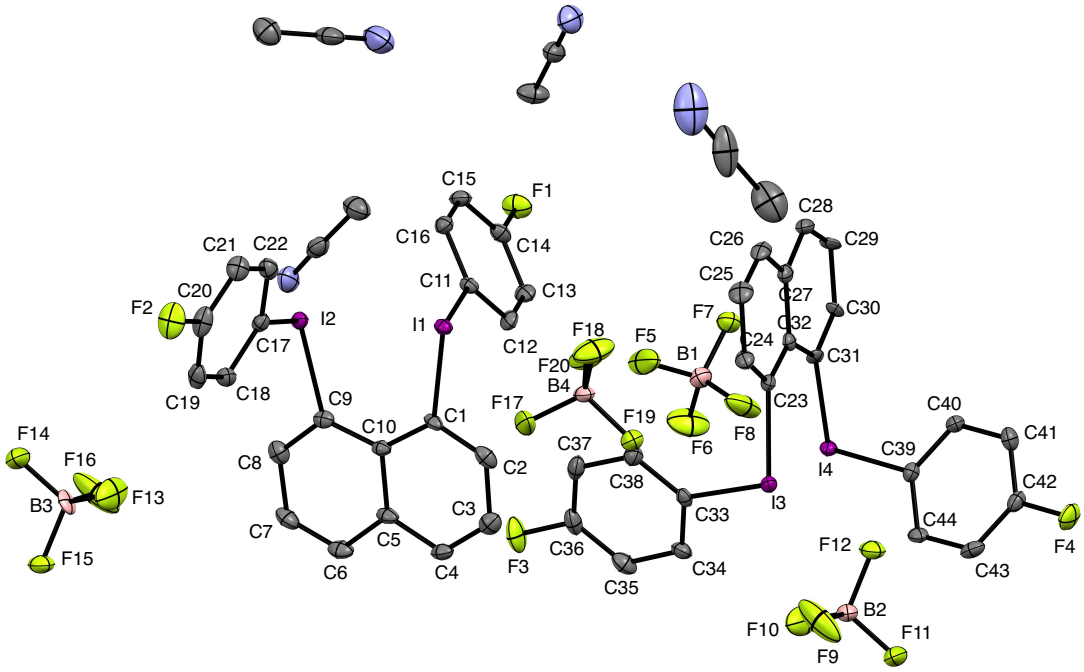

Figure 7.5. Single crystal structure (ORTEP drawing; hydrogen atoms were omitted) of **114e**. Thermal ellipsoids displayed with 50% probability.

Table 7.5. Crystal data and structure refinement for **114e**

Empirical formula	$C_{26}H_{20}B_2F_{10}I_2N_2$	μ/mm^{-1}	2.261
Formula weight	825.86	F(000)	3168
Temperature/K	100.01	Crystal size/mm^3	0.145 ×0.11 ×0.1
Crystal system	orthorhombic	Radiation	MoKα ($\lambda = 0.71073$)
Space group	$Pna2_1$	2Θ range for data collection/°	4.53 to 56.644
a/Å	11.8821(4)	Index ranges	$-15 \leq h \leq 15, -17 \leq k \leq 17, -49 \leq l \leq 49$
b/Å	13.2160(4)	Reflections collected	73891
c/Å	36.8141(11)	Independent reflections	14374 [$R_{int} = 0.0263, R_{sigma} = 0.0213$]
α/°	90	Data/restraints/parameters	14374/1/761
β/°	90	Goodness-of-fit on F^2	1.126
γ/°	90	Final R indexes [I >= 2σ (I)]	$R_1 = 0.0239, wR_2 = 0.0529$
Volume/$Å^3$	5781.1(3)	Final R indexes [all data]	$R_1 = 0.0251, wR_2 = 0.0533$
Z	8	Largest diff. peak/hole / e $Å^{-3}$	0.81/-1.84
ρ_{calc} gcm^{-3}	1.898	Flack parameter	0.014(4)

Naphthalene-1,8-diylbis(phenyliodonium) trifluoromethanesulfonate (114f)

Single crystals of **114f** were prepared by dissolving the substance in a minimum amount of acetonitrile. Diethyl ether was introduced via gas-phase diffusion to obtain a suitable crystal. (CCDC 2334665)

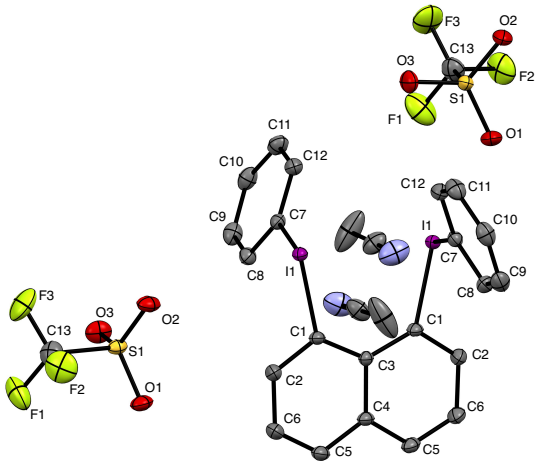

Figure 7.6. Single crystal structure (ORTEP drawing; hydrogen atoms were omitted) of **114f**. Thermal ellipsoids displayed with 50% probability.

Table 7.6. Crystal data and structure refinement for **114f**

Empirical formula	$C_{28}H_{22}F_6I_2N_2O_6S_2$	μ/mm^{-1}	2.116
Formula weight	914.39	F(000)	1776
Temperature/K	100	Crystal size/mm^3	0.22 ×0.11 ×0.09
Crystal system	orthorhombic	Radiation	MoKα ($\lambda = 0.71073$)
Space group	Pbcn	2Θ range for data collection/°	4.988 to 66.324
a/Å	13.2104(8)	Index ranges	$-20 \leq h \leq 19, -16 \leq k \leq 18, -31 \leq l \leq 28$
b/Å	12.0113(10)	Reflections collected	53721
c/Å	20.7291(11)	Independent reflections	6280 [$R_{int} = 0.0465, R_{sigma} = 0.0282$]
α/°	90	Data/restraints/parameters	6280/0/210
β/°	90	Goodness-of-fit on F^2	1.071
γ/°	90	Final R indexes [I >= 2σ (I)]	$R_1 = 0.0272, wR_2 = 0.0549$
Volume/$Å^3$	3289.2(4)	Final R indexes [all data]	$R_1 = 0.0365, wR_2 = 0.0578$
Z	4	Largest diff. peak/hole / e $Å^{-3}$	0.60/-0.90
ρ_{calc} g cm^{-3}	1.847		

(4-Bromophenyl)(8-iodonaphthalen-1-yl)iodonium tetrafluoroborate (116a)

Single crystals of **116a** were prepared by dissolving the substance in a minimum amount of acetonitrile. Diethyl ether was introduced via gas-phase diffusion to obtain a suitable crystal. (CCDC 2334666)

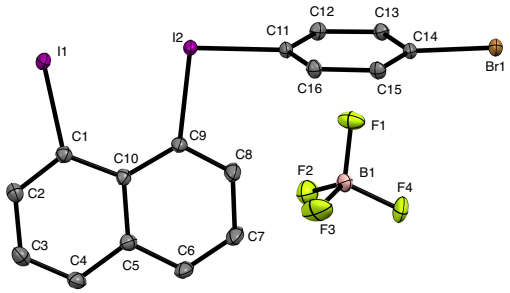

Figure 7.7. Single crystal structure (ORTEP drawing; hydrogen atoms were omitted) of **116a**. Thermal ellipsoids displayed with 50% probability.

Table 7.7. Crystal data and structure refinement for **116a**

Empirical formula	$C_{16}H_{10}BBrF_4I_2$	μ/mm^{-1}	5.985
Formula weight	622.76	F(000)	576
Temperature/K	100	Crystal size/mm^3	0.17 ×0.11 ×0.09
Crystal system	triclinic	Radiation	MoKα ($\lambda = 0.71073$)
Space group	P-1	2Θ range for data collection/°	5.234 to 56.646
a/Å	9.7615(3)	Index ranges	$-13 \leq h \leq 13, -14 \leq k \leq 14, -15 \leq l \leq 15$
b/Å	10.0058(3)	Reflections collected	37934
c/Å	10.9962(4)	Independent reflections	5270 [$R_{int} = 0.0356, R_{sigma} = 0.0194$]
α/°	107.3270(10)	Data/restraints/parameters	5270/0/217
β/°	102.9350(10)	Goodness-of-fit on F^2	1.133
γ/°	113.6010(10)	Final R indexes [I >= 2σ (I)]	$R_1 = 0.0192, wR_2 = 0.0450$
Volume/Å^3	864.24(5)	Final R indexes [all data]	$R_1 = 0.0196, wR_2 = 0.0455$
Z	2	Largest diff. peak/hole / e Å^{-3}	1.92/-1.67
ρ_{calc} g cm^{-3}	2.393		

(8-Iodonaphthalen-1-yl)(phenyl)iodonium tetrafluoroborate (116b)

Single crystals of **116b** were prepared by dissolving the substance in acetic acid and adding a minimum amount of methanol to reach full dissolution. Diethyl ether was introduced via gas-phase diffusion to obtain a suitable crystal. (CCDC 2334667)

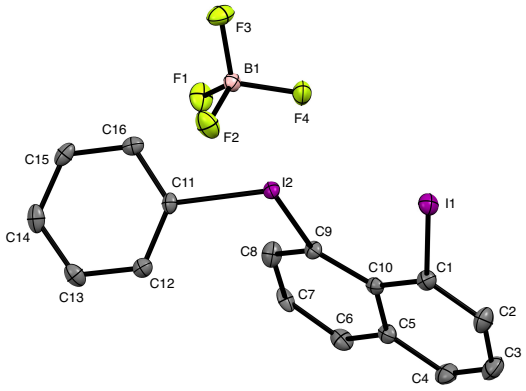

Figure 7.8. Single crystal structure (ORTEP drawing; hydrogen atoms were omitted) of **116b**. Thermal ellipsoids displayed with 50% probability.

Table 7.8. Crystal data and structure refinement for **116b**

Empirical formula	$C_{16}H_{11}BF_4I_2$	μ/mm^{-1}	3.944
Formula weight	543.86	F(000)	1016
Temperature/K	100	Crystal size/mm^3	0.14 ×0.13 ×0.12
Crystal system	monoclinic	Radiation	MoKα ($\lambda = 0.71073$)
Space group	$P2_1/c$	2Θ range for data collection/°	5.176 to 56.644
a/Å	11.9796(4)	Index ranges	$-15 \leq h \leq 15, -12 \leq k \leq 12, -19 \leq l \leq 19$
b/Å	9.4534(3)	Reflections collected	41492
c/Å	14.9115(6)	Independent reflections	4010 [$R_{int} = 0.0495, R_{sigma} = 0.0228$]
α/°	90	Data/restraints/parameters	4010/0/208
β/°	107.6780(10)	Goodness-of-fit on F^2	1.144
γ/°	90	Final R indexes [I >= 2σ (I)]	$R_1 = 0.0240, wR_2 = 0.0540$
Volume/$Å^3$	1608.95(10)	Final R indexes [all data]	$R_1 = 0.0262, wR_2 = 0.0548$
Z	4	Largest diff. peak/hole / e $Å^{-3}$	2.21/-0.82
ρ_{calc} gcm^{-3}	2.245		

(8-Iodonaphthalen-1-yl)(4-methoxyphenyl)iodonium tetrafluoroborate (116d)

Single crystals of **116d** were prepared by dissolving the substance in acetic acid and adding a minimum amount of methanol to reach full dissolution. Diethyl ether was introduced via gas-phase diffusion to obtain a suitable crystal. (CCDC 2334672)

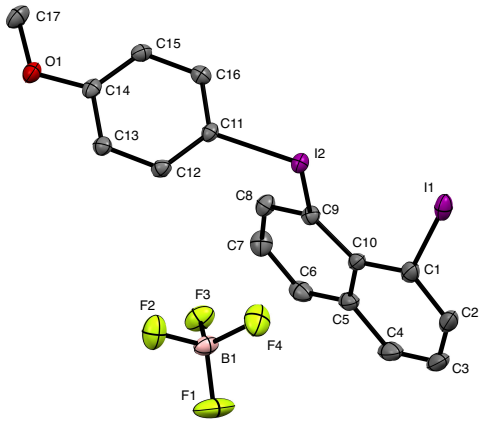

Figure 7.9. Single crystal structure (ORTEP drawing; hydrogen atoms were omitted) of **116d**. Thermal ellipsoids displayed with 50% probability.

Table 7.9. Crystal data and structure refinement for **116d**

Empirical formula	$C_{17}H_{13}BF_4I_2O$	μ/mm^{-1}	3.667
Formula weight	573.88	F(000)	1080
Temperature/K	100	Crystal size/mm^3	0.14 ×0.08 ×0.02
Crystal system	monoclinic	Radiation	MoKα ($\lambda = 0.71073$)
Space group	$P2_1/c$	2Θ range for data collection/°	4.932 to 56.596
a/Å	10.1315(5)	Index ranges	$-13 \leq h \leq 13, -19 \leq k \leq 19, -15 \leq l \leq 15$
b/Å	14.4172(7)	Reflections collected	43501
c/Å	11.9458(6)	Independent reflections	4302 [$R_{int} = 0.0273, R_{sigma} = 0.0138$]
α/°	90	Data/restraints/parameters	4302/0/227
β/°	95.928(2)	Goodness-of-fit on F^2	1.056
γ/°	90	Final R indexes [I >= 2σ (I)]	$R_1 = 0.0236, wR_2 = 0.0576$
Volume/$Å^3$	1735.57(15)	Final R indexes [all data]	$R_1 = 0.0251, wR_2 = 0.0586$
Z	4	Largest diff. peak/hole / e $Å^{-3}$	2.71/-1.29
ρ_{calc} g cm^{-3}	2.196		

(8-Iodonaphthalen-1-yl)(2,4,6-trimethoxyphenyl)iodonium tetrafluoroborate (116e)

Single crystals of **116d** were prepared by dissolving the substance in a minimum amount of acetonitrile. Diethyl ether was introduced via gas-phase diffusion to obtain a suitable crystal. (CCDC 2334671)

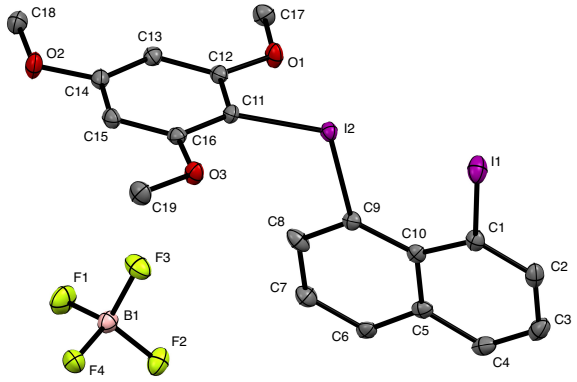

Figure 7.10. Single crystal structure (ORTEP drawing; hydrogen atoms were omitted) of **116e**. Thermal ellipsoids displayed with 50% probability.

Table 7.10. Crystal data and structure refinement for **116e**

Empirical formula	$C_{19}H_{17}BF_4I_2O_3$	μ/mm^{-1}	3.228
Formula weight	633.93	F(000)	1208
Temperature/K	100	Crystal size/mm^3	0.21 ×0.14 ×0.14
Crystal system	monoclinic	Radiation	MoKα ($\lambda = 0.71073$)
Space group	$P2_1/c$	2Θ range for data collection/°	5.234 to 56.646
a/Å	7.7949(3)	Index ranges	$-10 \leq h \leq 10, -21 \leq k \leq 21, -20 \leq l \leq 20$
b/Å	16.4401(7)	Reflections collected	63524
c/Å	15.4963(6)	Independent reflections	4944 [$R_{int} = 0.0358, R_{sigma} = 0.0155$]
α/°	90	Data/restraints/parameters	4944/0/265
β/°	93.164(2)	Goodness-of-fit on F^2	1.276
γ/°	90	Final R indexes [I >= 2σ (I)]	$R_1 = 0.0247, wR_2 = 0.0573$
Volume/$Å^3$	1982.81(14)	Final R indexes [all data]	$R_1 = 0.0248, wR_2 = 0.0574$
Z	4	Largest diff. peak/hole / e $Å^{-3}$	1.94/-0.89
ρ_{calc} gcm^{-3}	2.124		

7.1.4 NMR Data

Spectral data of compounds that were either not published in peer-reviewed journals or are insufficiently described.

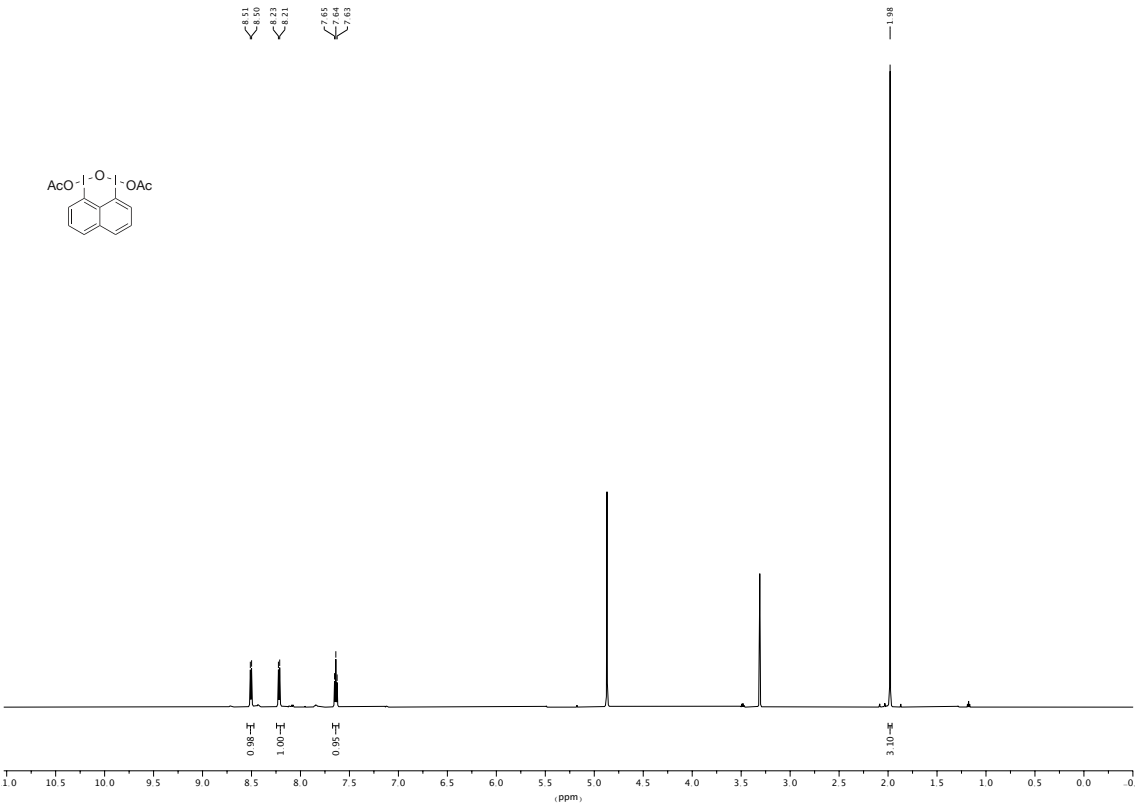

Figure 7.11. 600 MHz ^{1}H NMR spectrum of the compound **118** in CD_3OD.

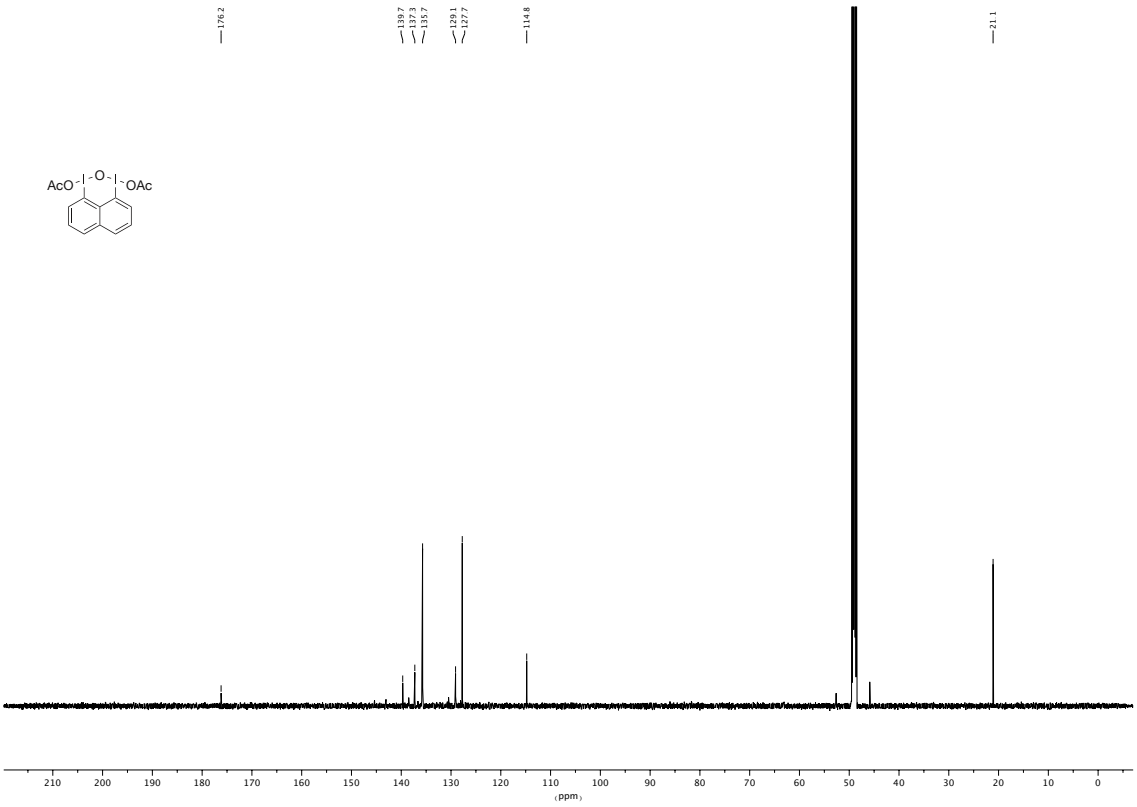

Figure 7.12. 151 MHz ^{13}C NMR spectrum of the compound **118** in CD_3OD.

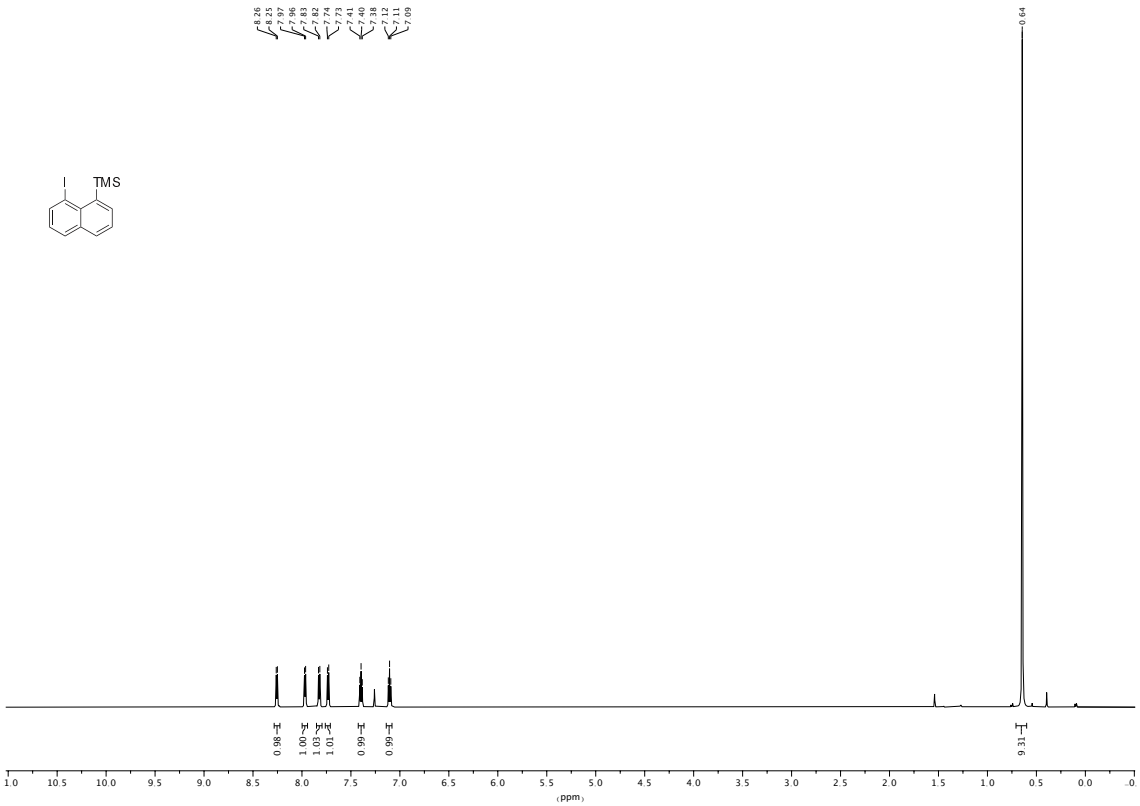

Figure 7.13. 600 MHz ^{1}H NMR spectrum of the compound **124** in $CDCl_3$.

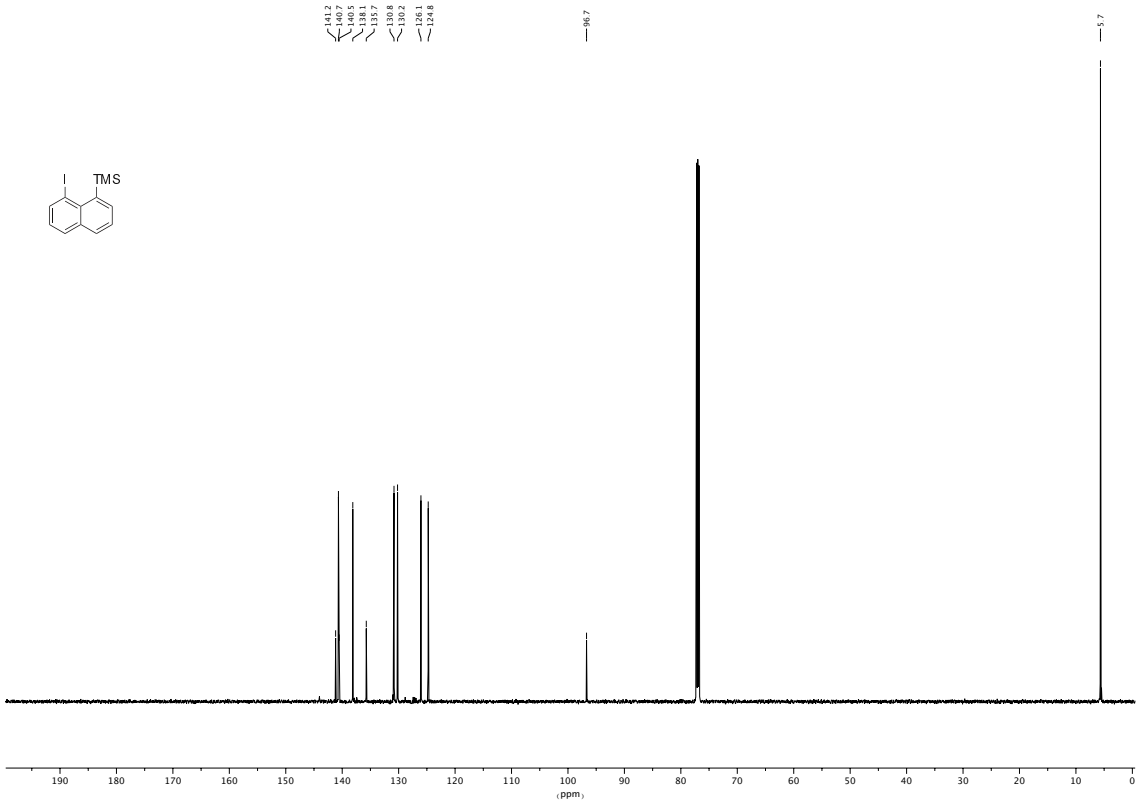

Figure 7.14. 151 MHz ^{13}C NMR spectrum of the compound **124** in $CDCl_3$.

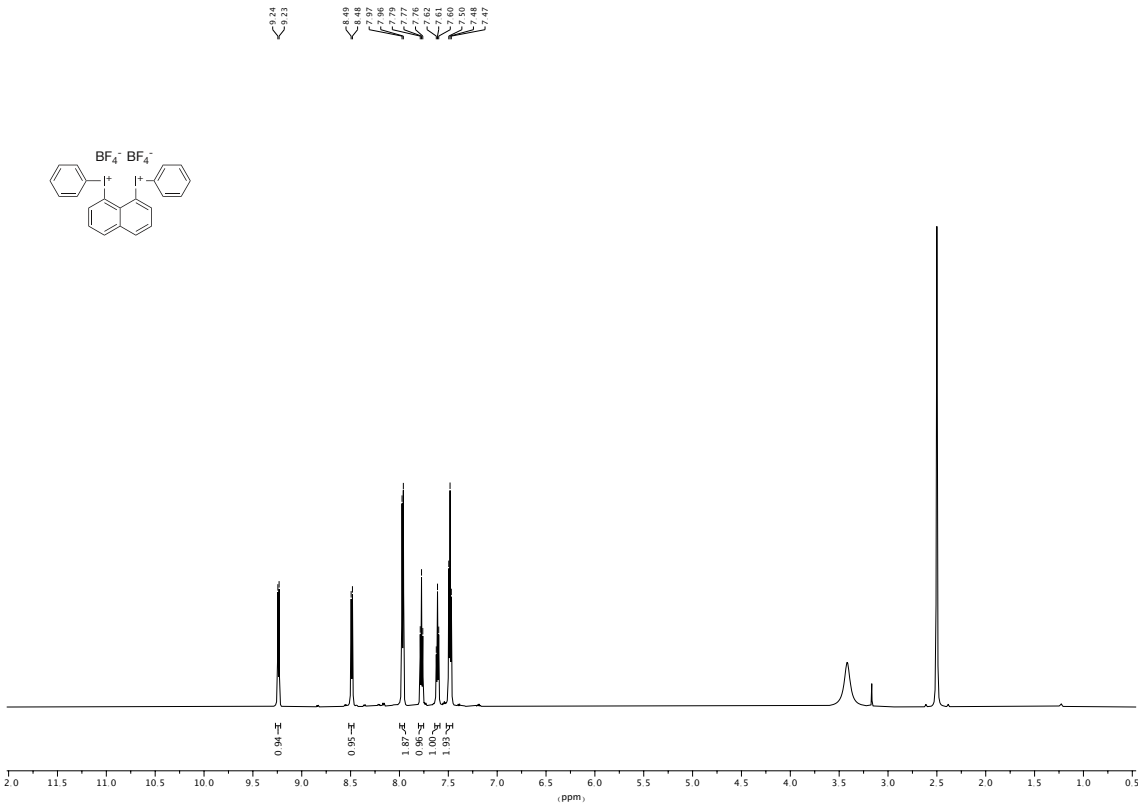

Figure 7.15. 601 MHz ^{1}H NMR spectrum of the compound **114a** in DMSO-d_6.

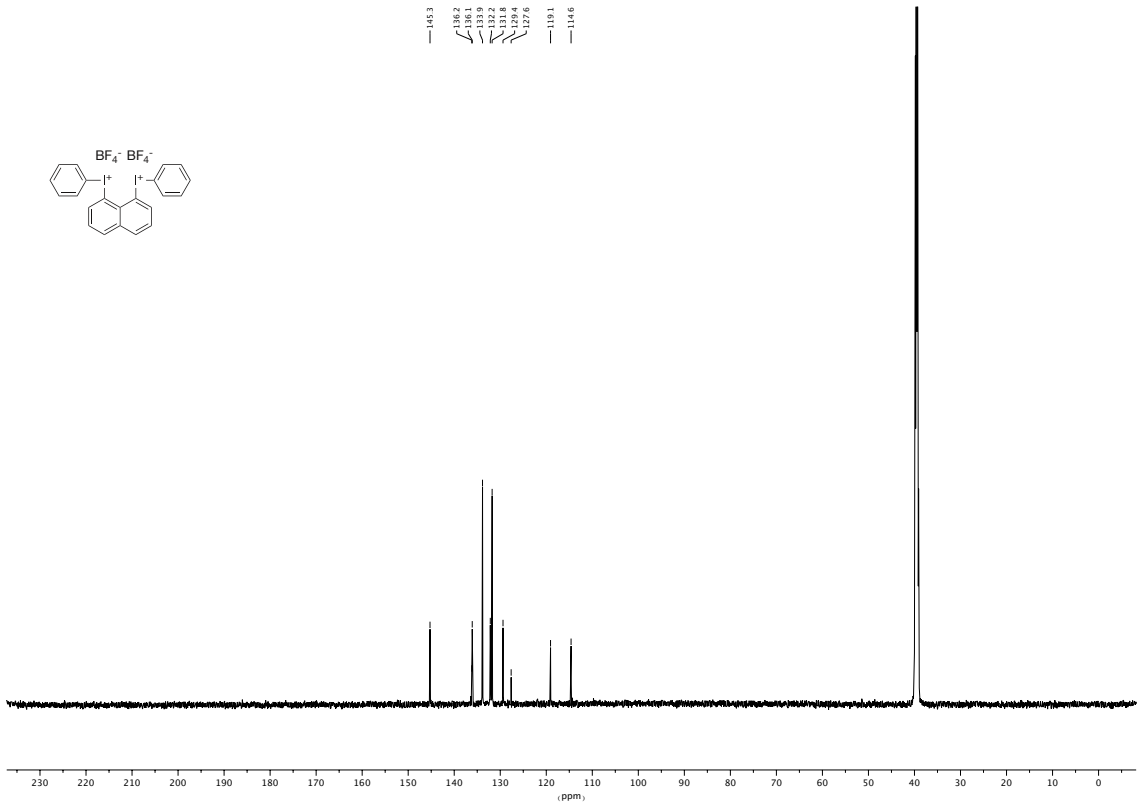

Figure 7.16. 151 MHz ^{13}C NMR spectrum of the compound **114a** in DMSO-d_6.

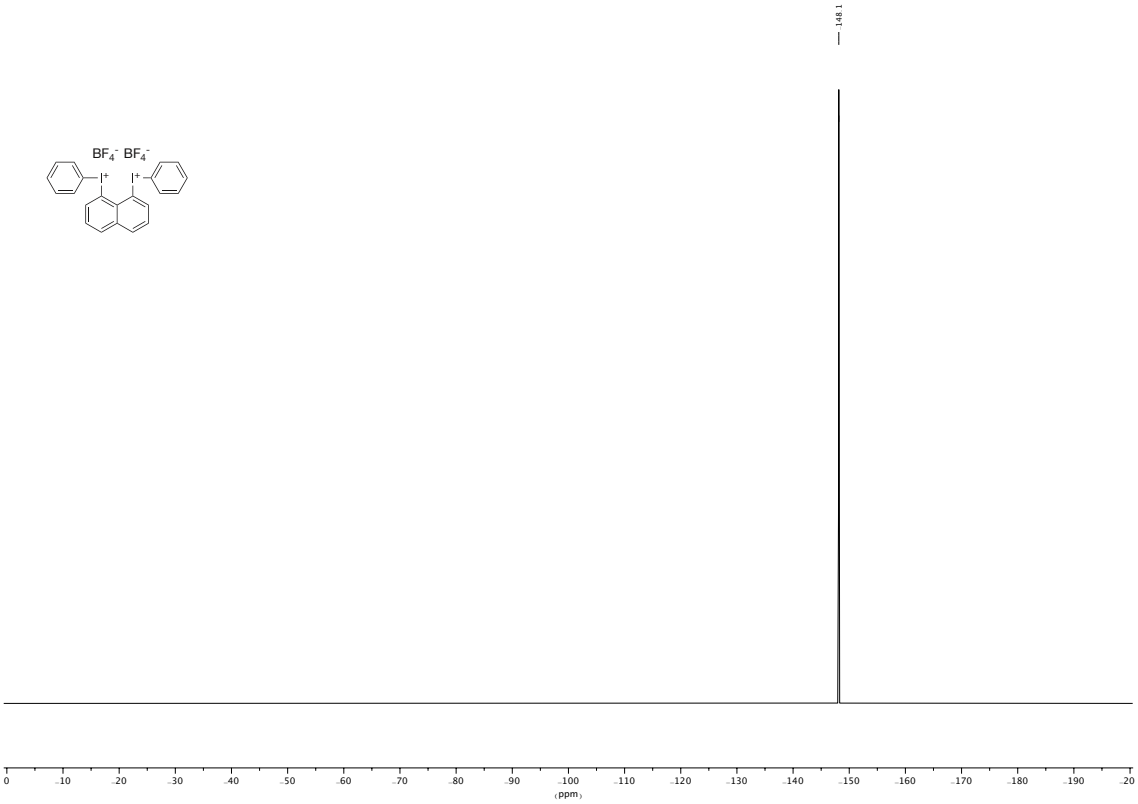

Figure 7.17. 565 MHz ^{19}F NMR spectrum of the compound **114a** in DMSO-d_6.

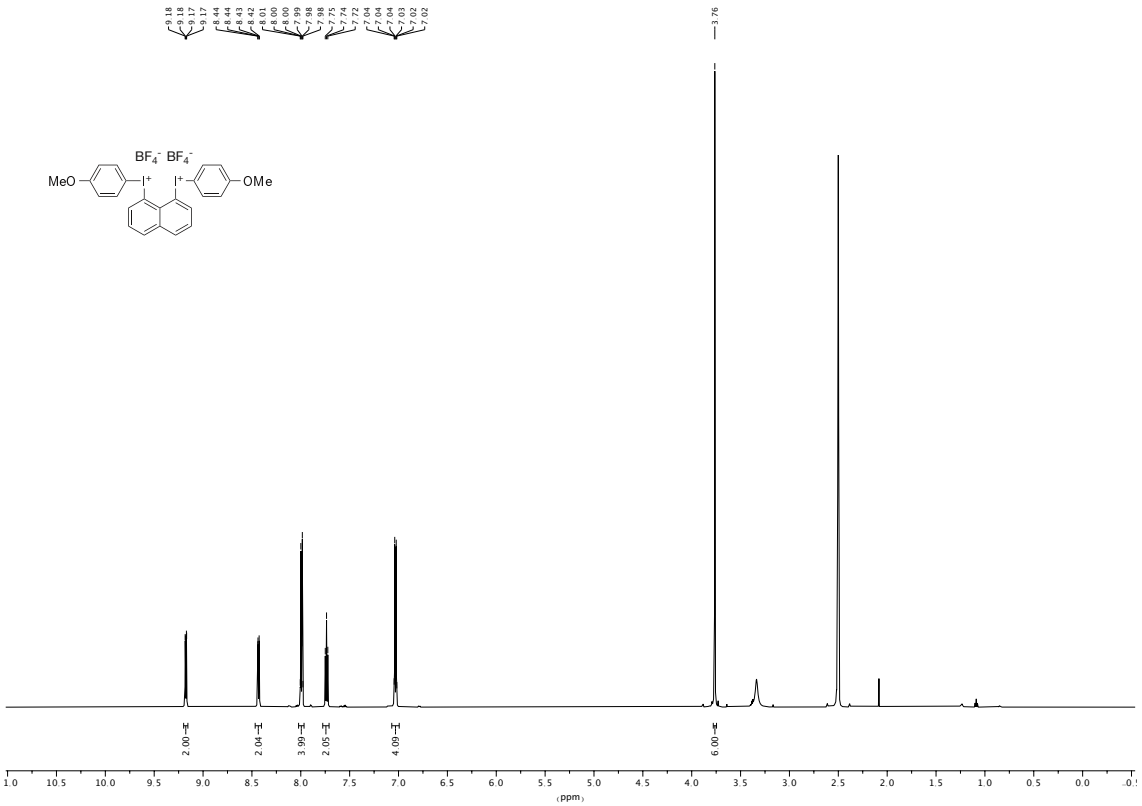

Figure 7.18. 600 MHz ^{1}H NMR spectrum of the compound **114b** in DMSO-d_6.

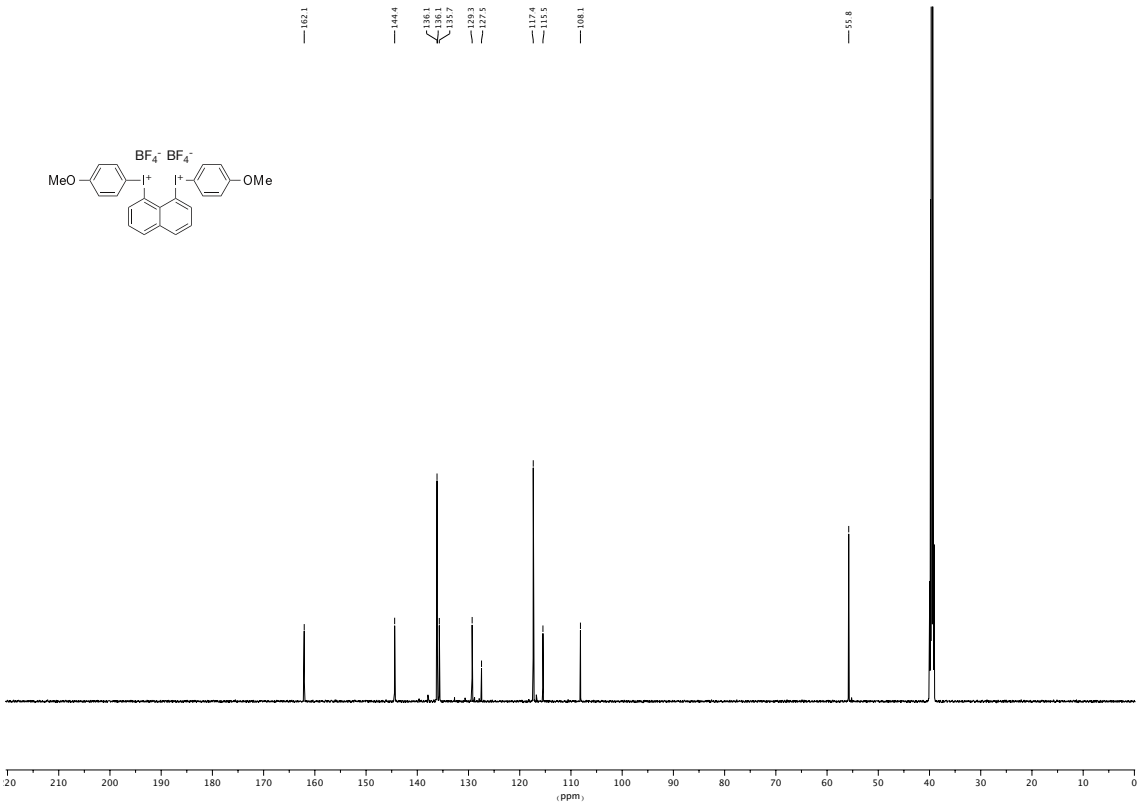

Figure 7.19. 151 MHz ^{13}C NMR spectrum of the compound **114b** in DMSO-d_6.

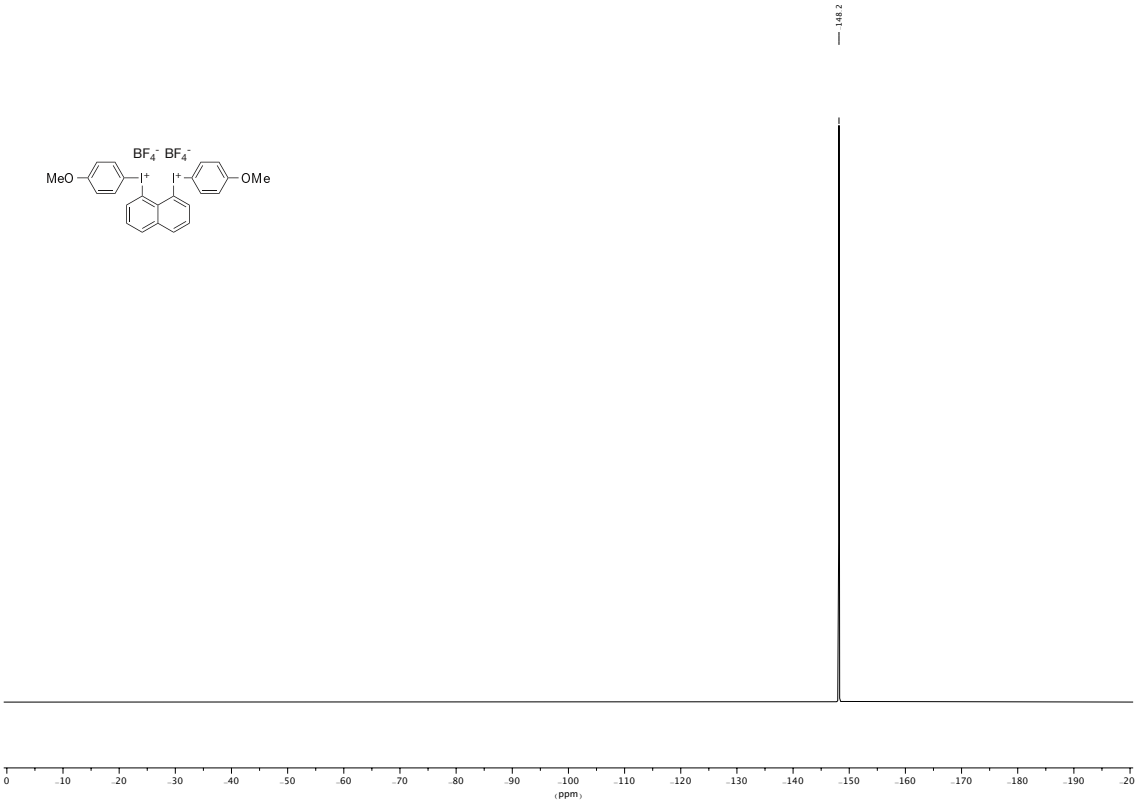

Figure 7.20. 565 MHz ^{19}F NMR spectrum of the compound **114b** in DMSO-d_6.

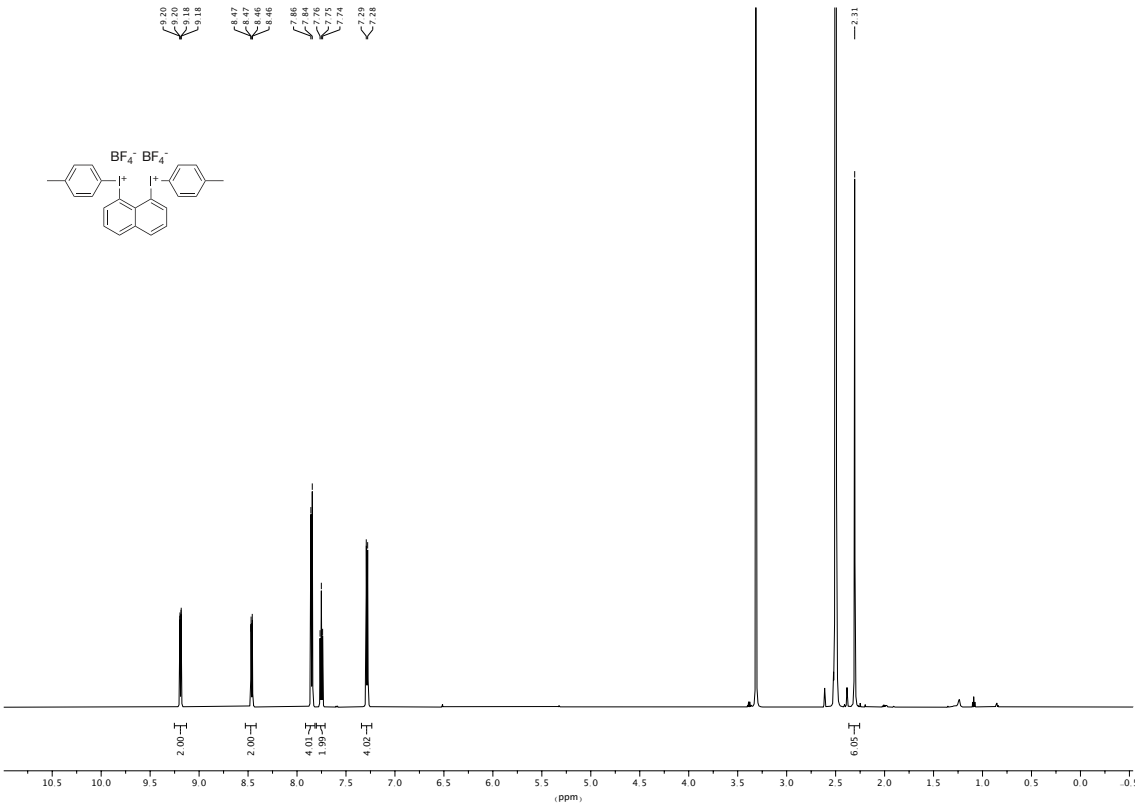

Figure 7.21. 600 MHz ^{1}H NMR spectrum of the compound **114c** in DMSO-d_6.

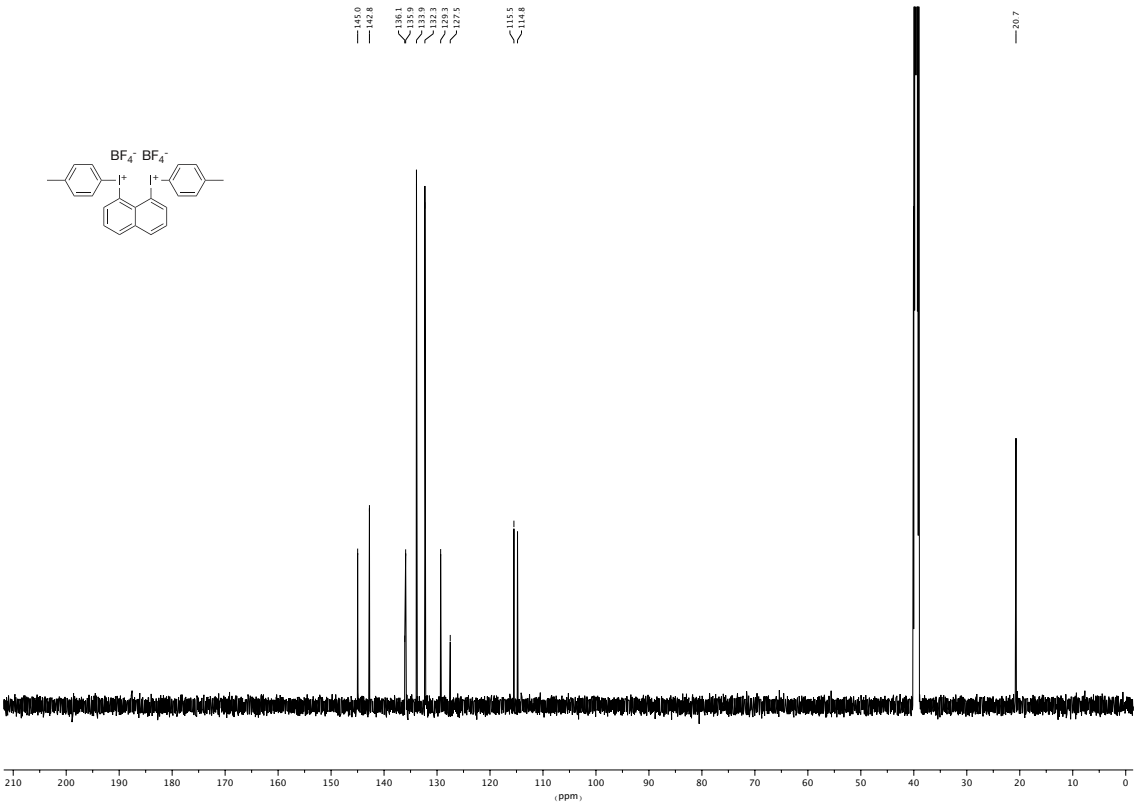

Figure 7.22. 151 MHz ^{13}C NMR spectrum of the compound **114c** in DMSO-d_6.

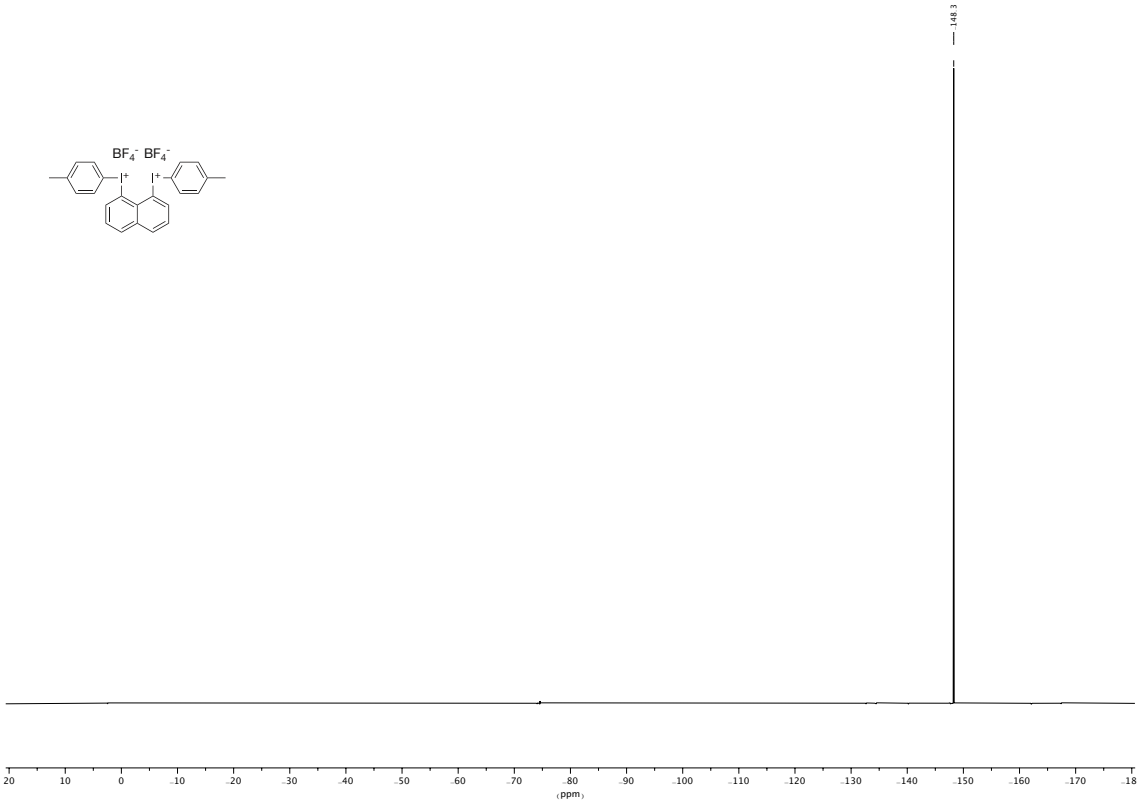

Figure 7.23. 565 MHz ^{19}F NMR spectrum of the compound **114c** in DMSO-d_6.

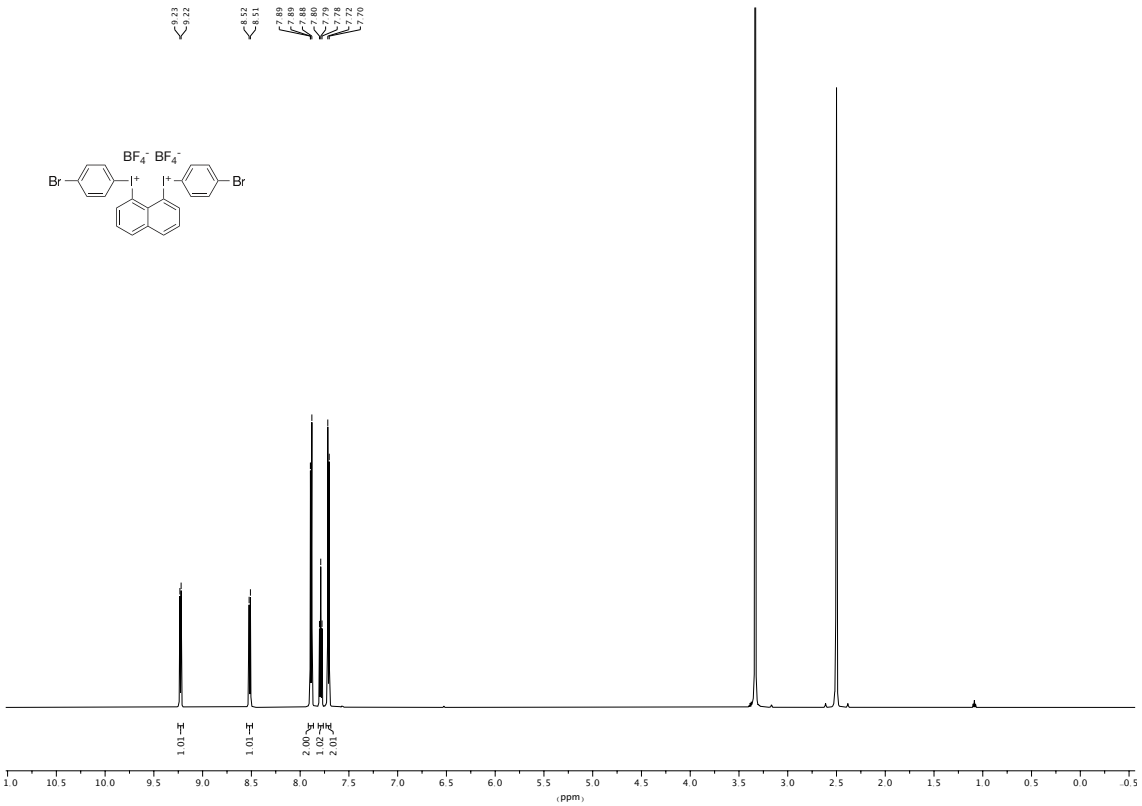

Figure 7.24. 600 MHz ^{1}H NMR spectrum of the compound **114d** in DMSO-d_6.

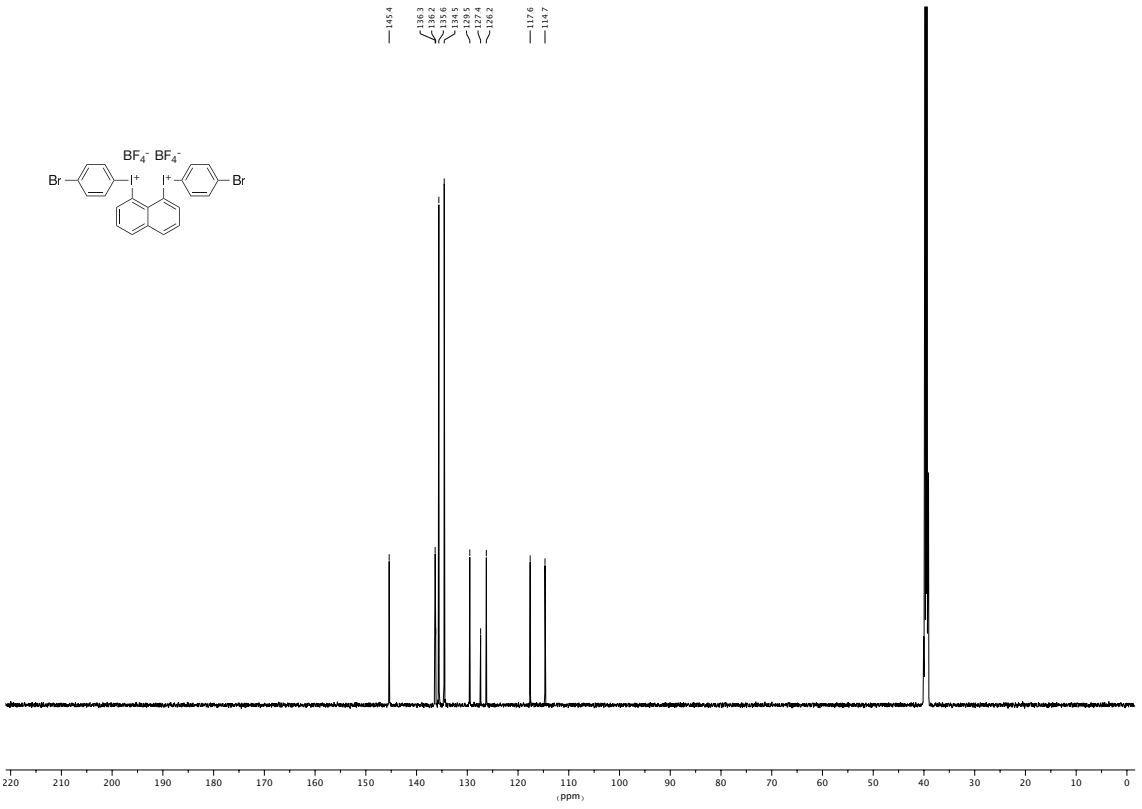

Figure 7.25. 151 MHz ^{13}C NMR spectrum of the compound **114d** in DMSO-d_6.

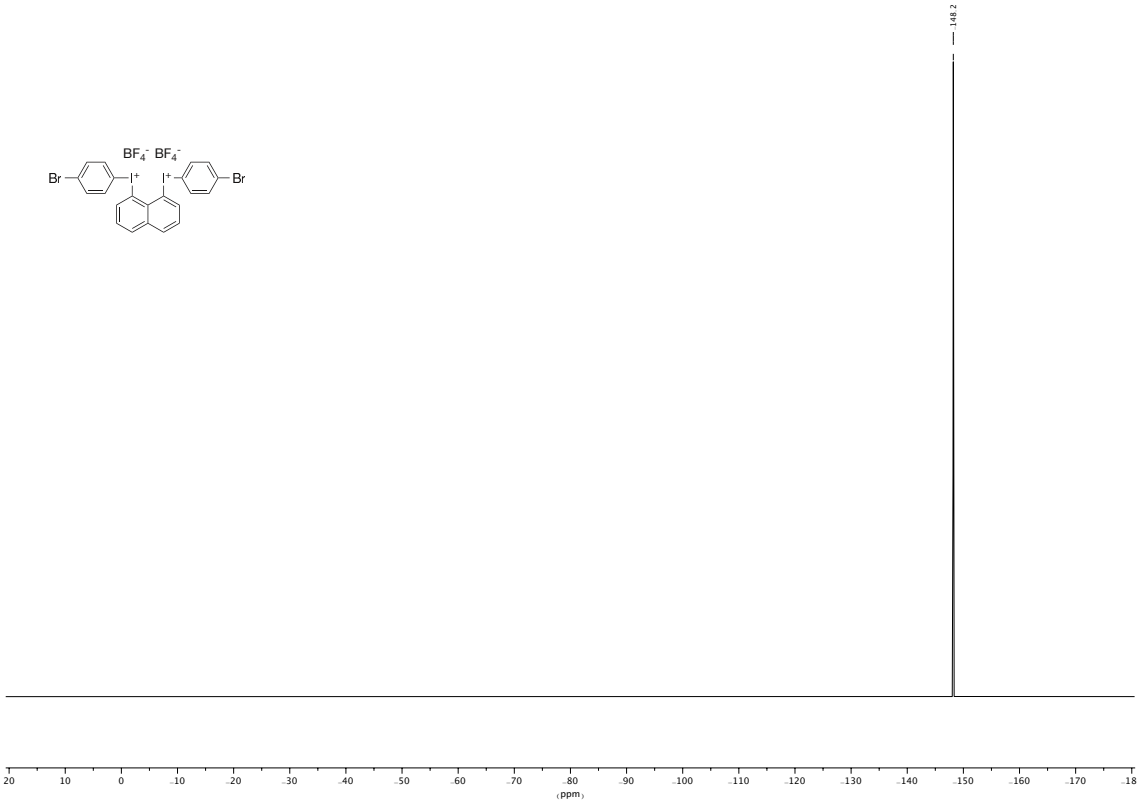

Figure 7.26. 565 MHz ^{19}F NMR spectrum of the compound **114d** in DMSO-d_6.

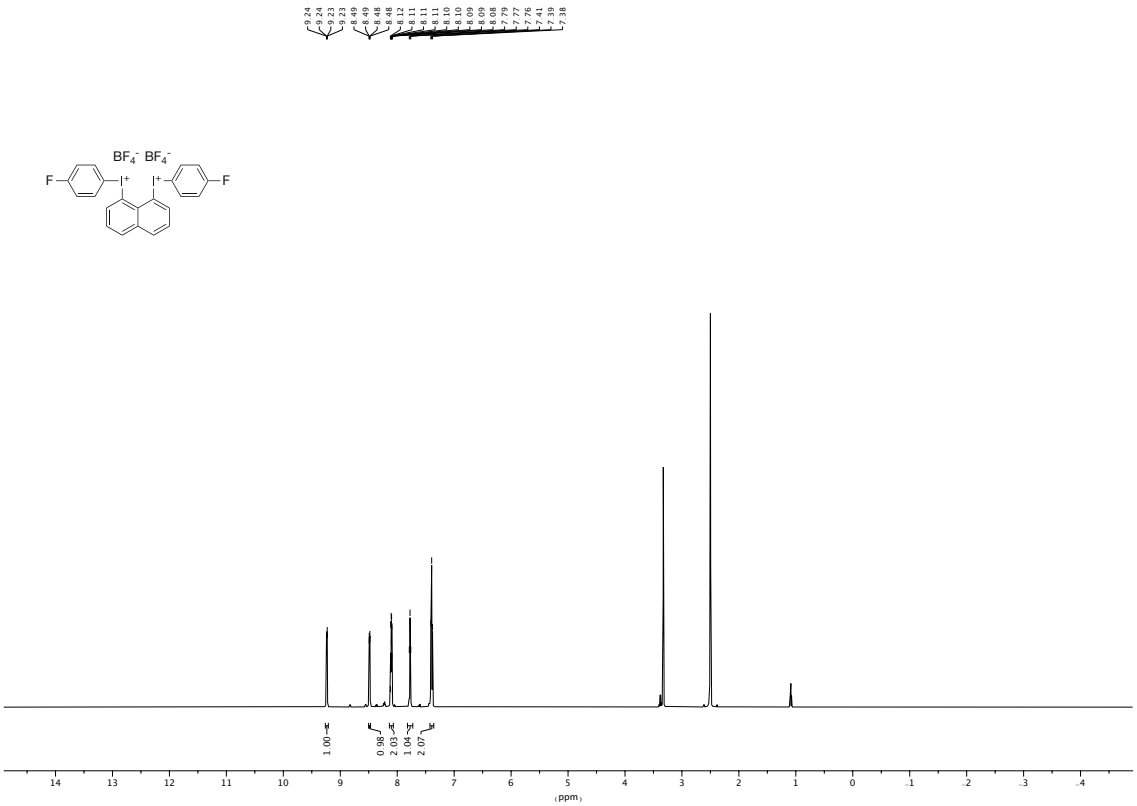

Figure 7.27. 600 MHz ^{1}H NMR spectrum of the compound **114e** in DMSO-d_6.

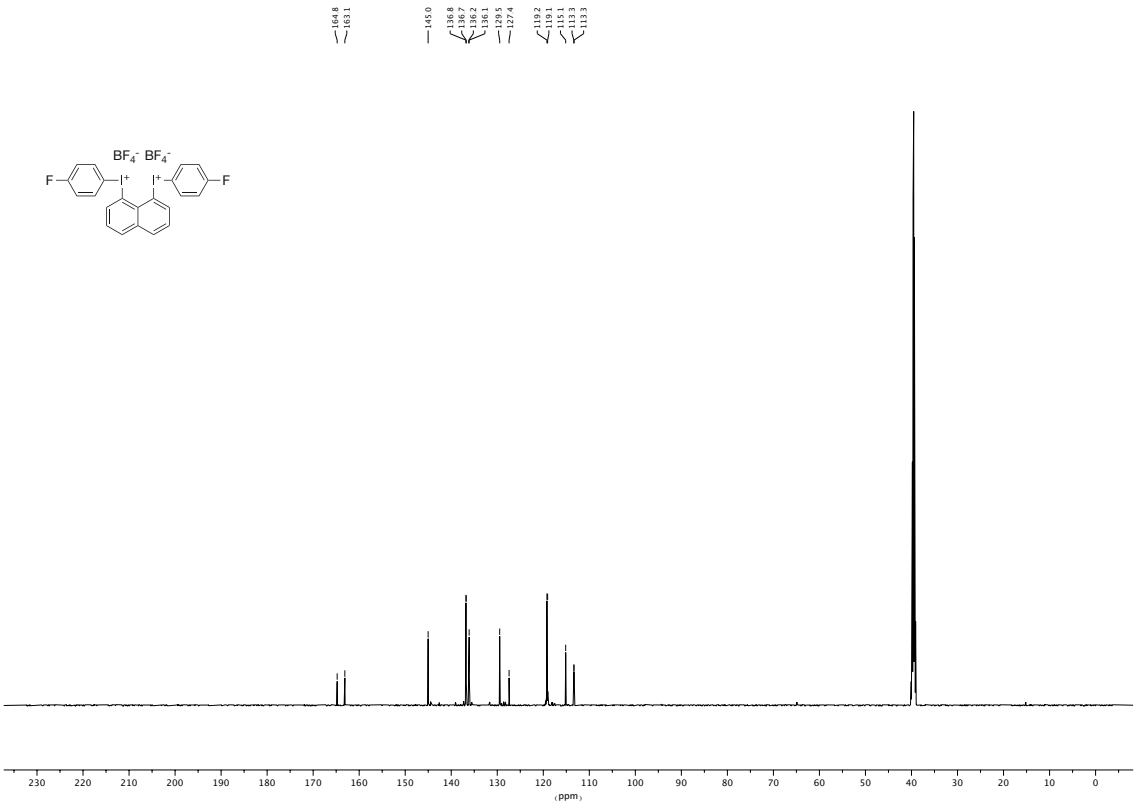

Figure 7.28. 151 MHz ^{13}C NMR spectrum of the compound **114e** in DMSO-d_6.

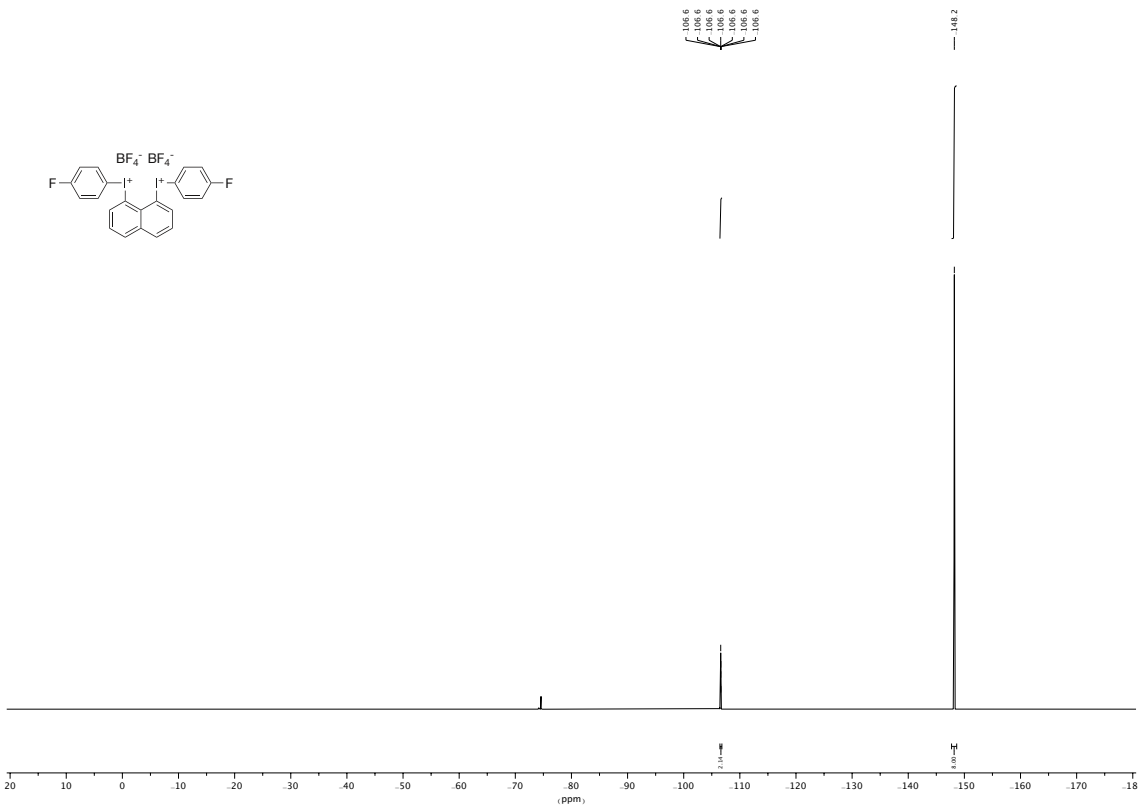

Figure 7.29. 565 MHz ^{19}F NMR spectrum of the compound **114e** in DMSO-d_6.

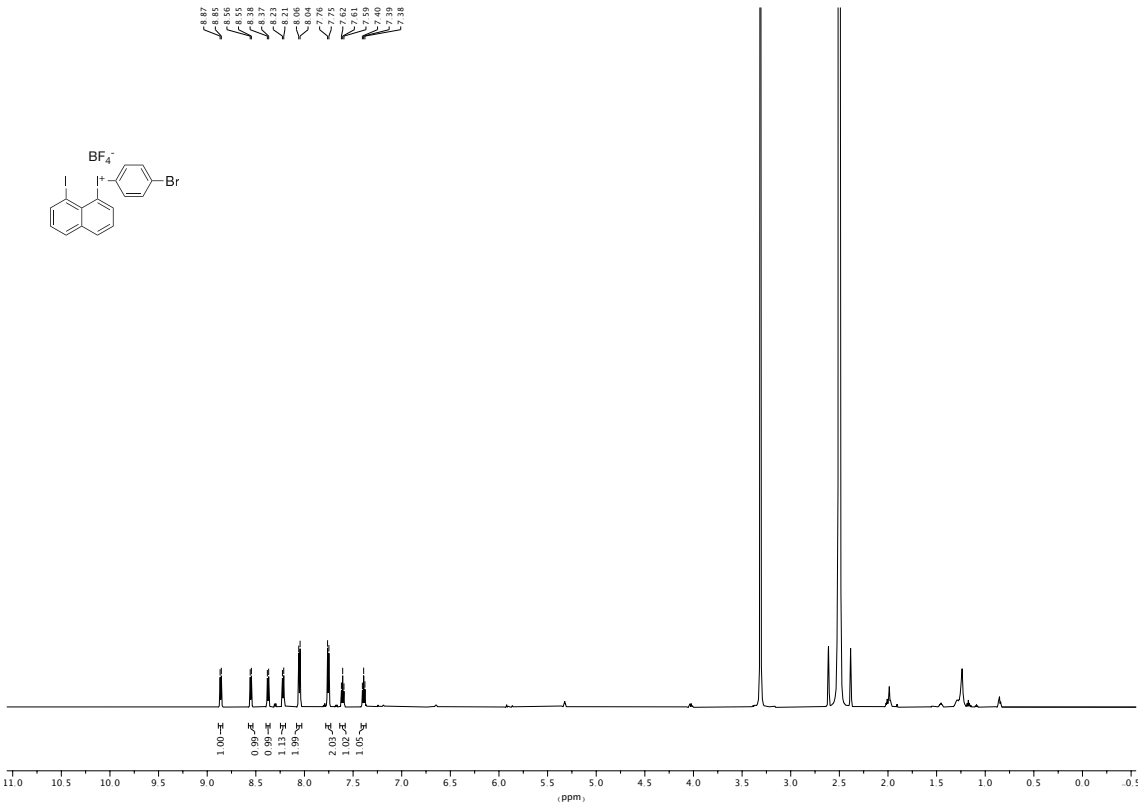

Figure 7.30. 600 MHz ^{1}H NMR spectrum of the compound **116a** in DMSO-d_6.

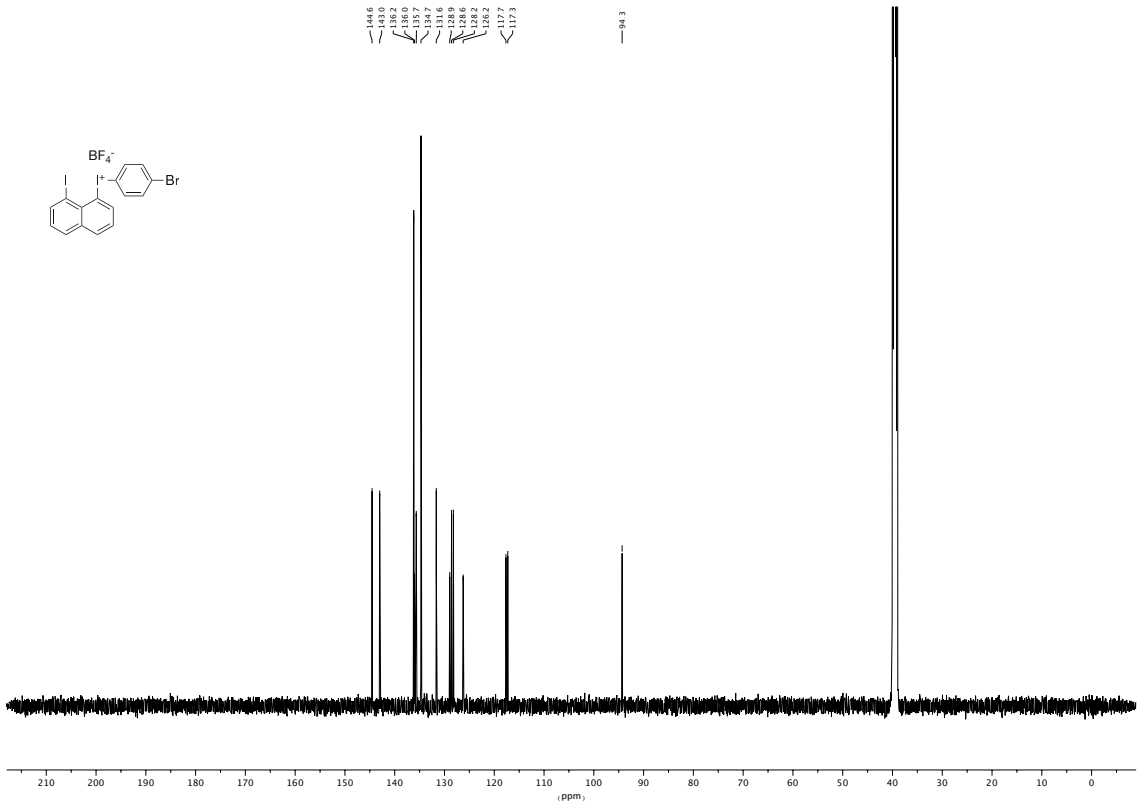

Figure 7.31. 151 MHz ^{13}C NMR spectrum of the compound **116a** in DMSO-d_6.

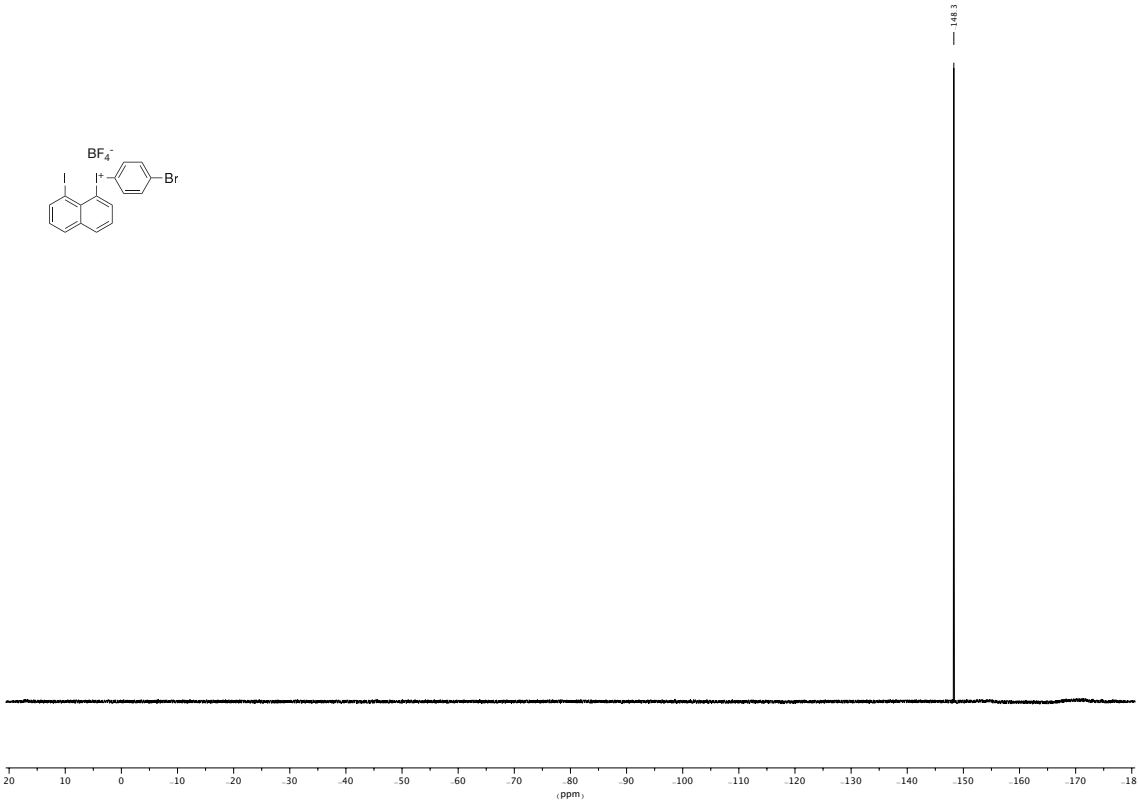

Figure 7.32. 565 MHz ^{19}F NMR spectrum of the compound **116a** in DMSO-d_6.

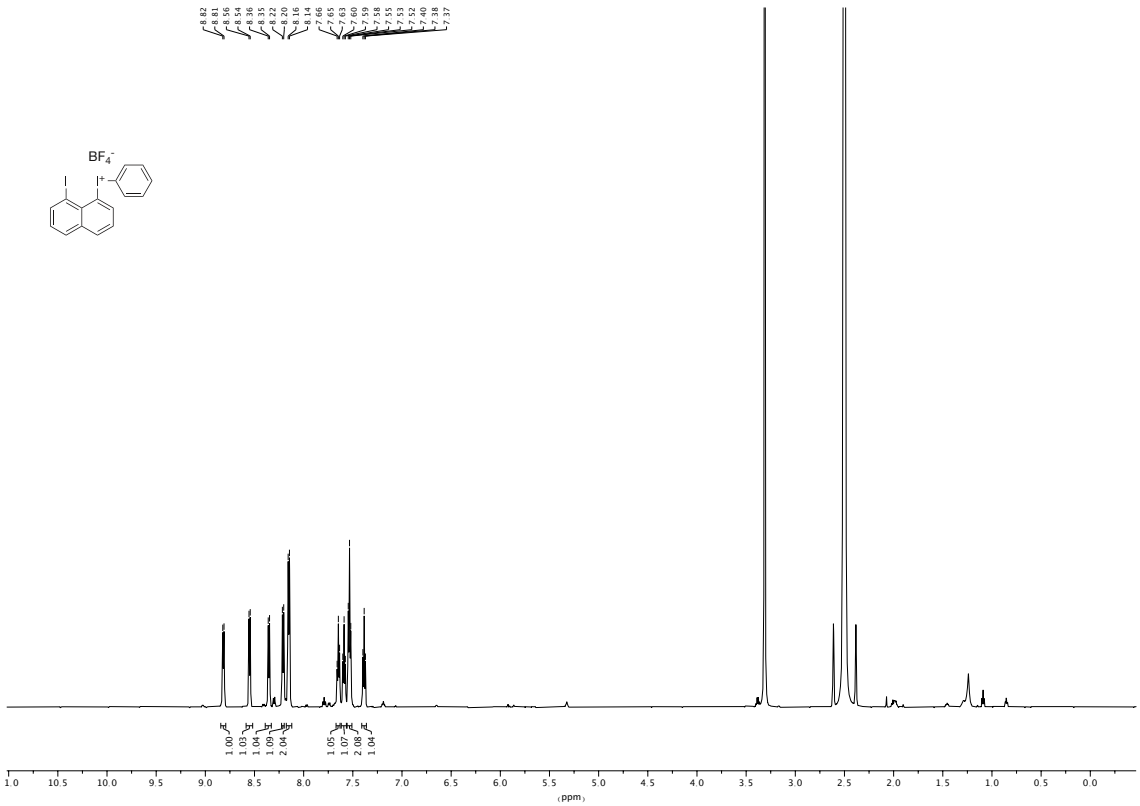

Figure 7.33. 600 MHz ^{1}H NMR spectrum of the compound **116b** in DMSO-d_6.

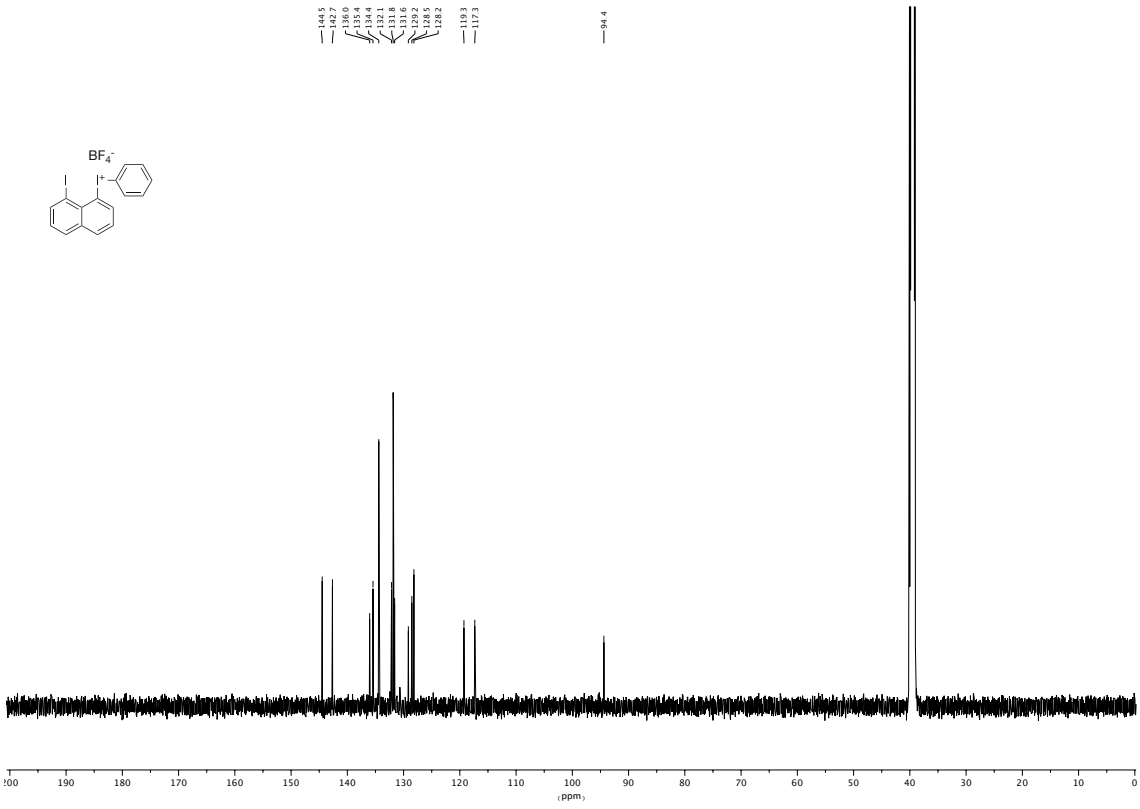

Figure 7.34. 151 MHz ^{13}C NMR spectrum of the compound **116b** in DMSO-d_6.

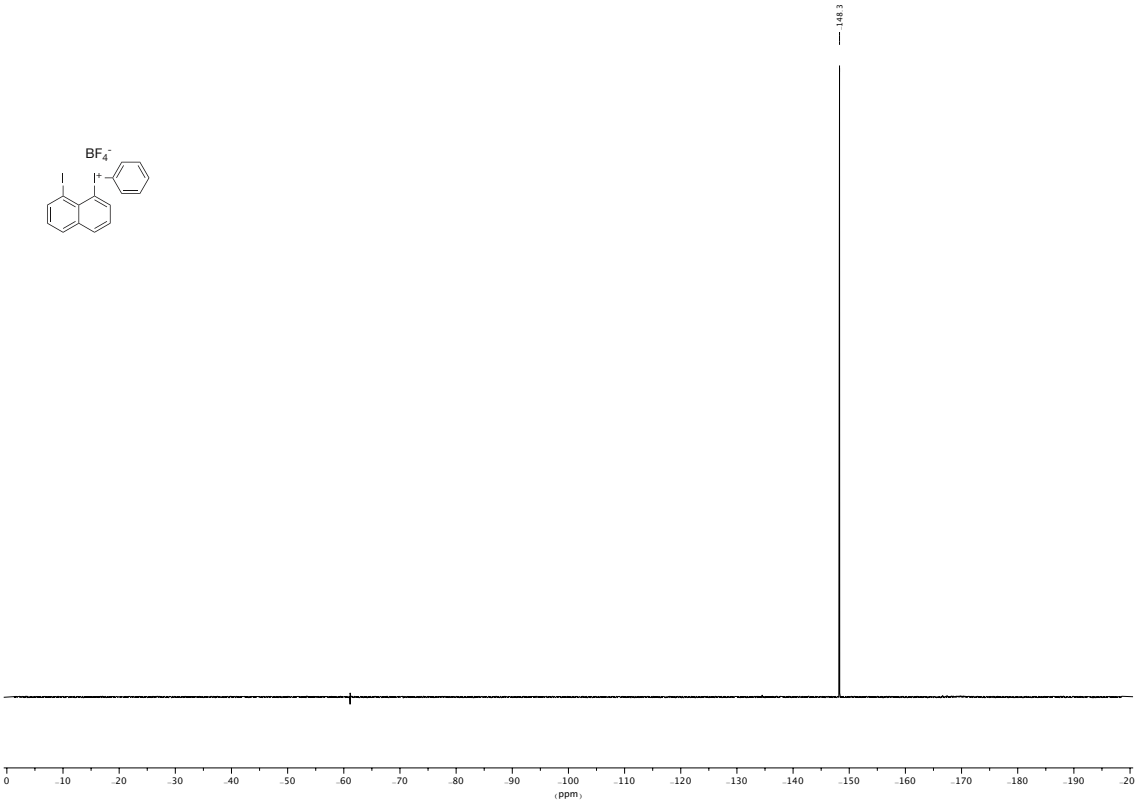

Figure 7.35. 565 MHz ^{19}F NMR spectrum of the compound **116b** in DMSO-d_6.

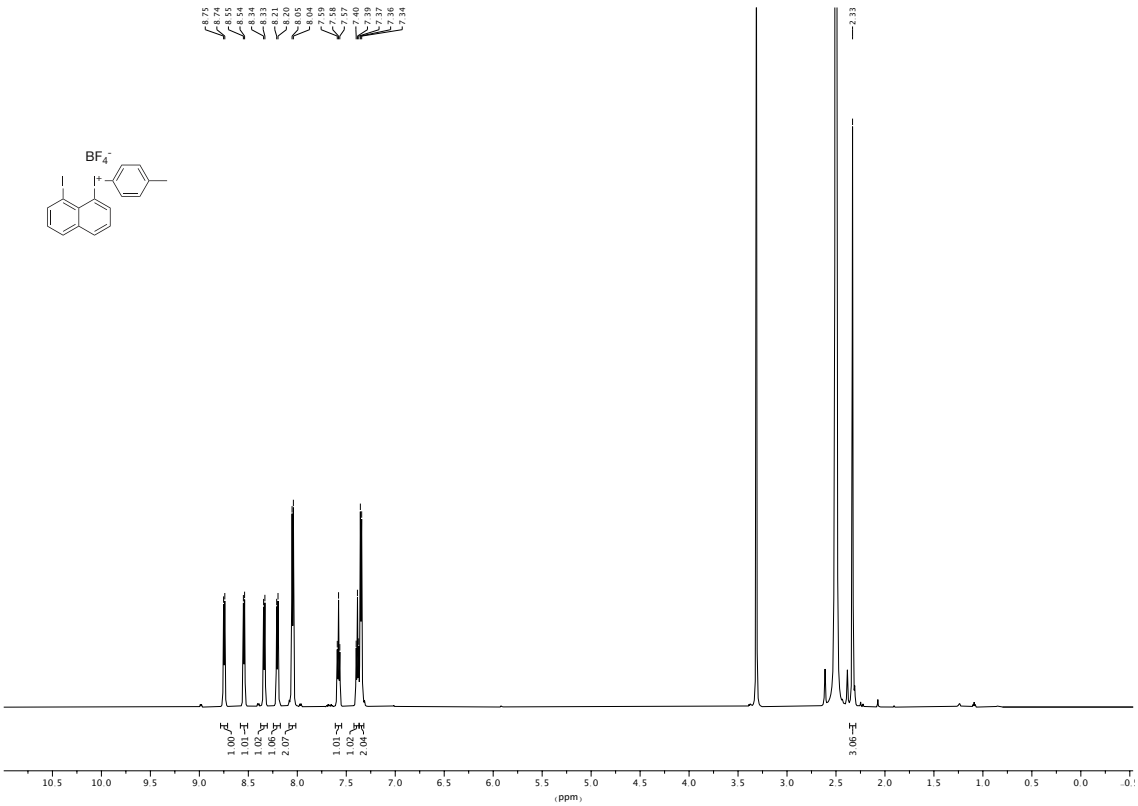

Figure 7.36. 600 MHz ^{1}H NMR spectrum of the compound **116c** in DMSO-d_6.

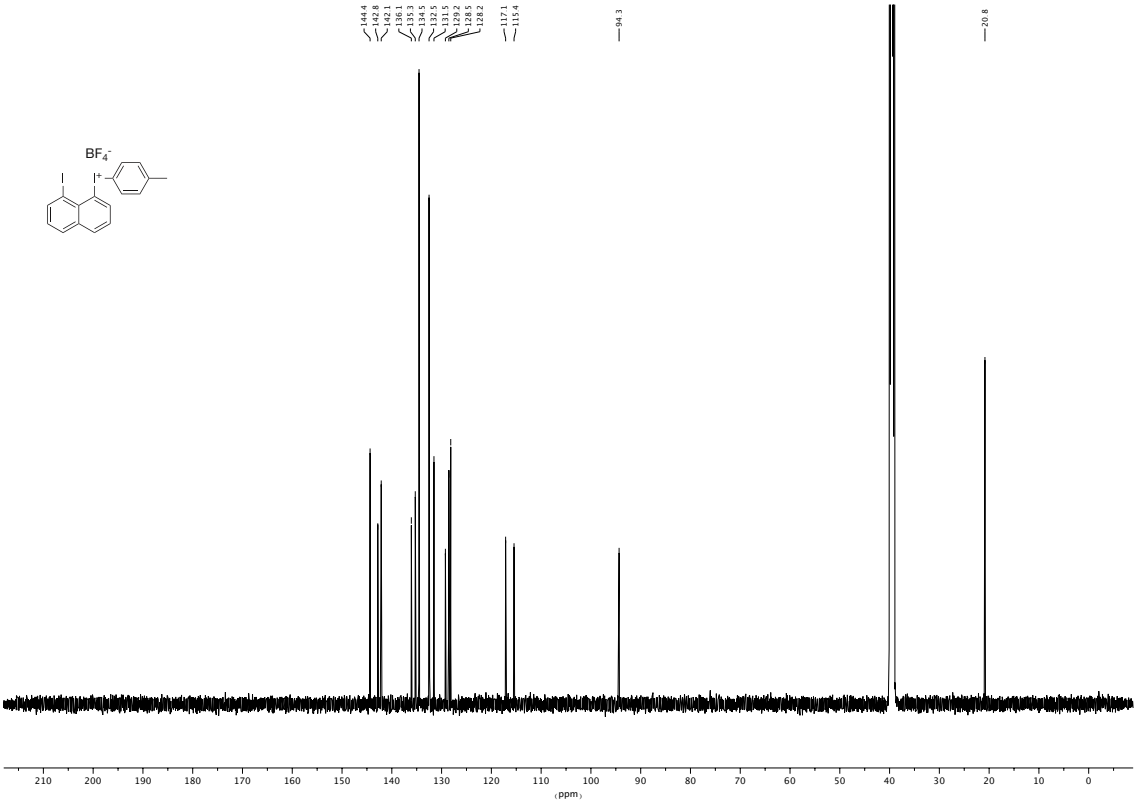

Figure 7.37. 151 MHz ^{13}C NMR spectrum of the compound **116c** in DMSO-d_6.

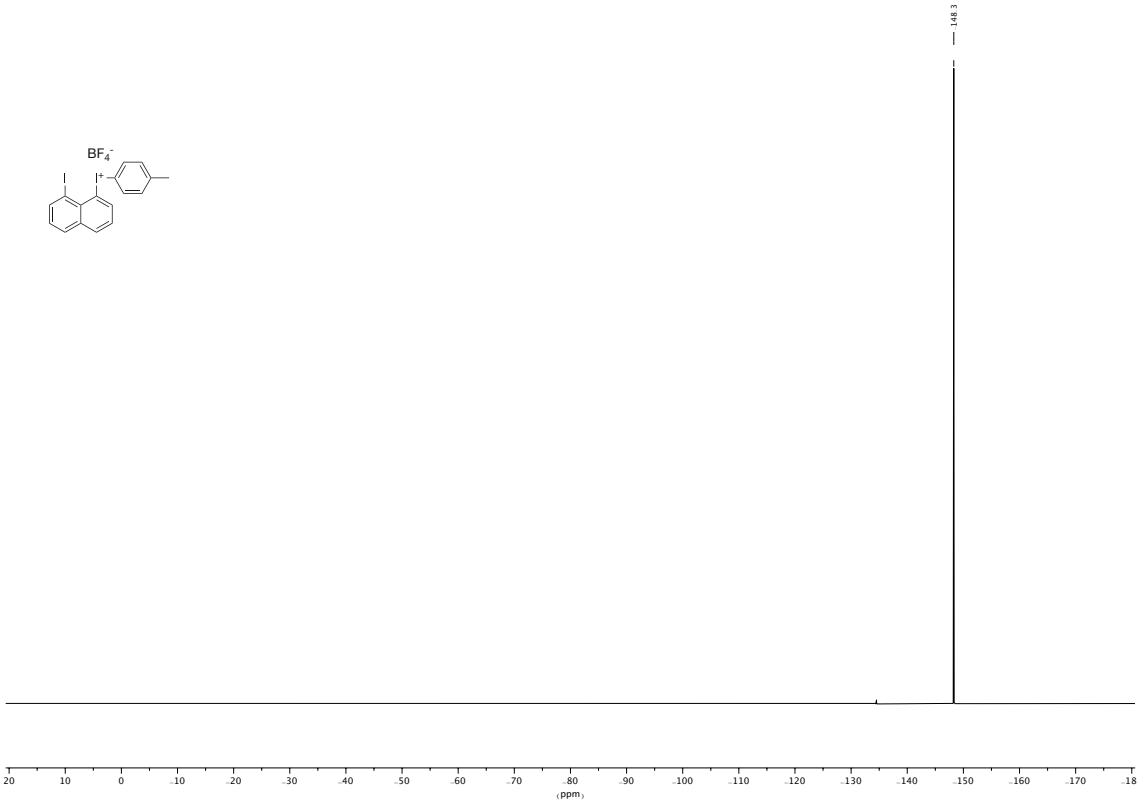

Figure 7.38. 565 MHz ^{19}F NMR spectrum of the compound **116c** in DMSO-d_6.

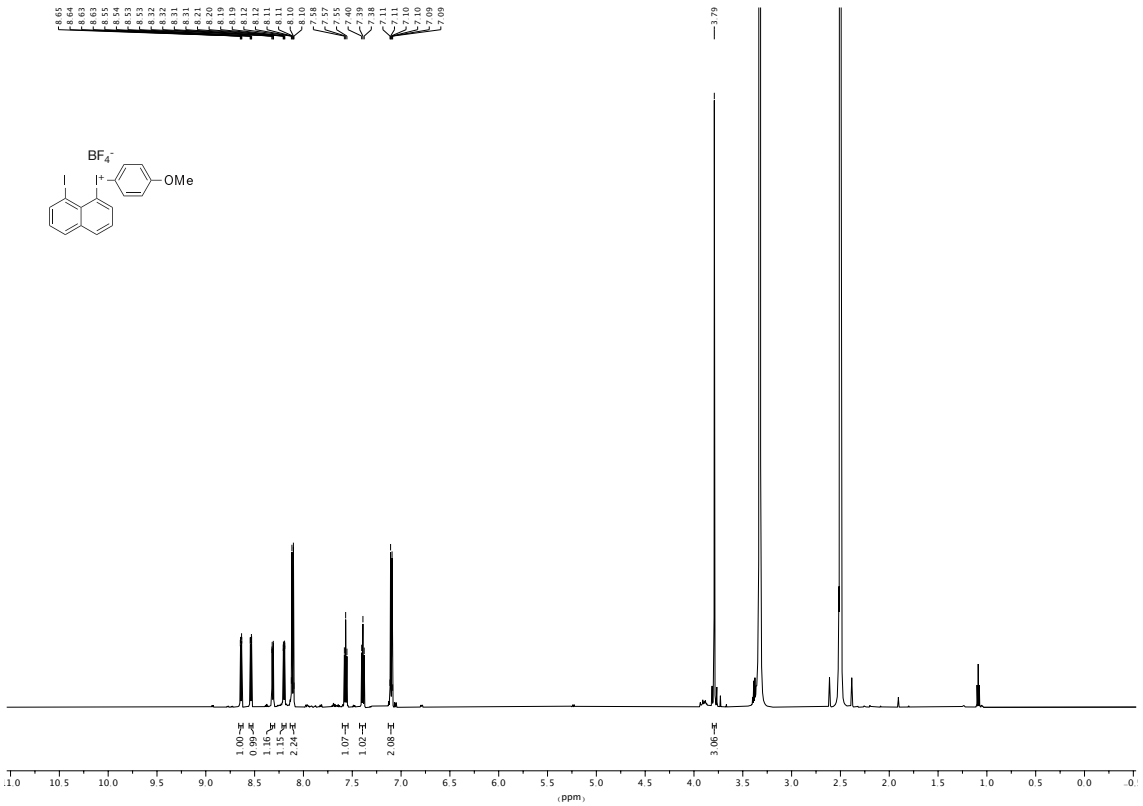

Figure 7.39. 600 MHz ^{1}H NMR spectrum of the compound **116d** in DMSO-d_6.

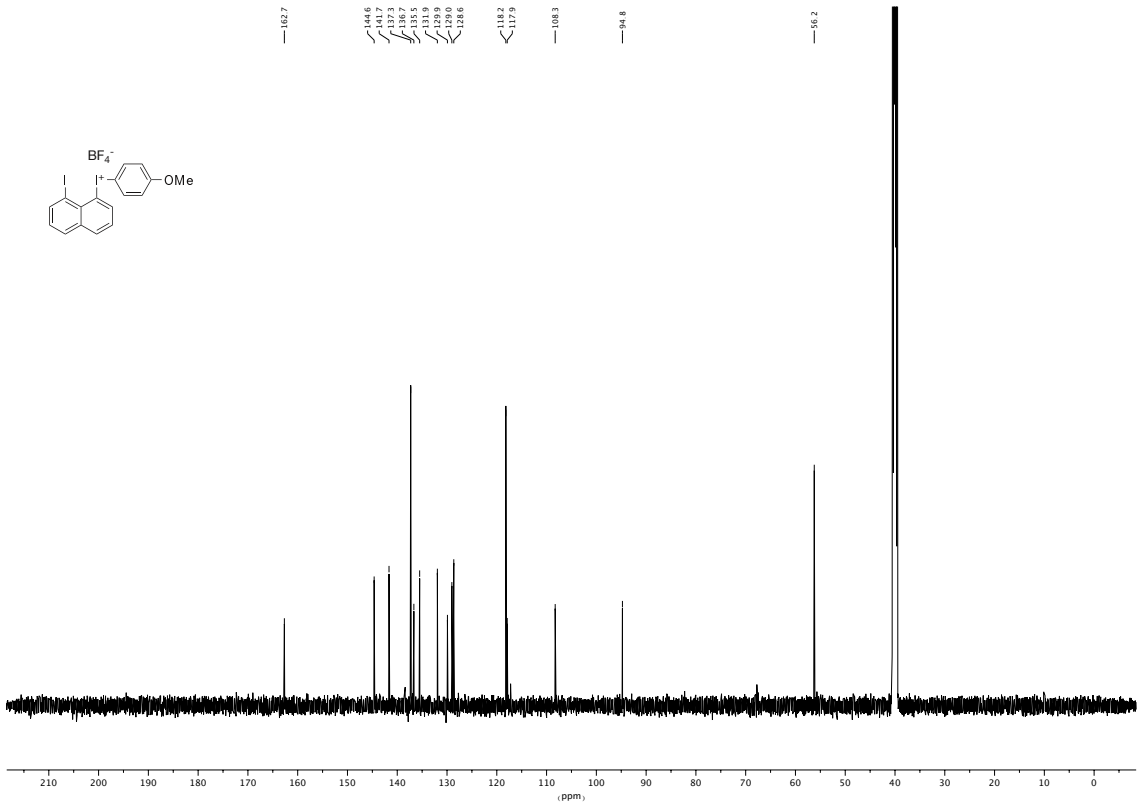

Figure 7.40. 151 MHz ^{13}C NMR spectrum of the compound **116d** in DMSO-d_6.

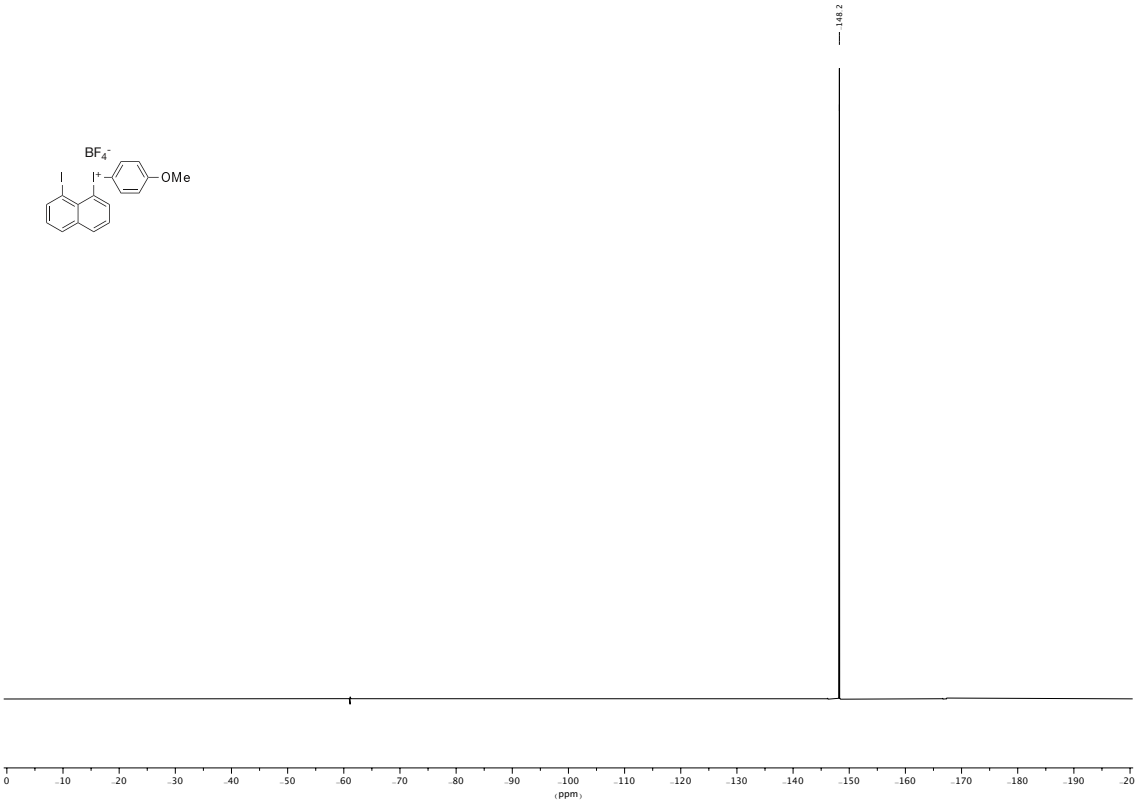

Figure 7.41. 565 MHz ^{19}F NMR spectrum of the compound **116d** in DMSO-d_6.

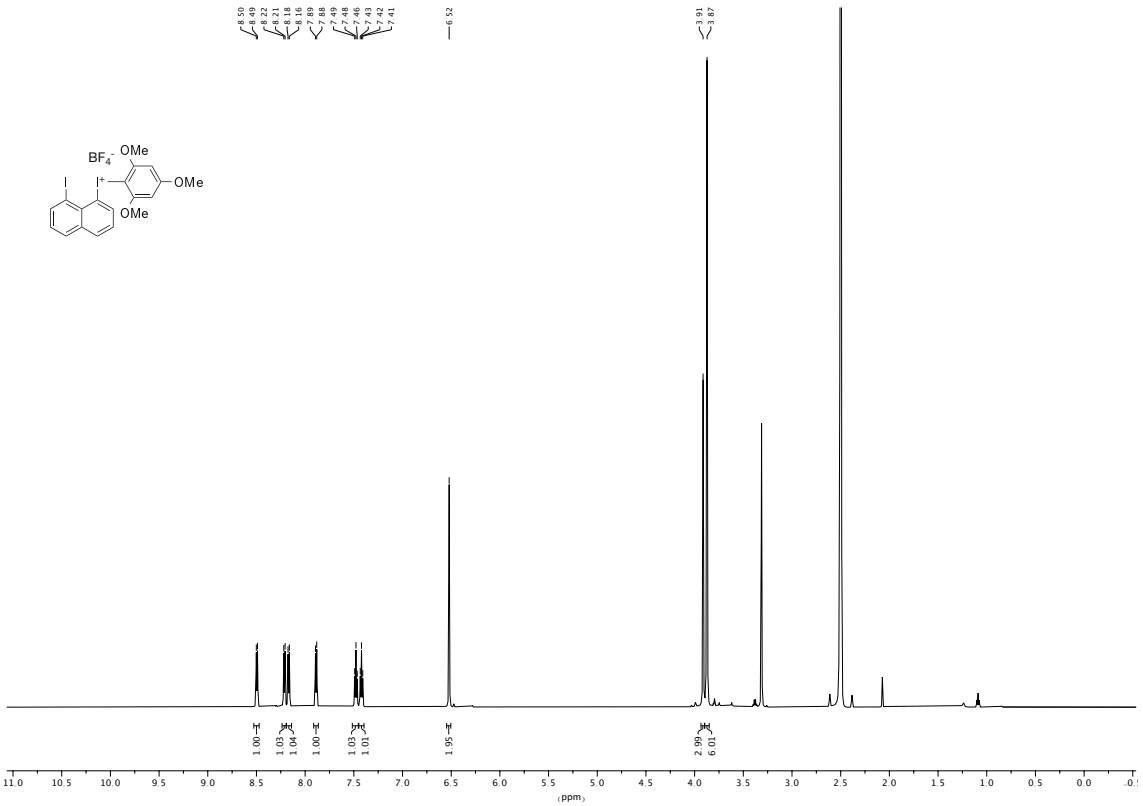

Figure 7.42. 600 MHz ^{1}H NMR spectrum of the compound **116e** in DMSO-d_6.

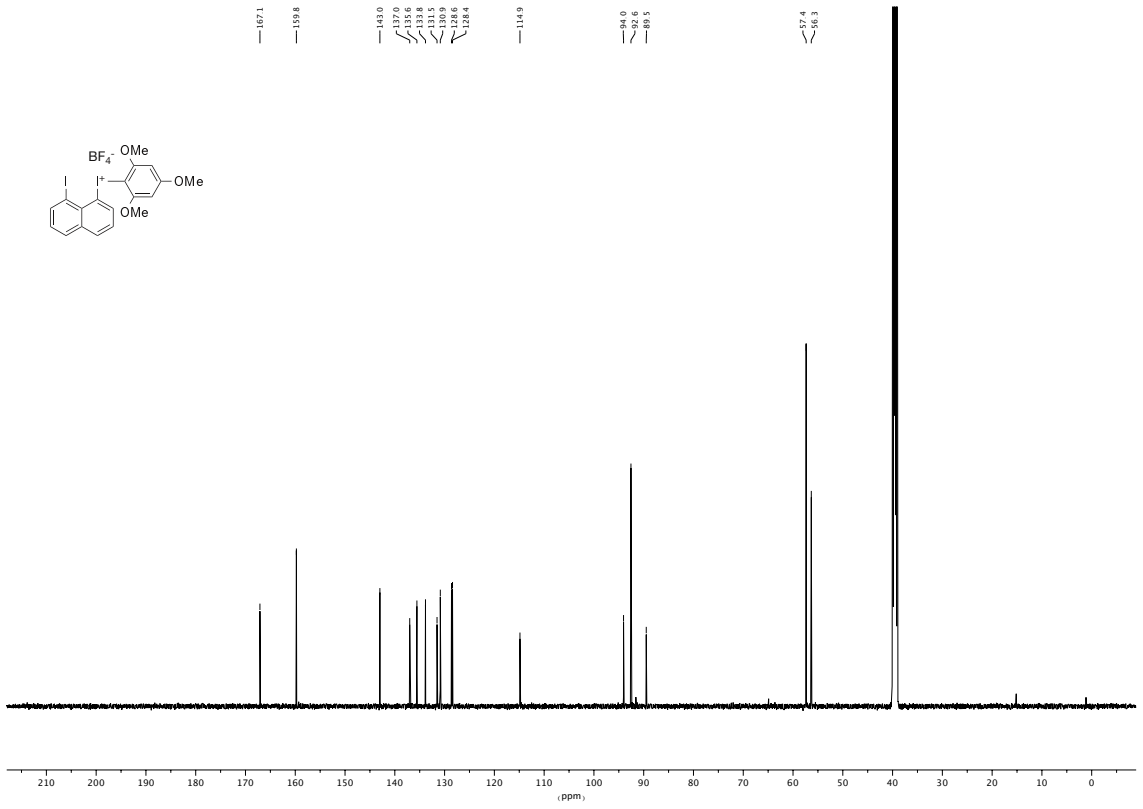

Figure 7.43. 151 MHz ^{13}C NMR spectrum of the compound **116e** in DMSO-d_6.

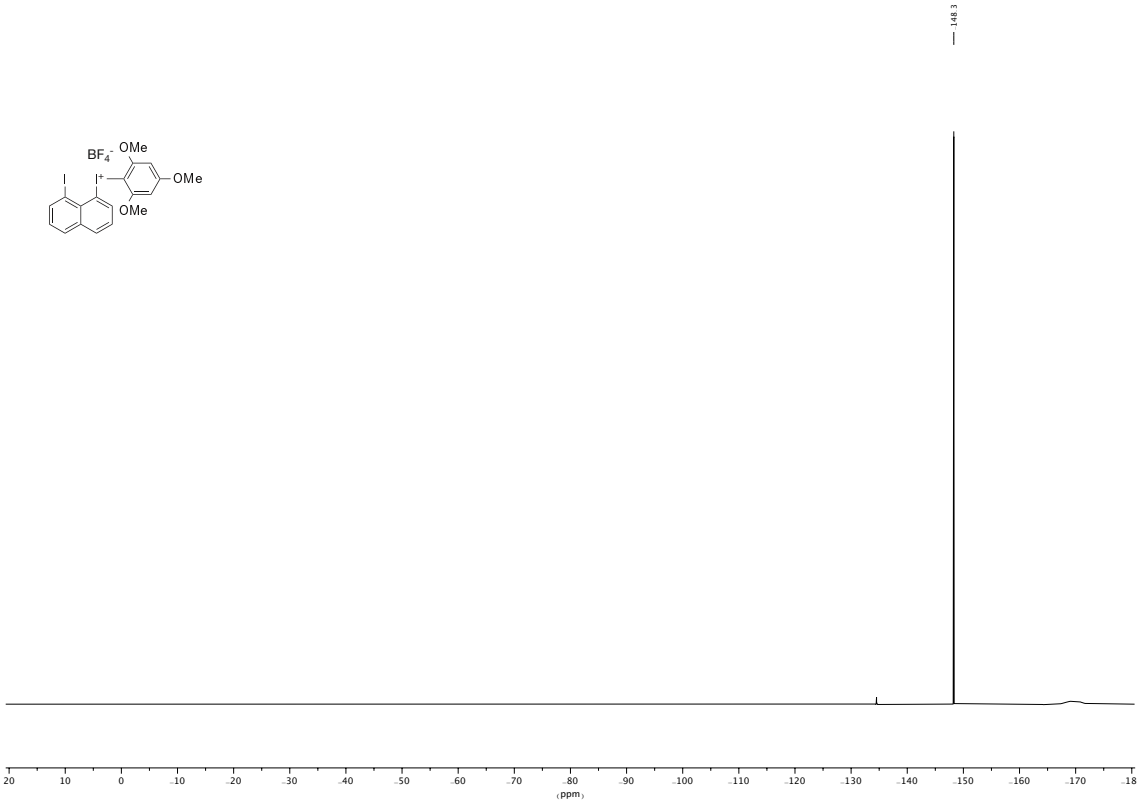

Figure 7.44. 565 MHz ^{19}F NMR spectrum of the compound **116e** in DMSO-d_6.

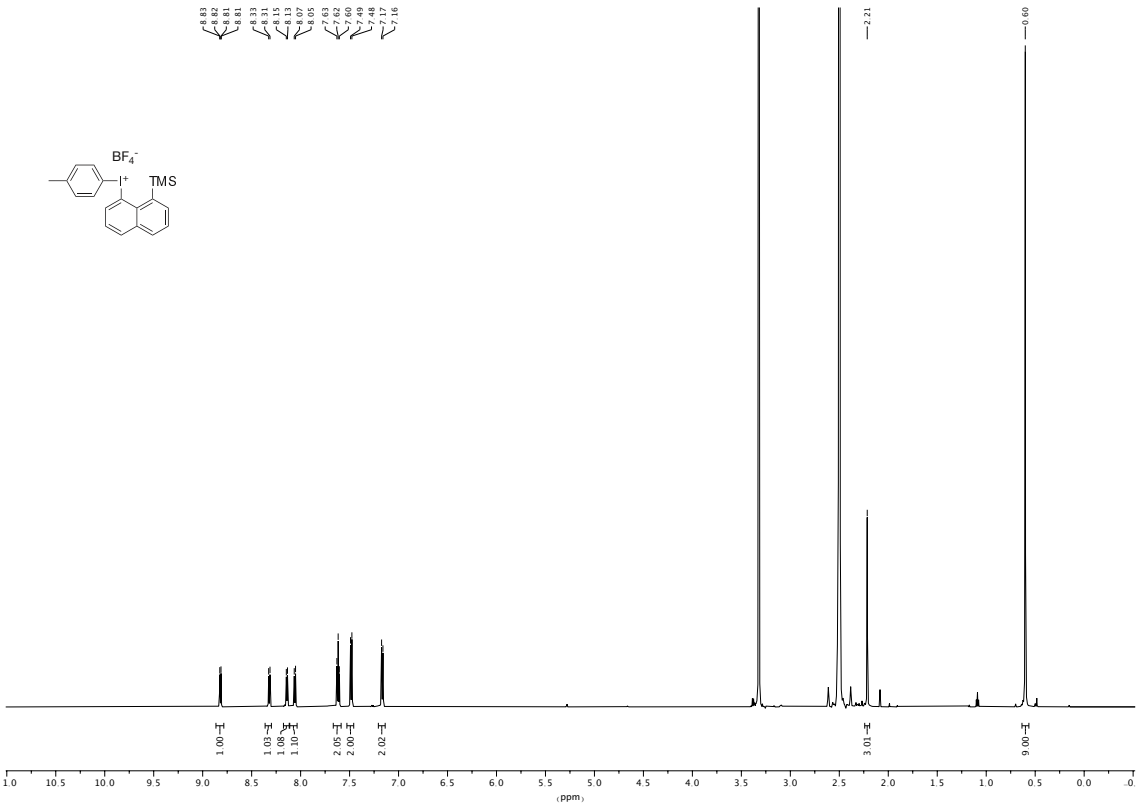

Figure 7.45. 601 MHz ^{1}H NMR spectrum of the compound **117a** in DMSO-d_6.

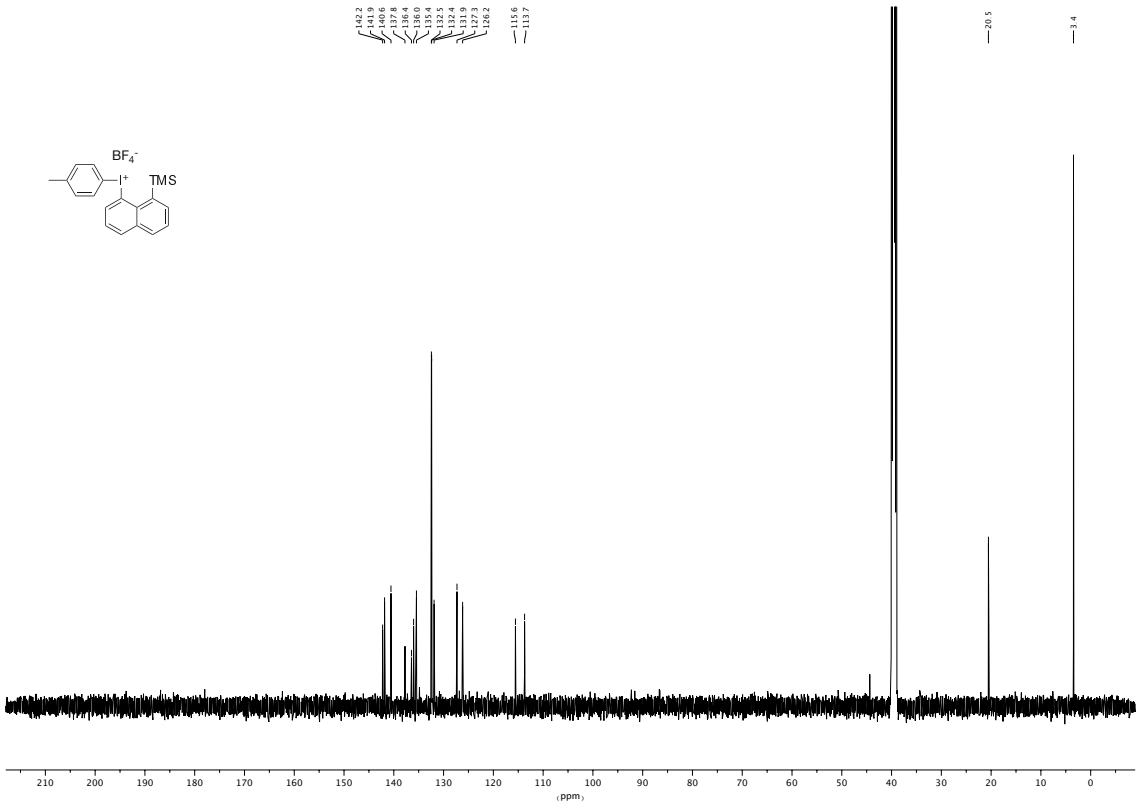

Figure 7.46. 151 MHz ^{13}C NMR spectrum of the compound **117a** in DMSO-d_6.

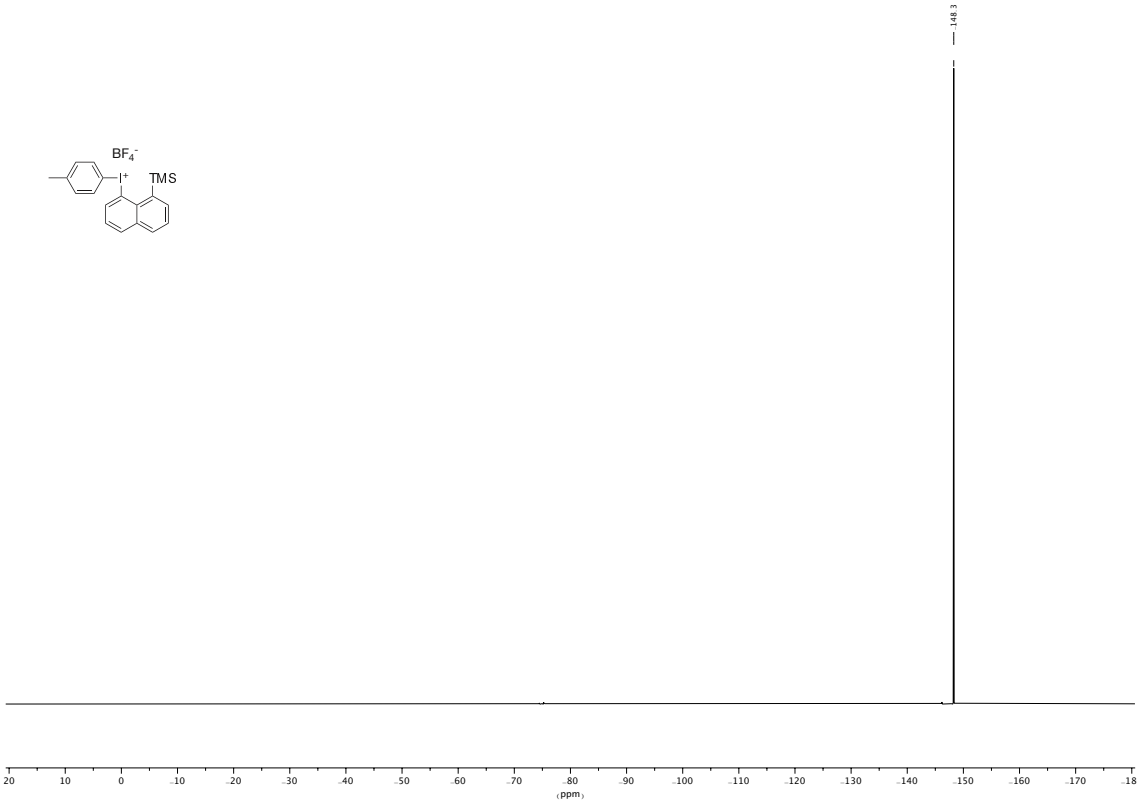

Figure 7.47. 565 MHz ^{19}F NMR spectrum of the compound **117a** in DMSO-d_6.

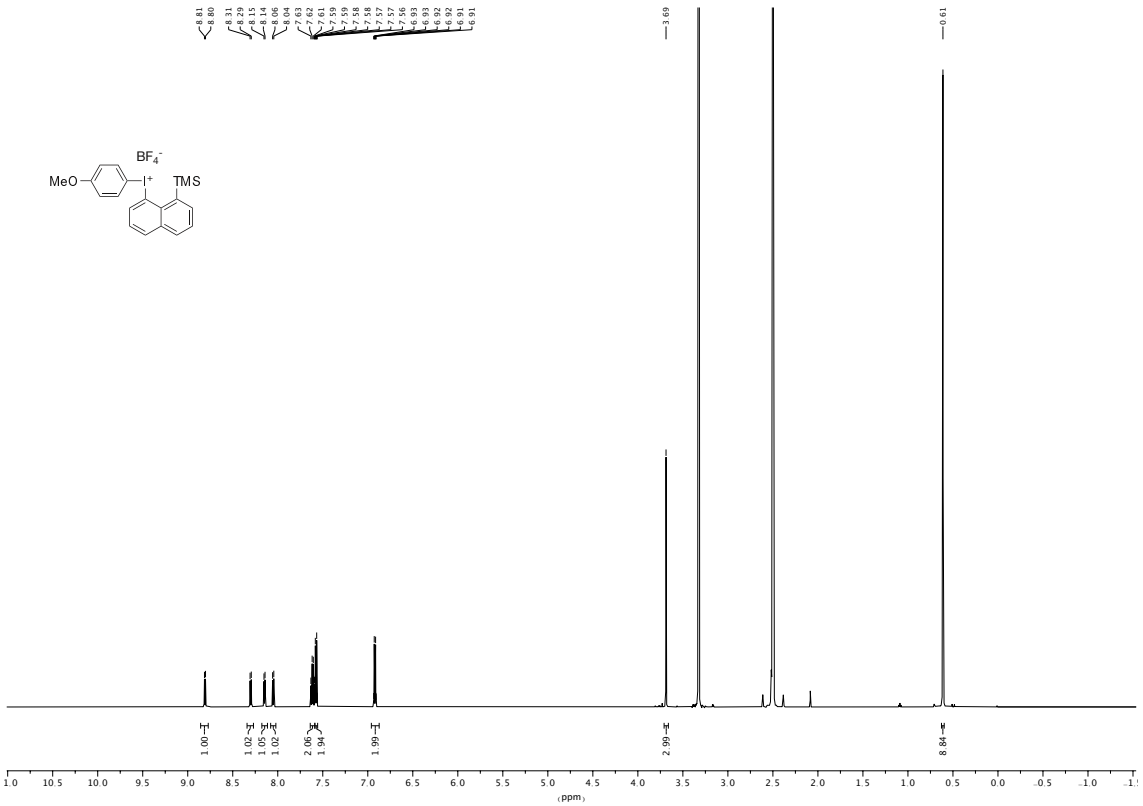

Figure 7.48. 600 MHz ^{1}H NMR spectrum of the compound **117b** in DMSO-d_6.

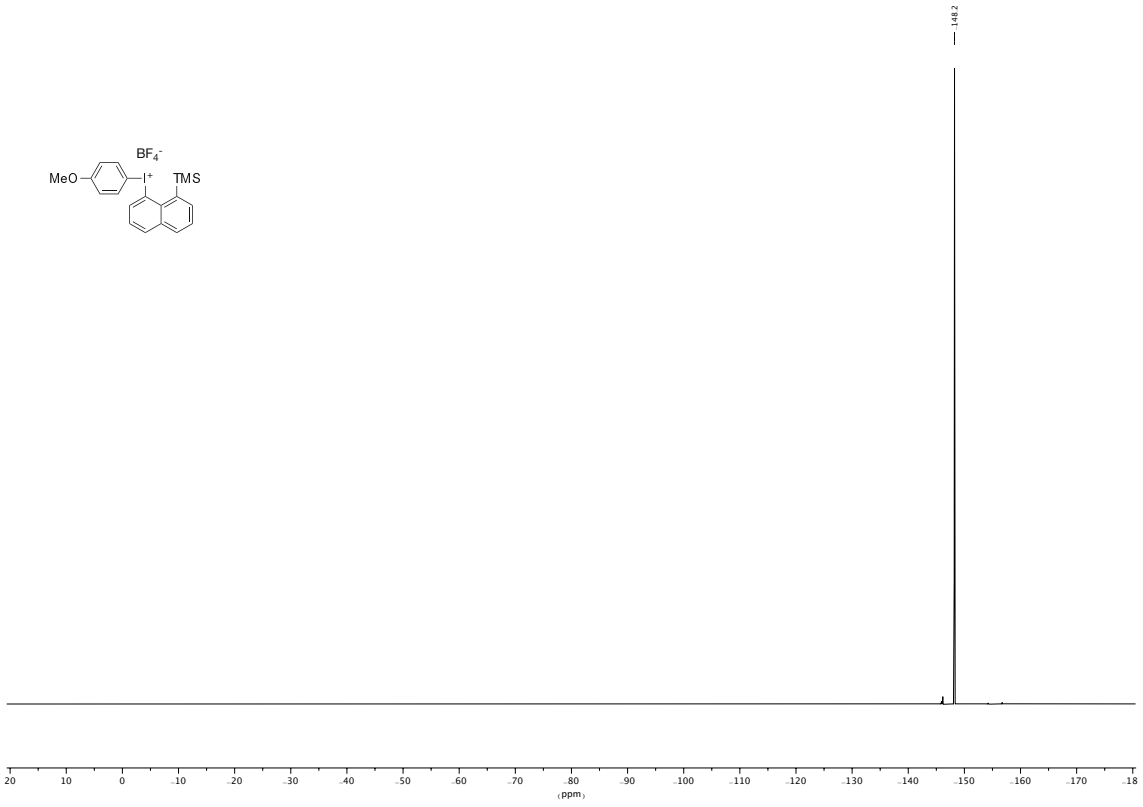

Figure 7.49. 151 MHz ^{13}C NMR spectrum of the compound **117b** in DMSO-d_6.

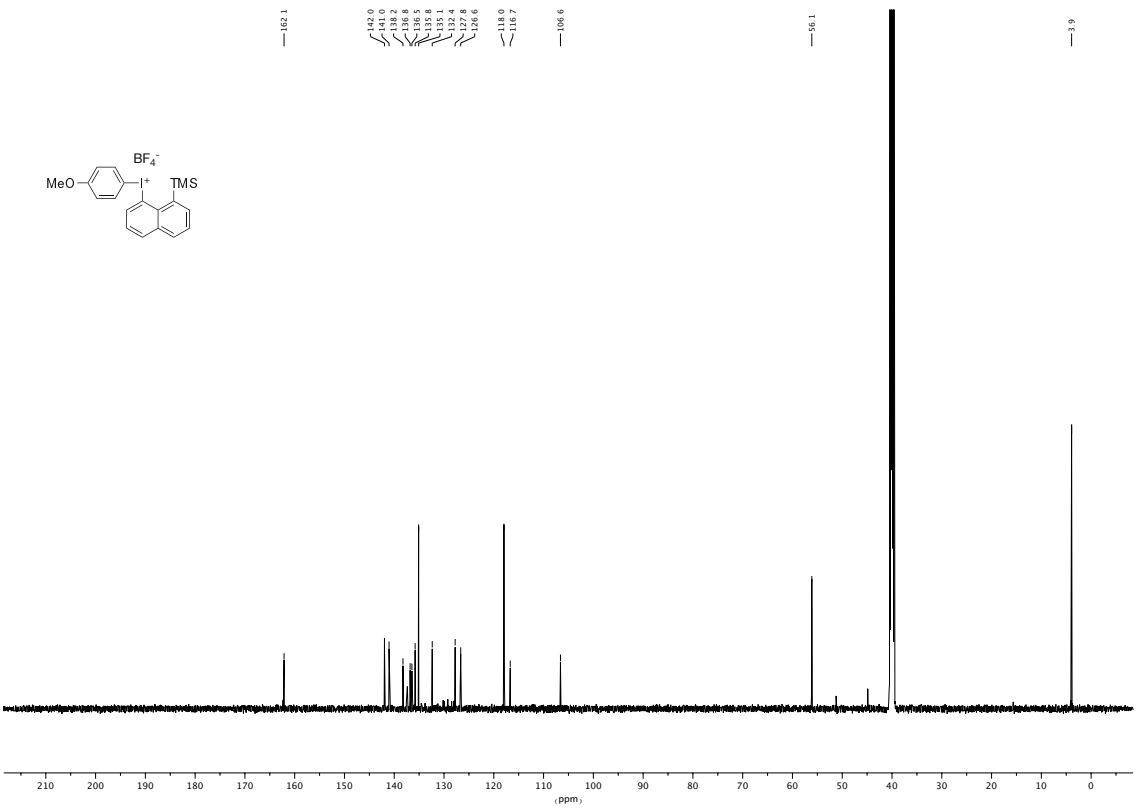

Figure 7.50. 565 MHz ^{19}F NMR spectrum of the compound **117b** in DMSO-d_6.

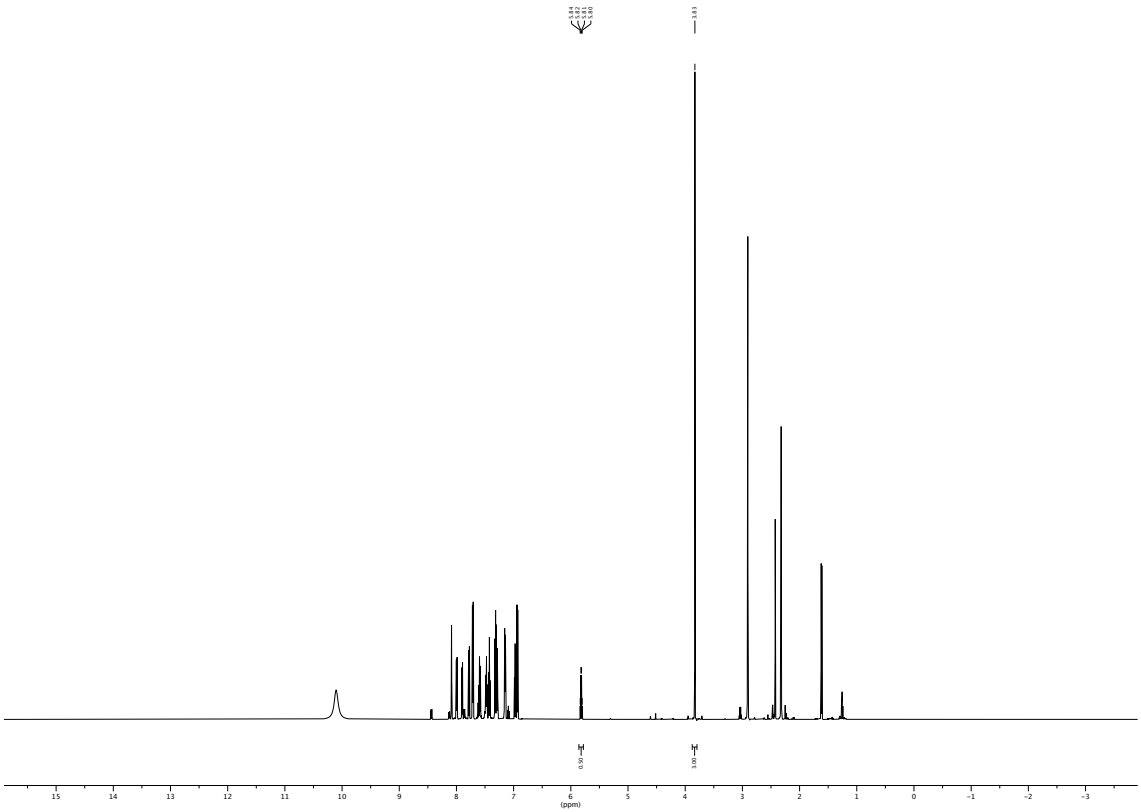

Figure 7.51. Spectrum of the α-tosyloxylation of propiophenone with 1,8-diiodonaphthalene (**112**) as a catalyst.

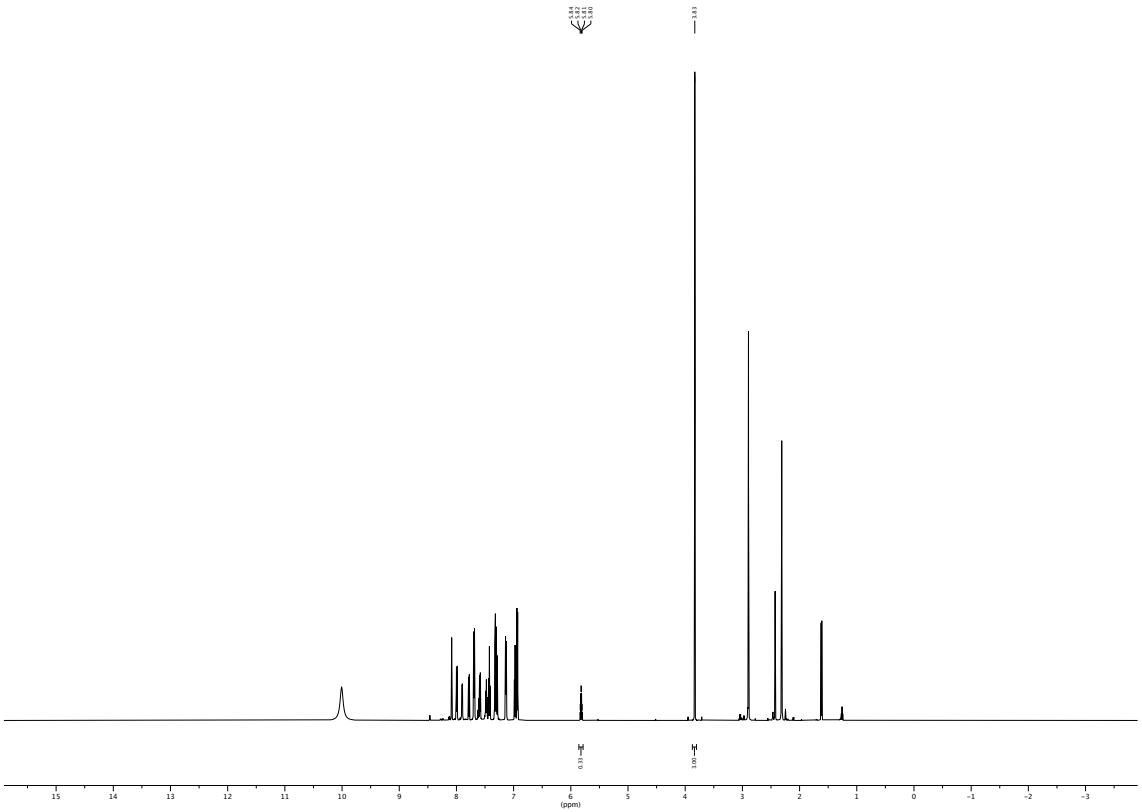

Figure 7.52. Spectrum of the α-tosyloxylation of propiophenone with 1-iodonaphthalene (**126**) as a catalyst.

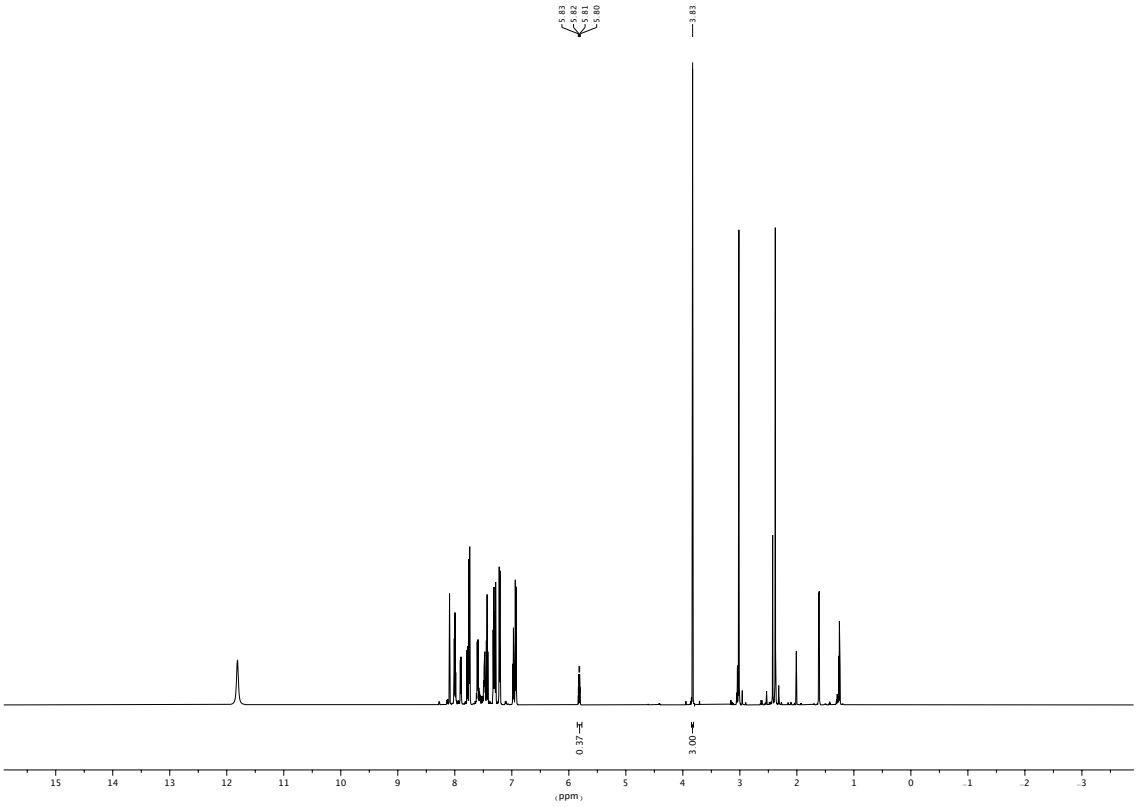

Figure 7.53. Spectrum of the α-tosyloxylation of propiophenone with **116a** as a catalyst.

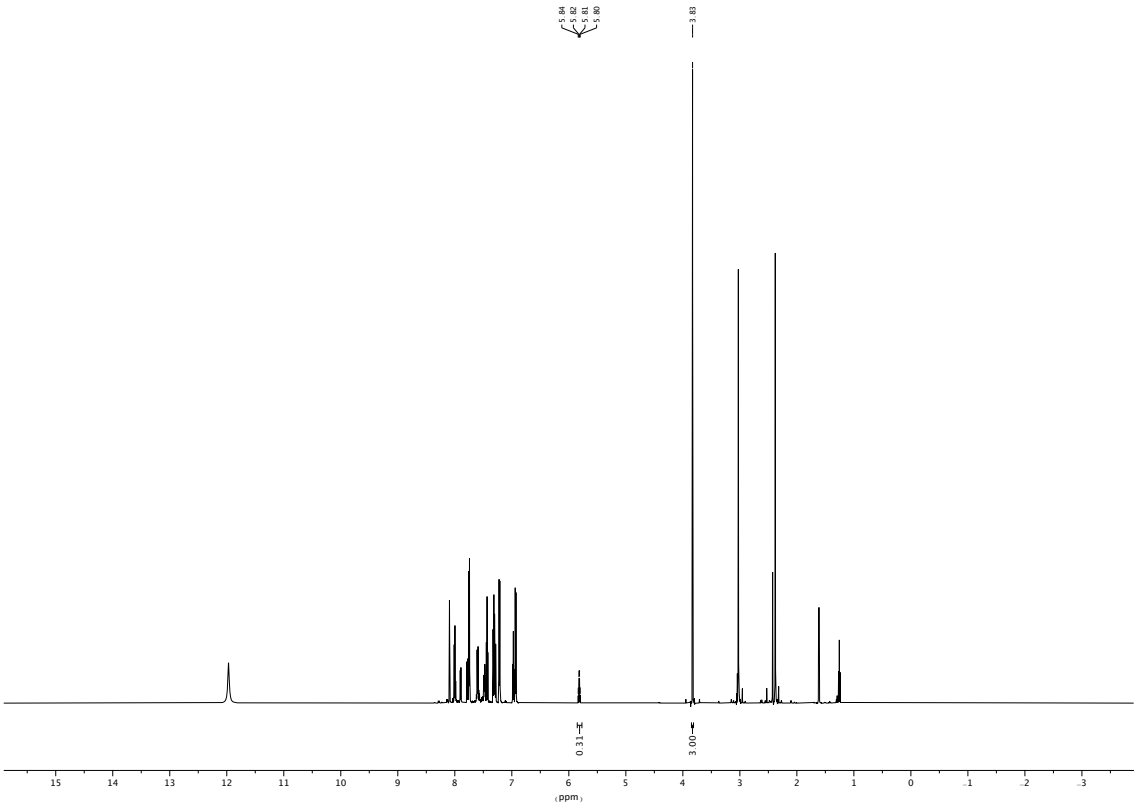

Figure 7.54. Spectrum of the α-tosyloxylation of propiophenone with **116b** as a catalyst.

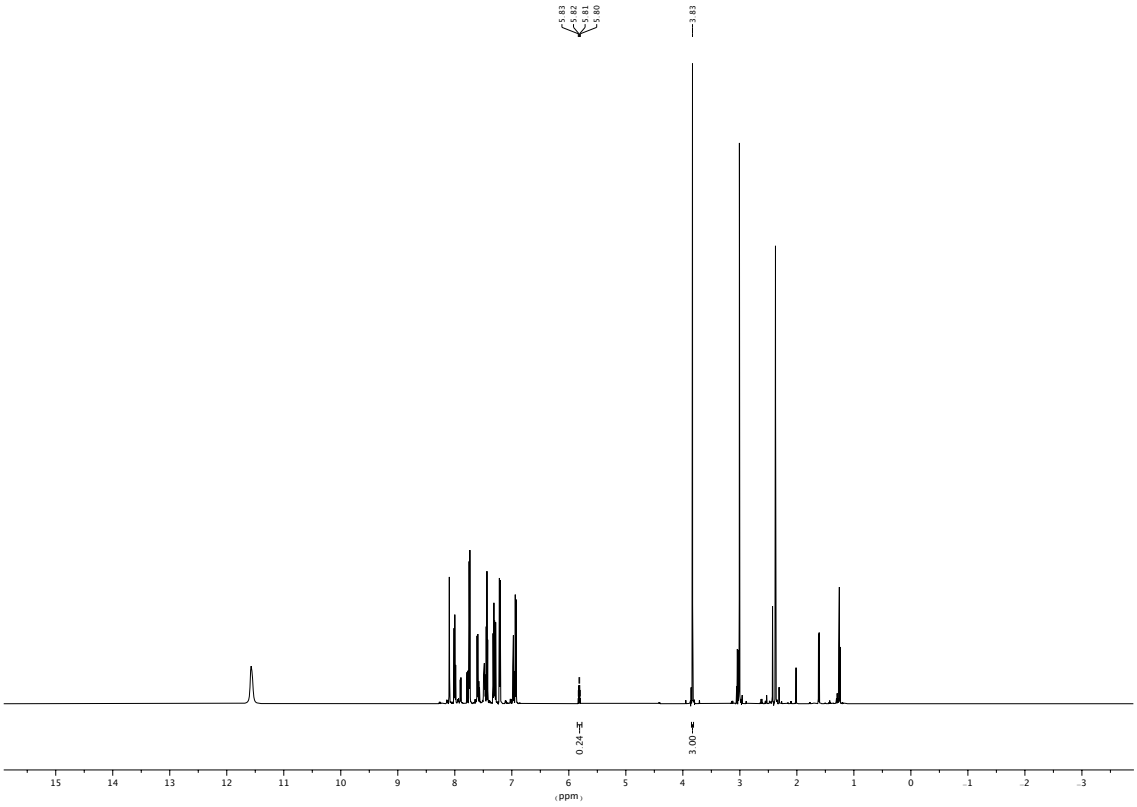

Figure 7.55. Spectrum of the α-tosyloxylation of propiophenone with **116d** as a catalyst.

7.2 Supporting Information for Section 3.2

BEILSTEIN JOURNAL OF ORGANIC CHEMISTRY

Supporting Information

for

Two-step continuous-flow synthesis of 6-membered cyclic iodonium salts via anodic oxidation

Julian Spils, Thomas Wirth and Boris J. Nachtsheim

Beilstein J. Org. Chem. **2023,** *19,* 27–32. doi:10.3762/bjoc.19.2

Experimental, analytical data and copies of NMR spectra

Table of Contents

1 General Information

Unless otherwise noted, all reactions were carried out under air. Reactions with chemicals sensitive to moisture or oxygen were carried out under a nitrogen atmosphere using standard Schlenk techniques. All chemicals were purchased from commercial suppliers and either used as received or purified according to "Purification of Laboratory Chemicals".[1] Anhydrous tetrahydrofuran (THF) and diethyl ether (Et_2O) were obtained from an Inert PS-MD-6 solvent purification system. All other solvents were dried using standard methods if necessary.[1]

Yields refer to isolated yields of compounds estimated to be >95% pure as determined by ^{1}H-NMR spectroscopy.

Thin layer chromatography was performed on fluorescence indicator marked precoated silica gel 60 plates (Macherey-Nagel, ALUGRAM Xtra SIL G/UV254) and visualized by UV light (254 nm/366 nm). Flash column chromatography was performed on silica gel (0.040–0.063 mm) with the solvents given in the procedures.

NMR spectra were recorded on a Bruker Avance 360WB spectrometer, a Bruker Avance Neo 600 MHz spectrometer with BBO probe head and a Bruker Avance Neo 600 MHz spectrometer with TXI probe head at 23 °C. Chemical shifts for ^{1}H-NMR spectra are reported as δ (parts per million) relative to the residual proton signal of $CDCl_3$ at 7.26 ppm (s), DMSO-d_6 at 2.50 ppm (quint). Chemical shifts for ^{13}C-NMR spectra are reported as δ (parts per million) relative to the signal of $CDCl_3$ at 77.0 ppm (t), DMSO-d_6 at 39.5 ppm (sept). Chemical shifts for ^{19}F-NMR spectra are reported as δ (parts per million) relative to the signal of $Si(CH_3)_4$ at 0.00 ppm. The following abbreviations are used to describe splitting patterns: br. = broad, s = singlet, d = doublet, t = triplet, q = quartet, quint = quintet, sept = septet, m = multiplet. Coupling constants J are given in Hz.

APCI mass spectra were recorded on an Advion Expression CMS^L via ASAP probe or direct inlet. Low Resolution ESI mass spectra were recorded on an Agilent 6120 Series LC/MSD system. Low resolution EI mass spectra were recorded on an Agilent 5977A Series GC/MSD system. High resolution (HR) EI mass spectra were recorded on a double focusing mass spectrometer ThermoQuest MAT 95 XL from Finnigan MAT. HR-ESI and HR-APCI mass spectra were recorded on a Bruker Impact II. All Signals are reported with the quotient from mass to charge m/z.

IR spectra were recorded on a Nicolet Thermo iS10 scientific spectrometer with a diamond ATR unit. The absorption bands $\tilde{\nu}$ are reported in cm^{-1}.

Melting points of solids were measured on a Büchi M-5600 Melting Point apparatus and are uncorrected. The measurements were performed with a heating rate of 2 °C/min and the melting point temperatures T are reported in °C.

The electrochemical reactions in batch were carried out using a IKA Electrasyn 2.0 in a 5 mL glass vial with GC and Pt electrodes. For electrochemical reactions in flow in a galvanostatic mode a PEAKTECH 6225 A galvanostat was used. Electrolysis experiments were carried out using a Vapourtec Ion Electrochemical Reactor. Electrode materials: Platinum (Pt, coated obtained from Vapourtec Ltd.), Glassy Carbon (GC, SIGRADUR® from HTW Hochtemperatur-Werkstoffe GmbH). The electrodes (5 × 5 cm^2) are separated by a 0.5 mm spacer with a channel volume of 0.6 mL and an exposed electrode surface area of 12 cm^2 (each electrode). The syringe pumps that were used were Landgraf Laborsysteme HLL GmbH LA-30 syringe pumps.

2 Optimization of Reaction Conditions

2.1.1 Optimization of the Oxidation and Cyclization in Batch

Table S1: Optimization of the Oxidation and Cyclization in Batch towards 10H-dibenzo[b,e]iodinin-5-ium salt (***1a***).

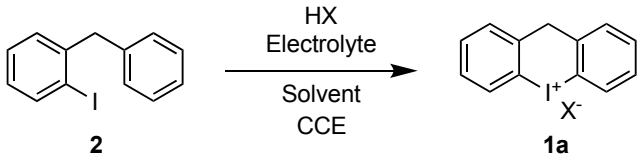

2 **1a**

#[a]	HX (equiv)	Electrolyte (mM)	Solv. (mM)	Anode/ Cathode	Current (mA)	X	Yield / %
1	H_2SO_4 (2 M)		MeCN/Ac_2O 3:1 (40)	Pt/Pt	30 (2.4 F)	I	---
2	H_2SO_4 (2 M) **TfOH (5)**		MeCN/Ac_2O 3:1 (40)	Pt/Pt	**10** (2.4 F)	TfO	19
3	TfOH (5)	**Bu_4NBF_4 (5)**	**TFE (40)**	**GC**/Pt	10 (2.1 F)	TfO	45
4	TfOH (5)	Bu_4NBF_4 (5)	**MeCN**/TFE 4:1 (40)	GC/Pt	10 (2.0 F)	TfO	40
5	TfOH (5)	Bu_4NBF_4 (5)	**CH_2Cl_2**/TFE 4:1 (40)	GC/Pt	10 (2.2 F)	TfO	46
6	**TfOH (15)**	Bu_4NBF_4 (5)	CH_2Cl_2/TFE 4:1 (40)	GC/Pt	10 (3.0 F)	TfO	44
7	TfOH (5)	**Bu_4NBF_4 (15)**	CH_2Cl_2/TFE 4:1 (40)	GC/Pt	10 (2.2 F)	TfO	44
8	TfOH (5)	Bu_4NBF_4 (5)	CH_2Cl_2/**HFIP** 4:1 (40)	GC/Pt	10 (2.0 F)	TfO	78
9	**TfOH (2)**	Bu_4NBF_4 (5)	CH_2Cl_2/HFIP 4:1 (40)	GC/Pt	10 (2.0 F)	TfO	76
10	TfOH (2)	Bu_4NBF_4 (5)	CH_2Cl_2/HFIP 4:1 (40)	GC/Pt	**30** (2.3 F)	TfO	57

[a] All reactions were performed on a 0.200 mmol scale with an IKA Electrasyn 2.0 in an undivided cell.

2.1.2 Optimization of the Oxidation and Cyclization in Flow

Table S2: Optimization of the Oxidation and Cyclization in Flow towards 10H-dibenzo[b,e]iodinin-5-ium salt (**1a**)**.**

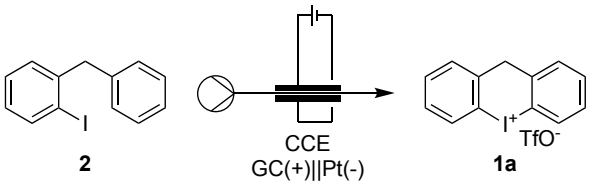

#[a]	HX (equiv)	Additives	Solv. (mM)	Anode/ Cathode	Current (mA)	Yield /%
7	TfOH (1)	Bu_4NBF_4 (5 mM)	CH_2Cl_2/TFE 1:1 (100)	GC/Pt	32 (2.0 F)	62
8	TfOH (2)	Bu_4NBF_4 (5 mM)	CH_2Cl_2/TFE 1:1 (100)	GC/Pt	32 (2.0 F)	74
9[b]	**HBF_4OEt_2 (1)**	Bu_4NBF_4 (5 mM)	CH_2Cl_2/TFE 1:1 (100)	GC/Pt	32 (2.0 F)	66
10[b]	HBF_4OEt_2 (1)	Bu_4NBF_4 (5 mM)	CH_2Cl_2/TFE 1:1 (100)	GC/Pt	**48 (3.0 F)**	62
11	TfOH (2)	Bu_4NBF_4 (5 mM) **PhH (9 equiv)**	**$MeNO_2$ (100)**	GC/Pt	32 (2.0 F)	48
13	TfOH (2)	Bu_4NBF_4 (5 mM) PhH (9 equiv)	**$MeNO_2$/TFE 1:1** (100)	GC/Pt	32 (2.0 F)	63
14	TfOH (2)	**PhH (9 equiv)**	$MeNO_2$/TFE 1:1 (100)	GC/Pt	32 (2.0 F)	62
15	TfOH (2)	PhH (9 equiv)	$MeNO_2$/TFE 1:1 (100)	GC/Pt	**48 (3.0 F)**	62

[a] Reaction was performed in a Vapourtec Ion electrochemical flow reactor with a glassy carbon (GC) anode, a Pt cathode and a 0.5 mm PTFE spacer in between. General reaction conditions: **1** (0.1 M), $TBABF_4$ (0.005 M). Flowrate: 0.1 ml min^{-1}. Yield is based on collecting for 20 min (0.200 mmol) after two reactor volumes had passed at the respective condition. [b] The corresponding tetrafluoroborate was isolated.

2.1.3 Final optimization of the one-pot-procedure in flow

*Table S1: Final optimization of the one-pot-procedure in flow towards 10H-dibenzo[b,e]iodinin-5-ium salt (**1a**).*

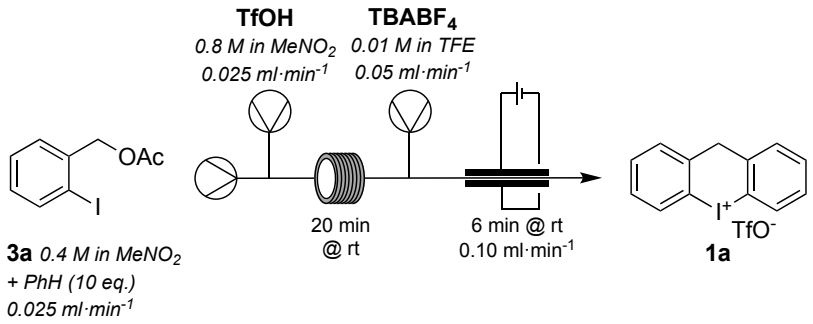

#[a]	Electrolyte	Current (mA)	Yield /%
1	Bu_4NBF_4	32 (2.0 F)	54
2	Bu_4NBF_4	**48 (3.0 F)**	54
3	---	32 (2.0 F)	49
4[b]	---	32 (2.0 F)	38 (46, 37, 34, 33)
5[b]	**Bu_4NBF_4**	32 (2.0 F)	43 (52, 41, 41, 38)

[a] Reaction was performed in a Vapourtec Ion electrochemical flow reactor with a glassy carbon (GC) anode, a Pt cathode and a 0.5 mm PTFE spacer in between. Yield is based on collecting for 20 min (0.200 mmol) after two reactor volumes had passed at the respective condition.

[b] **1a** was collected for 3 h 20 min (2.00 mmol) divided in four fractions each 50 min (0.500 mmol). Yields of each fraction is in brackets.

3 Preparation of Starting Materials

3.1 General Procedures for the Synthesis of the Starting Materials

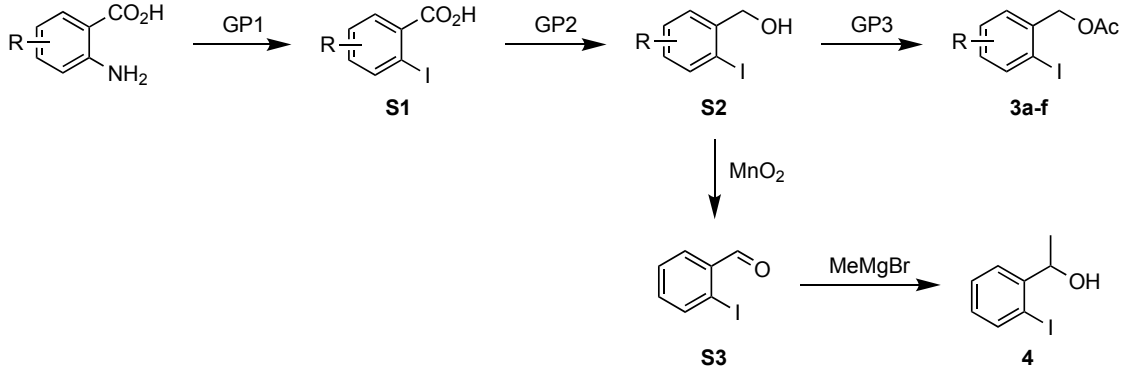

*Scheme S1: General scheme for the synthesis of primary benzyl acetates **3** and secondary benzyl alcohol **4**.*

3.1.1 Sandmeyer-type Iodination of Anthranilic acids (GP1)

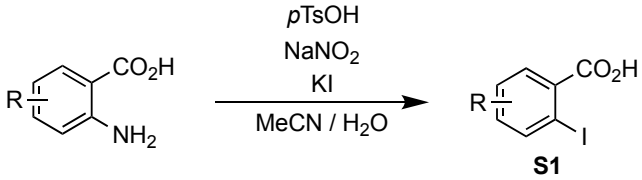

Following a reported procedure,[1] the anthranilic acid derivative (1.00 equiv) and $TsOH \cdot H_2O$ (3.00 equiv) were suspended in MeCN (0.125 M). The mixture was cooled to 10–15 °C. A solution of $NaNO_2$ (2.00 equiv) and KI (2.50 equiv) in H_2O (1.5 ml/mmol) was added dropwise over 1 h. After complete addition, the resulting dark coloured mixture was stirred for another 1 h and then 1 N HCl (5 ml/mmol) and EtOAc (10 ml/mmol) were added. The phases were separated and the aqueous phase was extracted with EtOAc (2 × 5 ml/mmol). The combined organic phases were washed with water (5 ml/mmol), $Na_2S_2O_3$ (10% *w*/*w*, 5 ml/mmol) and brine (2 ml/mmol), dried over Na_2SO_4 and concentrated under reduced pressure. The residue was either purified by filtration over silica or by column chromatography.

3.1.2 Borane-mediated Reduction of Carboxylic acids (GP2)

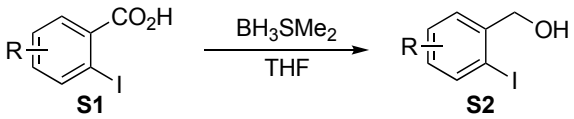

In modification of a reported procedure,[2] the *o*-iodobenzoic acid derivative (**S1**, 1.00 equiv) was dissolved in dry THF (1.00 M). After cooling to 0 °C, BH_3SMe_2 (1.20 equiv) were added dropwise over 15 min. After the addition, the mixture was allowed to warm to rt and stirred for 16 h. After completion of the reaction, the mixture was cooled to 0 °C and MeOH (40 µl/mmol) was carefully added. Afterwards, 1 M Na_2CO_3 solution (0.5 ml/mmol) was slowly added. The resulting mixture was diluted with water (3 ml/mmol) and extracted with Et_2O (3 × 5 ml/mmol). The combined organic phases were washed with brine (5 ml/mmol), dried over Na_2SO_4 and concentrated under reduced. The crude product was purified by column chromatography on silica gel.

3.1.3 Iodine catalysed Acetylation of Benzylic alcohols (GP3)

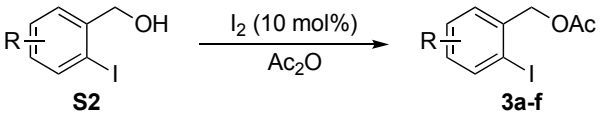

S2 **3a-f**

In modification of a reported procedure,[3] the *o*-iodobenzyl alcohol derivative (**S2**, 1.00 equiv) was suspended in Ac_2O (6.00 equiv). If necessary, dichloromethane (0.1–0.2 ml/mmol) was added. Iodine (0.100 equiv) was added and the mixture was stirred at rt. The conversion was monitored via TLC and after full conversion the mixture was diluted with water (0.5 ml/mmol) and sat. $NaHCO_3$ solution (2 ml/mmol). The aqueous phase was extracted with dichloromethane (1 ml/mmol). The combined organic phases were washed with sat. $Na_2S_2O_3$ solution, dried over Na_2SO_4 and concentrated under reduced pressure. The crude product was either used as received or purified by column chromatography on silica gel.

3.2 Synthesis of Starting Materials

3.2.1 Primary Benzyl Acetates

The *o*-iodobenzoic acid derivative **S1a** were commercially available and have been used as received for the synthesis of the corresponding alcohols.

2-Iodobenzyl acetate (3a)

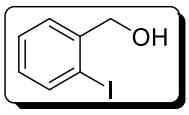

Following a reported procedure,[1] *o*-iodobenzoic acid (49.6 g, 200 mmol 1.00 equiv) was dissolved in dry THF (200 ml). After cooling to 0 °C, $NaBH_4$ (21.9 g, 580 mmol, 2.90 equiv) was added portionwise. To the resulting mixture, I_2 (38.1 g, 150 mmol, 0.750 equiv) in THF (300 ml) was slowly added over 5 h. After the addition, the mixture was allowed to warm to rt and stirred overnight. After completion of the reaction, the mixture was cooled to 0 °C and water (70 ml) was carefully added. Afterwards, 3 M HCl was slowly added until the solution was at pH 2. The resulting mixture was extracted with Et_2O (4 × 150 ml). The combined organic phases were washed with 1 M Na_2CO_3 (200 ml), sat. $Na_2S_2O_3$ (50 ml) and brine (200 ml), dried over Na_2SO_4, and concentrated under reduced pressure. Recrystallization of the crude product from cyclohexane gave (2-iodophenyl)methanol (**S2a**, 46.8 g, 200 mmol, quant.) as a white crystalline solid.

^{1}H-NMR (601 MHz, $CDCl_3$) δ = 7.83 (dd, *J* = 7.8, 1.2 Hz, 1H), 7.46 (dd, *J* = 7.6, 1.7 Hz, 1H), 7.37 (td, *J* = 7.5, 1.2 Hz, 1H), 7.00 (td, *J* = 7.6, 1.8 Hz, 1H), 4.68 (d, *J* = 6.3 Hz, 2H), 2.00 (t, *J* = 6.3 Hz, 1H). **^{13}C-NMR (151 MHz, CDCl3)** δ = 142.9, 139.5, 129.6, 128.8, 128.7, 97.7, 69.6. **FTIR (ATR, neat)** $\tilde{\nu}$ = 3262, 3061, 2887, 2843, 1434, 1321, 1195, 1033, 1009, 738. **MS (EI, 70 eV)** *m/z* = 234.0 $[M]^{+\cdot}$ **Mp** *T* = 91. The analytical data is in accordance with literature data.[1]

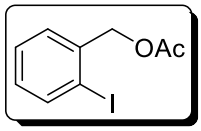

Following **GP3**, the reaction of (2-iodophenyl)methanol (**S2a**, 4.68 g, 20.0 mmol) in Ac_2O (11.3 ml, 120 mmol) with iodine (508 mg, 2.00 mmol) gave after a reaction time of 4 h and subsequent column chromatography (silica, cyclohexane) 2-Iodobenzyl acetate (**3a**, 5.53 g, 20.0 mmol, quant.) as a colourless liquid.

^{1}H-NMR (600 MHz, $CDCl_3$) δ = 7.86 (d, *J* = 7.9 Hz, 1H), 7.38 (dd, *J* = 7.6, 1.9 Hz, 1H), 7.35 (td, *J* = 7.4, 0.9 Hz, 1H), 7.03 (td, *J* = 7.6, 1.9 Hz, 1H), 5.13 (s, 2H), 2.15 (s, 3H). **^{13}C-NMR (151 MHz, $CDCl_3$)** δ = 170.6, 139.5, 138.3, 129.8, 129.5, 128.3, 98.4, 70.1, 20.9. **FTIR (ATR, neat)** $\tilde{\nu}$ = 3056, 2953, 1732, 1566, 1437,

1378, 1360, 1218, 1012, 746. **MS (EI, 70 eV)** *m/z* = 276.0 $[M]^{+\cdot}$, 149.1 $[M\text{-}I]^{+}$. The analytical data is in accordance with literature data.[1]

5-Fluoro-2-iodobenzyl acetate (3b)

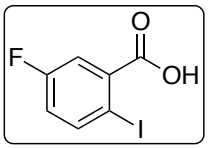

Following **GP1**, the reaction of 2-amino-5-fluorobenzoic acid (7.76 g, 50.0 mmol) and $TsOH{\cdot}H_2O$ (28.5 g, 150 mmol) in MeCN (400 ml) with $NaNO_2$ (6.90 g, 100 mmol) and KI (20.8 g, 125 mmol) in water (75 ml) gave 5-fluoro-2-iodobenzoic acid (**S1b**, 11.4 g, 43.0 mmol, 86%) as a yellow solid.

^{1}H-NMR (600 MHz, DMSO-*d*$_6$) δ = 8.31 (s, 1H), 7.88 (dd, *J* = 8.5, 2.6 Hz, 1H), 7.82 (dd, *J* = 8.7, 6.0 Hz, 1H), 7.35 (td, *J* = 8.4, 2.6 Hz, 1H). **^{13}C-NMR (151 MHz, DMSO-*d*$_6$)** δ = 167.1, 162.5 (d, *J* = 254.2 Hz), 132.9 (d, *J* = 2.4 Hz), 132.2 (d, *J* = 9.0 Hz), 127.5 (d, *J* = 23.7 Hz), 115.2 (d, *J* = 21.3 Hz), 95.3 (d, *J* = 8.5 Hz). **^{19}F-NMR (565 MHz, $CDCl_3$)** δ = -108.3 (m). **FTIR (ATR, neat)** $\tilde{\nu}$ = 2977, 2856, 2648, 1694, 1573, 1411, 1300, 1257, 1203, 768. **MS (EI, 70 eV)** *m/z* = 265.9 $[M]^{+\cdot}$. **Mp** *T* = 135 – 137. The analytical data is in accordance with literature data.[4]

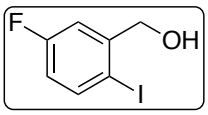

Following **GP2**, the reaction of 5-fluoro-2-iodobenzoic acid (**S1b**, 10.6 g, 40.0 mmol) in dry THF (40 ml) with BH_3SMe_2 (4.80 ml, 48.0 mmol) gave (5-fluoro-2-iodophenyl)methanol (**S2b**, 9.56 g, 37.9 mmol, 95%) as a colourless solid.

^{1}H-NMR (601 MHz, $CDCl_3$) δ = 7.74 (dd, *J* = 8.6, 3.1 Hz, 1H), 7.25 (dd, *J* = 9.3, 3.1 Hz, 1H), 6.76 (td, *J* = 8.3, 3.1 Hz, 1H), 4.63 (d, *J* = 6.1 Hz, 2H), 2.07 (t, *J* = 6.1 Hz, 1H). **^{13}C-NMR (151 MHz, $CDCl_3$)** δ = 163.1 (d, *J* = 247.8 Hz), 145.0 (d, *J* = 6.9 Hz), 140.1 (d, *J* = 7.6 Hz), 116.4 (d, *J* = 22.0 Hz), 115.5 (d, *J* = 23.4 Hz), 89.1 (d, *J* = 2.7 Hz), 68.8. **^{19}F-NMR (565 MHz, $CDCl_3$)** δ = −113.4. **FTIR (ATR, neat)** $\tilde{\nu}$ = 3286, 1578, 1458, 1437, 1356, 1263, 1149, 1058, 1013, 808. **MS (EI, 70 eV)** *m/z* = 251.9 $[M]^{+\cdot}$. **Mp** *T* = 111.5 – 113. The analytical data is in accordance with literature data.[1]

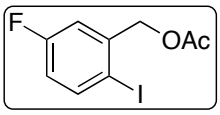

Following **GP3**, the reaction of (5-fluoro-2-iodophenyl)methanol (**S2b**, 1.76 g, 7.00 mmol) in Ac_2O (4.00 ml, 42.0 mmol) with iodine (178 mg, 0.700 mmol) gave after a reaction time of 4 h and subsequent column chromatography (silica, cyclohexane/ethyl acetate 1:0→19:1) 5-fluoro-2-iodobenzyl acetate (**3b**, 1.80 g, 6.12 mmol, 87%) as a colourless solid.

^{1}H-NMR (600 MHz, $CDCl_3$) δ = 7.59 (dd, *J* = 8.0, 2.6 Hz, 1H), 7.36 (dd, *J* = 8.6, 5.8 Hz, 1H), 7.08 (td, *J* = 8.3, 2.6 Hz, 1H), 5.10 (s, 2H), 2.13 (s, 3H). **^{13}C-NMR (151 MHz, $CDCl_3$)** δ = 170.6, 161.7 (d, *J* = 252.4 Hz), 134.4 (d, *J* = 3.5 Hz), 130.6 (d, *J* = 8.3 Hz), 126.5 (d, *J* = 23.8 Hz), 115.4 (d, *J* = 20.9 Hz), 97.9 (d, *J* = 8.3 Hz), 69.3, 20.9. **^{19}F-NMR (565 MHz, $CDCl_3$)** δ = -112.1. **FTIR (ATR, neat)** $\tilde{\nu}$ = 2928, 1731, 1716, 1584, 1480, 1438, 1359, 1237, 1220, 1048, 1026, 868. **HRMS (ESI+, MeOH)** *m/z* = 316.94410 $[M+Na]^{+}$. Calculated for $[C_9H_8FINaO_2]^{+}$: *m/z* = 316.94453. **Mp** *T* = 38 – 39.

5-Chloro-2-iodobenzyl acetate (3c)

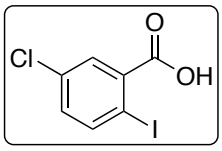

Following **GP1**, the reaction of 2-amino-5-chlorobenzoic acid (5.15 g, 30.0 mmol) and $TsOH{\cdot}H_2O$ (17.1 g, 90.0 mmol) in MeCN (240 ml) with $NaNO_2$ (4.14 g, 60.0 mmol) and KI (12.5 g, 75.0 mmol) in water (45 ml) gave 5-chloro-2-iodobenzoic acid (**S1c**, 8.21 g, 29.1 mmol, 97%) as a yellow solid.

^{1}H-NMR (600 MHz, DMSO-*d*$_6$) δ = 13.61 (brs, 1H), 7.97 (d, *J* = 8.4 Hz, 1H), 7.72 (d, *J* = 2.6 Hz, 1H), 7.32 (dd, *J* = 8.4, 2.6 Hz, 1H). **^{13}C-NMR (151 MHz, DMSO-*d*$_6$)** δ = 167.0, 142.1, 138.9, 133.2, 132.2, 129.5,

92.1. **FTIR (ATR, neat)** $\tilde{\nu}$ = 1694, 1673, 1574, 1400, 1290, 1246, 1117, 1017, 780, 749. **MS (EI, 70 eV)** *m/z*: 281.9 $[M]^{+\cdot}$. **Mp** *T* = 154 – 157. The analytical data is in accordance with literature data.[1]

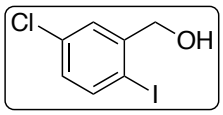

Following **GP2**, the reaction of 5-chloro-2-iodobenzoic acid (**S1c**, 20.0 mmol, 5.65 g) in dry THF (20 ml) with BH_3SMe_2 (24.0 mmol, 2.40 ml) gave after a subsequent column chromatography (silica, cyclohexane/ethyl acetate 1:0→9:1) (5-chloro-2-iodophenyl)methanol (**S2c**, 4.15 g, 15.5 mmol, 77%) as a colourless solid.

^{1}H-NMR (601 MHz, $CDCl_3$) δ = 7.71 (d, *J* = 8.3 Hz, 1H), 7.48 (d, *J* = 2.5 Hz, 1H), 6.99 (dd, *J* = 8.3, 2.6 Hz, 1H), 4.63 (s, 2H), 2.10 (s, 1H). **^{13}C-NMR (151 MHz, $CDCl_3$)** δ = 144.3, 140.0, 135.0, 129.2, 128.2, 93.6, 68.7. **FTIR (ATR, neat)** $\tilde{\nu}$ = 3289, 3212, 1452, 1436, 1391, 1193, 1101, 1055, 1007, 974, 808. **MS (EI, 70 eV)** *m/z*: 268.0 $[M]^{+\cdot}$, 233.9 $[M - Cl]^+$, 141.0 $[M - I]^+$. **Mp** *T* = 118 – 119.5. The analytical data is in accordance with literature data.[1]

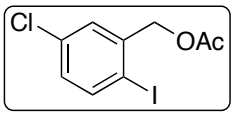

Following **GP3**, the reaction of (5-chloro-2-iodophenyl)methanol (**S2c**, 4.40 mmol, 1.18 g) in Ac_2O (26.4 mmol, 2.50 ml) with iodine (0.440 mmol, 112 mg) gave after a reaction time of 4 h and subsequent column chromatography (silica, cyclohexane/ethyl acetate 1:0→19:1) 5-chloro-2-iodobenzyl acetate (**3c**, 1.28 g, 4.12 mmol, 94%) as a colourless solid.

^{1}H-NMR (600 MHz, $CDCl_3$) δ = 7.76 (d, *J* = 8.4 Hz, 1H), 7.36 (d, *J* = 2.5 Hz, 1H), 7.02 (dd, *J* = 8.4, 2.6 Hz, 1H), 5.07 (s, 2H), 2.17 (s, 3H). **^{13}C-NMR (151 MHz, $CDCl_3$)** δ = 170.4, 140.4, 140.1, 134.8, 129.8, 129.1, 94.6, 69.4, 20.9. **FTIR (ATR, neat)** $\tilde{\nu}$ = 3054, 1730, 1437, 1375, 1360, 1248, 1240, 1094, 1047, 874, 819. **HRMS (ESI+, MeOH)** *m/z* = 332.91460 $[M+Na]^+$. Calculated for $[C_9H_8ClINaO_2]^+$: *m/z* = 332.91498. **Mp** *T* = 80 – 82.

2-Iodo-5-methyl-benzyl acetate (3d)

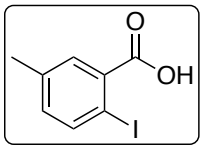

Following a modified literature procedure,[2] 2-amino-5-methylbenzoic acid (3.02 g, 20.0 mmol) was suspended in conc. HCl (15 ml) and was stirred for 15 min at 0 °C before $NaNO_2$ (1.79 g, 26.0 mmol) in H_2O (4 ml) was added dropwise over 10 min. Stirring continued for 1.5 h at 0 °C and afterwards KI (16.6 g, 100 mmol) in H_2O (20 mL) was added dropwise over 20 min. The reaction mixture was allowed to warm to room temperature and was stirred for 24 h. H_2O (40 mL) was added and extracted with EtOAc (3 × 40 mL). The combined organic phases were washed with sat. $Na_2S_2O_3$-solution (20 ml), brine (40 ml) and H_2O (40 ml), dried over Na_2SO_4, filtered and concentrated *in vacuo* to give 2-iodo-5-methylbenzoic acid (**S1d**, 5.04 g, 20.0 mmol, 96%) as a yellow solid.

^{1}H-NMR (600 MHz, $CDCl_3$) δ = 7.91 (d, *J* = 8.1 Hz, 1H), 7.84 (d, *J* = 2.2 Hz, 1H), 7.02 (dd, *J* = 8.2, 2.2 Hz, 1H), 2.35 (s, 3H). **^{13}C-NMR (151 MHz, $CDCl_3$)** δ = 13C NMR (151 MHz, CDCl3) δ = 171.7, 141.7, 138.2, 134.6, 132.8, 90.6, 20.8. **FTIR (ATR, neat)** $\tilde{\nu}$ = 2870, 2549, 1674, 1560, 1468, 1408, 1296, 1255, 1215, 1012, 756. **MS (EI, 70 eV)** *m/z* = 261.9 $[M]^{+\cdot}$. **Mp** *T* = 111 – 113. The analytical data is in accordance with literature data.[5]

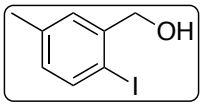

Following **GP2**, the reaction of 2-iodo-5-methylbenzoic acid (**S1d**, 15.0 mmol, 3.93 g) in dry THF (15 ml) with BH_3SMe_2 (18.0 mmol, 1.80 ml) gave (2-iodo-5-methylphenyl)methanol (**S2d**, 3.72 g, 15.0 mmol, quant.) as a colourless solid, which was analysed via ^{1}H-NMR and used without further purification.

^{1}H-NMR (600 MHz, $CDCl_3$) δ = 7.68 (d, *J* = 8.0 Hz, 1H), 7.28 (d, *J* = 2.2 Hz, 1H), 6.83 (dd, *J* = 8.0, 2.2 Hz, 1H), 4.65 (s, 2H), 3.77 – 3.73 (m, 1H), 2.32 (s, 3H). The analytical data is in accordance with literature data.[6]

Following **GP3**, the reaction of (2-iodo-5-methylphenyl)methanol (**S2d**, 10.0 mmol, 2.48 g) in Ac_2O (60.0 mmol, 5.67 ml) with iodine (1.00 mmol, 254 mg) gave after a reaction time of 4 h and subsequent column chromatography (silica, cyclohexane/ethyl acetate 1:0→19:1) 2-iodo-3-methylbenzyl acetate (**3d**, 2.27 g, 7.82 mmol, 78%) as a yellow solid.

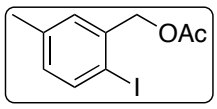

^{1}H-NMR (600 MHz, $CDCl_3$) δ = 7.72 (d, *J* = 8.0 Hz, 1H), 7.19 (d, *J* = 2.2 Hz, 1H), 6.85 (dd, *J* = 8.0, 2.2 Hz, 1H), 5.09 (s, 2H), 2.31 (s, 3H), 2.14 (s, 3H). **^{13}C-NMR (151 MHz, $CDCl_3$)** δ = 170.6, 139.3, 138.5, 137.9, 130.9, 130.5, 129.0, 94.4, 70.1, 20.9. **FTIR (ATR, neat)** $\tilde{\nu}$ = 2974, 2916, 1727, 1443, 1375, 1357, 1233, 1045, 1020, 812. **HRMS (ESI+, MeOH)** *m/z* = 312.96956 $[M+Na]^+$. Calculated for $[C_{10}H_{11}INaO_2]^+$: *m/z* = 312.96960. **Mp** *T* = 103 – 104.

4-Bromo-2-iodobenzyl acetate (3e)

Following **GP1**, the reaction of 2-amino-4-bromobenzoic acid (10.0 mmol, 2.16 g) in MeCN (80 ml) with $NaNO_2$ (1.38 g, 20.0 mmol) and KI (4.15 g, 25.0 mmol) in water (15 ml) gave 4-bromo-2-iodobenzoic acid (**S1e**, 2.65 g, 8.11 mmol, 81%) as a colourless solid.

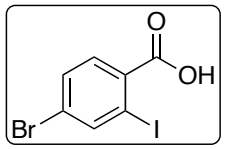

^{1}H-NMR (600 MHz, DMSO-d_6) δ = 13.47 (s, 1H), 8.19 (d, *J* = 1.8 Hz, 1H), 7.70 (dd, *J* = 8.3, 1.8 Hz, 1H), 7.65 (d, *J* = 8.3 Hz, 1H). **^{13}C-NMR (151 MHz, DMSO- d_6)** δ = 167.4, 142.1, 136.0, 131.5, 131.2, 125.0, 95.7. **FTIR (ATR, neat)** $\tilde{\nu}$ = 3064, 1672, 1422, 1291, 1542, 1291, 1249, 1023, 838, 771. **MS (EI, 70 eV)** *m/z* = 325.8 $[M]^{+\cdot}$. **Mp** *T* = 175 – 177. The analytical data is in accordance with literature data.[1]

Following **GP2**, the reaction of 4-bromo-2-iodobenzoic acid (**S1e**, 7.50 mmol, 2.45 g) in dry THF (7.5 ml) with BH_3SMe_2 (9.00 mmol, 900 µl) gave after a subsequent column chromatography (silica, cyclohexane/ethyl acetate 1:0→9:1) (2-iodo-4-bromophenyl)methanol (**S2e**, 1.63 g, 5.21 mmol, 69%) as a colourless solid.

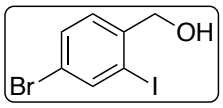

^{1}H-NMR (600 MHz, $CDCl_3$) δ = 7.96 (d, *J* = 1.9 Hz, 1H), 7.50 (dd, *J* = 8.2, 1.9 Hz, 1H), 7.33 (d, *J* = 8.2 Hz, 1H), 4.62 (d, *J* = 5.6 Hz, 2H), 2.06 (t, *J* = 6.0 Hz, 1H). **^{13}C-NMR (151 MHz, $CDCl_3$)** δ = 141.6, 140.9, 131.5, 129.3, 121.7, 97.3, 68.6. **FTIR (ATR, neat)** $\tilde{\nu}$ = 3315, 3226, 1572, 1550, 1467, 1377, 1056, 1008, 801, 705. **MS (EI, 70 eV)** *m/z* = 311.8 $[M]^{+\cdot}$. **Mp** *T* = 104 – 105. The analytical data is in accordance with literature data.[1]

Following **GP3**, the reaction of (2-iodo-4-bromophenyl)methanol (**S2e**, 5.11 mmol, 1.60 g) in Ac_2O (30.7 mmol, 3.13 ml) with iodine (0.511 mmol, 130 mg) gave after a reaction time of 4 h and subsequent column chromatography (silica, cyclohexane/ethyl acetate 1:0 → 19:1) 5-chloro-2-iodobenzyl acetate (**3e**, 1.73 g, 4.87 mmol, 95%) as a colourless liquid.

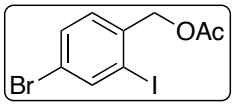

^{1}H-NMR (600 MHz, $CDCl_3$) δ = 7.69 (d, *J* = 8.3 Hz, 1H), 7.50 (d, *J* = 2.3 Hz, 1H), 7.16 (dd, *J* = 8.4, 2.4 Hz, 1H), 5.07 (s, 2H), 2.17 (s, 3H). **^{13}C-NMR (151 MHz, $CDCl_3$)** δ = 170.4, 140.7, 140.4, 132.8, 132.0, 122.7,

95.7, 69.3, 20.9. **FTIR (ATR, neat)** $\tilde{\nu}$ = 3079, 2934, 1734, 1574, 1552, 1462, 1367, 1216, 1020, 809. **HRMS (ESI+, MeOH)** *m/z* = 376.86414 $[M+Na]^+$. Calculated for $[C_9H_8BrINaO_2]^+$: *m/z* = 376.86446.

2-Iodo-3-methylbenzyl acetate (3f)

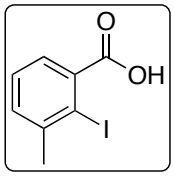

Following **GP1**, the reaction of 2-amino-3-methylbenzoic acid (30.0 mmol, 4.53 g) in MeCN (240 ml) with $NaNO_2$ (4.14 g, 60.0 mmol) and KI (12.5 g, 75.0 mmol) in water (45 ml) gave 2-iodo-3-methylbenzoic acid (**S1f**, 3.26 g, 12.4 mmol, 41%) as a yellow solid.

^{1}H-NMR (600 MHz, DMSO-*d*$_6$) δ = 13.07 (s, 1H), 7.42 (dd, *J* = 7.2, 2.1 Hz, 1H), 7.34 (t, *J* = 7.4 Hz, 1H), 7.30 (dd, *J* = 7.6, 2.2 Hz, 1H), 2.43 (s, 3H). **^{13}C-NMR (151 MHz, DMSO-*d*$_6$)** δ = 169.7, 142.4, 140.3, 131.2, 128.0, 126.1, 99.6, 29.0. **FTIR (ATR, neat)** $\tilde{\nu}$ = 2975, 2805, 2545, 1698, 1671, 1568, 1413, 1290, 1187, 929. **MS (EI, 70 eV)** *m/z*: 261.9 $[M]^{+\cdot}$. **Mp** *T* = 151 – 152. The analytical data is in accordance with literature data.[7]

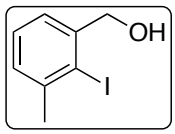

Following **GP2**, the reaction of 2-iodo-3-methylbenzoic acid (**S1f**, 11.3 mmol, 2.97 g) in dry THF (11 ml) with BH_3SMe_2 (13.6 mmol, 1.36 ml) gave after a subsequent column chromatography (silica, cyclohexane/ethyl acetate 1:0 → 9:1) (2-iodo-3-methylphenyl)methanol (**S2f**, 2.10 g, 8.47 mmol, 75%) as a colourless solid.

^{1}H-NMR (360 MHz, $CDCl_3$) δ = 7.28 – 7.23 (m, 2H), 7.25 – 7.14 (m, 1H), 4.71 (s, 2H), 2.48 (s, 3H). **^{13}C-NMR (91 MHz, $CDCl_3$)** δ = 143.2, 142.1, 129.0, 128.1, 125.7, 104.7, 70.3, 29.1. **FTIR (ATR, neat)** $\tilde{\nu}$ = 3251, 3070, 2891, 1573, 1445, 1375, 1312, 1169, 1055. 1000. **MS (EI, 70 eV)** *m/z*: 248.0 $[M]^{+\cdot}$. **Mp** *T* = 70 – 71. The analytical data is in accordance with literature data.[8]

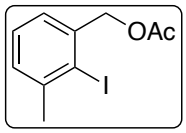

Following **GP3**, the reaction of (2-iodo-3-methylphenyl)methanol (**S2f**, 8.00 mmol, 1.98 g) in Ac_2O (48.0 mmol, 4.54 ml) with iodine (0.800 mmol, 203 mg) gave after a reaction time of 4 h and subsequent column chromatography (silica, cyclohexane/ethyl acetate 1:0 → 19:1) 2-iodo-3-methylbenzyl acetate (**3f**, 2.19 g, 7.57 mmol, 95%) as a colourless liquid.

^{1}H-NMR (600 MHz, $CDCl_3$) δ = 7.25 – 7.19 (m, 2H), 7.17 (dd, J = 7.2, 2.0 Hz, 1H), 5.17 (s, 2H), 2.49 (s, 3H), 2.15 (s, 3H). **^{13}C-NMR (151 MHz, $CDCl_3$)** δ = 170.7, 142.6, 138.8, 129.5, 128.0, 126.6, 105.5, 71.1, 29.3, 21.0. **FTIR (ATR, neat)** $\tilde{\nu}$ = 3049, 2948, 1734, 1532, 1450, 1372, 1218, 1054, 1010, 773. **HRMS (ESI+, MeOH)** *m/z* = 312.96922 $[M+Na]^+$. Calculated for $[C_{10}H_{11}INaO_2]^+$: *m/z* = 312.96960.

3.2.2 Secondary Benzyl Alcohols

1-(2-Iodophenyl)ethan-1-ol (4)

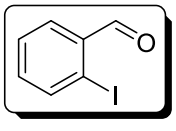

(2-Iodophenyl)methanol (**S2a**, 24.9 g, 106 mmol, 1.00 equiv) was dissolved in $CHCl_3$ (265 mL), activated MnO_2 (92.4 g, 1.06 mol, 10.0 equiv) was added and the suspension was stirred for 24 h at rt. The mixture was filtrated over Celite and the filter material was washed with ethyl acetate (300 mL). After removal of the solvent under reduced pressure, 2-iodobenzaldehyde (**S3**, 21.9 g, 94.4 mmol, 89%) was obtained as a colourless solid.

^{1}H-NMR (600 MHz, $CDCl_3$) δ = 10.07 (d, *J* = 0.7 Hz, 1H), 7.96 (dd, *J* = 7.9, 1.1 Hz, 1H), 7.89 (dd, *J* = 7.7, 1.8 Hz, 1H), 7.47 (t, *J* = 7.5 Hz, 1H), 7.29 (ddd, *J* = 7.9, 7.4, 1.8 Hz, 1H). **^{13}C-NMR (151 MHz, $CDCl_3$)** δ =

196.0, 140.8, 135.7, 135.2, 130.4, 128.9, 100.9. **FTIR (ATR, neat)** $\tilde{\nu}$ = 2849, 2833, 2746, 1683, 1578, 1436, 1388, 1261, 1200, 1015, 748. **MS (EI, 70 eV)** *m/z* = 232.0 $[M]^{+\cdot}$, 203.0 $[M\text{-}CHO]^{+}$. **Mp** *T* = 34 – 35 °C. The analytical data is in accordance with literature data.[1]

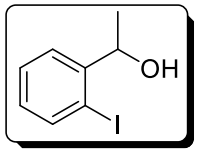

To a solution of 2-iodobenzaldehyde (**S3**, 3.02 g, 13.0 mmol, 1.00 equiv) in dry THF (26 mL) at 0 °C MeMgBr (4.80 mL, 3 M in THF, 14.3 mmol, 1.10 equiv) was added at a rate of 0.8 mL/min. The mixture was allowed to warm to rt overnight and sat. NH_4Cl (10 mL) and Et_2O (10 mL) were added. The phases were separated and the aqueous phase was extracted with Et_2O (2 × 10 mL). The combined organic phases were dried over Na_2SO_4, concentrated under reduced pressure and the residue was purified via column chromatography (silica, cyclohexane/ethyl acetate 1:0→10:1) to obtain 1-(2-iodophenyl)ethan-1-ol (**4**, 2.84 g, 8.38 mmol, 88%) as a colourless liquid.

^{1}H-NMR (600 MHz, $CDCl_3$) δ = 7.80 (dd, *J* = 7.9, 1.2 Hz, 1H), 7.57 (dd, *J* = 7.8, 1.7 Hz, 1H), 7.38 (td, *J* = 7.6, 1.3 Hz, 1H) 6.97 (td, *J* = 7.7, 1.8 Hz, 1H), 5.08 (qd, *J* = 6.4, 3.3 Hz, 1H), 1.96 (d, J = 3.3 Hz, 1H), 1.47 (d, *J* = 6.4 Hz, 3H). **^{13}C-NMR (151 MHz, $CDCl_3$)** δ = 147.6, 139.5, 129.3, 128.9, 126.5, 97.4, 73.9, 23.9. **FTIR (ATR, neat)** $\tilde{\nu}$ = 3312, 3057, 2970, 2924, 1584, 1563, 1462, 1435, 1367, 1260, 1199, 1124, 1086, 1067, 1045, 1007, 897, 751, 720, 652. **MS (EI, 70 eV)** *m/z* = 248.0 $[M]^{+\cdot}$, 233.0 $[M\text{-}CH_3]^{+}$. The analytical data is in accordance with literature data.[1]

4 Substrate synthesis

4.1 General Procedures for the One-Pot Reaction Utilizing Primary Benzyl Acetates 3 and Secondary Benzyl Alcohol 4 (OPP1)

4.1.1 Standard conditions employing primary benzyl acetates 3 (OPP1a)

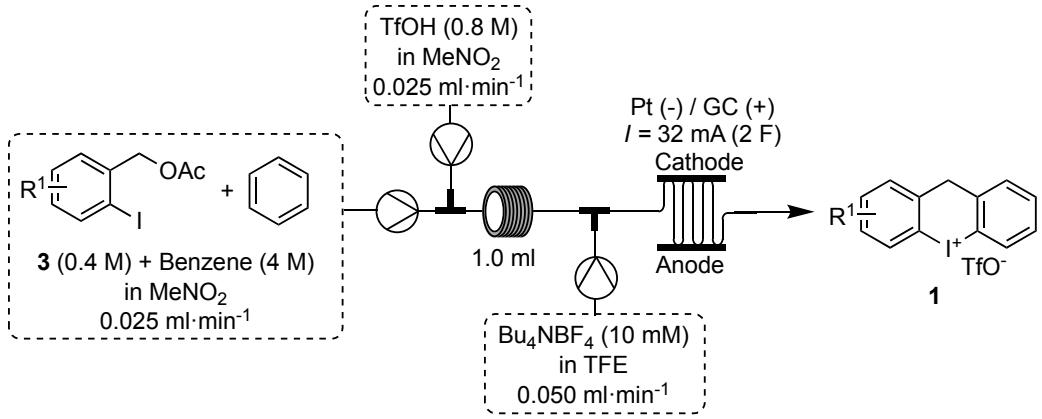

*Scheme S2: General scheme for the synthesis of iodinium salts **1** from primary benzyl acetates **3**.*

The reaction was performed in a continuous flow reactor based on three syringe pumps, one reaction chamber (1.0 ml) at room temperature and an electrochemical Flow Reactor (*Vapourtec - Ion Electrochemical Flow Reactor*, Volume = 0.60 ml, spacer 0.50 mm, 0.10 ml·min^{-1}). All parts were joined with T-Pieces as shown in scheme **S2**. A solution of benzyl acetate **3** (0.4 M, 1.00 equiv) and benzene (4.0 M, 10.0 equiv) in $MeNO_2$ was mixed in flow with a solution of TfOH (0.8 M, 2.00 equiv) in $MeNO_2$ and reacted at rt for 20 min at a combined flowrate of 0.05 ml·min^{-1}. Afterwards a solution of *n*-BuN_4BF_4 (10 mM) in TFE was added to the stream and the flow was subjected to electrolysis by employing a glassy carbon (GC) anode and a platinum cathode. The electrolysis was performed under CCE (j = 2.67 mA·cm^{-2}, 2 F) at a total combined flowrate of 0.10 ml·min^{-1}. The first two reactor volumes were discarded to reach a steady state. After collecting for 3 h 20 min the solution was concentrated by reduced pressure and the product was first precipitated and afterwards washed with Et_2O to obtain the corresponding iodininium salt.

4.1.2 Standard conditions employing secondary benzyl alcohol 4 (OPP1b)

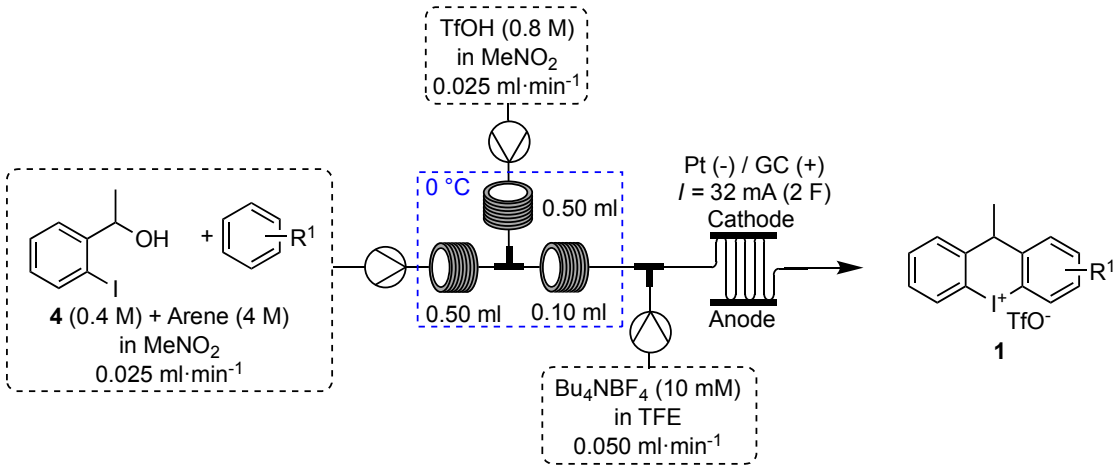

*Scheme S3: General scheme for the synthesis of iodinium salts **1** from secondary benzyl alcohols **4**.*

The reaction was performed in a continuous flow reactor based on three syringe pumps, one reaction chamber (0.10 ml) at room temperature and an electrochemical Flow Reactor (*Vapourtec - Ion Electrochemical Flow Reactor*, Volume = 0.60 ml, spacer 0.50 mm, 0.10 ml·min^{-1}). All parts were joined with T-Pieces as shown in scheme **S3**. An in flow precooled (for 20 min @ 0 °C) solution of benzyl alcohol **4** (0.4 M, 1.00 equiv) and the corresponding arene (4.0 M, 10.0 equiv) in $MeNO_2$ was mixed with an in flow precooled (for 20 min @ 0 °C) solution of TfOH (0.8 M, 2.00 equiv) in $MeNO_2$ and reacted at 0 °C for 2 min at a combined flowrate of 0.05 ml·min^{-1}. Afterwards a solution of *n*-BuN_4BF_4 (10 mM) in TFE was added to the stream and the flow was subjected to electrolysis by employing a glassy carbon (GC) anode and a platinum cathode. The electrolysis was performed under CCE (*j* = 2.67 mA·cm^{-2}, 2 F) at a total combined flowrate of 0.10 ml·min^{-1}. The first two reactor volumes were discarded to reach a steady state. After collecting for 3 h 20 min the solution was concentrated by reduced pressure and the product was first precipitated and afterwards washed with Et_2O to obtain the corresponding iodininium salt.

4.2 Substrates from Primary Benzyl Acetates and Secondary Benzyl Alcohols

10*H*-Dibenzo[*b,e*]iodinin-5-ium trifluoromethanesulfonate (1a)

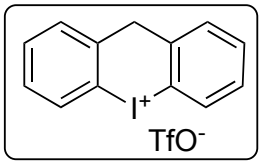

Following **OPP1a**, the reaction of 2-iodobenzyl acetate (**3a**, 552 mg, 2.00 mmol) gave the product **1a** (373 mg, 0.844 mmol, 42%) as a colourless solid.

^{1}H-NMR (601 MHz, DMSO-d_6) δ = 8.10 (dd, *J* = 8.1, 1.2 Hz, 2H), 7.81 (dd, *J* = 7.6, 1.6 Hz, 2H), 7.61 (td, *J* = 7.5, 1.2 Hz, 2H), 7.43 (td, *J* = 7.7, 1.6 Hz, 2H), 4.32 (s, 2H). **^{13}C-NMR (151 MHz, DMSO-d_6)** δ = 138.9, 133.7, 131.8, 130.5, 129.1, 120.7 (q, *J* = 322.7 Hz), 116.0, 45.7. **^{19}F-NMR (565 MHz, DMSO-d_6)** δ = -77.7. **FTIR (ATR, neat)** $\tilde{\nu}$ = 3094, 3059, 1457, 1441, 1426, 1237, 1220, 1152, 1023, 751. **MS (ESI$^+$, MeCN/H_2O)** *m/z* = 292.9 [M-OTf]$^+$. **Mp** *T* = 219 – 221 °C (decomp.). The analytical data is in accordance with literature data.[1]

2-Fluoro-10*H*-dibenzo[*b,e*]iodinin-5-ium trifluoromethanesulfonate (1b)

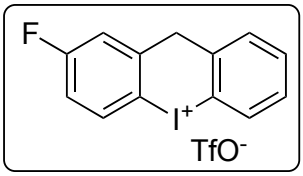

Following **OPP1a**, the reaction of 5-fluoro-2-iodobenzyl acetate (**3b**, 588 mg, 2.00 mmol) gave the product **1b** (135 mg, 0.294 mmol, 15%) as a colourless solid.

^{1}H-NMR (601 MHz, DMSO-d_6) δ = 8.12 (dd, *J* = 8.9, 5.3 Hz, 1H), 8.09 (dd, *J* = 8.1, 1.2 Hz, 1H), 7.77 (dd, *J* = 7.6, 1.6 Hz, 1H), 7.74 (dd, *J* = 9.3, 3.0 Hz, 1H), 7.62 (td, *J* = 7.5, 1.2 Hz, 1H), 7.44 (ddd, *J* = 8.2, 7.4, 1.6 Hz, 1H), 7.36 (td, *J* = 8.7, 3.0 Hz, 1H), 4.34 (s, 2H). **^{13}C-NMR (151 MHz, DMSO-d_6)** δ = 163.8 (d, *J* = 249.8 Hz), 142.2 (d, *J* = 8.8 Hz), 138.4, 135.7 (d, *J* = 9.0 Hz), 133.6, 131.8, 130.6, 129.2, 120.7 (q, *J* = 322.3 Hz), 117.6 (d, *J* = 23.6 Hz), 116.3 (d, *J* = 24.2 Hz), 116.2, 110.1 (d, *J* = 2.4 Hz), 45.3. **^{19}F-NMR (565 MHz, DMSO-d_6)** δ = -77.7, -109.3 (td, *J* = 8.8, 5.3 Hz). **FTIR (ATR, neat)** $\tilde{\nu}$ = 3098, 1573, 1460, 1272, 1220, 1173, 1021, 998, 817, 758. **MS (ESI$^+$, MeCN/H_2O)** *m/z* = 310.9 [M-OTf]$^+$. **Mp** *T* = 225 – 230 (decomp.). The analytical data is in accordance with literature data.[1]

2-Chloro-10*H*-dibenzo[*b,e*]iodinin-5-ium trifluoromethanesulfonate (1c)

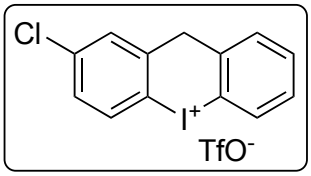

Following **OPP1a**, the reaction of 5-chloro-2-iodobenzyl acetate (**3c**, 621 mg, 2.00 mmol) gave the product **1c** (249 mg, 0.523 mmol, 26%) as a colourless solid.

^{1}H-NMR (601 MHz, DMSO-d_6) δ = 8.09 (dd, *J* = 8.1, 1.2 Hz, 1H), 8.08 (d, *J* = 8.6 Hz, 1H), 7.95 (d, *J* = 2.5 Hz, 1H), 7.77 (dd, *J* = 7.6, 1.6 Hz, 1H), 7.62 (td, *J* = 7.5, 1.2 Hz, 1H), 7.54 (dd, *J* = 8.6, 2.5 Hz, 1H), 7.44 (td, *J* = 8.1, 1.6 Hz, 1H), 4.33 (s, 2H). **^{13}C-NMR (151 MHz, DMSO-d_6)** δ = 141.4, 138.4, 136.6, 135.2, 133.6, 131.9, 130.7, 130.1, 129.2, 128.8, 120.7 (q, *J* = 322.2 Hz), 116.2, 114.1, 45.1. **^{19}F-NMR (565 MHz, DMSO-d_6)** δ = -77.7. **FTIR (ATR, neat)** $\tilde{\nu}$ = 3085, 1556, 1453, 1276, 1220, 1171, 1021, 993, 785, 756. **MS (ESI$^+$, MeCN/H_2O)** *m/z* = 344.9 [M+H_2O-OTf]$^+$. **Mp** *T* = 216 – 218. The analytical data is in accordance with literature data.[1]

2-Methyl-10*H*-dibenzo[*b,e*]iodinin-5-ium trifluoromethanesulfonate (1d)

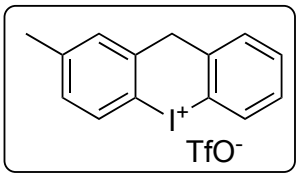

Following **OPP1a**, the reaction of 2-iodo-5-methylbenzyl acetate (**3d**, 580 mg, 2.00 mmol) gave the product **1d** (496 mg, 1.09 mmol, 54%) as a colourless solid.

^{1}H-NMR (600 MHz, DMSO-d_6) δ = 8.08 (dd, *J* = 8.1, 1.2 Hz, 1H), 7.95 (d, *J* = 8.2 Hz, 1H), 7.79 (dd, *J* = 7.5, 1.6 Hz, 1H), 7.63 (d, *J* = 2.1 Hz, 1H), 7.60 (td, *J* = 7.4, 1.1 Hz, 1H), 7.42 (td, *J* = 7.7, 1.7 Hz, 1H), 7.25 (dd, *J* = 8.3, 2.1 Hz, 1H), 4.26 (s, 2H), 2.37 (s, 3H). **^{13}C-NMR (151 MHz, DMSO-d_6)** δ = 142.0, 139.0, 138.7, 133.6, 133.3, 131.7, 131.1, 130.5, 129.7, 129.0, 120.7 (q, *J* = 322.2 Hz), 116.0, 112.2, 45.6, 20.6. **^{19}F-NMR (565 MHz, DMSO-d_6)** δ = -77.7. **FTIR (ATR, neat)** $\tilde{\nu}$ = 3046, 1594, 1460, 1443, 1388, 1277, 1243, 1152, 1025, 746. **HRMS (ESI$^+$, MeOH)** *m/z* = 306.99760 [M-OTf]$^+$. Calculated for $[C_{14}H_{12}I]^{+\cdot}$: *m/z* = 306.99782. **Mp** *T* = 200 – 205 (decomp.).

3-Bromo-10*H*-dibenzo[*b,e*]iodinin-5-ium trifluoromethanesulfonate (1e)

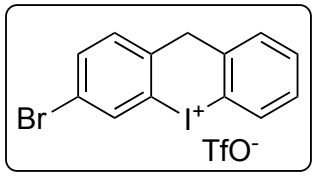

Following **OPP1a**, the reaction of 3-bromo-2-iodobenzyl acetate (**3e**, 710 mg, 2.00 mmol) gave the product **1e** (171 mg, 0.329 mmol, 16%) as a colourless solid.

^{1}H-NMR (600 MHz, DMSO-d_6) δ = 8.27 (d, *J* = 2.0 Hz, 1H), 8.10 (dd, *J* = 8.1, 1.2 Hz, 1H), 7.83 (dd, *J* = 8.1, 2.0 Hz, 1H), 7.79 (dd, *J* = 7.6, 1.6 Hz, 1H), 7.75 (d, *J* = 8.2 Hz, 1H), 7.62 (td, *J* = 7.5, 1.2 Hz, 1H), 7.44 (td, *J* = 7.7, 1.7 Hz, 1H), 4.30 (s, 2H). **^{13}C-NMR (151 MHz, DMSO-d_6)** δ = 138.7, 138.5, 135.5, 134.5, 133.7, 131.9, 131.8, 130.6, 129.2, 121.8 (q, *J* = 322 Hz), 120.4, 117.0, 116.2, 44.9. **^{19}F-NMR (565 MHz, DMSO-d_6)** δ = -77.7. **FTIR (ATR, neat)** $\tilde{\nu}$ = 3097, 1576, 1457, 1379, 1282, 1233, 1159, 1025, 842, 751. **MS (ESI$^+$, MeCN/H_2O)** *m/z* = 3790.8 [M-OTf]$^+$. **Mp** *T* = 210 – 215 (decomp.). The analytical data is in accordance with literature data.[1]

4-Methyl-10*H*-dibenzo[*b,e*]iodinin-5-ium trifluoromethanesulfonate (1f)

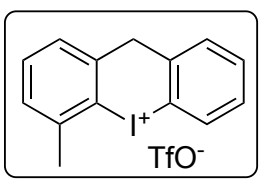

Following **OPP1a**, the reaction of 2-iodo-3-methylbenzyl acetate (**3f**, 580 mg, 2.00 mmol) gave the product **1f** (313 mg, 0.686 mmol, 34%) as a colourless solid.

^{1}H-NMR (600 MHz, DMSO-d_6) δ 8.10 (dd, *J* = 8.2, 1.1 Hz, 1H), 7.82 (dd, *J* = 7.6, 1.6 Hz, 1H), 7. 64 (d, *J* = 7.4 Hz, 1H), 7.62 (td, *J* = 7.5, 1.2 Hz, 1H), 7.52 (t,

J = 7.4 Hz, 1H), 7.42 (td, *J* = 8.2, 1.6 Hz, 1H), 7.39 (d, *J* = 7.3 Hz, 1H), 4.35 (s, 2H), 2.63 (s, 3H). **^{13}C-NMR (151 MHz, DMSO-*d*$_6$)** δ = 140.6, 139.7, 139.0, 133.7, 131.9, 131.7, 130.3, 129.5, 129.0, 128.0, 120.7 (q, *J* = 322.3 Hz), 120.5, 117.0, 47.2, 24.6 **^{19}F-NMR (565 MHz, DMSO-*d*$_6$)** δ = -77.7. **FTIR (ATR, neat)** $\tilde{\nu}$ = 1460, 1440, 1425, 1275, 1228, 1172, 1021, 994, 810, 745. **HRMS (ESI$^+$, MeOH)** *m/z* = 306.99762 [M-OTf]$^+$. Calculated for $[C_{14}H_{12}I]^{+\cdot}$: *m/z* = 306.99782. **Mp** *T* = 120 – 125 (decomp.).

10-Methyl-10*H*-dibenzo[*b,e*]iodinin-5-ium trifluoromethanesulfonate (1g)

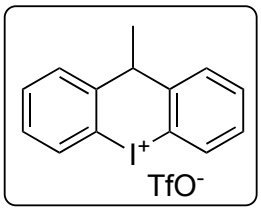

Following **OPP1b**, the reaction of 1-(2-iodophenyl)ethan-1-ol (**4**, 710 mg, 2.00 mmol) with benzene (1.56 g, 1.78 ml, 20.0 mmol) gave the product **1g** (346 mg, 0.759 mmol, 38%) as a colourless solid.

^{1}H-NMR (600 MHz, DMSO-*d*$_6$) δ = 8.13 (dd, *J* = 8.0, 1.2 Hz, 1H), 7.74 (dd, *J* = 7.8, 1.6 Hz, 1H), 7.64 (td, *J* = 7.5, 1.2 Hz, 1H), 7.43 (td, *J* = 7.7, 1.6 Hz, 1H), 4.25 (bs, 1H), 1.75 (bs, 2H). **^{13}C-NMR (151 MHz, DMSO-*d*$_6$)** δ = 141.6, 133.9, 131.8, 129.0, 128.8, 120.6 (q, *J* = 323 Hz), 47.8. Two Signals are missing due to signal broadening. **^{19}F-NMR (565 MHz, DMSO-*d*$_6$)** δ = -77.7. **FTIR (ATR, neat)** $\tilde{\nu}$ = 3257, 3077, 2990, 1589, 1559, 1446, 1362, 1307, 1280, 1260, 1245, 1198, 1178, 1134, 1108, 1081, 1067, 1025, 906, 831, 777, 763, 746. **HRMS (ESI$^+$, MeOH)** *m/z* = 306.99751 [M-OTf]$^+$. Calculated for $[C_{14}H_{12}I]^{+\cdot}$: *m/z* = 306.99782. **Mp** *T* = 255 – 257.

3,10-Dimethyl-10*H*-dibenzo[*b,e*]iodinin-5-ium trifluoromethanesulfonate (1h)

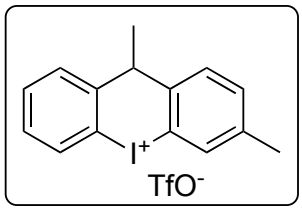

Following **OPP1b**, the reaction of 1-(2-iodophenyl)ethan-1-ol (**4**, 710 mg, 2.00 mmol) with toluene (1.84 g, 2.12 ml, 20.0 mmol) gave the product **1h** (347 mg, 0.738 mmol, 37%) as a colourless solid.

^{1}H-NMR (DMSO-*d*$_6$, 600 MHz) δ = 8.11 (dd, *J* = 8.2, 1.2 Hz, 1H), 7.93 (d, 1H), 7.73 (d, *J* = 6.8 Hz, 1H), 7.63 (td, *J* = 7.5, 1.2 Hz, 1H), 7.62 (d, *J* = 8.0 Hz, 1H), 7.45 (dd, *J* = 7.9, 1.6 Hz, 1H), 7.42 (td, *J* = 7.7, 1.6 Hz, 1H), 4.21 (bs, 1H), 2.36 (s, 3H), 1.72 (bs, 3H). **^{13}C-NMR (DMSO-*d*$_6$, 151 MHz)** δ = 141.8, 138.9, 138.6, 133.9, 133.8, 132.4, 131.8, 129.0, 128.5 (m, 2C), 120.7 (q, *J* = 322.6 Hz), 47.3, 20.2, 16.3. Two Signals are missing due to signal broadening. **^{19}F-NMR (DMSO-*d*$_6$, 565 MHz)** δ = -77.7. **FTIR (ATR, neat)** $\tilde{\nu}$ = 3096, 2976, 2926, 1458, 1438, 1386, 1015, 831, 769, 745. **HRMS (ESI$^+$, MeOH)** *m/z* = 321.01324 [M-TfO]$^+$. Calculated for $C_{15}H_{14}I^{+*}$: *m/z* = 321.01347. **Mp** *T* = 176-178. The analytical data (^{1}H- and ^{13}C-NMR) are in agreement with the by us previously reported corresponding tetrafluoroborate.[1]

4.3 Substrates that could not be successfully synthesized

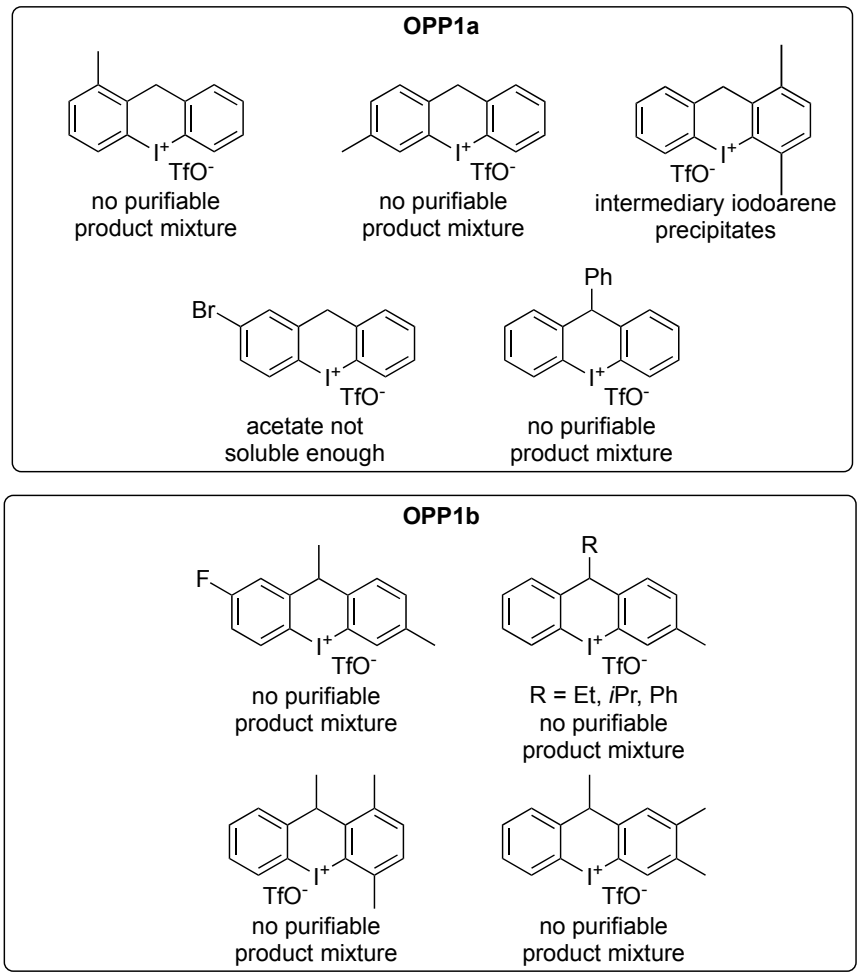

Figure S2: Substrates that could not successfully be synthesized with OPP1a or OPP1b.

5 NMR-Spectra of New Substrates

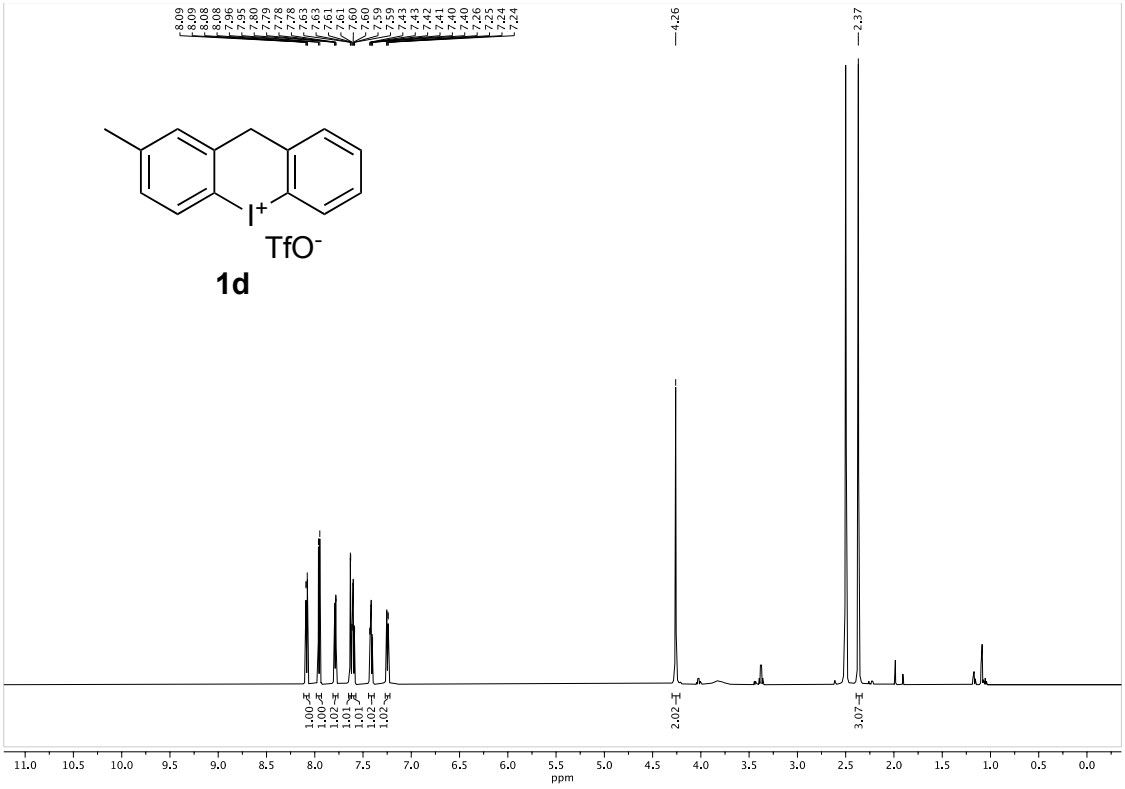

*Figure S2: 600 MHz ^{1}H-NMR spectrum of compound **1d**.*

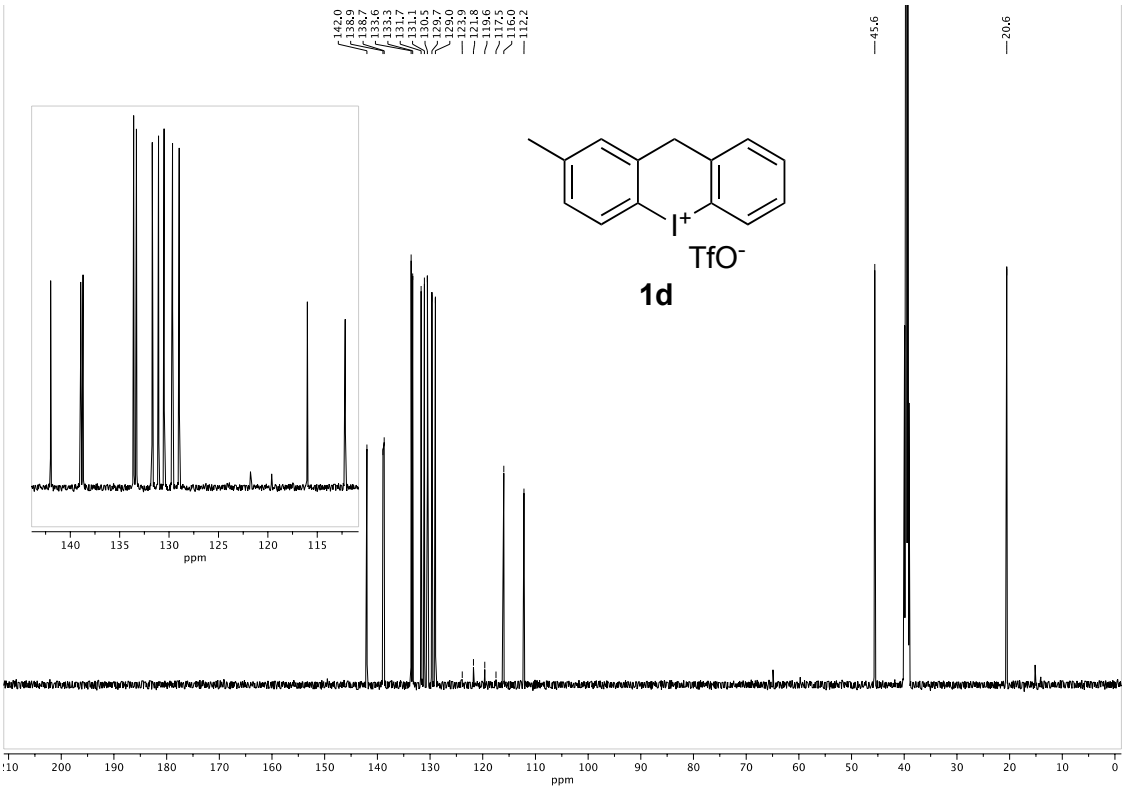

*Figure S3: 151 MHz ^{13}C-NMR spectrum of compound **1d**.*

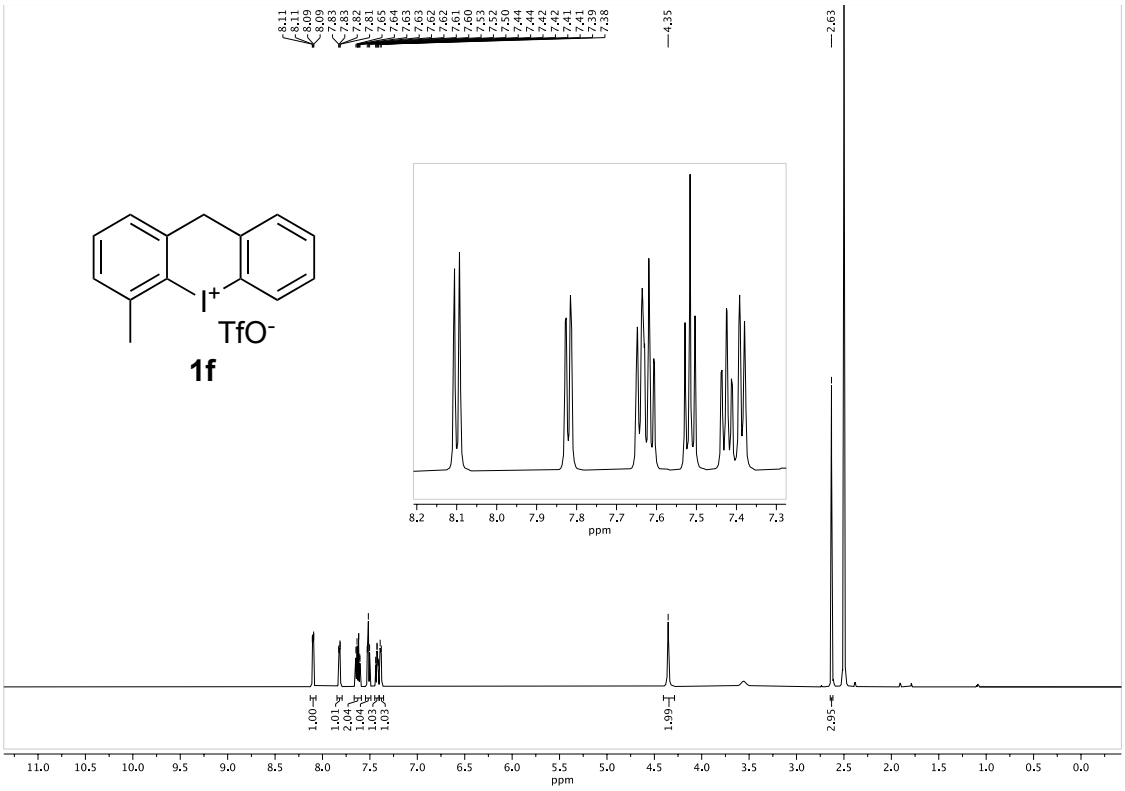

*Figure S4: 600 MHz ^{1}H-NMR spectrum of compound **1f**.*

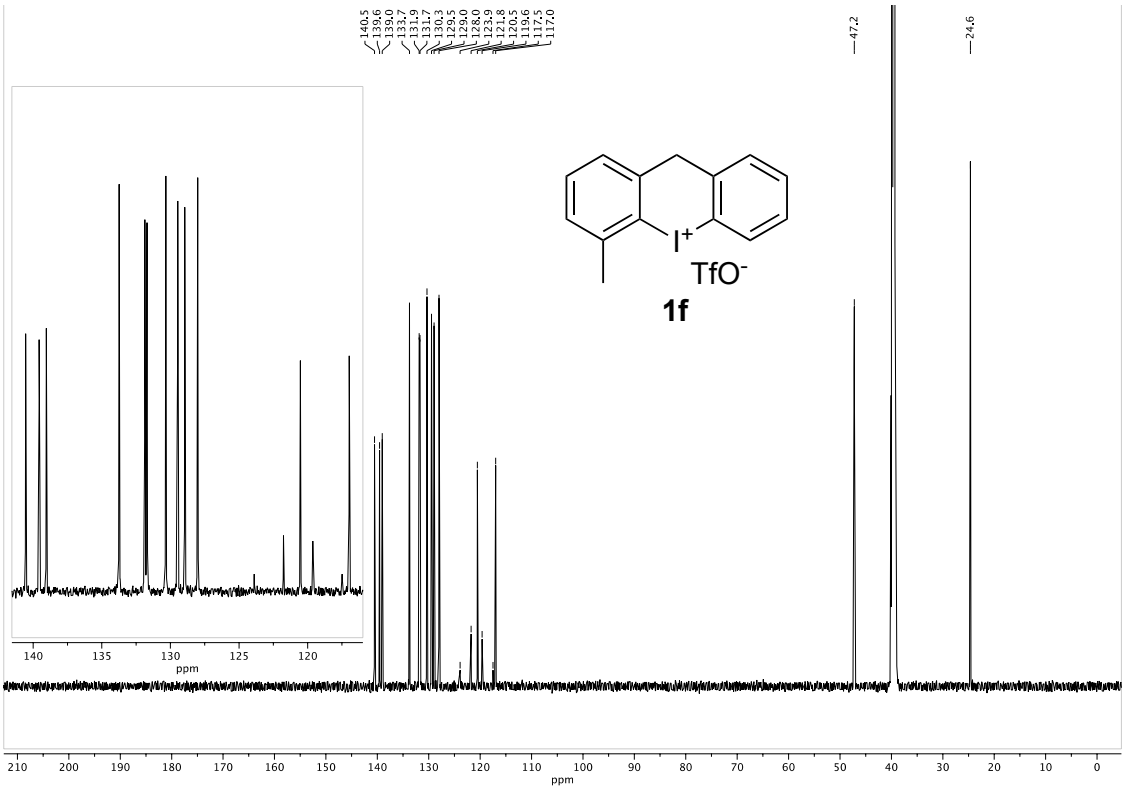

*Figure S5: 151 MHz ^{13}C-NMR spectrum of compound **1f**.*

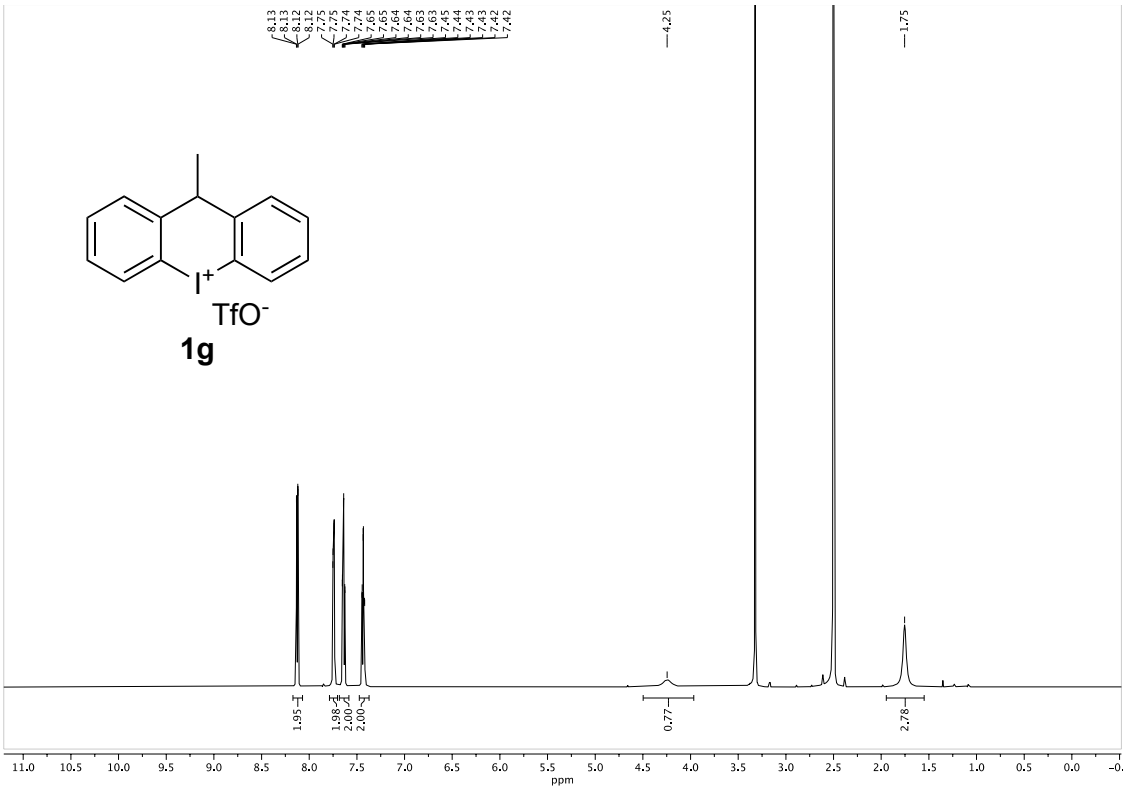

*Figure S6: 600 MHz ^{1}H-NMR spectrum of compound **1g**.*

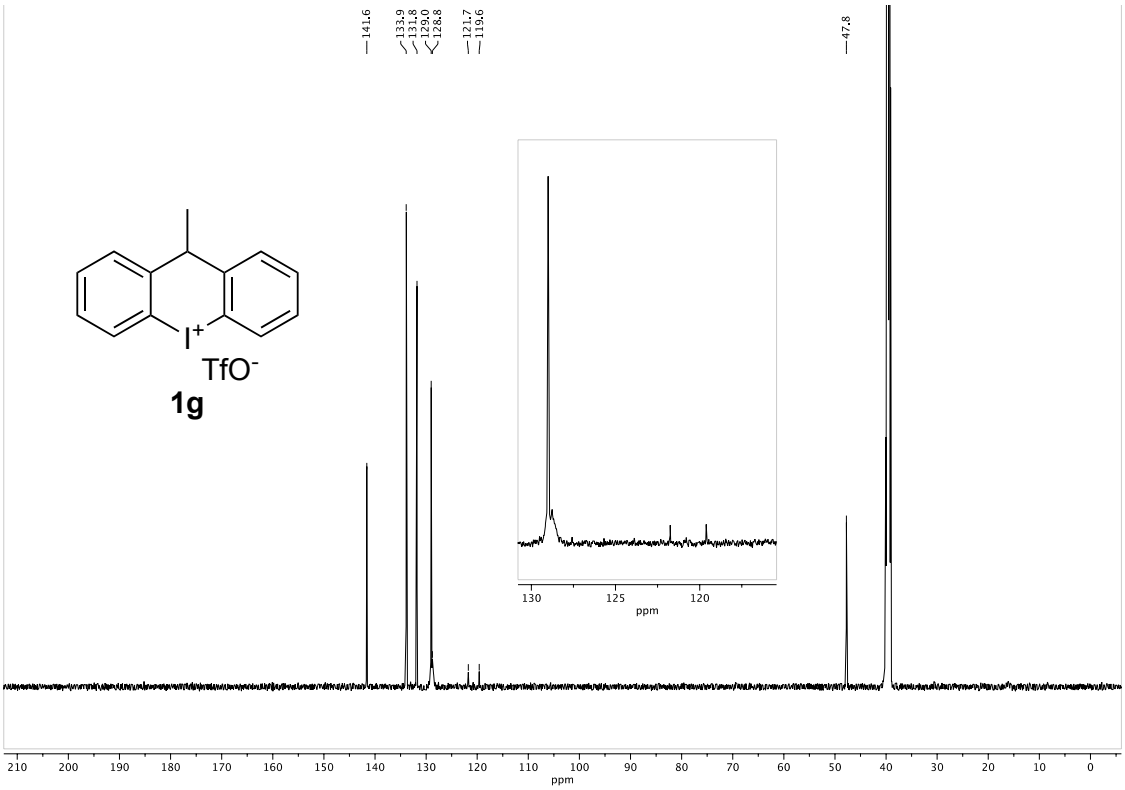

*Figure S7: 151 MHz ^{13}C-NMR spectrum of compound **1g**.*

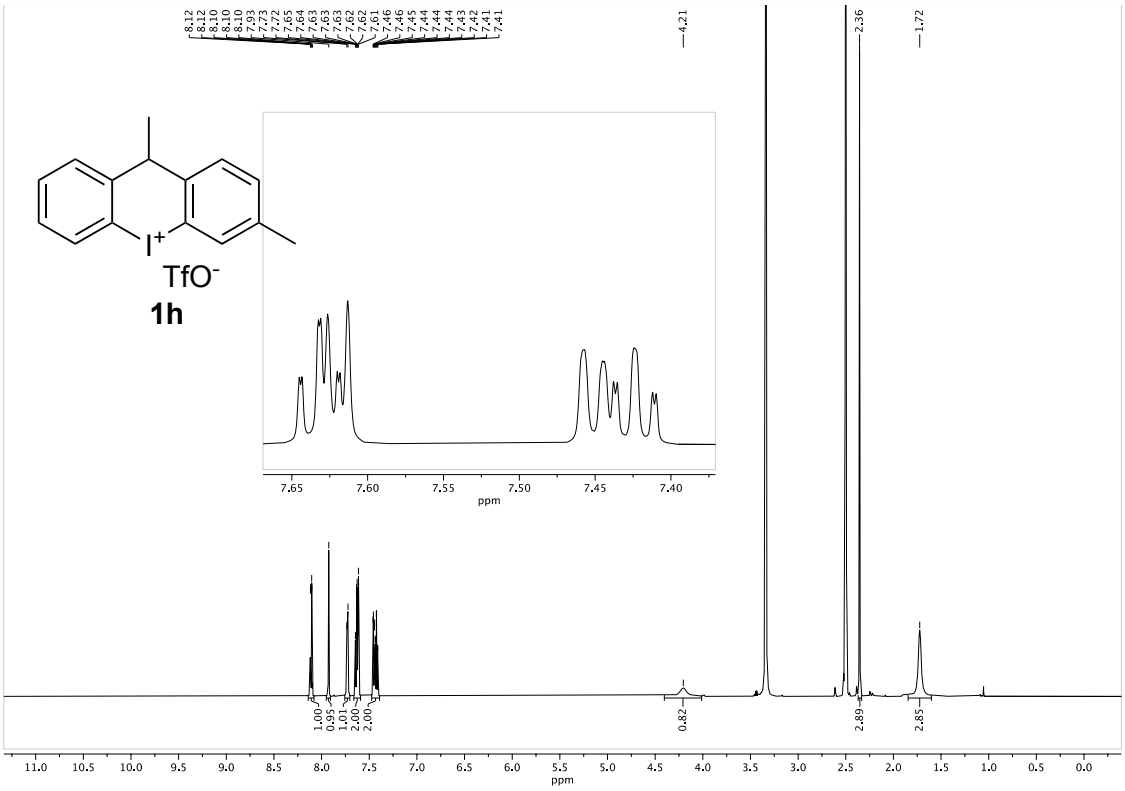

*Figure S8: 600 MHz ^{1}H-NMR spectrum of compound **1h**.*

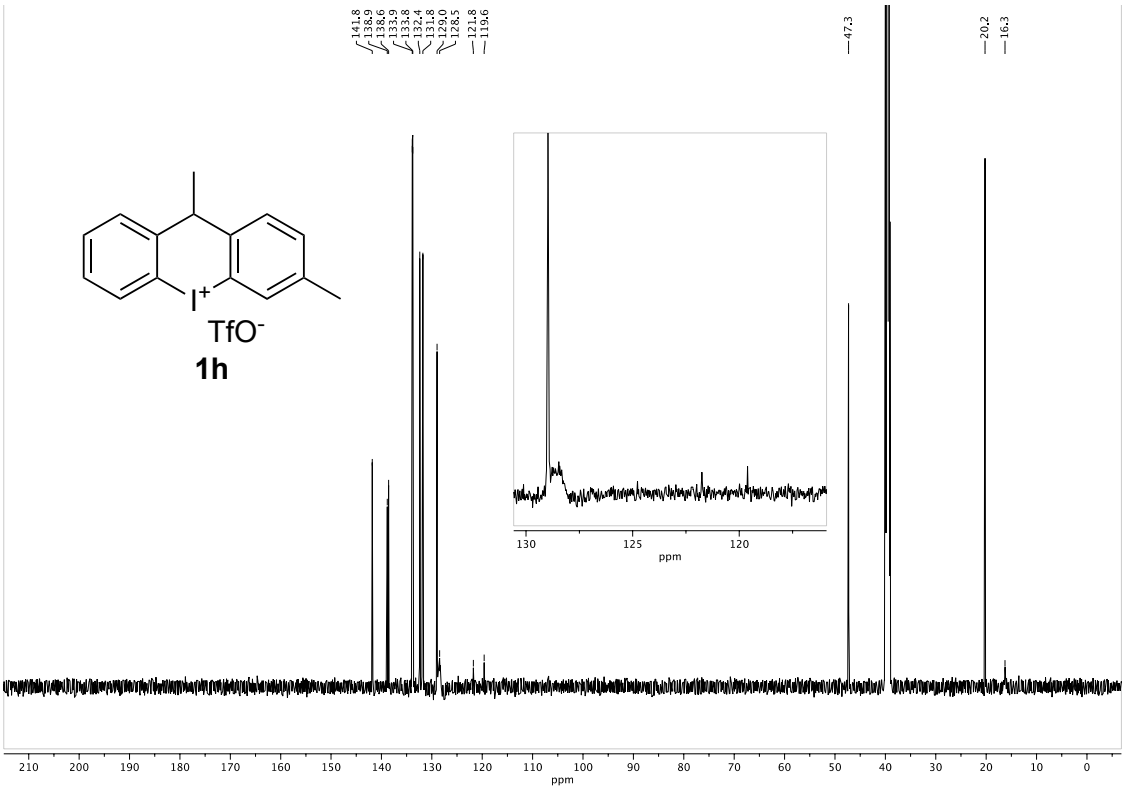

*Figure S9: 151 MHz ^{13}C-NMR spectrum of compound **1h**.*

6 Literature

[1] Caspers, L. D., Spils, J., Damrath, M., Lork, E., Nachtsheim, B. J., *J. Org. Chem.* **2020**, *85*, 9161-9178.
[2] Boelke, A., Nachtsheim, B. J., *Adv. Synth. Catal.* **2019**, *362*, 184-191.
[3] Borah, R., Deka, N., Sarma, J. C., *J. Chem. Res., Synop* . **1997**, 110-111.
[4] Miles, K. C., Le, C. C., Stambuli, J. P., *Chem. - Eur. J.* **2014**, *20*, 11336-11339.
[5] Mei, T. S., Giri, R., Maugel, N., Yu, J. Q., *Angew. Chem. Int. Ed. Engl.* **2008**, *47*, 5215-5219.
[6] Kim, H., Inoue, K., Yoshida, J. I., *Angew. Chem. Int. Ed. Engl.* **2017**, *56*, 7863-7866.
[7] Moorthy, J. N., Senapati, K., Parida, K. N., Jhulki, S., Sooraj, K., Nair, N. N., *J. Org. Chem.* **2011**, *76*, 9593-9601.
[8] Imbos, R., Minnaard, A. J., Feringa, B. L., *J. Am. Chem. Soc.* **2002**, *124*, 184-185.

7.3 Supporting Information for Section 3.3

Oxidative Cyclization and Enzyme-free Deiodination of Thyroid Hormones

Supporting Information

Julian Spils,[a] Lucien D. Caspers,[a] Pim Puylaert,[b] and Boris Nachtsheim*[a]

[a] Institute for Organic and Analytical Chemistry, University of Bremen, Leobener Straße 7, 28359 Bremen, Germany

[b] Institute for Inorganic Chemistry and Crystallography, University of Bremen, Leobener Straße 7, 28359 Bremen, Germany.

Prof. Dr. Boris J. Nachtsheim, nachtsheim@uni-bremen.de

Table of Contents

1 General Information

Unless otherwise noted, all reactions were carried out under air. Reactions with chemicals sensitive to moisture or oxygen were carried out under a nitrogen atmosphere using standard Schlenk techniques. All chemicals were purchased from commercial suppliers and either used as received or purified according to "Purification of Laboratory Chemicals". All other solvents were dried using standard methods if necessary.[1]

Thin layer chromatography was performed on fluorescence indicator marked precoated silica gel 60 plates (Macherey-Nagel, ALUGRAM Xtra SIL G/UV254) and visualized by UV light (254 nm/366 nm). Flash column chromatography was performed on silica gel (0.040 – 0.063 mm) with the solvents given in the procedures.

NMR spectra were recorded on a Bruker Avance II+ 400 or a Bruker Avance Neo 600. Spectra of compounds **1**, **6** and **7** are recorded with a repetition time of 20 s due to high relaxation times (see. [2]). Chemical shifts for ^{1}H-NMR spectra are reported as δ (parts per million) relative to the residual proton signal of $CDCl_3$ at 7.26 ppm (s), DMSO-d_6 at 2.50 ppm (quint) and CD_3OD at 3.31 ppm (quint). Chemical shifts for ^{13}C-NMR spectra are reported as δ (parts per million) relative to the signal of $CDCl_3$ at 77.0 ppm (t), DMSO-d_6 at 39.5 ppm (sept) and CD_3OD at 49.0 ppm (sept). Chemical shifts for ^{19}F-NMR spectra are reported as δ (parts per million) relative to the signal of $Si(CH_3)_4$ at 0.00 ppm. The following abbreviations are used to describe splitting patterns: br. = broad, s = singlet, d = doublet, t = triplet, q = quartet, quint = quintet, sept = septet, m = multiplet. Coupling constants *J* are given in Hz.

Low-resolution ESI mass spectra were recorded on an Agilent 6120 Series LC/MSD system. High-resolution (HR) EI mass spectra were recorded on a double-focusing mass spectrometer ThermoQuest MAT 95 XL from Finnigan MAT. HR-ESI and HR-APCI mass spectra were recorded on a Bruker Impact II. All Signals are reported with the quotient from mass to charge *m/z*.

IR spectra were recorded on a Nicolet Thermo iS10 scientific spectrometer with a diamond ATR unit. The absorption bands $\tilde{\nu}$ are reported in cm^{-1}.

Melting points of solids were measured on a Büchi M-5600 Melting Point apparatus and are uncorrected. The measurements were performed with a heating rate of 2 °C/min and the melting point temperatures *T* are reported in °C.

Intensity data of suitable single crystals were collected on a Bruker Venture D8 diffractometer at 100 K with Mo Kα (0.7107 Å) radiation. All structures were solved by direct methods and refined based on F^2 by the use of the SHELX program package as implemented in Olex2.[3-5] All non-hydrogen atoms were refined using anisotropic displacement parameters. Hydrogen atoms attached to carbon atoms were included in geometrically calculated positions using a rigid model. The ORTEP drawing was made using the program Mercury from the CCDC.[6] Crystallographic data for the structural analyses have been deposited with the Cambridge Crystallographic Data Centre. Copies of this information may be obtained free of charge from The Director, CCDC, 12 Union Road, Cambridge CB2 1EZ, U.K. (Fax: +44-1223-336033; e-mail: deposit@ccdc.cam.ac.uk or http://www.ccdc.cam.ac.uk/).

2 Preparation of Starting Materials

2.1 Aryliodides

2-(4-methoxyphenoxy)-5-methyl-1,3-dinitrobenzene (S1)

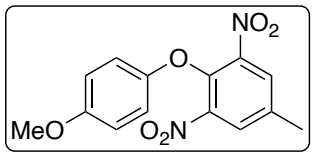

Based on a literature procedure[7] 2,4-dinitro-*p*-cresol (4.95 g, 25.0 mmol) and *p*-TsCl (5.24 g, 27.5 mmol) were dissolved in dry pyridine (40 ml) and stirred for 30 min at 95 °C. *p*-methoxyphenol (6.83 g, 55.0 mmol) was added and the mixture was stirred for 2 h under reflux. After full conv. (TLC) pyridine was removed by reduced pressure and the residue was dissolved in CH_2Cl_2 (80 ml). The solution was washed with aq. HCl (2N, 40 ml), H_2O (40 ml) and aq. NaOH (2N, 2x 40 ml), was dried over Na_2SO_4 and concentrated under reduced pressure. Purification by column chromatography (silica, Cy/EtOAc, 7:1) afforded the product **S1** (6.92 g, 22.7 mmol, 91%) as a colourless solid.

^{1}H-NMR (400 MHz, $CDCl_3$) δ = 7.93 (d, *J* = 0.7 Hz, 2H), 6.80 (s, 4H), 3.76 (s, 3H), 2.52 (s, 3H). **^{13}C-NMR (100 MHz, $CDCl_3$)** δ = 155.8, 151.1, 144.4, 140.2, 136.2, 129.6, 116.5, 114.7, 55.6, 20.7. **FTIR (ATR, neat)** $\tilde{\nu}$ = 3354, 2936, 2837, 1538, 1501, 1229, 1180, 1024, 833, 782. **HRMS (ESI$^+$, MeOH)** *m/z* = 327.0592 $[M+Na]^+$. Calculated for $C_{14}H_{12}N_2NaO_6^+$ *m/z* = 327.0588. **Mp** *T* = 140 – 143 °C.

1,3-diiodo-2-(4-methoxyphenoxy)-5-methylbenzene (S2)

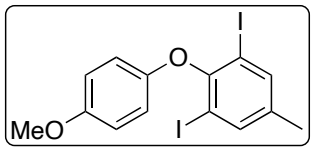

In slight deviation from a literature procedure[7] **S1** (988 mg, 3.25 mmol) was suspended under N_2-atmosphere in AcOH (40 ml) and Pd/C (10% w/w, 311 mg, 0.290 mmol) was added. After hydrogenation in a Parr-apparatus (p(H_2) = 3 bar) the suspension was filtered over Celite® and washed with AcOH (2x 20 ml). The filtrate was concentrated to around 15 ml in total and cold aq. H_2SO_4 (50% v/v, 40 ml) was carefully added. Afterwards, a solution of NaNO2 (493 mg, 7.15 mmol) in H2O (7.5 ml) was carefully added over 60 min at 0 °C. After 30 min urea (244 mg, 4.06 mmol) was added and the tetrazonium was added to a vigorously stirred emulsion of NaI (2.44 g, 16.3 mmol), I_2 (2.06 g, 8.13 mmol), H_2O (35 ml) and $CHCl_3$ (15 ml) at 45 °C. The emulsion was stirred for a further 20 min at 45 °C and after cooling to rt the phases were separated. The aqueous phase was extracted with $CHCl_3$ (2x 40 ml) and the combined org. phases were washed with H_2O (2x 20 ml), aq. $Na_2S_2O_3$ (10% w/w, 20 ml) and again H_2O (2x 20 ml), dried over Na_2SO_4 and concentrated under reduced pressure. Purification by column chromatography (silica, Cy/EtOAc, 30:1) afforded the product **S2** (1.18 g, 2.53 mmol, 78%) as a colourless solid.

^{1}H-NMR (400 MHz, $CDCl_3$) δ = 7.68 (s, 2H), 6.83 – 6.87 (m, 2H), 6.72 – 6.76 (m, 2H), 3.78 (s, 3H), 2.31 (s, 3H). **^{13}C-NMR (100 MHz, $CDCl_3$)** δ = 154.7, 152.0, 150.4, 140.6, 138.6, 116.2, 114.6, 90.9, 55.6, 19.8. **FTIR (ATR, neat)** $\tilde{\nu}$ = 2993, 2834, 1502, 1460, 1432, 1240, 1191, 1176, 1028, 822. **HRMS (ESI$^+$, MeOH)** *m/z* = 488.8817 $[M+Na]^+$. Calculated for $C_{14}H_{11}I_3O_2^+$ *m/z* = 488.8819. **Mp** *T* = 106 – 107.5 °C.

4-(2,6-diiodo-4-methylphenoxy)phenol (S3)

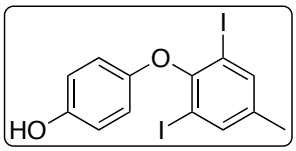

In slight deviation from a literature procedure[7] **S2** (300 mg, 0.640 mmol) was suspended in a mixture of AcOH (1.9 ml) and aq. HI (47%, 1.9 ml) and stirred at 120 °C for 2.5 h. Aft er full conv. the reaction was poured onto ice (5 g) and extracted with toluene (3x 10 ml). The combined org. phases were washed with aq. $Na_2S_2O_3$ (10% w/w, 10 ml) and H_2O (10 ml), were dried

over Na_2SO_4 and concentrated under reduced pressure. Purification by column chromatography (silica, Cy/EtOAc, 15:1) afforded the product **S3** (262 mg, 0.580 mmol, 91%) as a colourless solid.

^{1}H-NMR (400 MHz, $CDCl_3$) δ = 7.68 (d, *J* = 0.6 Hz, 2H), 6.75 – 6.79 (m, 2H), 6.65 – 6.70 (m, 2H), 4.55 (brs, 1H), 2.31 (s, 3H). **^{13}C-NMR (100 MHz, $CDCl_3$)** δ = 152.0, 150.5, 150.4, 140.7, 138.7, 116.4, 116.2, 90.8, 19.8. **FTIR (ATR, neat)** $\tilde{\nu}$ = 3385, 1500, 1433, 1260, 1234, 1193, 1097, 827, 801, 768. **HRMS (ESI$^-$, MeOH)** *m/z* = 450.8702 $[M-H]^-$. Calculated for $C_{13}H_9I_2O_2^-$ *m/z* = 450.8698. **Mp** *T* = 147 – 148.5 °C.

4-(2,6-diiodo-4-methylphenoxy)-2,6-diiodophenol (S4)

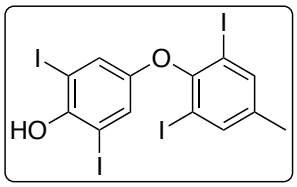

In slight deviation from a literature procedure[7] **S3** (4.52 g, 10.0 mmol) was dissolved in a mixture of EtOH (100 ml) and $MeNH_2$ (25% w/w, 100 ml) and a solution of KI (13.3 g, 40 mmol) and I_2 (5.58 g, 22.0 mmol) in H_2O (36 ml) was added dropwise at 0 °C to 5 °C for 1 h. Afterwards, it was stirred for another 90 min and the mixture was acidified at 0 °C by conc. HCl to pH 1. CH_2Cl_2 (150 ml) was added, the phases were separated and the aqueous phase was extracted with CH_2Cl_2 (2x 150 ml). The combined org. phases were washed with aq. $Na_2S_2O_3$ (50 ml, 10% w/w) and H_2O (50 ml), were dried over Na_2SO_4 and concentrated under reduced pressure. Purification by column chromatography (silica, Cy/CH_2Cl_2, 3:1) afforded the product **S4** (5.85 g, 8.31 mmol, 83%) as a colourless solid and the side product **S5** (620 mg, 1.07 mmol, 11%).

^{1}H-NMR (400 MHz, $CDCl_3$) δ = 7.68 (d, *J* = 0.6 Hz, 2H), 7.13 (s, 2H), 5.46 (s, 1H), 2.33 (s, 3H). **^{13}C-NMR (100 MHz, $CDCl_3$)** δ = 151.2, 150.3, 149.2, 140.8, 139.4, 128.9, 90.4, 81.5, 19.8. **FTIR (ATR, neat)** $\tilde{\nu}$ = 3452, 1581, 1550, 1505, 1435, 1316, 1182, 1143, 848, 709. **HRMS (ESI$^-$, MeOH)** *m/z* = 702.6630 $[M]^-$. Calculated for $C_{14}H_{11}I_3O_2^-$ *m/z* = 702.6631. **Mp** *T* = 209 – 210 °C.

2-(3,5-diiodo-4-methoxyphenoxy)-1,3-diiodo-5-methylbenzene (2a)

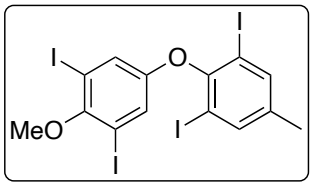

The phenol **S4** (70.4 mg, 100 µmol), MeI (62.5 µl, 142 mg, 1.00 mmol) and K_2CO_3 (1.10 g, 800 µmol) were suspended in acetone (14 ml) and stirred at 55 °C for 1 h. Afterwards, NEt_3 (5 ml) was added and stirred for 1 h at rt. CH_2Cl_2 (20 ml) and H_2O (20 ml) were added, phases were separated and the aq. phase was extracted with CH_2Cl_2 (2x 20 ml), the combined org. phases were washed with aq. HCl (1N, 20 ml) and brine (10 ml), were dried over Na_2SO_4 and concentrated under reduced pressure. Purification by column chromatography (silica, Cy/EtOAc, 30:1) afforded the product **2a** (67.0 mg, 93.3 µmol, 93%) as a colourless solid.

^{1}H-NMR (400 MHz, $CDCl_3$) δ = 7.68 (s, 2H), 7.18 (s, 2H), 3.85 (s, 3H), 2.33 (s, 3H). **^{13}C-NMR (100 MHz, $CDCl_3$)** δ = 154.2, 152.9, 151.0, 140.8, 139.5, 126.4, 90.3, 89.8, 60.9, 19.9. **FTIR (ATR, neat)** $\tilde{\nu}$ = 1581, 1565, 1458, 1435, 1410, 1235, 1171, 1002, 912, 851. **HRMS (ESI$^+$, MeOH)** *m/z* = 756.6494 $[M+K]^+$. Calculated for $C_{14}H_{10}I_4KO_2^+$ *m/z* =. **Mp** *T* = 182 – 183.5 °C.

4-(2,6-diiodo-4-methylphenoxy)-2-iodophenol (S5)

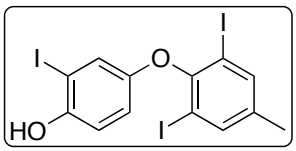

In slight deviation from a literature procedure[7] **S3** (4.52 g, 10.0 mmol) was dissolved in a mixture of EtOH (100 ml) and $MeNH_2$ (25% w/w, 100 ml) and a solution of KI (5.98 g, 36.0 mmol) and I_2 (2.58 g, 10.2 mmol) in H_2O (36 ml) was added dropwise at 0 °C to 5 °C for 1 h. Afterwards, it was stirred for another 90 min and the mixture was acidified at 0 °C by conc. HCl to pH 1. CH_2Cl_2 (150 ml) was added, the phases were separated and the aqueous phase was extracted with CH_2Cl_2 (2x 150 ml). The combined org. phases were washed with aq. $Na_2S_2O_3$ (50 ml, 10% w/w) and H_2O (50 ml), were dried over Na_2SO_4 and concentrated under reduced pressure. Purification by column chromatography (silica, Cy/CH_2Cl_2, 3:1) afforded the product **S5** (4.95 g, 8.57 mmol, 86%) as a colourless solid and the side product **S5** (450 mg, 0.639 mmol, 6.3%).

^{1}H-NMR (400 MHz, $CDCl_3$) δ = 7.67 (d, *J* = 0.5 Hz, 2H), 7.08 (d, *J* = 2.8 Hz, 1H), 6.92 (d, *J* = 8.9 Hz, 1H), 6.71 (dd, *J* = 8.9, 2.8 Hz, 1H), 5.05 (bs, 1H), 2.32 (s, 3H). **^{13}C-NMR (100 MHz, $CDCl_3$)** δ = 151.5, 150.3, 150.2, 140.7, 139.0, 124.5, 117.3, 115.1, 90.6, 85.3, 19.8. **FTIR (ATR, neat)** $\tilde{\nu}$ = . **HRMS (ESI$^-$, MeOH)** *m/z* = 576.7665 $[M]^-$. Calculated for $C_{13}H_8I_3O_2^-$ *m/z* = 576.7664. **Mp** *T* = 143 – 144 °C.

1,3-diiodo-2-(3-iodo-4-methoxyphenoxy)-5-methylbenzene (2b)

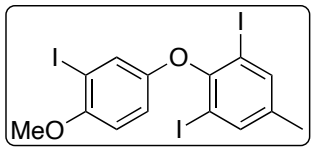

The phenol **S5** (57.8 mg, 100 µmol), MeI (62.5 µl, 142 mg, 1.00 mmol) and K_2CO_3 (1.10 g, 800 µmol) were suspended in acetone (14 ml) and stirred at 55 °C for 1 h. Afterwards, NEt_3 (5 ml) was added and stirred for 1 h at rt. CH_2Cl_2 (20 ml) and H_2O (20 ml) were added, phases were separated and the aq. phase was extracted with CH_2Cl_2 (2x 20 ml), the combined org. phases were washed with aq. HCl (1N, 20 ml) and brine (10 ml), were dried over Na_2SO_4 and concentrated under reduced pressure. Purification by column chromatography (silica, Cy/EtOAc, 30:1) afforded the product **2b** (57.9 mg, 97.8 µmol, 98%) as a colourless solid.

^{1}H-NMR (400 MHz, $CDCl_3$) δ = 7.68 (d, *J* = 0.5 Hz, 2H), 7.25 (dd, *J* = 2.1, 0.9 Hz, 1H), 6.73 (m, 2H),3.85 (s, 3H), 2.32 (s, 3H). **^{13}C-NMR (100 MHz, $CDCl_3$)** δ = 153.7, 151.6, 150.6, 140.8, 139.0, 126.5, 115.9, 111.1, 90.6, 86.1, 56.8, 19.8. **FTIR (ATR, neat)** $\tilde{\nu}$ = 2824, 1591, 1477, 1432, 1292, 1265, 1235, 1177, 1043, 800. **HRMS (ESI$^+$, MeOH)** *m/z* = 630.7523 $[M+K]^+$. Calculated for $C_{14}H_{11}I_3KO_2^+$ *m/z* = 630.7525. **Mp** *T* = 138 – 139 °C.

1-(4-Methoxyphenoxy)-4-methyl-2-nitrobenzene (S6)

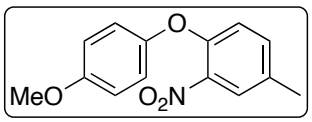

Dried *p*-methoxyphenol (15.6 g, 126 mmol) and K_2CO_3 (19.9 g, 144 mmol) were suspended in dried DMF (60 ml). 3-nitro-4-chlorotoluene (20.6 g, 120 mmol) was added and the mixture was heated at 120 °C for 24 h under N_2-atmosphere. The mixture was diluted with H_2O (500 ml) and extracted with Et_2O (4x 50 ml). The combined org. phases were washed with H_2O (50 ml) and brine (50 ml), dried over Na_2SO_4 and concentrated under reduced pressure. Purification by column chromatography (silica, Cy/EtOAc, 30:1→6:1) afforded the product **S6** (25.3 g, 97.7 mmol, 81%) as an orange-coloured oil.

^{1}H-NMR (360 MHz, $CDCl_3$) δ = 7.71 (dd, *J* = 2.2, 0.4 Hz, 1H), 7.25 (ddd, *J* = 8.5, 2.2, 0.6 Hz, 1H), 7.00 - 6.93 (m, 2H), 6.91 – 6.85 (m, 2H), 6.82 (d, *J* = 8.5 Hz, 1H), 3.79 (s, 2H), 2.36 (s, 3H). **^{13}C-NMR (91 MHz, $CDCl_3$)** δ = 156.3, 149.3, 149.1, 140.3, 134.7, 132.6, 125.5, 120.4, 119.3, 114.9, 55.5, 20.2. **FTIR (ATR, neat)** $\tilde{\nu}$ = 2930, 2836, 1621, 1527, 1502, 1490, 1348, 1031, 821, 810. **HRMS (EI, 70 eV)** *m/z* = 259.0841 $[M]^{+\cdot}$. Calculated for $C_{14}H_{13}NO_4^{+\cdot}$ *m/z* = 259.0839.

2-(4-Methoxyphenoxy)-5-methylaniline (S7)

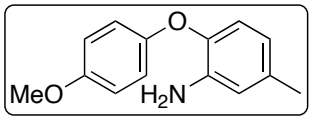

Compound **S6** (1.07 g, 4.00 mmol) was dissolved in a mixture of EtOH (8 ml) and AcOH (8 ml), Fe-powder (1.12 g, 20 mmol) was added and the mixture was stirred at 90 °C for 1 h. Afterwards, the mixture was filtered over silica, further washed (Cy/EtOAc, 4:1, 100 ml) and concentrated under reduced pressure to obtain the product **S7** (0.900 g, 3.90 mmol, 98%) as a colourless solid.

^{1}H-NMR (360 MHz, $CDCl_3$) δ = 6.98 - 6.90 (m, 2H), 6.90 - 6.82 (m, 2H), 6.71 (d, *J* = 8.1 Hz, 1H), 6.64 (d, *J* = 1.8 Hz, 1H), 6.52 (ddd, *J* = 8.1, 2.0, 0.5 Hz, 1H), 3.79 (s, 3H), 3.77 (s, 2H), 2.28 (s, 3H). **^{13}C-NMR (91 MHz, $CDCl_3$)** δ = 155.1, 151.2, 142.0, 138.0, 133.9, 119.2, 119.0, 118.4, 116.9, 114.7, 55.6, 20.9. **FTIR (ATR, neat)** $\tilde{\nu}$ = 3487, 3391, 2955, 1611, 1497, 1462, 1298, 1207, 1195, 1032, 841. **HRMS (EI, 70 eV)** *m/z* = 229.1096 $[M]^{+\cdot}$. Calculated for $C_{14}H_{15}NO_2^{+\cdot}$ *m/z* = 229.1097. **Mp** *T* = 70 - 70.5 °C.

2-Iodo-1-(4-methoxyphenoxy)-4-methylbenzene (S8)

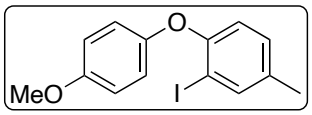

The reaction was based on a literature procedure.[7] The amine **S7** (17.4 g, 75.9 mmol) and *p*-TsOH·H_2O (43.4 g, 228 mmol) were suspended in MeCN (304 ml) and a solution of $NaNO_2$ (10.5 g, 152 mmol) and KI (31.5 g, 190 mmol) in H_2O (46 ml) was added dropwise over 3 h at 10 – 15 °C. After an additional 1 h at rt, the reaction was diluted with aq. Na_2CO_3 (2N, 150 ml) and conc. aq. $Na_2S_2O_3$ (10 ml). The phases were separated and the aqueous phase was extracted with Et_2O. The combined org. phases were dried over Na_2SO_4 and concentrated under reduced pressure. Purification by column chromatography (silica, Cy/EtOAc, 200:1) afforded the product **S8** (22.2 g, 65.2 mmol, 86%) as a colourless solid.

^{1}H-NMR (360 MHz, $CDCl_3$) δ = 7.67 (dd, *J* = 2.0, 0.6 Hz, 1H), 7.05 (ddd, *J* = 8.3, 2.1, 0.7 Hz, 1H), 6.96 – 6.84 (m, 4H), 6.70 (d, *J* = 8.3 Hz, 1H), 3.80 (s, 3H), 2.30 (s, 3H). **^{13}C-NMR (91 MHz, $CDCl_3$)** δ = 155.7, 155.1, 150.5, 139.9, 134.5, 130.1, 119.7, 118.0, 114.7, 87.9, 55.6, 20.1. **FTIR (ATR, neat)** $\tilde{\nu}$ = 2997, 2926, 2832, 1592, 1503, 1474, 1231, 1195, 1035, 811. **HRMS (EI, 70 eV)** *m/z* = 339.9958 $[M]^{+\cdot}$. Calculated for $C_{14}H_{13}IO_2^{+\cdot}$ *m/z* = 339.9955. **Mp** *T* = 50 – 51.5 °C.

4-(2-Iodo-4-methylphenoxy)phenol (S9)

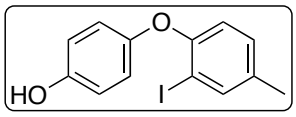

The iodoarene **S8** (1.02 g, 3.00 mmol) was dissolved in CH_2Cl_2 (30 ml) and BBr_3 (1M in CH_2Cl_2, 6 ml) was added dropwise at 0 °C. The mixture was stirred at rt for 1 h and afterwards, H_2O (20 ml) was added at 0 °C. The phases were separated, the aqueous phase was extracted with CH_2Cl_2 (2x 30 ml) and the org. phase was dried over Na_2SO_4 concentrated under reduced pressure. Purification by column chromatography (silica, Cy/EtOAc, 4:1) afforded the product **S9** (971 mg, 2.98 mmol, 99%) as a colourless solid.

^{1}H-NMR (360 MHz, $CDCl_3$) δ = 7.70 – 7.62 (m, 1H), 7.05 (ddd, *J* = 8.3, 2.1, 0.6 Hz, 1H), 6.90 – 6.76 (m, 4H), 6.70 (d, *J* = 8.3 Hz, 1H), 4.99 (s, 1H), 2.29 (s, 3H). **^{13}C-NMR (91 MHz, $CDCl_3$)** δ = 155.0, 151.4, 150.7, 139.9, 134.7, 130.2, 119.9, 118.1, 116.3, 88.0, 20.1. **FTIR (ATR, neat)** $\tilde{\nu}$ = 3384, 1502, 1477, 1444, 1359, 1219, 1198, 1036, 852, 794. **HRMS (EI, 70 eV)** *m/z* = 325.9797 $[M]^{+\cdot}$. Calculated for $C_{13}H_{11}IO_2^{+\cdot}$ *m/z* = 325.9798. **Mp** *T* = 105 – 106 °C.

2,6-Diiodo-4-(2-iodo-4-methylphenoxy)phenol (S10)

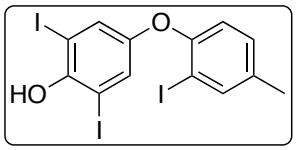

Based on a literature procedure[7] the phenol **S9** (4.08 g, 12.5 mmol) was dissolved in a mixture of EtOH (62.5 ml) and aq. $MeNH_2$ (25% w/w, 62.5 ml). A solution of KI (10.4 g, 62.5 mmol) and I_2 (6.98 g, 27.5 mmol) in H_2O (100 ml) was added dropwise over 1 h at 0 °C. Afterwards, the mixture was stirred for 1 h at 0 °C and carefully acidified with conc. HCl until pH = 1. The reaction was extracted with CH_2Cl_2 (2x 50 ml) and the org. phases were washed with $Na_2S_2O_3$ (10% w/w, 50 ml). The aq. phase was further extracted with CH_2Cl_2 (2x 50 ml) and the combined org. phases were dried over Na_2SO_4 and concentrated under reduced pressure. Purification by column chromatography (silica, Cy/CH_2Cl_2, 7:1 + 1% AcOH) afforded the product **S10** (6.59 g, 11.4 mmol, 91%) as a colourless solid. During the whole purification process, the solid should be kept acidified with AcOH.

^{1}H-NMR (360 MHz, $CDCl_3$) δ = 7.67 (s, 1H), 7.30 (s, 2H), 7.10 (d, *J* = 8.3 Hz, 1H), 6.76 (d, *J* = 8.3 Hz, 1H), 5.53 (s, 1H), 2.31 (s, 3H). **^{13}C-NMR (91 MHz, $CDCl_3$)** δ = 153.7, 151.1, 149.9, 140.2, 135.8, 130.5, 128.5, 119.0, 88.4, 81.4, 20.2. **FTIR (ATR, neat)** $\tilde{\nu}$ = 3440, 2917, 1580, 1481, 1448, 1308, 1207, 1184, 1141, 807, 796. **HRMS (EI, 70 eV)** *m/z* = 577.7736 $[M]^{+\cdot}$. Calculated for $C_{13}H_9I_3O_2^{+\cdot}$ *m/z* = 577.7731. **Mp** *T* = 117 – 118 °C.

1,3-Diiodo-5-(2-iodo-4-methylphenoxy)-2-methoxybenzene (2c)

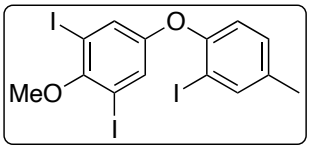

KO*t*Bu (2.52 g, 22.5 mmol) was suspended in THF (50 ml). The phenol **S10** (2.26 g, 5.00 mmol) was mixed with AcOH (150 mg, 2.50 mmol) followed by Et_2O (50 ml) and added dropwise over 10 min to the first solution. Afterwards, MeI (3.13 ml, 7.10 g, 50.0 mmol) was added and stirred for 48 h at rt. Et_3N (15 ml) was added and the mixture was stirred for 1 h at rt. H_2O (50 ml) and Et_2O (100 ml) were added and the phases were separated. The aq. phase was extracted with Et_2O (2x 50 ml). The combined org. phases were washed with aq. HCl (1N, 50 ml), dried over Na_2SO_4 and concentrated under reduced pressure. Purification by column chromatography (silica, Cy/EtOAc, 100:1) afforded the product **2c** (2.94 g, 4.97 mmol, 99%) as a colourless solid.

^{1}H-NMR (360 MHz, $CDCl_3$) δ = 7.68 (d, *J* = 1.9 Hz, 1H), 7.32 (s, 2H), 7.12 (dd, *J* = 8.2, 2.1 Hz, 1H), 6.82 (d, *J* = 8.2 Hz, 1H), 3.83 (s, 3H), 2.32 (s, 3H). **^{13}C-NMR (91 MHz, $CDCl_3$)** δ = 154.5, 154.1, 153.0, 140.2, 136.3, 130.6, 128.2, 119.9, 89.9, 89.0, 60.8, 20.3. **FTIR (ATR, neat)** $\tilde{\nu}$ = 3061, 2932, 1568, 1455, 1407, 1223, 1037, 994, 851, 725. **HRMS (EI, 70 eV)** *m/z* = 591.7886 $[M]^{+\cdot}$. Calculated for $C_{14}H_{11}I_3O_2^{+\cdot}$ *m/z* = 591.7888. **Mp** *T* = 107 – 108.5 °C.

Methyl (*S*)-2-acetamido-3-(4-(4-acetoxy-3,5-diiodophenoxy)-3,5-diiodophenyl)propanoate (Ac-Thx(Ac)-OMe)

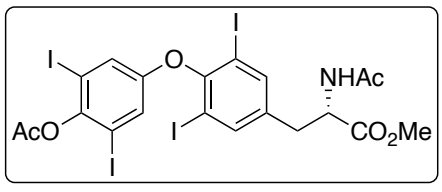

To a solution of L-Thyroxine (1.55 g, 2.00 mmol) in MeOH (10 ml) was added $SOCl_2$ (435 µl, 6.00 mmol) and the mixture is heated to 60 °C for 12 h. After cooling down Et_2O (10 ml) was added and the solution was decanted and washed further with Et_2O (5x 20 ml). The residue was dried under reduced pressure to obtain crude H-Thx-OMe. This

was dissolved in CH_2Cl_2 (10 ml), Ac_2O (11 mmol, 1.04 ml) and pyridine (21 mmol, 1.69 ml) were added and the solution was left to stir overnight at rt. After completion, the reaction mixture was diluted with water (50 ml) and extracted with CH_2Cl_2 (3x 10 ml). The combined organic phases were dried over Na_2SO_4, concentrated under reduced pressure and purified via column chromatography (silica, EtOAc/Cy, 1:1➞2:1) to give Ac-Thx(Ac)-OMe (1.63 g, 1.86 mmol, 93%) as a beige solid.

^{1}H-NMR (600 MHz, $CDCl_3$) δ = 7.62 (s, 2H), 7.18 (s, 2H), 6.03 (d, *J* = 7.4 Hz, 1H), 4.84 (q, *J* = 6.3 Hz, 1H), 3.77 (s, 3H), 3.11 (dd, *J* = 13.8, 6.1 Hz, 1H), 3.03 (dd, *J* = 13.8, 5.7 Hz, 1H), 2.39 (s, 3H), 2.05 (s, 3H). **^{13}C-NMR (151 MHz, $CDCl_3$)** δ = 171.5, 169.6, 167.5, 153.8, 152.3, 147.0, 141.2, 137.8, 126.2, 90.5, 89.9, 53.1, 52.6, 36.5, 23.2, 21.3. **FTIR (ATR, neat)** $\tilde{\nu}$ = 3270, 3063, 2949, 1738, 1652, 1538, 1427, 1367, 1196, 1163. **HRMS (ESI$^+$, MeOH)** *m/z* = 897.7115 $[M+Na]^+$. Calculated for $C_{20}H_{17}I_4NNaO_6^+$ *m/z* = 897.7127. **Mp** *T* = 152-156 °C.

3 Substrate synthesis

3.1 Optimisation and screening for the synthesis of model substrates 3

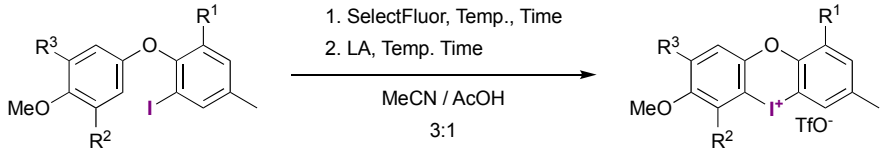

				1st Step			2nd Step			
#[a]	R^1	R^2	R^3	SelectFluor® (eq.)	Temp (°C)	Time (h)	LA (eq.)	Temp (°C)	Time (h)	Yield
1	**I**	**I**	**I**	4	rt	72	TfOH (5)	rt	24	16%
2	**I**	**I**	**I**	2.5	0 - rt	72	**TfOH (2.5)**	0 - 80	1.5	21%
3[b]	**I**	**I**	**I**	2.5	0 - rt	72	**BF_3OEt_2 (2.5)**	0 - 80	1.5	9%
4	**I**	**I**	**I**	2.5	**rt - 50**	**4**	TfOH (2.5)	0 - 80	1.5	35%
5	**I**	**I**	**I**	2.5	**rt - 80**	**1.5**	TfOH (2.5)	0 - 80	1.5	16%
6	**I**	**I**	**I**	**3.5**	**50**	**4**	TfOH (2.5)	rt	64	73%
7	**I**	**I**	**I**	3.5	**50**	**4**	**TfOH (1.5)**	rt - 80	24+1	21%
8[c]	**I**	**I**	**I**	3.5	**50**	**4**	TfOH (2.5)	rt	24	44%
9[d]	**I**	**I**	**I**	3.5	50	4	TfOH (2.5)	rt	72	35%
10	**I**	**H**	**I**	3.5	50	4	TfOH (2.5)	rt	72	0%
11	**I**	**H**	**H**	3.5	50	4	TfOH (2.5)	rt	72	0%
12	**H**	**H**	**I**	3.5	50	4	TfOH (2.5)	rt	72	0%
13	**H**	**I**	**I**	3.5	50	4	TfOH (2.5)	rt	72	23%

[a]All reactions were performed on a 50.0 µmol scale at a conc. of 0.05 M. [b]The corresponding tetrafluoroborate was isolated. [c]Conc. of 0.1 M. [d]500 µmol scale.

3.2 Model Substrates 3 - 5

1,6,8-Triiodo-7-methoxy-3-methyldibenzo[*b*,*e*][1,4]iodaoxin-5-ium trifluoromethanesulfonate (3a)

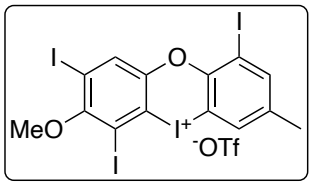

A solution of **2a** (359 mg, 0.500 mmol) and SelectFluor® (620 mg, 1.75 mmol) in MeCN/AcOH (10 ml, 3:1) was heated at 50 °C for 4 h. TfOH (111 µl, 1.25 mmol) was added at 0 °C and the mixture was stirred for 3 d at rt. After dilution with water (40 ml) and extraction with CH_2Cl_2 (3x 20 ml), the organic phases were dried over Na_2SO_4 and concentrated under reduced pressure. The resulting solid was washed with Et_2O to obtain **3a** (150 mg, 0.173 mmol, 35%) as a slightly orange solid.

^{1}H-NMR (601 MHz, DMSO-d_6) δ = 8.09 (s, 1H), 8.00 (s, 1H), 7.91 (s, 1H), 3.76 (s, 3H), 2.35 (s, 3H). **^{13}C-NMR (151 MHz, DMSO-d_6)** δ = 159.0, 151.1, 149.6, 142.6, 140.2, 133.7, 131.7, 120.7 (q, *J* = 322.1 Hz), 118.8, 106.7, 98.7, 95.9, 89.1, 60.7, 19.7. **^{19}F-NMR (565 MHz, DMSO-d_6)** δ = -77.7. **FTIR (ATR, neat)** $\tilde{\nu}$ = 3059, 2938, 2857, 1441, 1390, 1272, 1215, 1158, 1034, 926. **HRMS (ESI$^+$, MeOH)** *m/z* = 716.6766 [M-OTf]$^+$. Calculated for $C_{14}H_9I_4O_2^+$ *m/z* = 716.6776. **Mp** decomp. at 250 °C.

2,4-Diiodo-3-methoxy-7-methyldibenzo[b,e][1,4]iodaoxin-5-ium trifluoromethanesulfonate (3c)

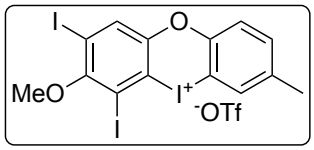

A solution of **2c** (296 mg, 0.500 mmol) and SelectFluor® (620 mg, 1.75 mmol) in MeCN/AcOH (10 ml, 3:1) was heated at 50 °C for 4 h. TfOH (111 µl, 1.25 mmol) was added at 0 °C and the mixture was stirred for 3 d at rt. After dilution with water (40 ml) and extraction with CH_2Cl_2 (3x 20 ml), the organic phases were dried over Na_2SO_4 and concentrated under reduced pressure. The resulting solid was washed with Et_2O to obtain **3c** (128 mg, 0.173 mmol, 35%) as a slightly orange solid.

^{1}H-NMR (600 MHz, DMSO-d_6) δ = 8.30 (s, 1H), 7.91 (d, *J* = 1.9 Hz, 1H), 7.65 (d, *J* = 8.3 Hz, 1H), 7.51 (dd, *J* = 8.3, 2.0 Hz, 1H), 3.76 (s, 3H), 2.39 (s, 3H). **^{13}C-NMR (151 MHz, DMSO-d_6)** δ = 158.6, 151.4, 150.6, 138.5, 134.2, 133.2, 131.5, 120.9, 120.7 (q, *J* = 322.4 Hz), 117.0, 106.4, 98.4, 95.9, 60.7, 20.2. **^{19}F-NMR (565 MHz, DMSO-d_6)** δ = -77.7. **FTIR (ATR, neat)** $\tilde{\nu}$ = 3085, 2942, 1659, 1519, 1484, 1449, 1393, 1225, 971, 955. **HRMS (ESI$^+$, MeCN/H_2O)** *m/z* = 590.7805 [M-OTf]$^+$. Calculated for $C_{14}H_{10}I_3O_2^+$ *m/z* = 590.7810. **Mp** decomp. at 140 °C.

7-Hydroxy-1,6,8-triiodo-3-methyldibenzo[*b*,*e*][1,4]iodaoxin-5-ium bromide (4a)

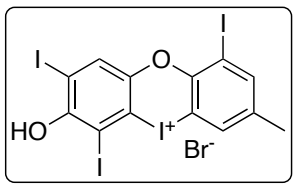

To a suspension of **3a** (433 mg, 0.500 mmol) in CH_2Cl_2 (5 ml) was added BBr_3 (1.65 ml, 1.50 mmol, 0.91 M in CH_2Cl_2) and the mixture was heated to 60 °C for 1 d. After completion, the mixture was diluted with Et_2O and the resulting solid was washed multiple times with Et_2O to obtain **4a** (321 mg, 0.411 mmol, 82%) as a colourless solid.

^{1}H-NMR (600 MHz, DMSO-d_6) δ = 10.25 (bs, 1H), 8.18 – 8.15 (m, 1H), 7.95 (s, 1H), 7.94 – 7.93 (m, 1H), 2.33 (s, 3H). **^{13}C-NMR (151 MHz, DMSO-d_6)** δ = 155.8, 150.2, 148.8, 142.0, 139.7, 134.5, 130.5, 123.5, 108.7, 92.9, 90.4, 88.6, 19.7. **FTIR (ATR, neat)** $\tilde{\nu}$ = 3043, 2115, 1527, 1449, 1412, 1345, 1231, 1063, 1036, 1007. **HRMS (ESI$^+$, MeOH)** *m/z* = 702.6613 [M-Br]$^+$. Calculated for $C_{13}H_7I_4O_2^+$ *m/z* = 702.6620. **Mp** decomp. at 160 °C.

7-Hydroxy-1,6,8-triiodo-3-methyldibenzo[*b*,*e*][1,4]iodaoxin-5-ium trifluoromethanesulfonate (4b)

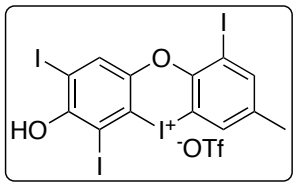

To a suspension of **4a** (78.3 mg, 0.100 mmol) in MeCN (1 ml) was added AgOTf (28.3 mg, 0.110 mmol) and the mixture was stirred for 14 h. The mixture was filtered through a syringe filter (PTFE, 0.45 µm). The reaction vessel and filter were washed with MeOH (2x 1 ml). The resulting solution was concentrated and precipitated with Et_2O to give **4b** (68.7 mg, 80.7 µmol, 81%) as a beige solid.

^{1}H-NMR (600 MHz, CD_3OD) δ = 8.18 (s, 1H), 8.01 (d, *J* = 1.0 Hz, 1H), 7.86 (d, *J* = 0.9 Hz, 1H), 2.42 (s, 3H). **^{13}C-NMR (151 MHz, CD_3OD)** δ = 156.1, 149.2, 147.0, 142.8, 140.2, 132.1, 131.5, 119.6 (d, *J* = 318.7 Hz), 115.2, 103.5, 88.4, 87.9, 86.7, 18.1. **^{19}F-NMR (565 MHz, CD_3OD)** δ = -80.1. ^{19}F content was checked by the addition of PhF (see spectra Fig. 41). **FTIR (ATR, neat)** $\tilde{\nu}$ = 3419, 1540, 1447, 1414, 1366, 1271, 1212, 1169, 1014, 819. **HRMS (ESI$^+$, MeOH)** *m/z* = 702.6613 $[M\text{-}OTf]^+$. Calculated for $C_{13}H_7I_4O_2^+$ *m/z* = 702.6620. **Mp** decomp. at 200 °C.

2,4,9-Triiodo-7-methyldibenzo[*b*,*e*][1,4]iodaoxin-5-ium-3-olate (5)

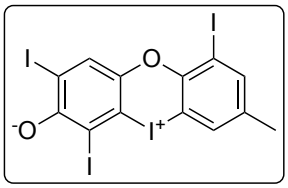

To a solution of iodaoxinium salt **4b** (29.8 mg, 35 µmol) in MeOH (0.7 ml) was added NaOH (38.5 µl, 38.5 µmol, 1 M) to form an orange precipitate. The suspension was stirred for 10 min, Et_2O (10 ml) was added, and the solution was centrifugated (6000 rpm, 10 min) and decanted. The solid was suspended in H_2O (10 ml), centrifugated and decanted. To obtain, after drying, **5** (22.7 mg, 32.4 µmol, 92%) as an orange solid.

^{1}H-NMR (601 MHz, DMSO-d_6) δ = 7.94 (s, 1H), 7.90 (s, 1H), 7.79 (s, 1H), 2.33 (s, 3H). Due to poor solubility and instability of the compound in DMSO the quality of the **^{1}H-NMR** quality is reduced and it was not possible to record a **^{13}C-NMR** spectrum. **FTIR (ATR, neat)** $\tilde{\nu}$ = 3052, 2912, 1541, 1493, 1406, 1236, 1210, 857, 824, 702. **HRMS (ESI$^+$, MeOH)** *m/z* = 702.6613 $[M+H]^+$. Calculated for $C_{13}H_7I_4O_2^+$ *m/z* = 702.6620. **Mp** decomp. at 212 °C.

3.3 Thyroxine-derived Salts 1 and 6

(*S*)-3-(2-Acetamido-3-methoxy-3-oxopropyl)-7-hydroxy-1,6,8-triiododibenzo[*b*,*e*][1,4]iodaoxin-5-ium trifluoromethanesulfonate (6a)

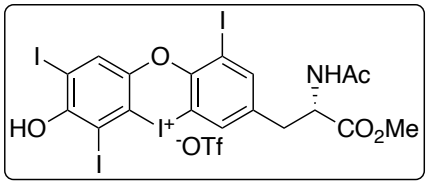

To a solution of Ac-Thx(Ac)-OMe (0.500 mmol, 437 mg) in MeCN/HFIP (10 ml, 1:1) was added mCPBA (0.550 mmol, 112 mg, 85%) at 0 °C. The solution was stirred for 10 min, TfOH (2.50 mmol, 221 µl) was added and the solution was stirred for 3 d. The reaction was monitored via HPLC-MS and after full conversion of the Iodoarene and subsequent *O*-deacylation the mixture was concentrated under reduced pressure and coevaporated with EtOAc (5 x 10 ml). The resulting solid was washed with Et_2O to obtain **6a** (261 mg, 0.266 mmol, 53%) as a colourless to beige solid.

^{1}H-NMR (600 MHz, DMSO-d_6) δ = 10.47 (brs, 1H), 8.35 (d, *J* = 7.9 Hz, 1H), 8.02 (s, 1H), 8.00 (d, *J* = 1.9 Hz, 1H), 7.95 (d, *J* = 1.9 Hz, 1H), 4.48 (ddd, *J* = 9.5, 7.9, 5.4 Hz, 1H), 3.62 (s, 3H), 3.10 (dd, *J* = 14.0, 5.3 Hz, 1H), 2.91 (dd, *J* = 14.0, 9.4 Hz, 1H), 1.79 (s, 3H). **^{13}C-NMR (151 MHz, DMSO-d_6)** δ = 171.59, 169.46, 156.51, 150.69, 147.91, 143.00, 139.65, 133.95, 131.16, 120.7 (q, *J* = 322.0 Hz), 118.13, 106.84, 93.59, 91.65, 89.05, 53.00, 52.07, 35.15, 22.26. **^{19}F-NMR (565 MHz, DMSO-d_6)** δ = -77.7. **FTIR (ATR, neat)** $\tilde{\nu}$ =

3319, 3064, 1726, 1633, 1542, 1423, 1372, 1219, 1166, 1020, 831. **HRMS (ESI$^+$, MeOH)** *m/z* = 831.7022 [M-OTf]$^+$. Calculated for $C_{18}H_{14}I_4NO_5^+$ *m/z* = 831.7045. **Mp** *T* = 220 °C, with decomp. immediately afterwards.

(*S*)-3-(2-Acetamido-3-methoxy-3-oxopropyl)-7-hydroxy-1,6,8-triiododibenzo[*b*,*e*][1,4]iodaoxin-5-ium chloride (6b)

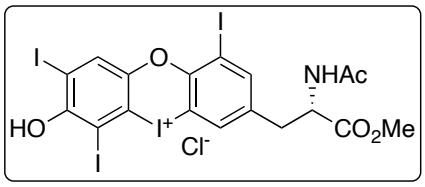

To a solution of iodaoxinium salt **6a** (49.1 mg, 50.0 µmol) in MeOH (0.5 ml) was added HCl (100 µl, 1 M) and the suspension was stirred for 10 min. Et_2O (8 ml) was added and the suspension was centrifugated (6000 rpm, 10 min) and decanted. This was repeated two times to obtain **6b** (40.2 mg, 47.0 mmol, 94%) as a colourless solid.

^{1}H-NMR (601 MHz, DMSO-*d*$_6$) δ = 10.20 (s, 1H), 8.28 (d, *J* = 7.8 Hz, 1H), 8.23 (d, *J* = 1.9 Hz, 1H), 7.96 – 7.91 (m, 2H), 4.42 (td, *J* = 8.5, 5.4 Hz, 1H), 3.62 (s, 3H), 3.06 (dd, *J* = 14.0, 5.1 Hz, 1H), 2.92 (dd, *J* = 14.0, 9.3 Hz, 1H), 1.80 (s, 3H). **^{13}C-NMR (151 MHz, DMSO-*d*$_6$)** δ = 171.5, 169.5, 155.7, 151.1, 149.0, 142.3, 139.2, 134.7, 130.4, 124.9, 109.9, 92.8, 90.1, 88.7, 53.1, 52.0, 35.1, 22.3. **FTIR (ATR, neat)** $\tilde{\nu}$ = 3250, 3046, 1728, 1644, 1527, 1418, 1530, 1275, 1230, 1194, 929. **HRMS (ESI$^+$, MeOH)** *m/z* = 831.7037 [M-Cl]$^+$. Calculated for $C_{18}H_{14}I_4NO_5^+$ *m/z* = 831.7045 **Mp** decomp at 178 °C.

(*S*)-7-(2-Acetamido-3-methoxy-3-oxopropyl)-2,4,9-triiododibenzo[*b*,*e*][1,4]iodaoxin-5-ium-3-olate (7)

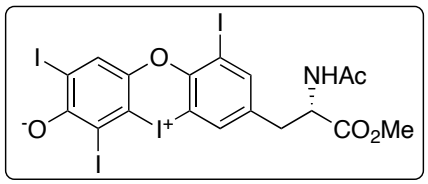

To a solution of iodaoxinium salt **6a** (49.1 mg, 50.0 µmol) in MeOH (1 ml) was added NaOH (55 µl, 1 M) to form an orange precipitate. The suspension was stirred for 1 h, H_2O (4 ml) was added and the suspension was washed with H_2O (4 ml) and MeOH (4 ml) to obtain **7** (29.3 mg, 35.9 µmol, 72%) as an orange solid.

^{1}H-NMR (600 MHz, DMSO-*d*$_6$) δ = 8.32 (d, *J* = 7.9 Hz, 1H), 7.92 (d, *J* = 2.8 Hz, 2H), 7.80 (s, 1H), 4.46 (td, *J* = 8.5, 5.3 Hz, 1H), 3.61 (s, 3H), 3.06 (dd, *J* = 14.0, 5.3 Hz, 1H), 2.91 (dd, *J* = 14.0, 9.3 Hz, 1H), 1.79 (s, 3H). **^{13}C-NMR** was not possible to record due to poor solubility and instability of the compound in DMSO. **FTIR (ATR, neat)** $\tilde{\nu}$ = 3287, 1716, 1636, 1549, 1411, 1347, 1233, 1043, 838. **HRMS (ESI$^+$, MeOH)** *m/z* = 831.7022 [M+H]$^+$. Calculated for $C_{18}H_{14}I_4NO_5^+$ *m/z* = 831.7045. **Mp** decomp. at 190 °C.

3-(2-Ammonio-2-carboxyethyl)-7-hydroxy-1,6,8-triiododibenzo[*b*,*e*][1,4]iodaoxin-5-ium chloride (1a)

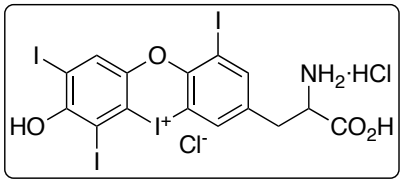

Iodaoxinium salt **6a** (49.1 mg, 50 µmol) was suspended in HCl (7.5 ml, 1 N) and heated to 120 °C for 4 h. The resulting suspension was centrifugated (6000 rpm, 10 min) and decanted. The resulting solid was washed by precipitation from MeOH with Et_2O, centrifugated and decanted. The resulting solid was then extracted from the solid by precipitation with MeCN from a suspension in MeOH, afterwards centrifugated and decanted. The resulting solution was concentrated and dried to obtain **1a** (24.0 mg, 28.3 µmol, 57%) as a colourless solid.

^{1}H-NMR (600 MHz, CD_3OD) δ = 8.39 (s, 1H), 8.11 (s, 1H), 8.06 (d, *J* = 1.6 Hz, 1H), 4.33 (t, *J* = 6.7 Hz, 1H), 3.41 (dd, *J* = 14.8, 5.4 Hz, 1H), 3.21 (dd, *J* = 14.7, 7.9 Hz, 1H). **^{13}C-NMR (151 MHz, CD_3OD)** δ = 170.6, 157.8, 153.5, 149.8, 145.0, 138.1, 136.2, 133.2, 122.7, 109.4, 90.1, 89.4, 89.1, 54.6, 35.8. **FTIR (ATR, neat)** $\tilde{\nu}$ = 2845, 2114, 1916, 1727, 1585, 1505, 1416, 1350, 1281, 1195, 1135, 826. **HRMS (ESI$^+$, MeOH)** *m/z* = 775.6775 $[M\text{-}HCl_2]^+$. Calculated for $C_{15}H_{10}I_4NO_4^+$ *m/z* = 775.6783. **Mp** decomp. at 200 °C.

3-(2-Ammonio-2-carboxyethyl)-7-hydroxy-1,8-diiododibenzo[*b*,*e*][1,4]iodaoxin-5-ium chloride (1b)

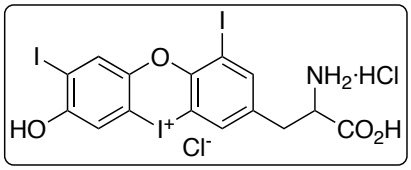

Iodaoxinium salt **6a** (98.1 mg, 100 µmol) was suspended in HCl (15 ml, 1 N) and heated to 100 °C for 1 d. The resulting suspension was diluted with HCl (5 ml, 1 N), centrifugated (6000 rpm, 10 min) and decanted. The resulting solid was suspended in MeOH (~1 ml) and diluted with Et_2O (9 ml), centrifugated and decanted to obtain **1b** (50.0 mg, 69.3 µmol, 69%) as a colourless solid.

^{1}H-NMR (600 MHz, DMSO-d_6 + 10% D_2O) δ = 8.00 (s, 1H), 7.88 (d, *J* = 1.8 Hz, 1H), 7.84 (s, 1H), 7.66 (s, 1H), 3.99 (t, *J* = 6.4 Hz, 1H), 3.16 – 3.10 (m, 1H), 3.04 (dd, *J* = 14.5, 7.1 Hz, 1H). **^{13}C-NMR (151 MHz, DMSO-d_6)** δ = 170.2, 156.3, 153.2, 147.5, 142.8, 137.0, 135.2, 130.9, 118.0, 108.9, 108.9, 90.0, 88.9, 53.7, 34.7. **FTIR (ATR, neat)** $\tilde{\nu}$ = 3335, 3040, 2860, 2115, 1916, 1724, 1606, 1374, 1229, 1174, 1040, 871, 823. **HRMS (ESI$^+$, MeOH)** *m/z* = 649.7809 $[M\text{-}HCl_2]^+$. Calculated for $C_{15}H_{11}I_3NO_4^+$ *m/z* = 649.7817. **Mp** decomp. at 235 °C.

3.4 Interaction of compound 6a with different amounts of tetra-*n*-butylammonium chloride (TBACl)

To a solution of Iodaoxinium salt **6a** (9.81 mg, 10.0 µmol) in DMSO-d_6 (0.5 ml) were added different amounts of a solution of tetra-*n*-butylammonium chloride in DMSO-d_6 (2 M). Afterwards ^{13}C-NMR spectra of the resulting solutions were measured.

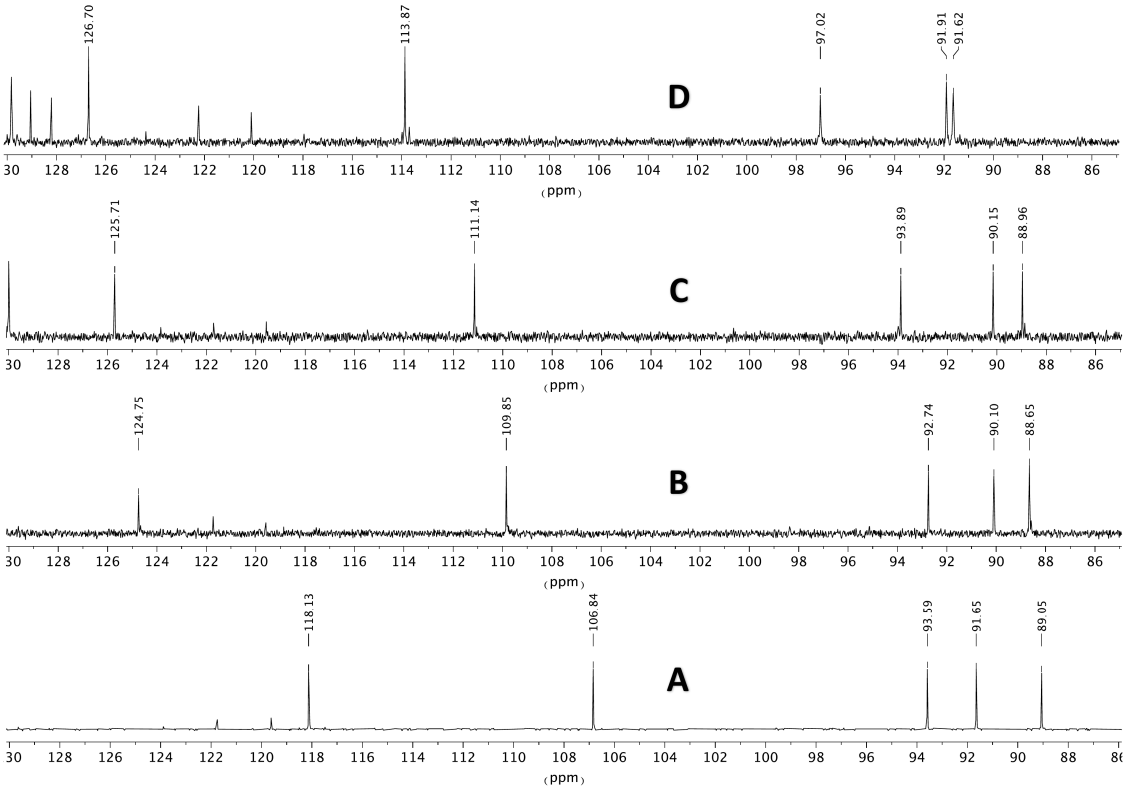

*Figure 1 - NMR Data with annotated peaks for compound **6a** (**A**), **6a** + 1 eq. TBACl (B), **6a** + 5 eq. TBACl (**C**), **6a** + 50 eq. TBACl (**D**) in DMSO-d_6 at 24 °C.*

4 Crystal Structures

Single crystals of **6a** were prepared by dissolving the substance in a minimum amount of methanol. Diethyl ether was introduced via gas-phase diffusion to obtain a suitable crystal. (CCDC 2291802)

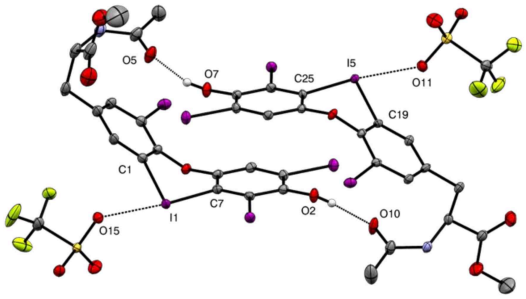

Figure S1: Structure of **6a** showing 50% probability ellipsoids. Selected bond parameters [Å, °]: I1-O15: 2.757(2); I5-O11: 2.752(2); O5-O7: 2.563(4); O2-O10: 2.606(4); C1-I1-C7: 90.0(1); C19-I5-C25: 89.7(1); C7-I1-O15: 175.2(1); C25-I5-O11: 172.69(9).

Table S2: Crystal data and structure refinement for **6a**.

Empirical formula	$C_{19}H_{14}F_3I_4NO_8S$
Formula weight	980.97
Temperature/K	100.00
Crystal system	Trigonal
Space group	R3
a/Å	34.2779(8)
b/Å	34.2779(8)
c/Å	13.8411(5)
α/°	90
β/°	90
γ/°	120
Volume/Å^3	14084.1(8)
Z	18
ρ_{calc}g/cm^3	2.082
μ/mm^{-1}	4.104
F(000)	8172.0
Crystal size/mm^3	0.245 × 0.18 × 0.125
Radiation	MoKα (λ = 0.71073)
2Θ range for data collection/°	4.024 to 72.87
Index ranges	-57 ≤ h ≤ 57, -57 ≤ k ≤ 57, -23 ≤ l ≤ 23
Reflections collected	262320
Independent reflections	30489 [R_{int} = 0.0460, R_{sigma} = 0.0265]
Data/restraints/parameters	30489/1/669
Goodness-of-fit on F^2	1.050
Final R indexes [I>=2σ (I)]	R_1 = 0.0199, wR_2 = 0.0402
Final R indexes [all data]	R_1 = 0.0230, wR_2 = 0.0409
Largest diff. peak/hole / e Å^{-3}	1.42/-0.68
Flack parameter	0.063(4)

5 Computational Details

The DFT calculations were performed with ORCA 5.0.4.[8] Structure optimisations were performed on a PBE0-D3(BJ)/def2-SVP+CPCM level of theory, a combination of the PBE0 functional[9] with Becke-Johnson damping[10, 11], the def2-SVP basis set[12], an auxiliary basis set for the RI approximation[13] and the Conductor-like Polarizable Continuum Model[14]. On the optimised structure single point calculations were performed on a PBE0-D3(BJ)/def2-TZVP+CPCM level of theory, a combination of the PBE0 functional[9] with Becke-Johnson damping[10, 11], the def2-TZVP basis set[12], an auxiliary basis set for the RI approximation[13] and the Conductor-like Polarizable Continuum Model[14]. Transition states were verified by the implemented method of Morokuma et al.[15]. The corresponding geometries are attached as a separate file.

Table S3: PBE0-D3(BJ)/def2-TZVP+CPCM(Water) computed imaginary frequency (ImF), Gibbs free-energy (G) and the energy relative to the corresponding conformer of **1a** (ΔG).

	Conformer	Direction of attack	Im / cm^{-1}	G / Eh	ΔG / kcal mol^{-1}
1a + HCl	**1**		**0**	**-3504.76521948**	**0.00**
	2		**0**	**-3504.76589810**	**0.00**
1a-1-HCl	1	a	0	-3504.74728099	11.26
		b	0	-3504.74980229	9.67
	2	**a**	**0**	**-3504.74918803**	**10.49**
		b	0	-3504.75027868	9.80
TS1	1	a	833.86i	-3504.71854128	29.29
		b	765.90i	-3504.71953144	28.67
	2	**a**	**802.46i**	**-3504.72076594**	**28.32**
		b	756.87i	-3504.72008974	28.75
1b''-1-ICl	1	a	0	-3504.76963102	-2.77
		b	0	-3504.73888234	16.53
	2	**a**	**0**	**-3504.77251990**	**-4.16**
		b	0	-3504.74007346	16.21
1b'' + ICl	1		0	-3504.75404517	7.01
	2		**0**	**-3504.75431142**	**7.27**
1a-6-HCl	**1**	a	0	-3504.75031644	9.35
		b	**0**	**-3504.75051335**	**9.23**
	2	a	0	-3504.75189973	8.78
		b	0	-3504.75209454	8.66
TS6	**1**	a	1062.77i	-3504.72551074	24.92
		b	**530.12i**	**-3504.72656243**	**24.26**
	2	a	1058.97i	-3504.72603908	25.01
		b	458.37i	-3504.72710899	24.34
1b-6-ICl	**1**	a	0	-3504.75400566	7.04
		b	**0**	**-3504.77316283**	**-4.98**
	2	a	0	-3504.75481173	6.96
		b	0	-3504.77422553	-5.23
1b + ICl	**1**		**0**	**-3504.76109736**	**2.59**
	2		0	-3504.76191018	2.50
1a-8-HCl	**1**	**a**	**0**	**-3504.74913224**	**10.09**
		b	0	-3504.74960774	9.80
	2	a	0	-3504.74991549	10.03
		b	0	-3504.75042736	9.71
TS8	**1**	**a**	**1117.63i**	**-3504.71973968**	**28.54**
		b	1113.81i	-3504.71948467	28.70

	2	a	1105.42i	-3504.71964787	29.02
		b	1108.86i	-3504.71990273	28.86
1b'-8-ICl	**1**	**a**	**0**	**-3504.75125351**	**8.76**
		b	0	-3504.75086519	9.01
	2	a	0	-3504.75148539	9.04
		b	0	-3504.75106779	9.31
1b' + ICl	**1**		**0**	**-3504.75505375**	**6.38**
	2		0	-3504.75537039	6.61

6 NMR-Spectra of New Substrates

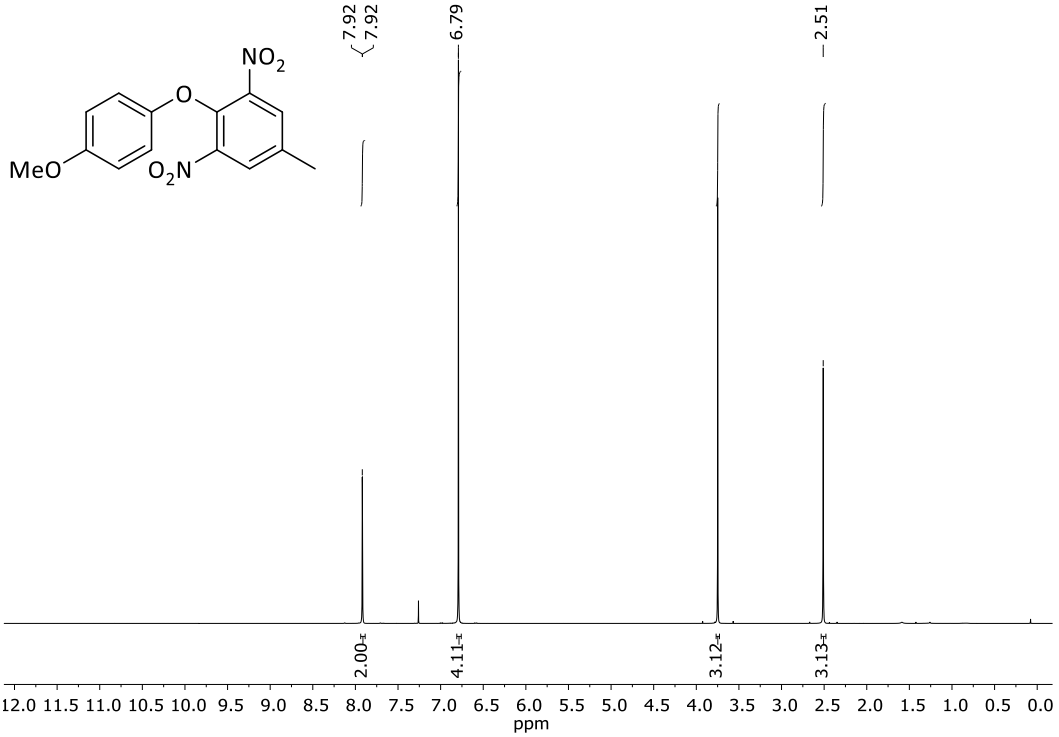

*Figure S2: 400 MHz ^{1}H-NMR spectrum of compound **S1** in $CDCl_3$.*

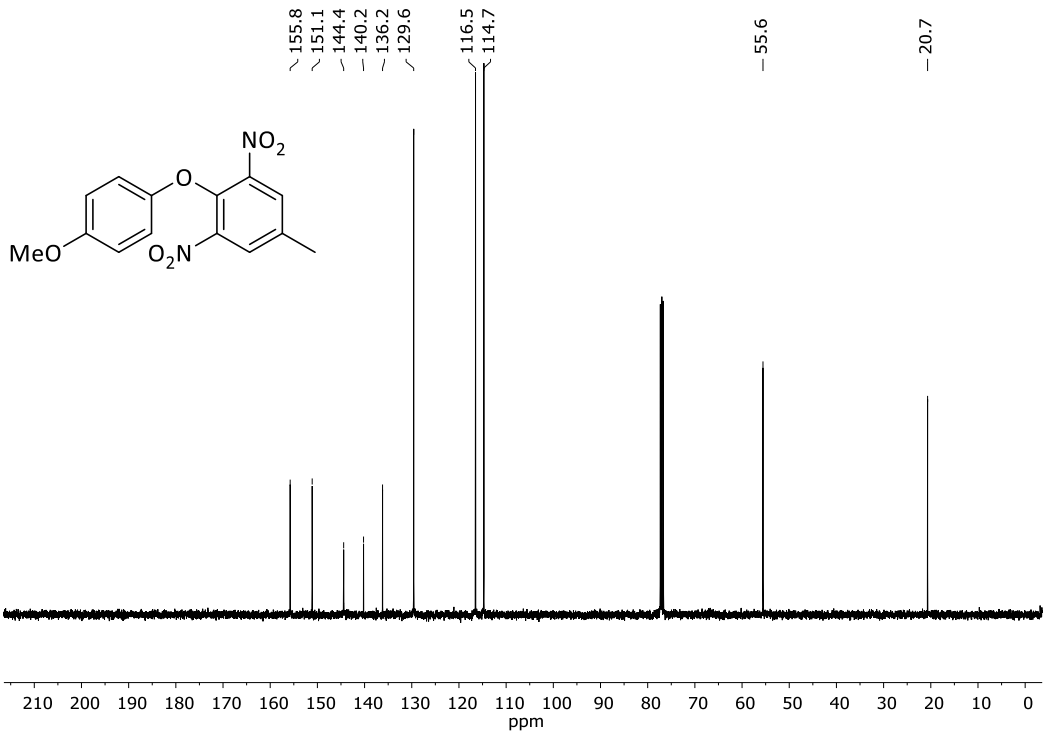

*Figure S3: 100 MHz ^{13}C-NMR spectrum of compound **S1** in $CDCl_3$.*

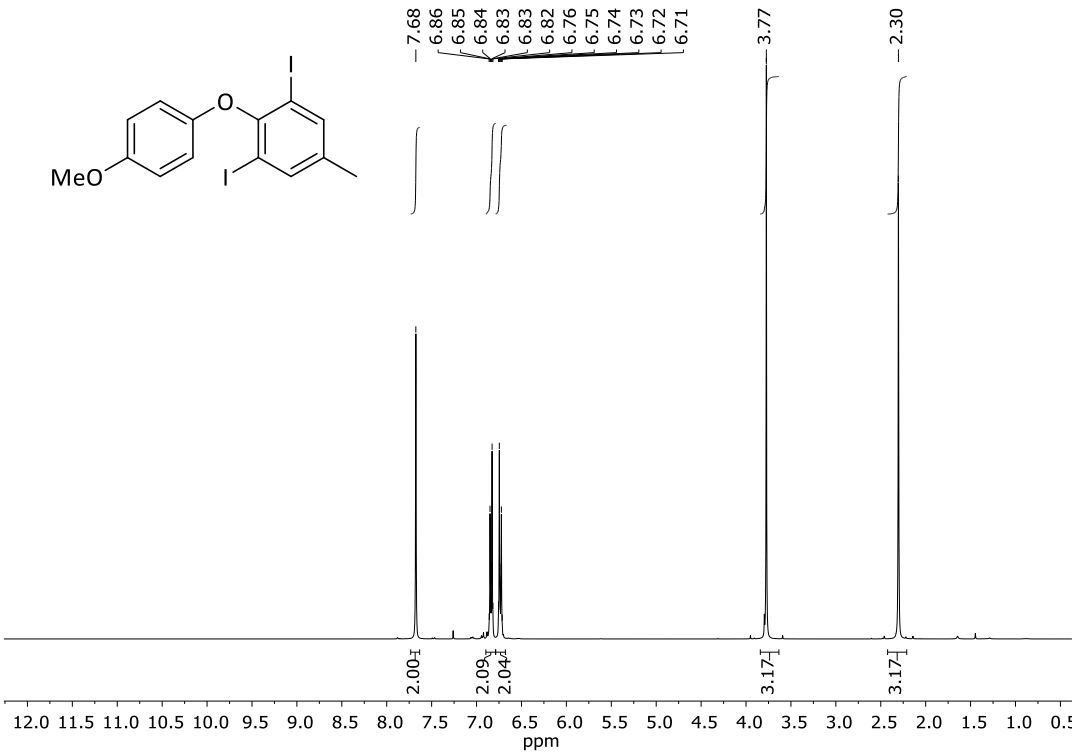

*Figure S4: 400 MHz ^{1}H-NMR spectrum of compound **S2** in $CDCl_3$.*

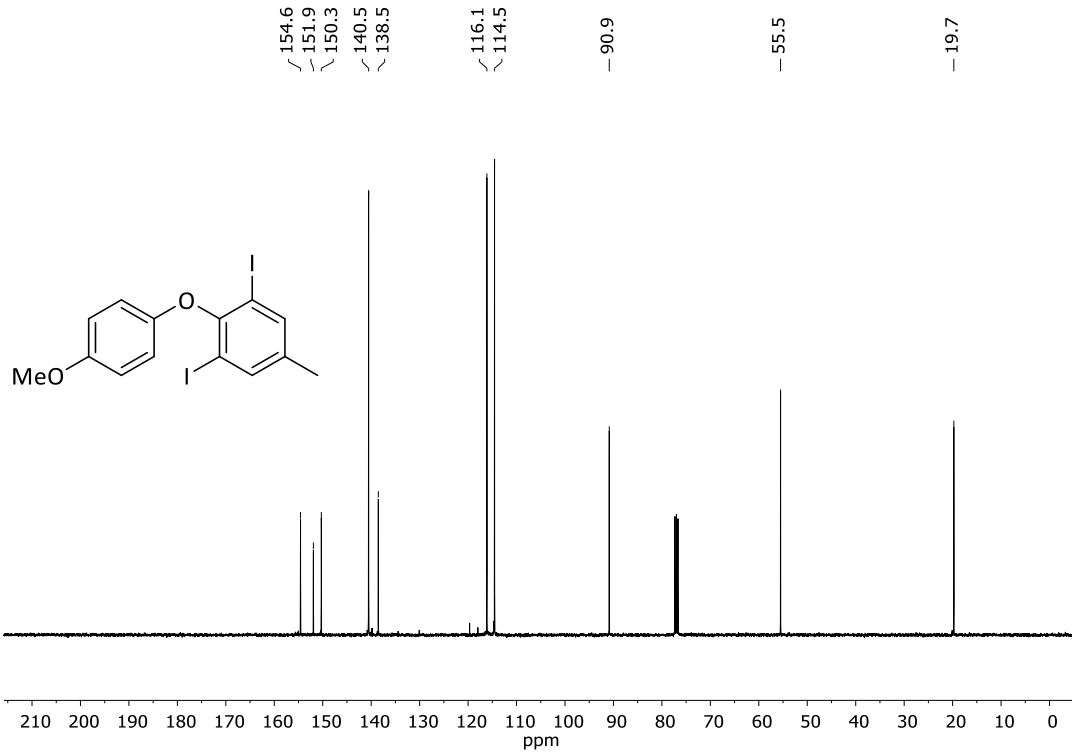

*Figure S5: 100 MHz ^{13}C-NMR spectrum of compound **S2** in $CDCl_3$.*

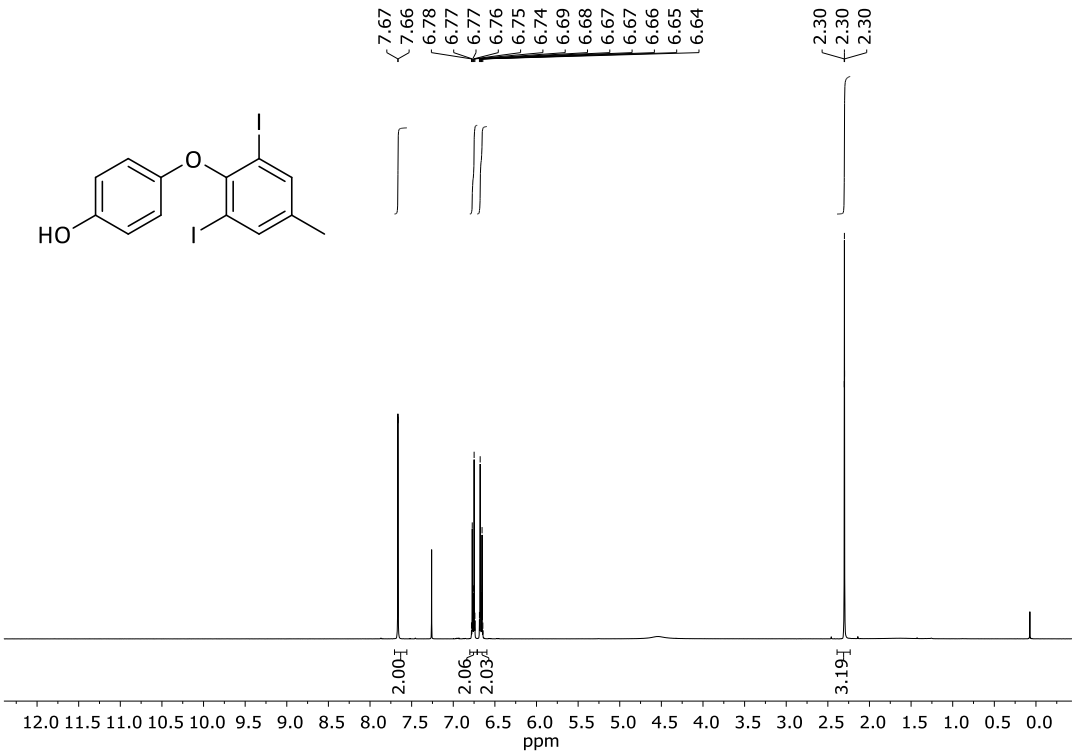

*Figure S6: 400 MHz ^{1}H-NMR spectrum of compound **S3** in $CDCl_3$.*

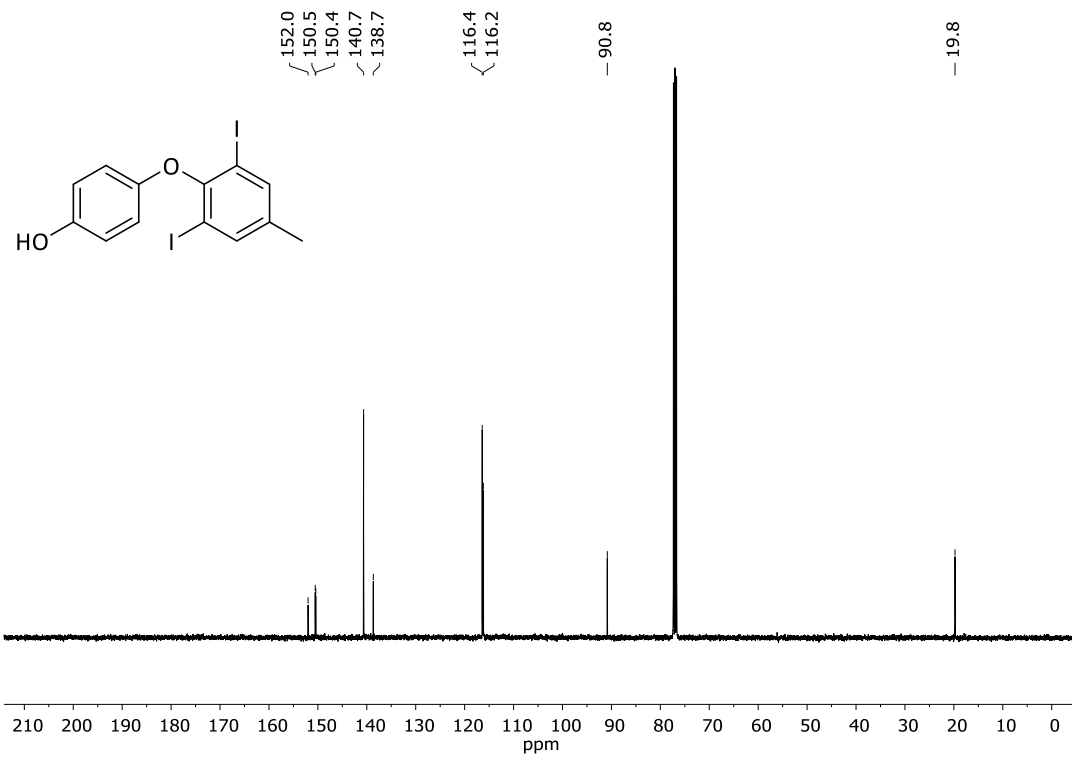

*Figure S7: 100 MHz ^{13}C-NMR spectrum of compound **S3** in $CDCl_3$.*

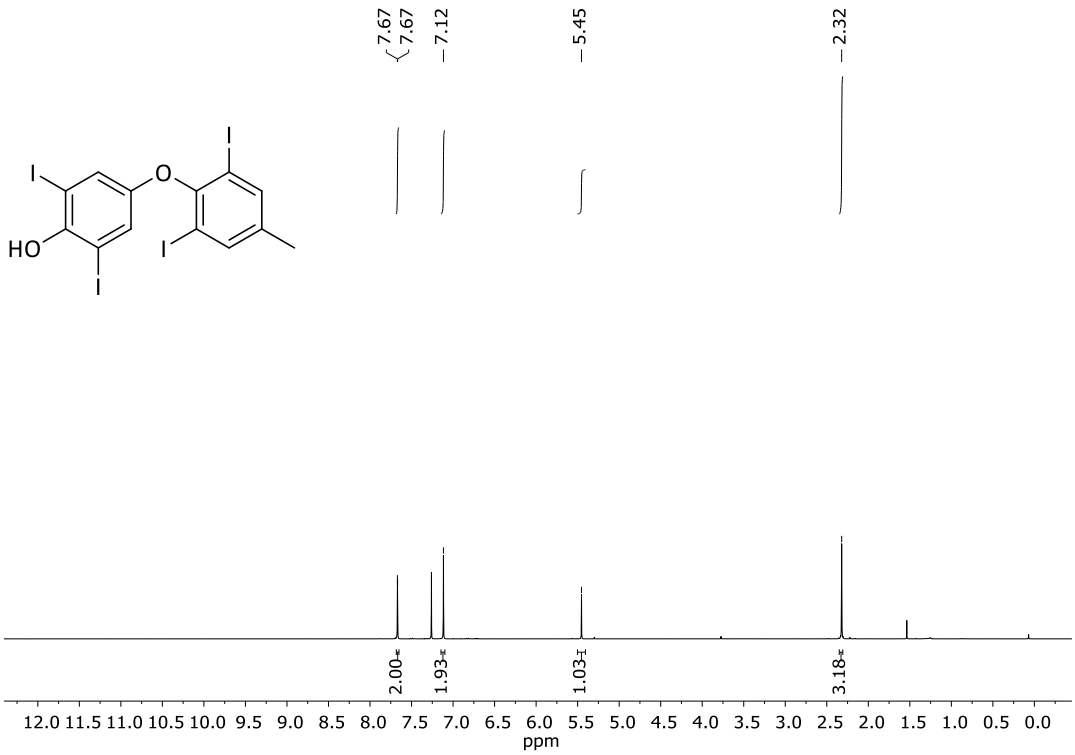

*Figure S8: 400 MHz ^{1}H-NMR spectrum of compound **S4** in $CDCl_3$.*

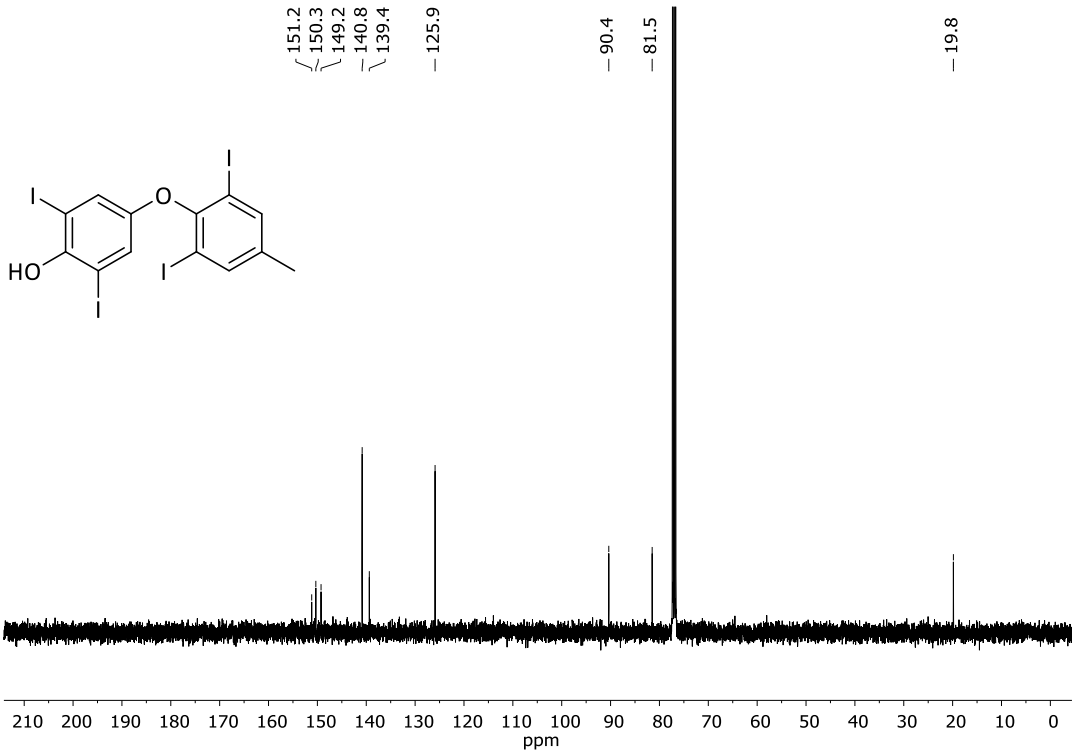

*Figure S9: 100 MHz ^{13}C-NMR spectrum of compound **S4** in $CDCl_3$.*

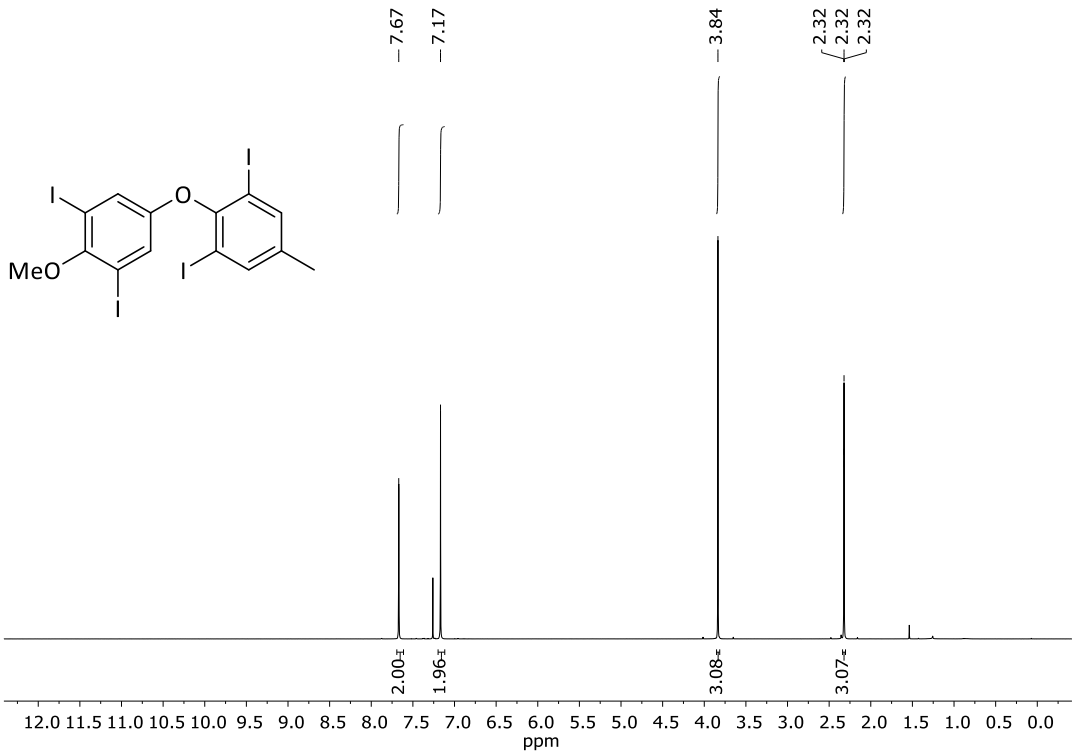

*Figure S10: 400 MHz ^{1}H-NMR spectrum of compound **2a** in $CDCl_3$.*

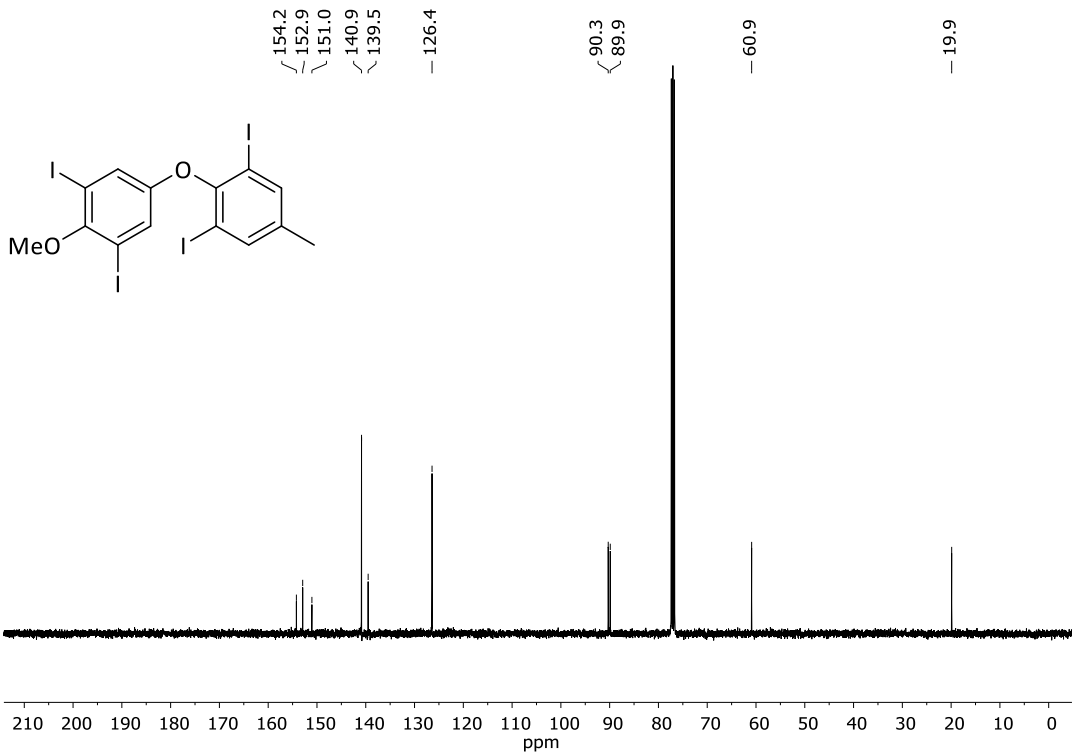

*Figure S11: 100 MHz ^{13}C-NMR spectrum of compound **2a** in $CDCl_3$.*

*Figure S12: 400 MHz ^{1}H-NMR spectrum of compound **S5** in $CDCl_3$.*

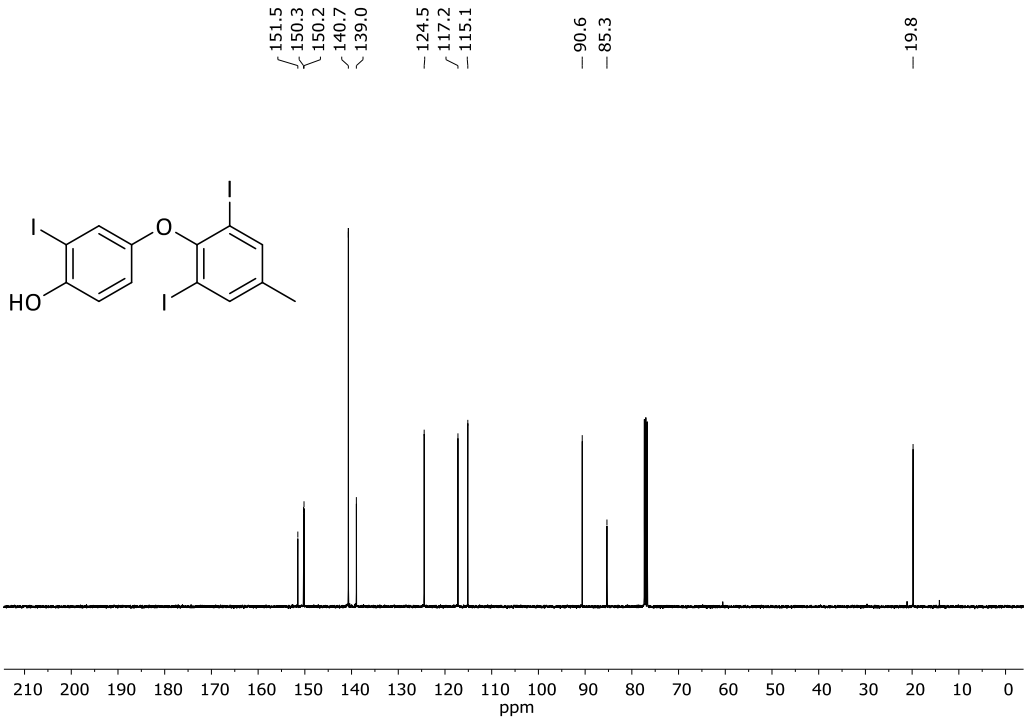

*Figure S13: 100 MHz ^{13}C-NMR spectrum of compound **S5** in $CDCl_3$.*

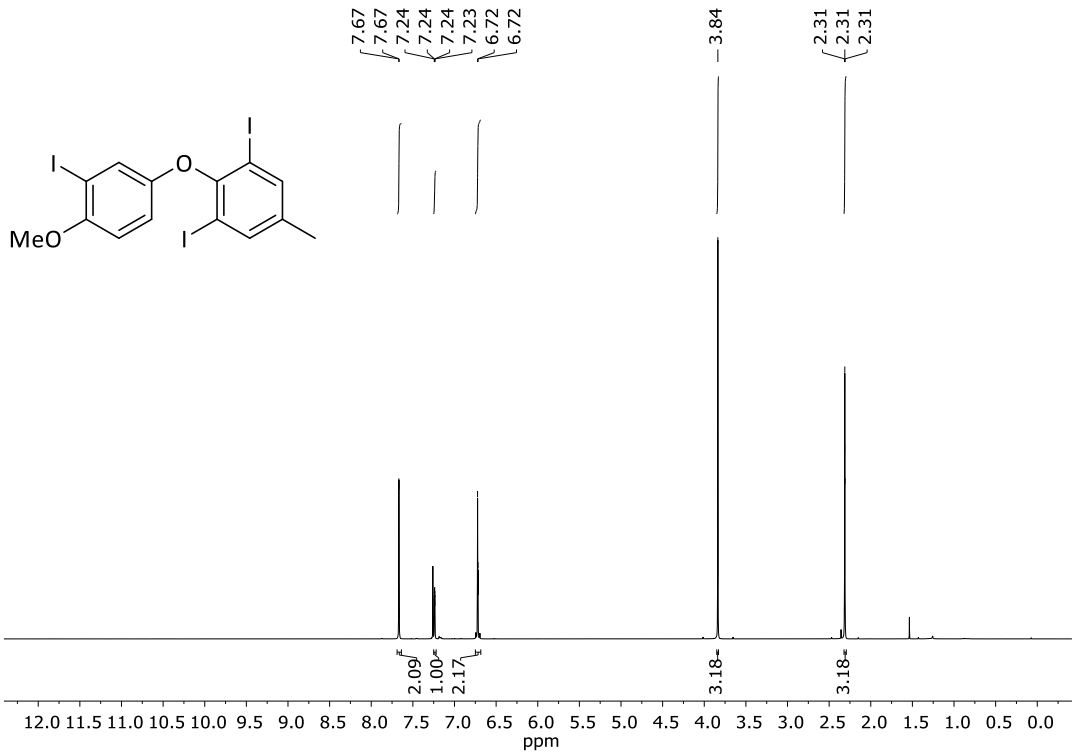

*Figure S14: 400 MHz ^{1}H-NMR spectrum of compound **2b** in $CDCl_3$.*

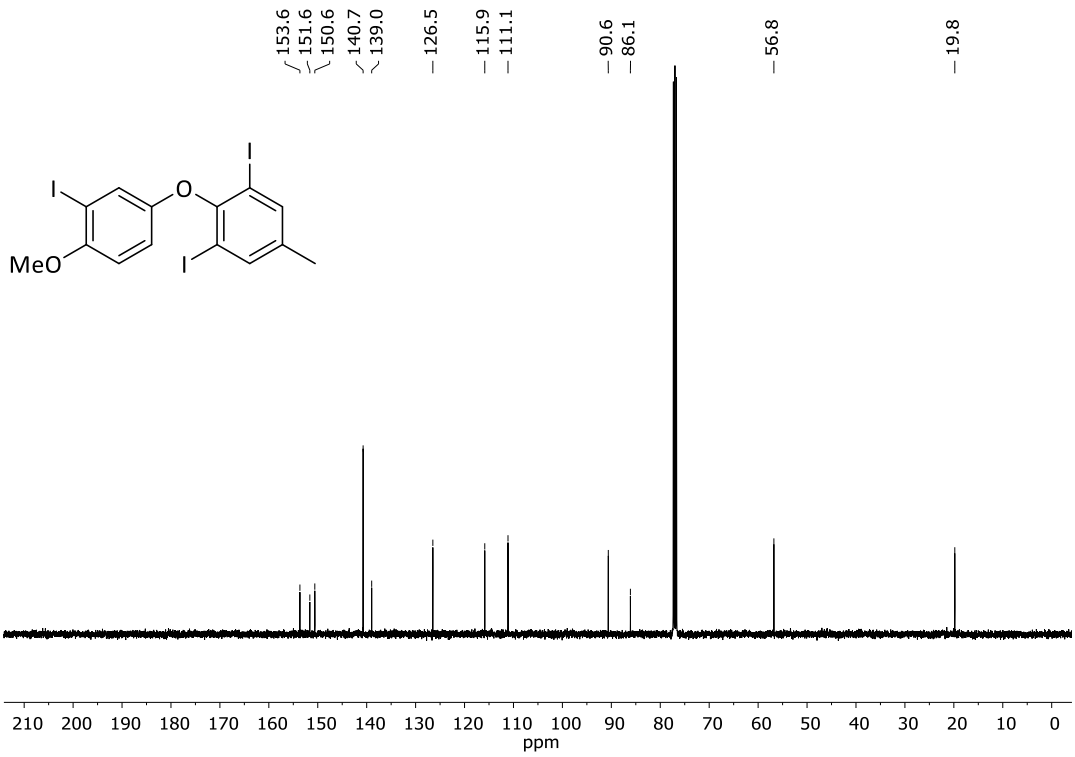

*Figure S15: 100 MHz ^{13}C-NMR spectrum of compound **2b** in $CDCl_3$.*

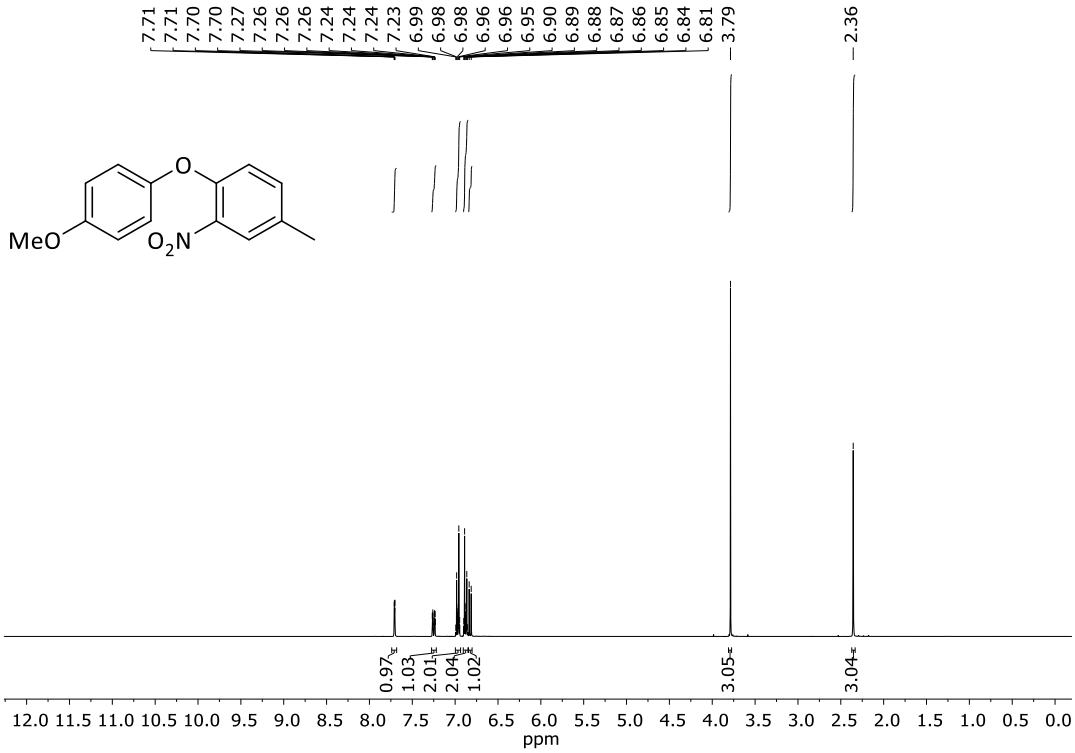

*Figure S16: 360 MHz ^{1}H-NMR spectrum of compound **S6** in $CDCl_3$.*

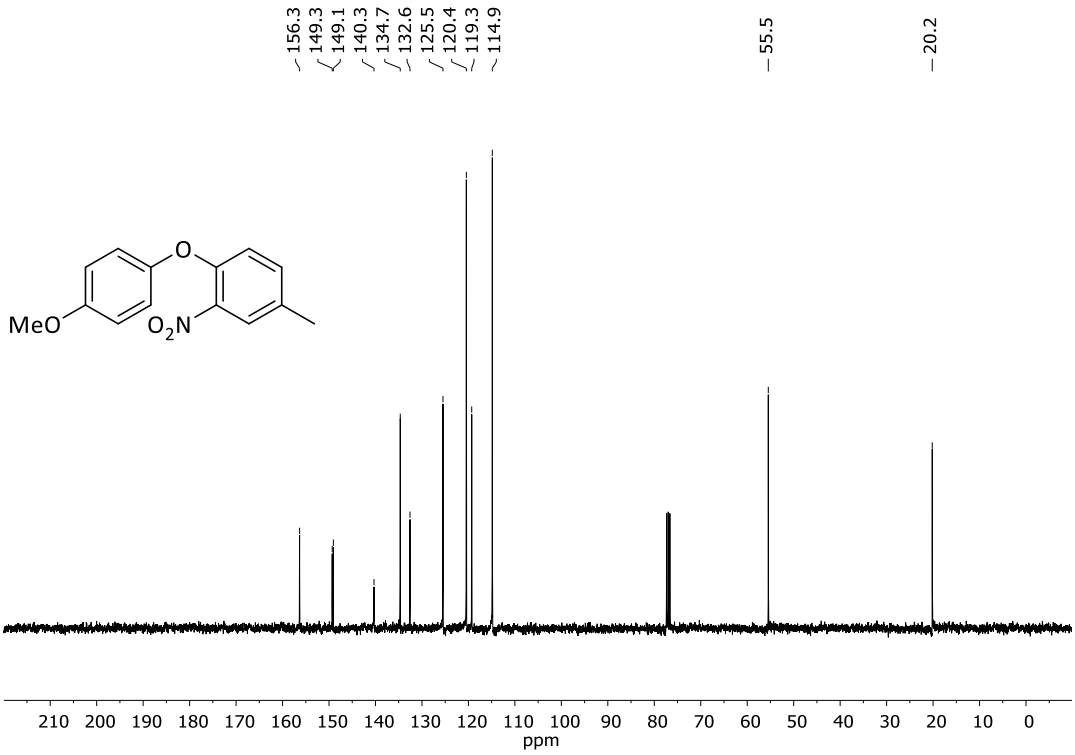

*Figure S17: 90 MHz ^{13}C-NMR spectrum of compound **S6** in $CDCl_3$.*

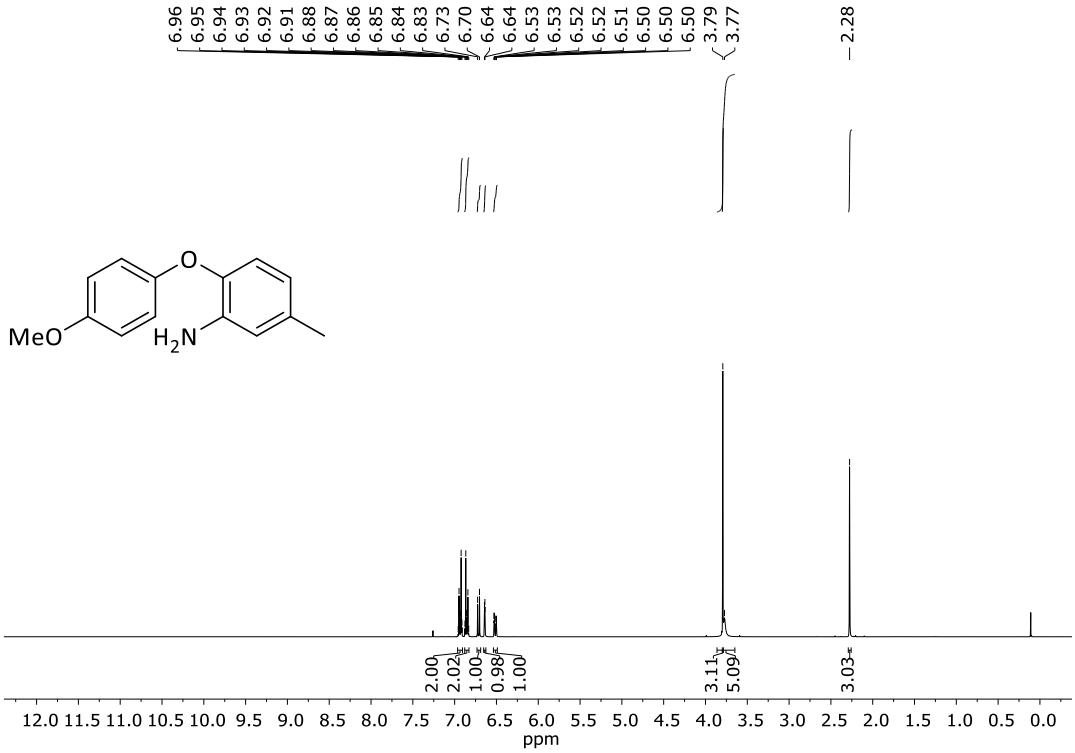

*Figure S18: 360 MHz ^{1}H-NMR spectrum of compound **S7** in $CDCl_3$.*

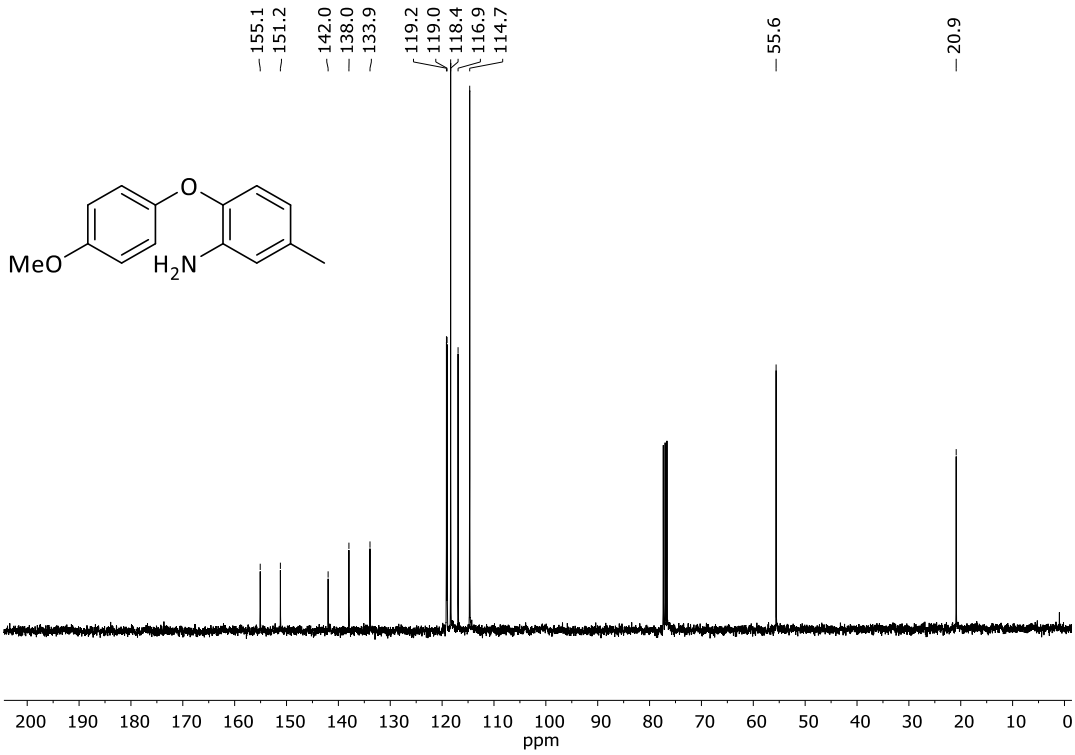

*Figure S19: 90 MHz ^{13}C-NMR spectrum of compound **S7** in $CDCl_3$.*

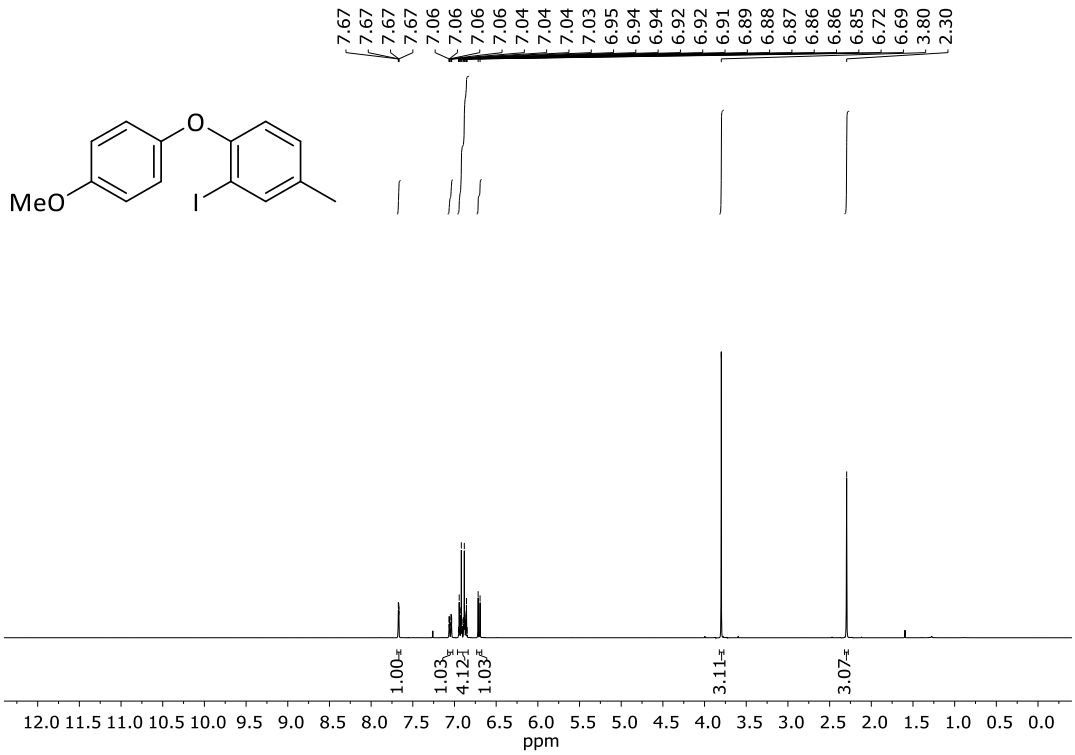

*Figure S20: 360 MHz ^{1}H-NMR spectrum of compound **S8** in $CDCl_3$.*

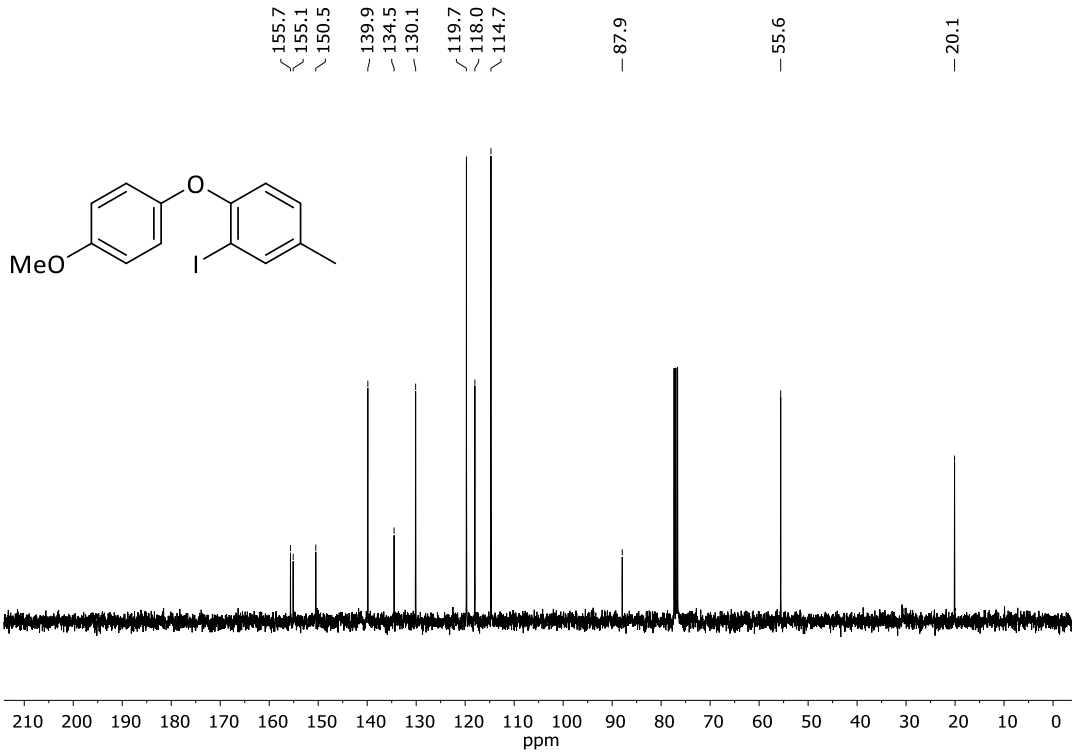

*Figure S21: 90 MHz ^{13}C-NMR spectrum of compound **S8** in $CDCl_3$.*

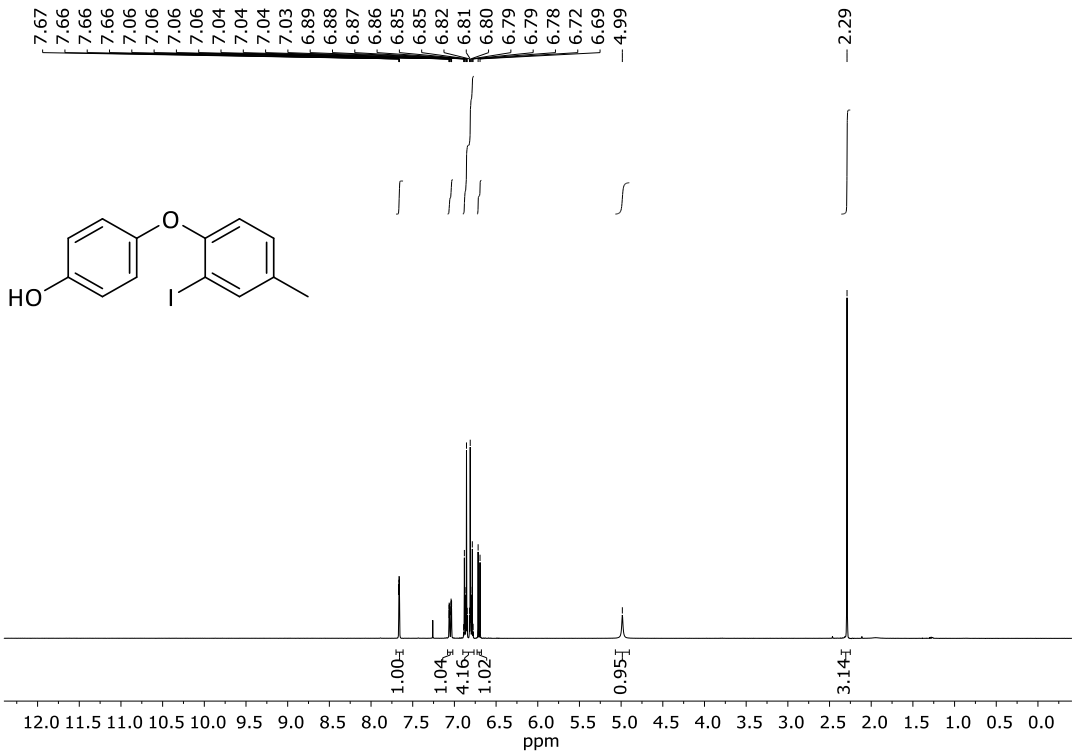

*Figure S22: 360 MHz ^{1}H-NMR spectrum of compound **S9** in $CDCl_3$.*

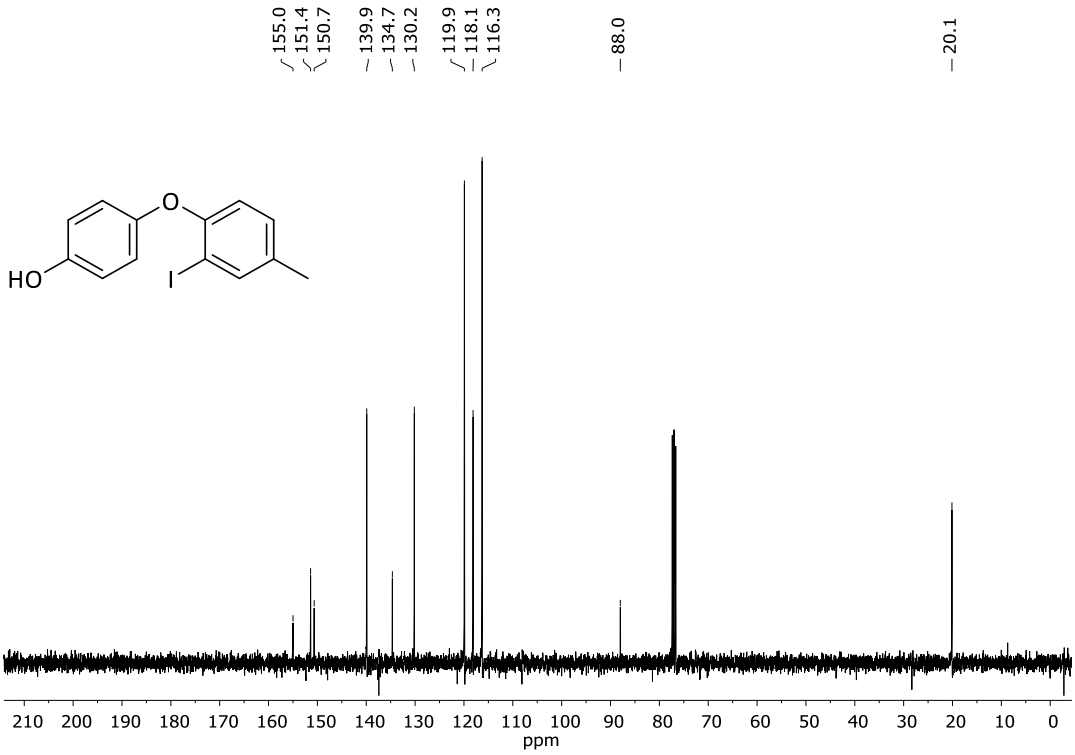

*Figure S23: 90 MHz ^{13}C-NMR spectrum of compound **S9** in $CDCl_3$.*

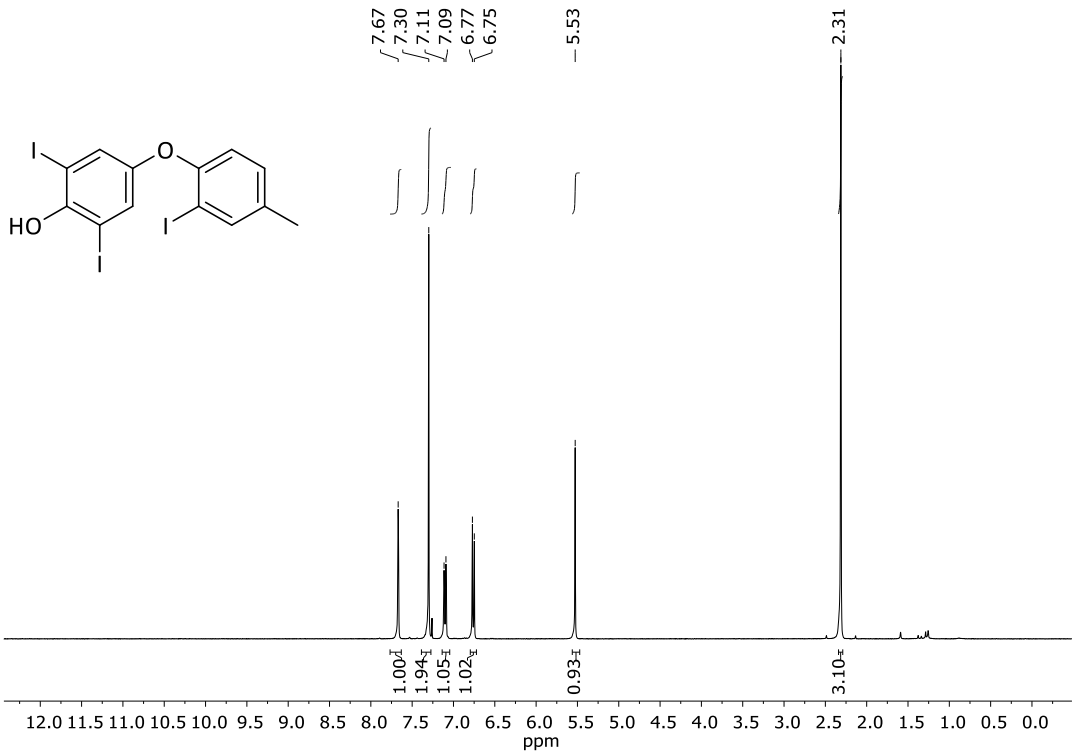

*Figure S24: 360 MHz ^{1}H-NMR spectrum of compound **S10** in $CDCl_3$.*

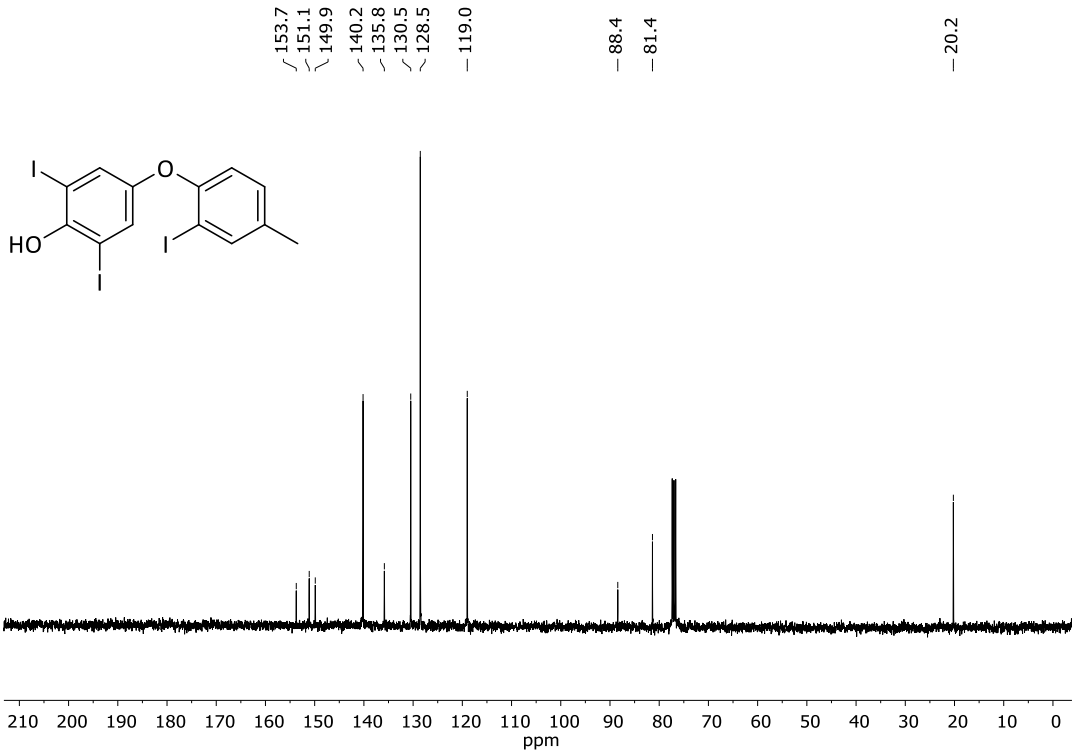

*Figure S25: 90 MHz ^{13}C-NMR spectrum of compound **S10** in $CDCl_3$.*

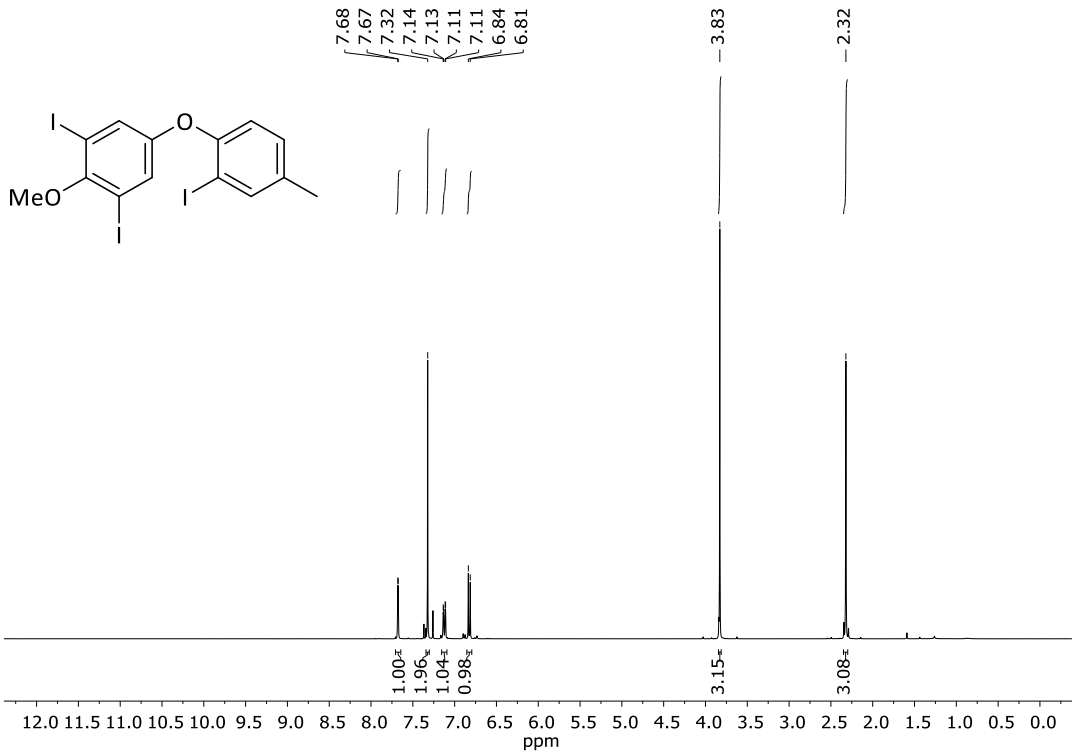

*Figure S26: 360 MHz ^{1}H-NMR spectrum of compound **2c** in $CDCl_3$.*

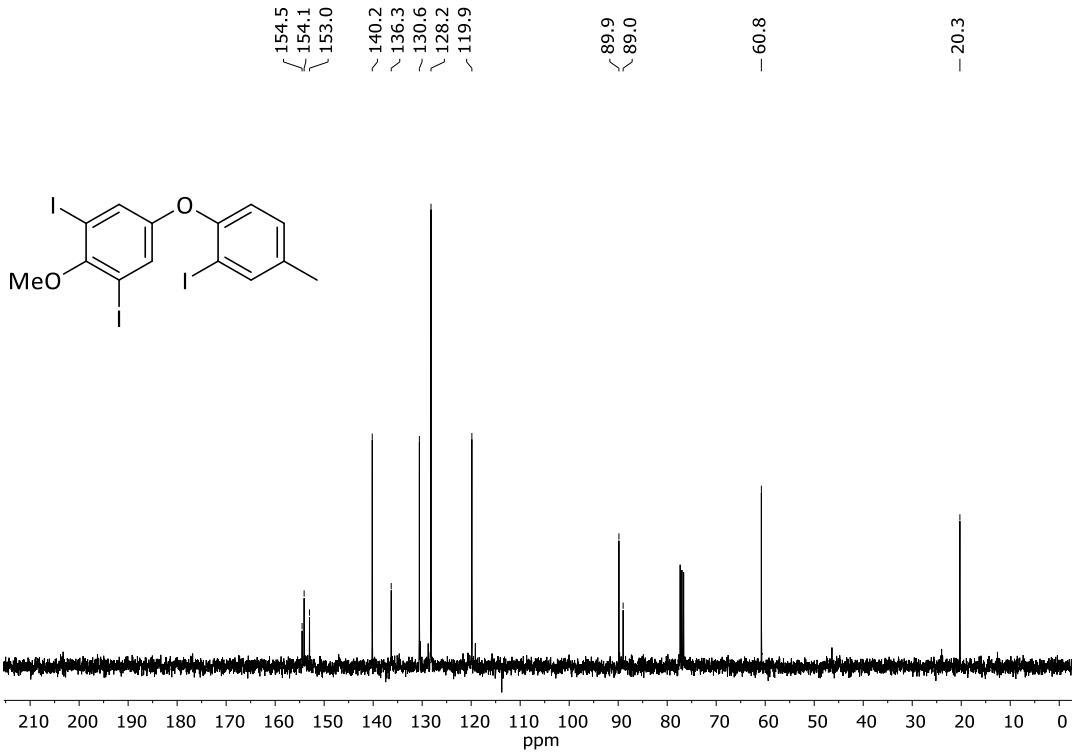

*Figure S27: 90 MHz ^{13}C-NMR spectrum of compound **2c** in $CDCl_3$.*

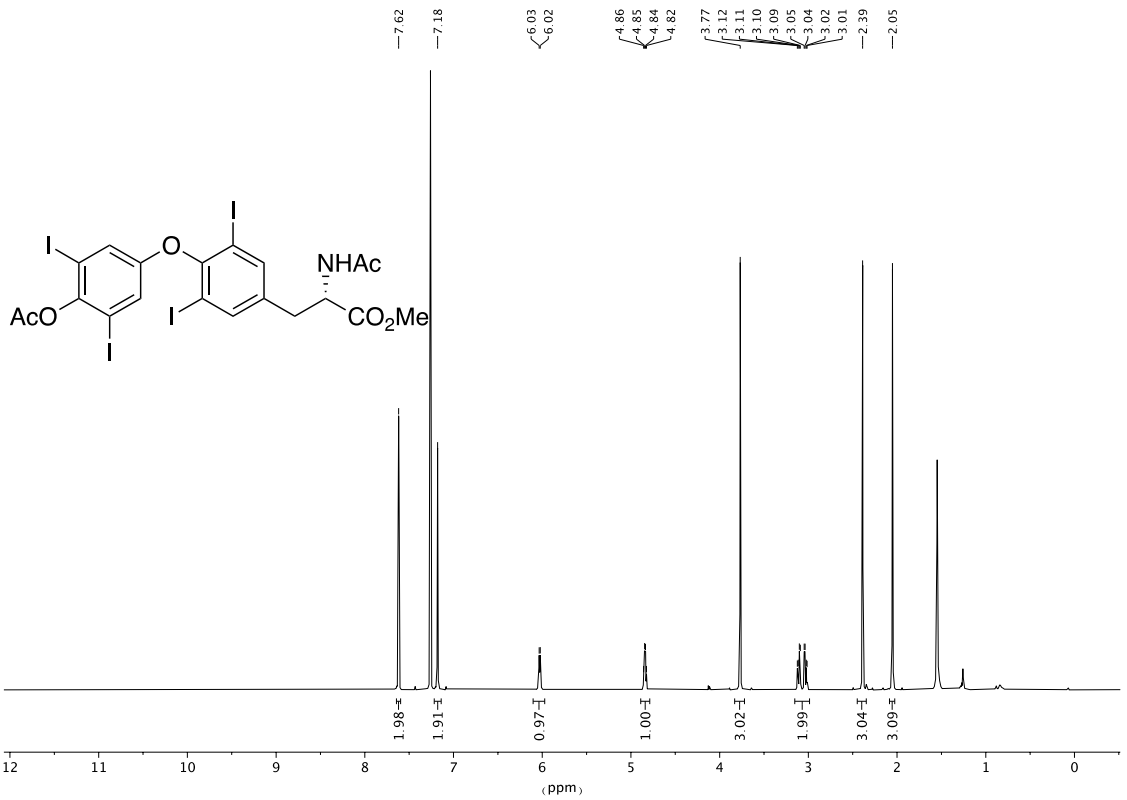

*Figure S28: 600 MHz ^{1}H-NMR spectrum of compound **Ac-Thx(Ac)-OMe** in $CDCl_3$.*

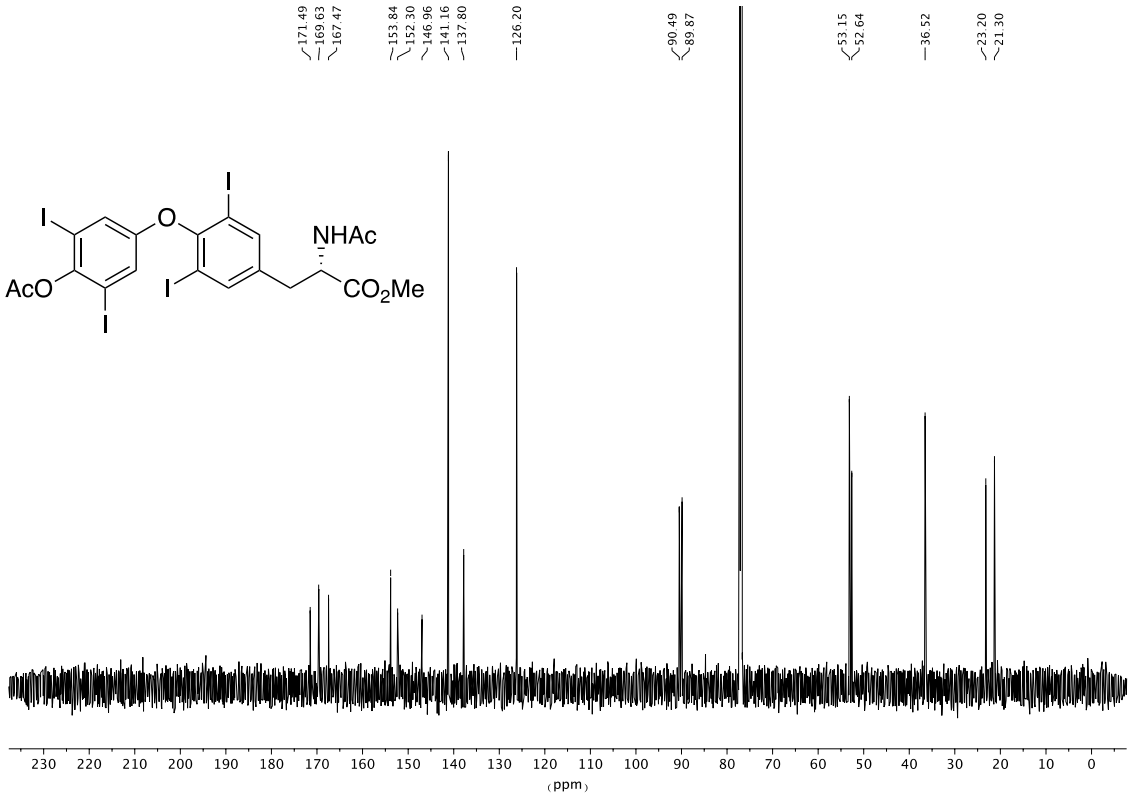

*Figure S29: 151 MHz ^{13}C-NMR spectrum of compound **Ac-Thx(Ac)-OMe** in $CDCl_3$.*

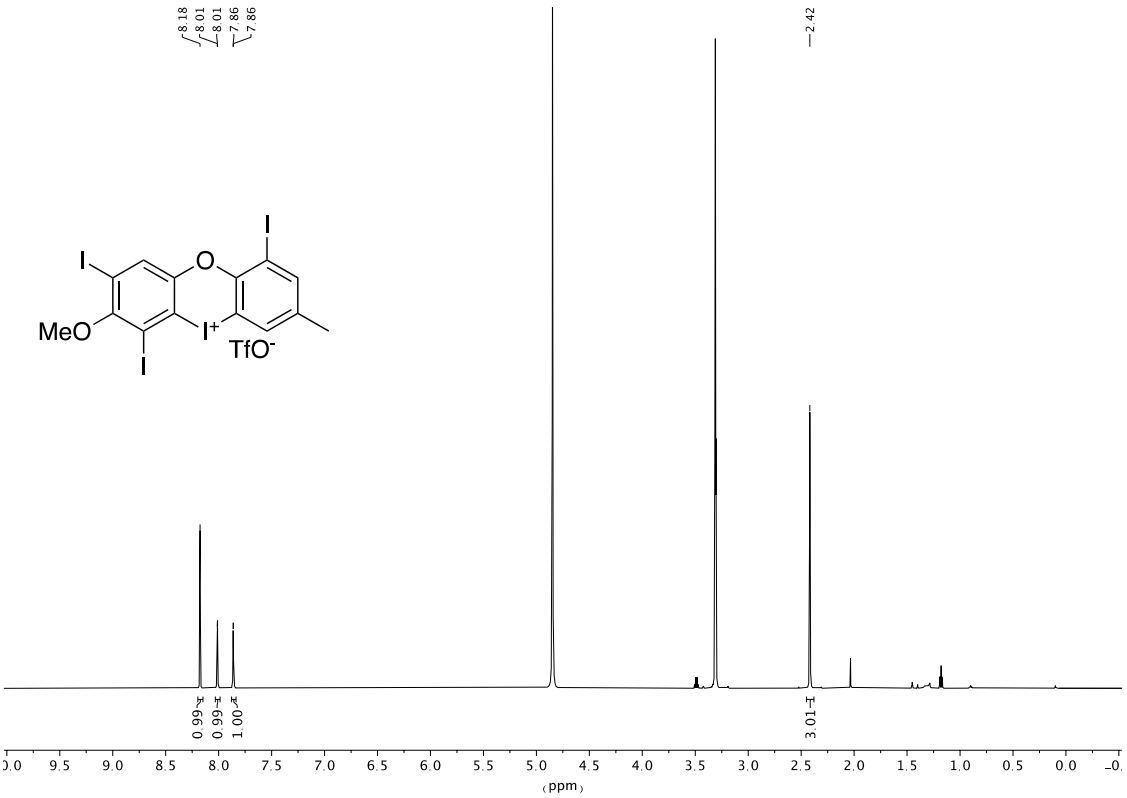

*Figure S30: 600 MHz ^{1}H-NMR spectrum of compound **3a** in DMSO-d_6.*

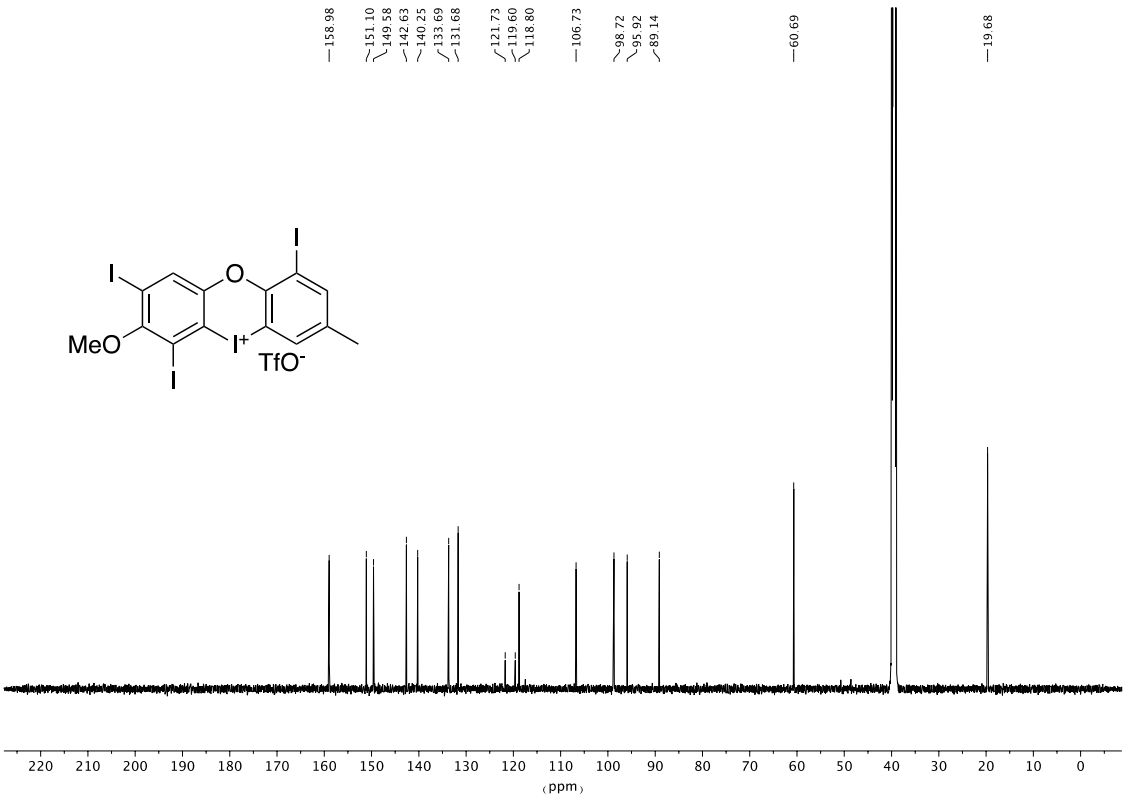

*Figure S31: 151 MHz ^{13}C-NMR spectrum of compound **3a** in DMSO-d_6.*

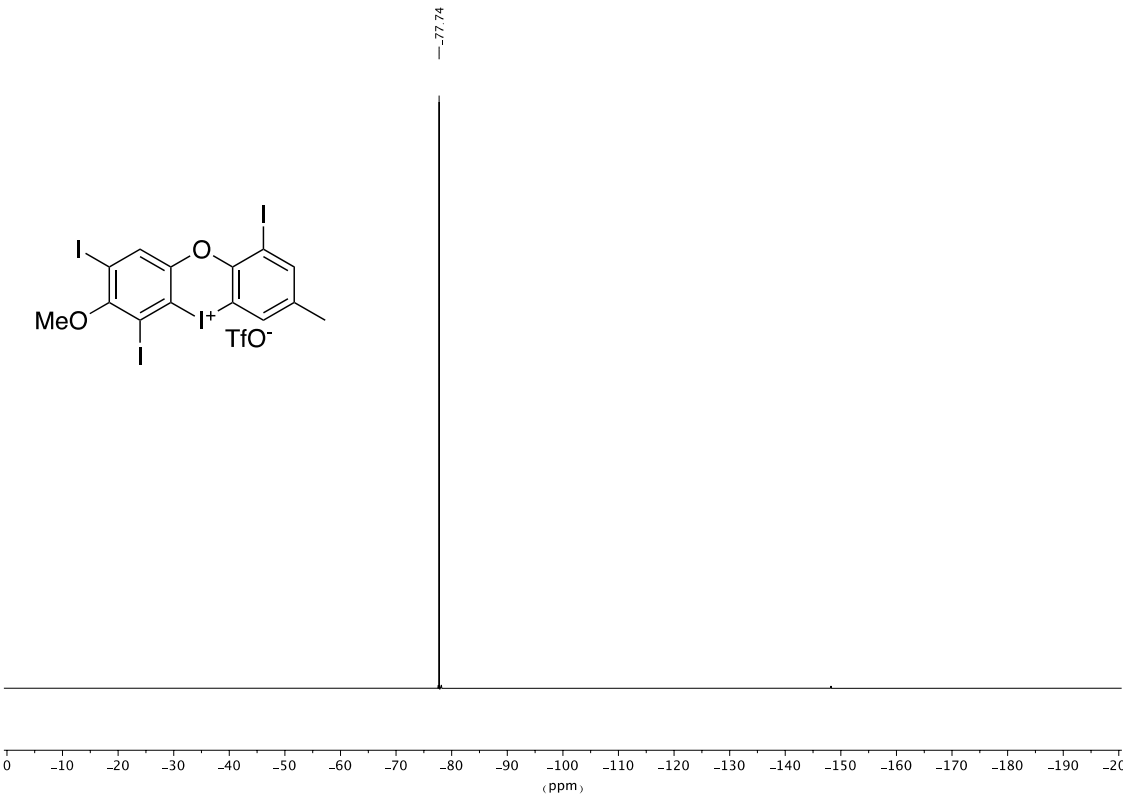

*Figure S32: 565 MHz ^{19}F-NMR spectrum of compound **3a** in DMSO-d_6.*

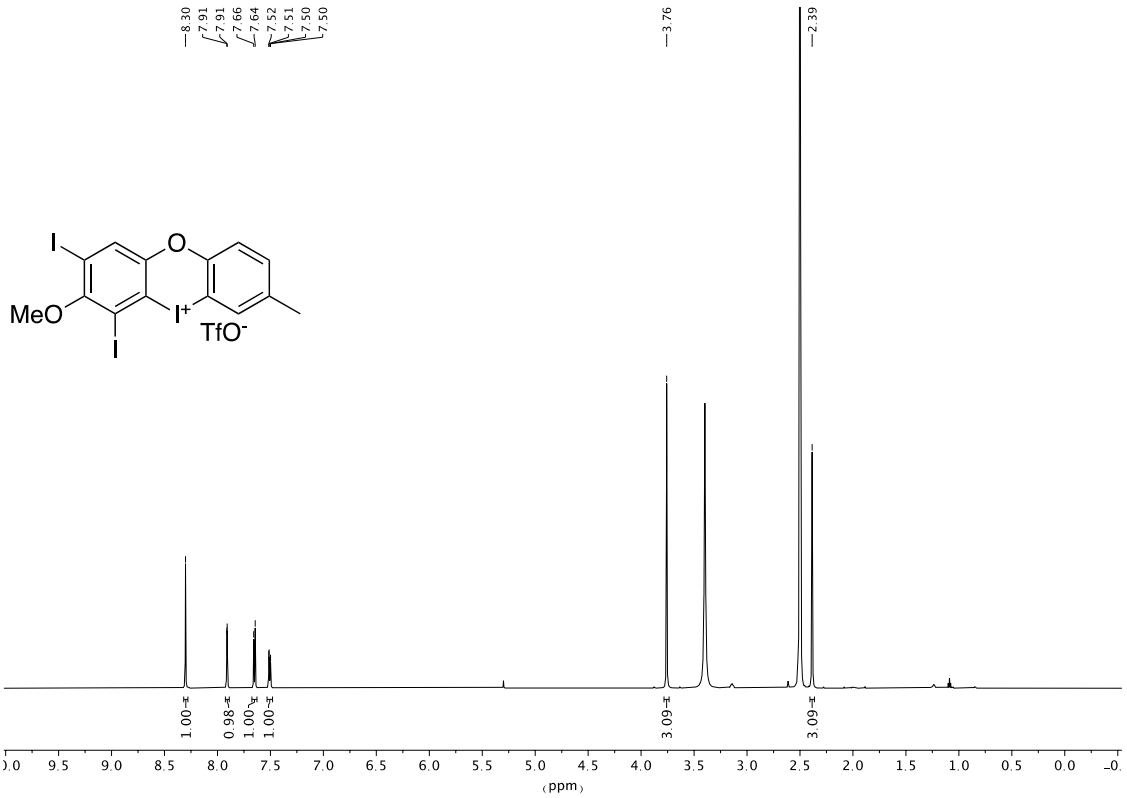

*Figure S33: 600 MHz ^{1}H-NMR spectrum of compound **3c** in DMSO-d_6.*

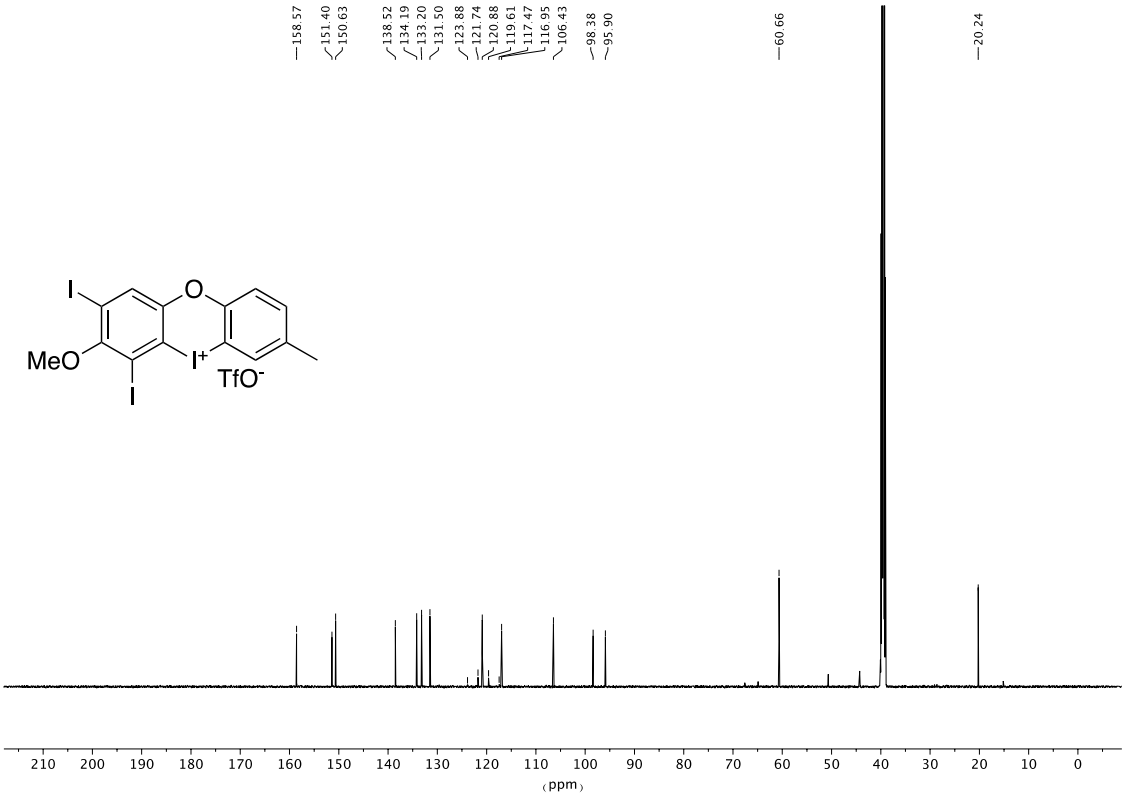

*Figure S34: 151 MHz ^{13}C-NMR spectrum of compound **3c** in DMSO-d_6.*

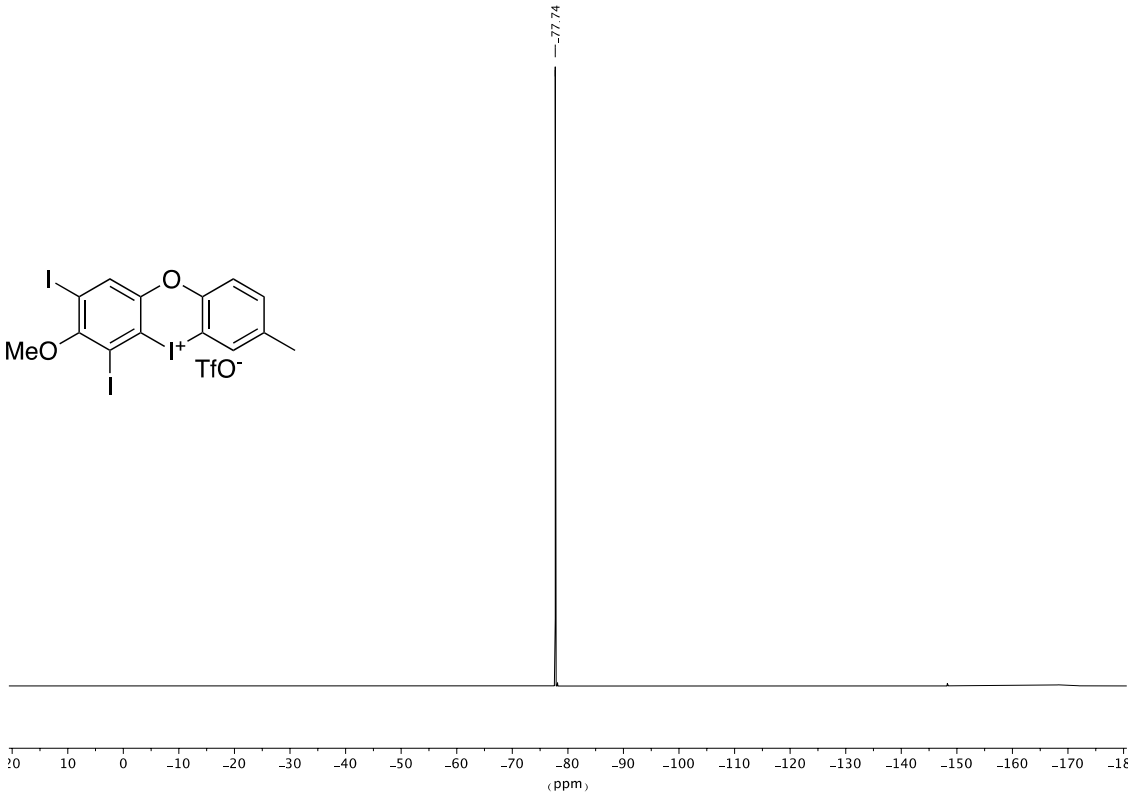

*Figure S35: 565 MHz ^{19}F-NMR spectrum of compound **3c** in DMSO-d_6.*

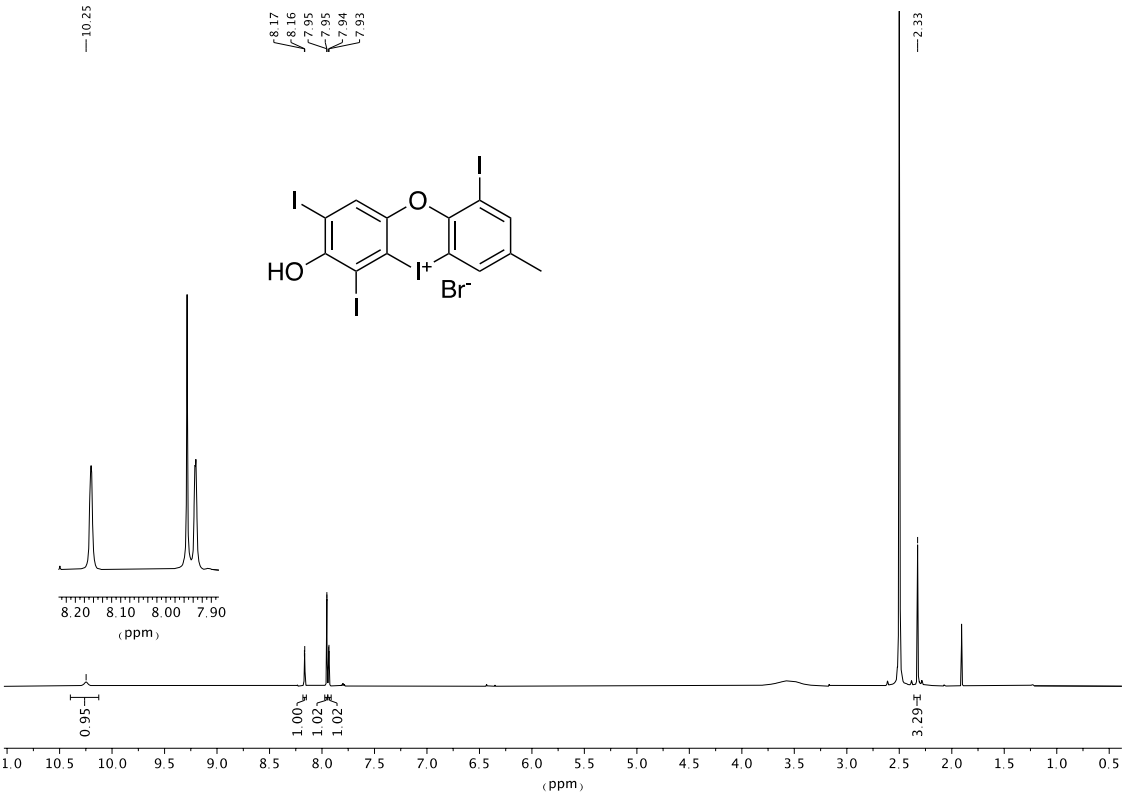

*Figure S36: 601 MHz ^{1}H-NMR spectrum of compound **4a** in DMSO-d_6.*

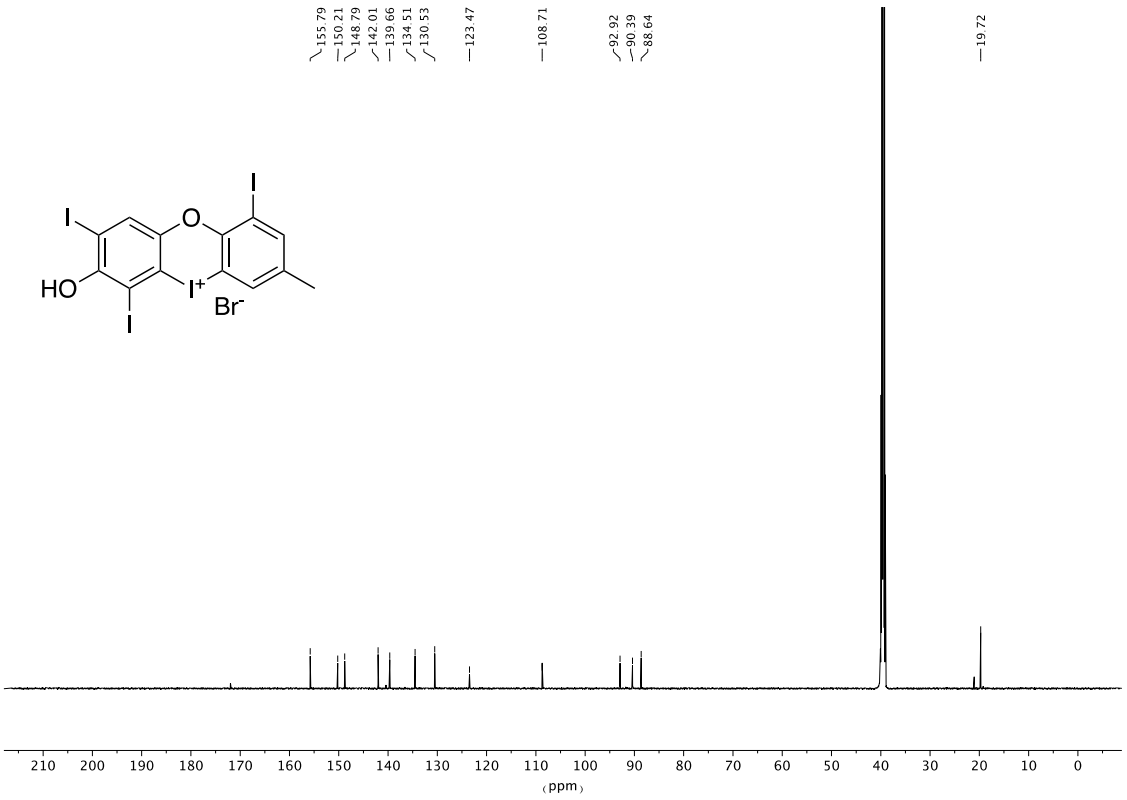

*Figure S37: 151 MHz ^{13}C-NMR spectrum of compound **4a** in DMSO-d_6.*

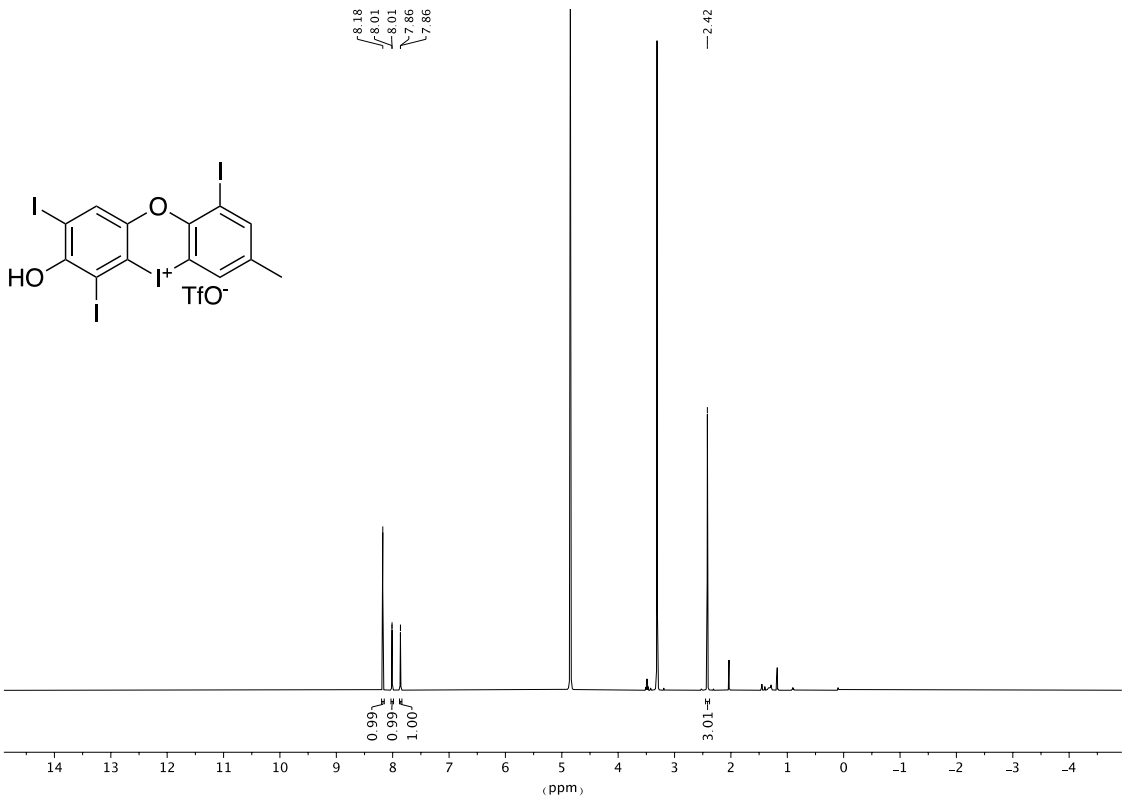

*Figure S38: 600 MHz ^{1}H-NMR spectrum of compound **4b** in CD_3OD.*

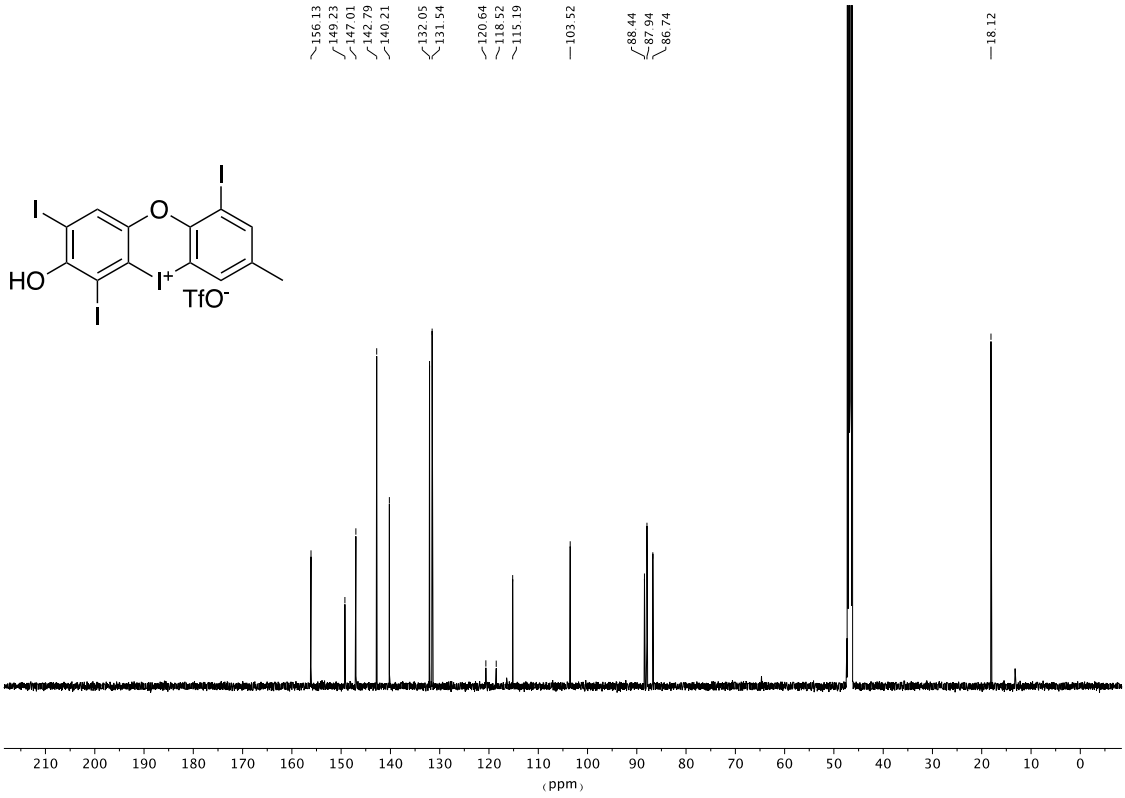

*Figure S39: 151 MHz ^{13}C-NMR spectrum of compound **4b** in CD_3OD.*

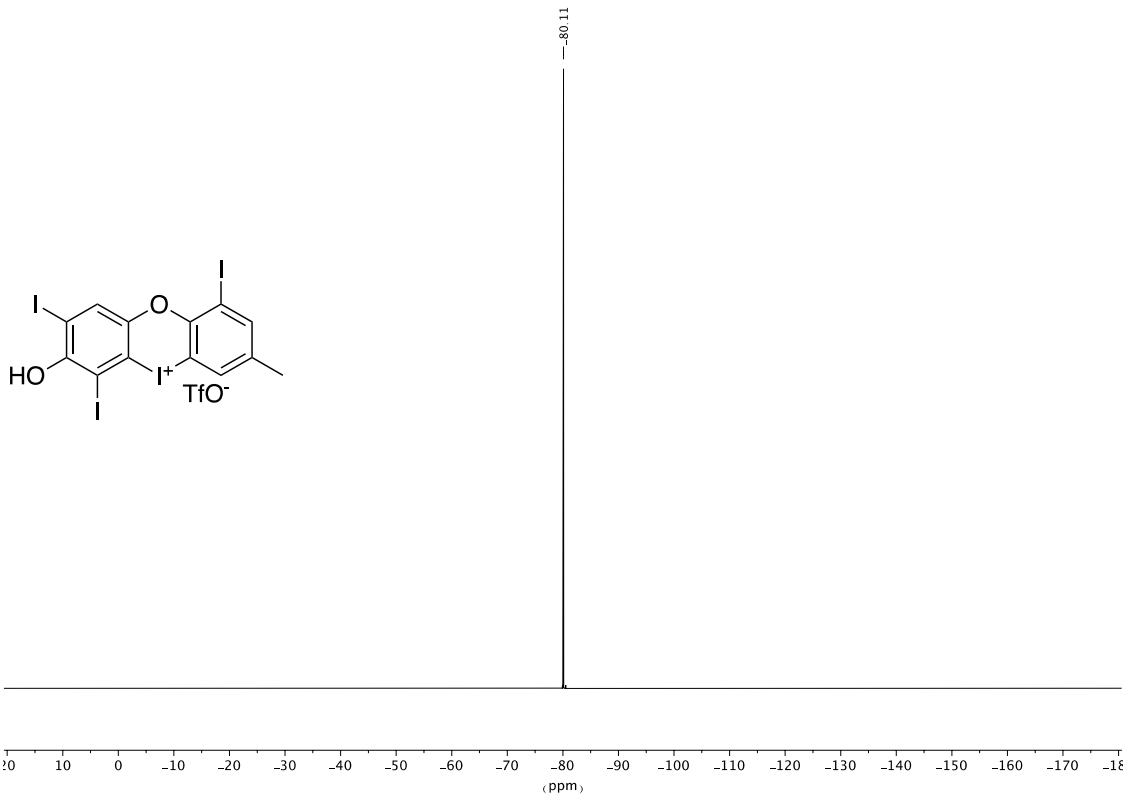

*Figure S40: 565 MHz ^{19}F-NMR spectrum of compound **4b** in CD_3OD.*

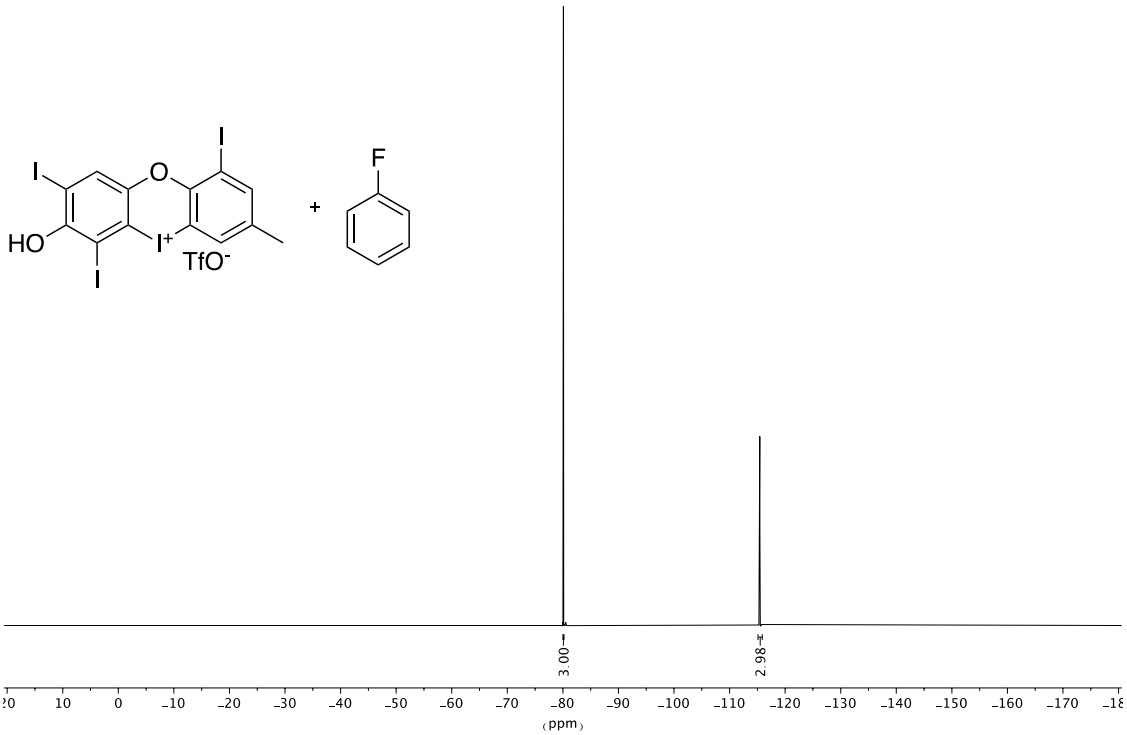

*Figure S41: 565 MHz ^{19}F-NMR spectrum of compound **4b + 3 eq. of PhF** in CD_3OD.*

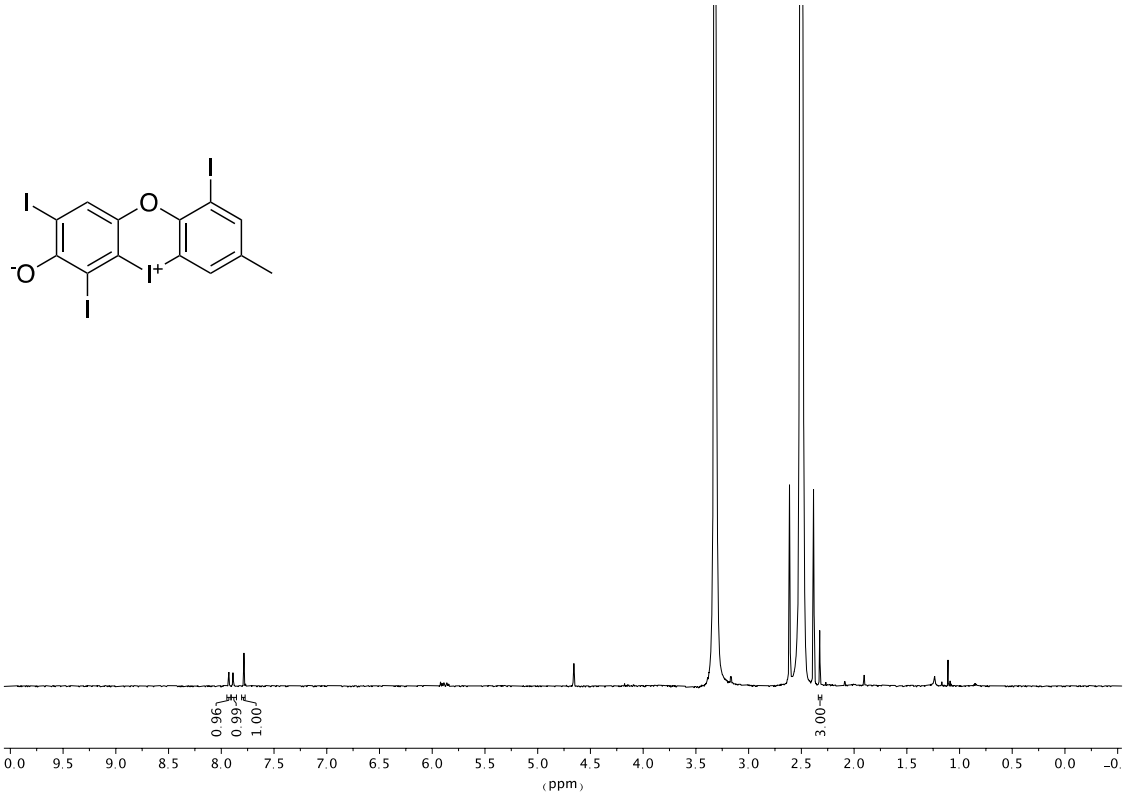

*Figure S42: 600 MHz ^{1}H-NMR spectrum of compound **5** in DMSO-d_6.*

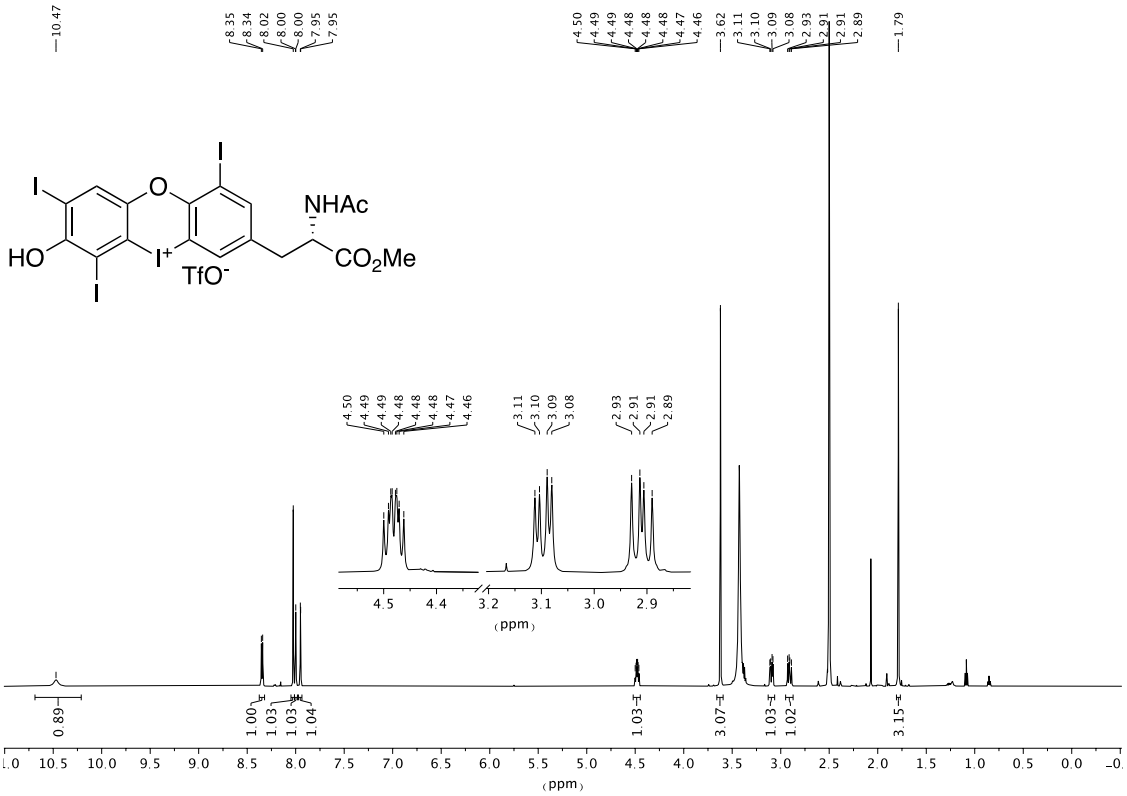

*Figure S43: 600 MHz ^{1}H-NMR spectrum of compound **6a** in DMSO-d_6.*

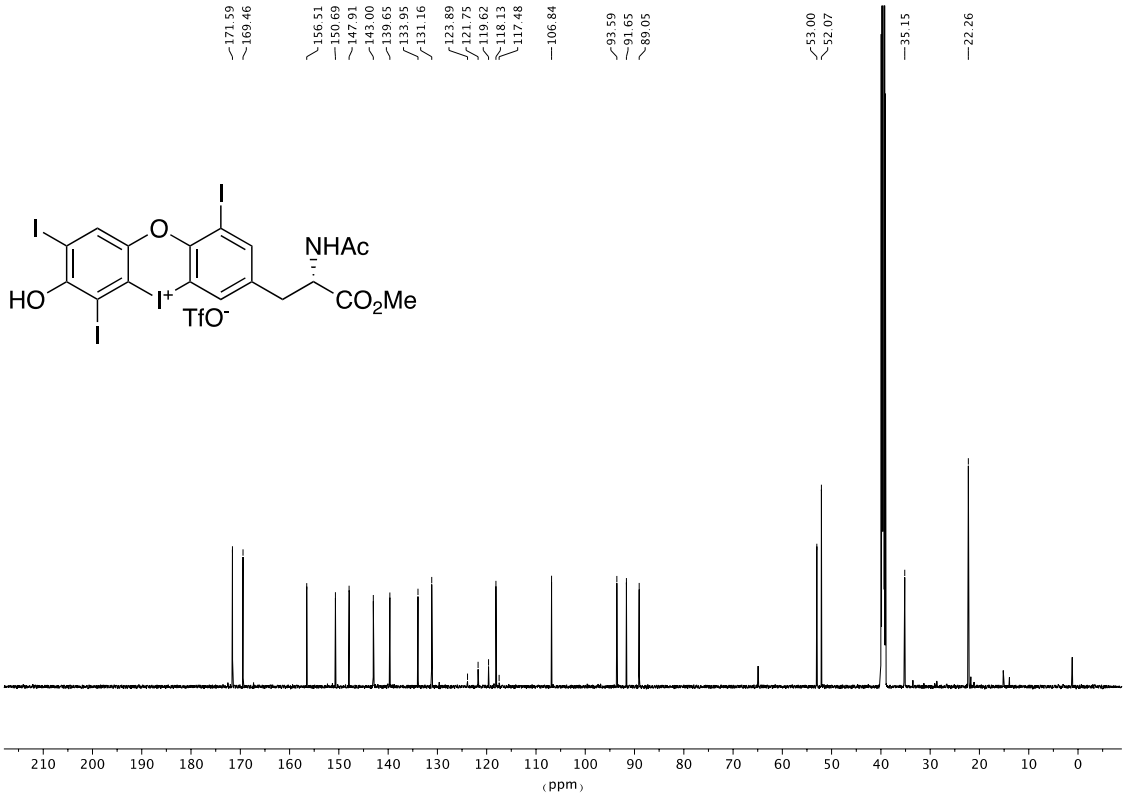

*Figure S44: 151 MHz ^{13}C-NMR spectrum of compound **6a** in DMSO-d_6.*

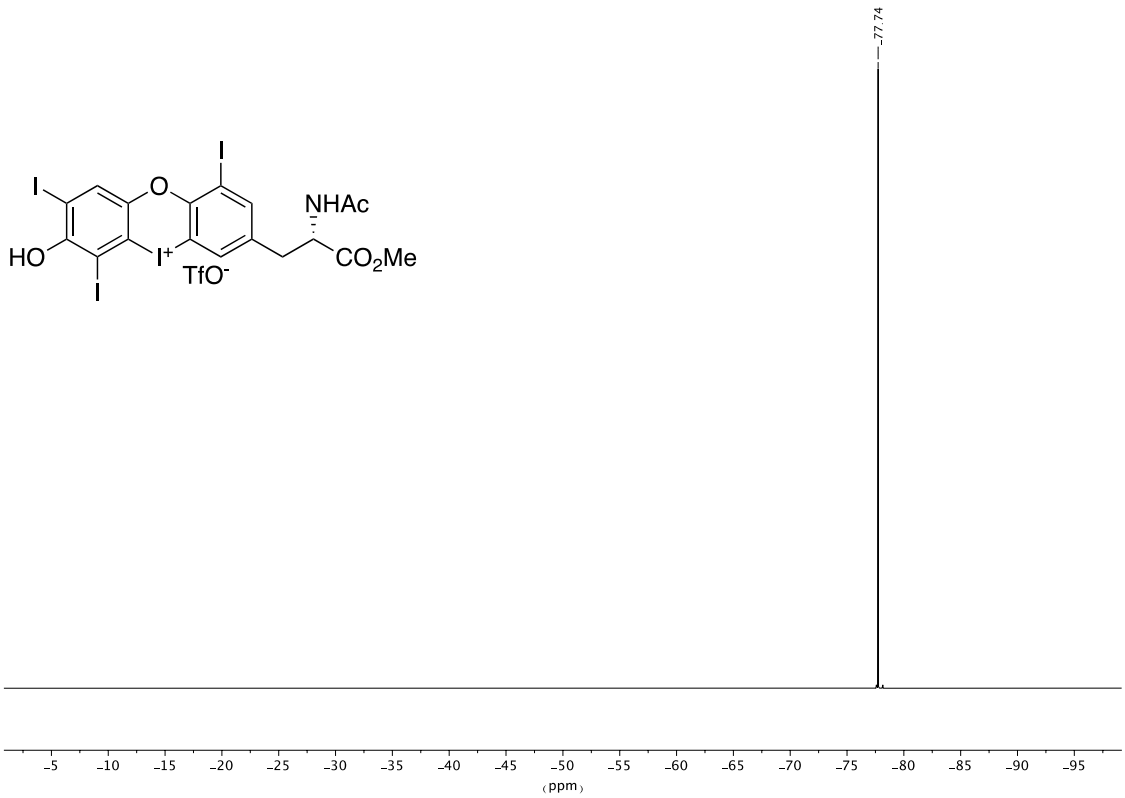

*Figure S45: 565 MHz ^{19}F-NMR spectrum of compound **6a** in DMSO-d_6.*

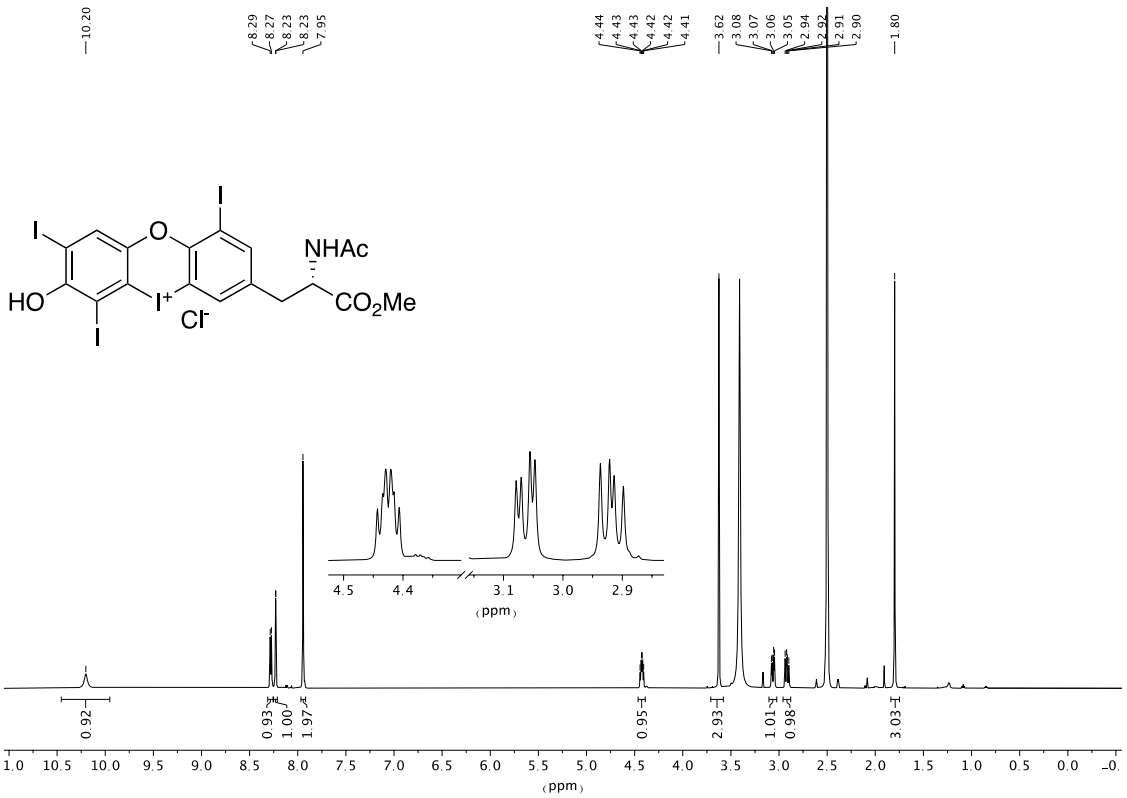

*Figure S46: 600 MHz ^{1}H-NMR spectrum of compound **6b** in DMSO-d_6.*

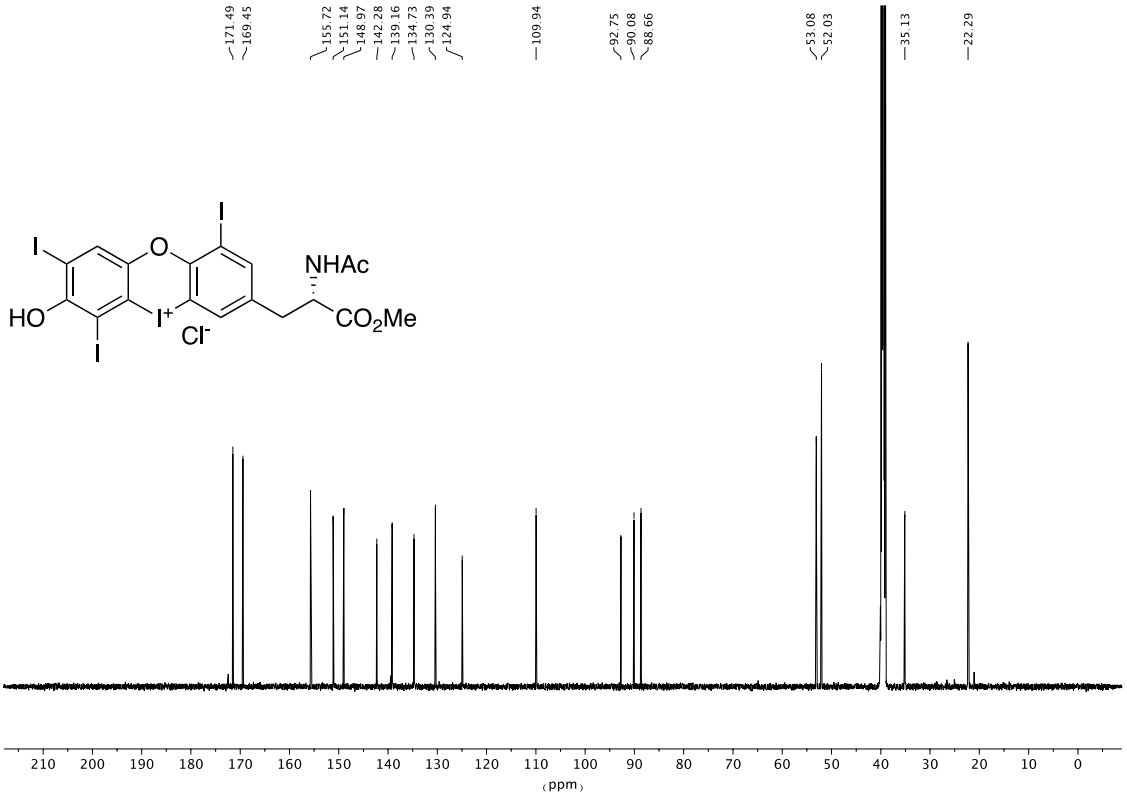

*Figure S47: 151 MHz ^{13}C-NMR spectrum of compound **6b** in DMSO-d_6.*

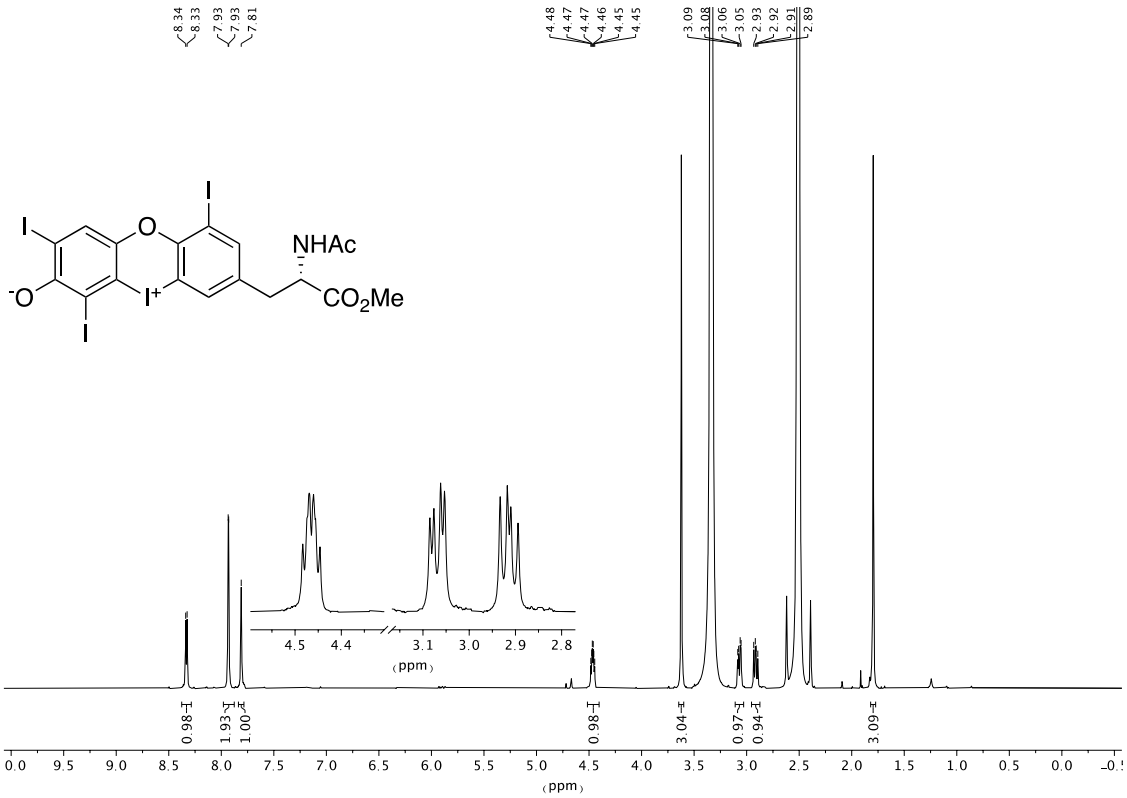

*Figure S48: 600 MHz ^{1}H-NMR spectrum of compound **7** in DMSO-d_6.*

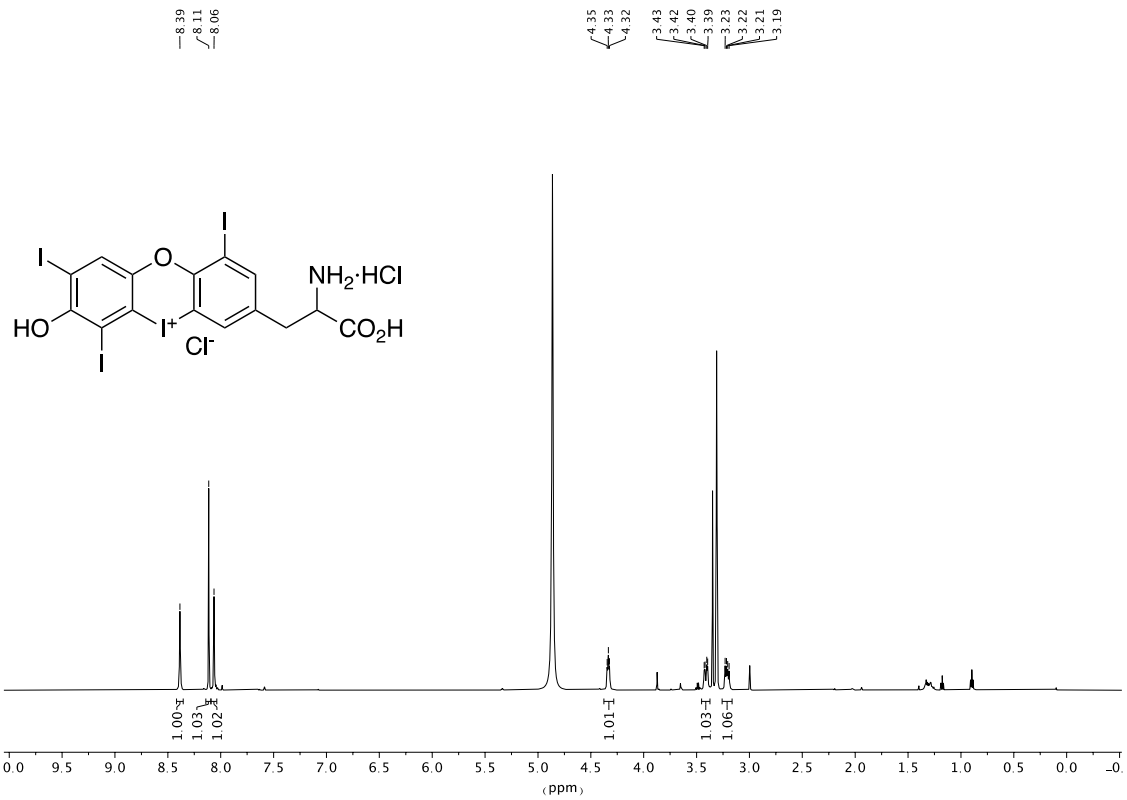

*Figure S49: 600 MHz ^{1}H-NMR spectrum of compound **1a** in CD_3OD.*

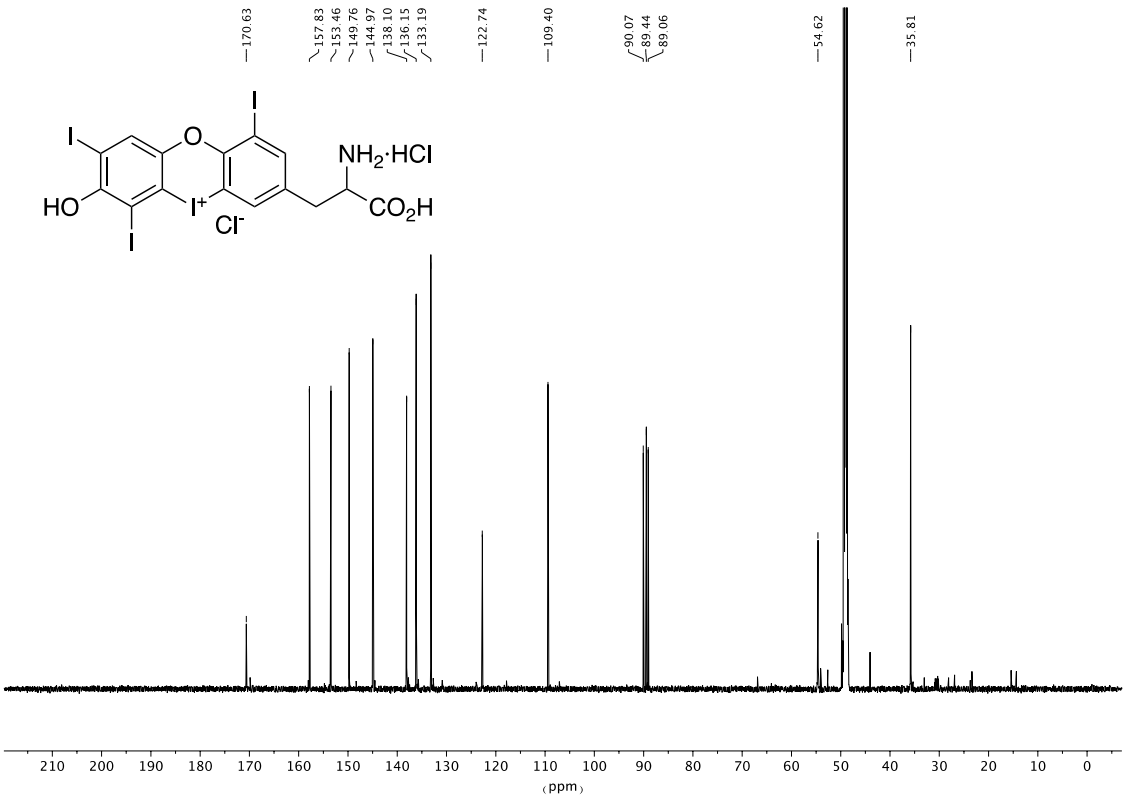

*Figure S50: 151 MHz ^{13}C-NMR spectrum of compound **1a** in CD_3OD.*

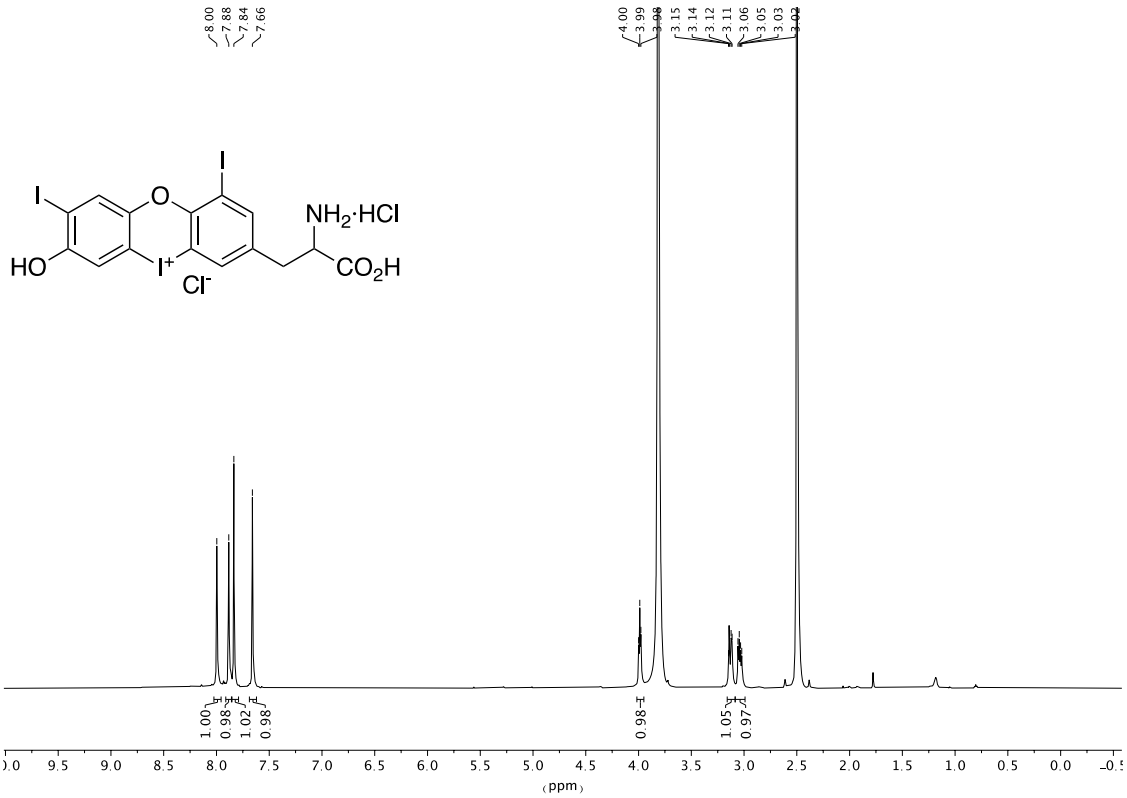

*Figure S51: 600 MHz ^{1}H-NMR spectrum of compound **1b** in DMSO-d_6 + 10% D_2O.*

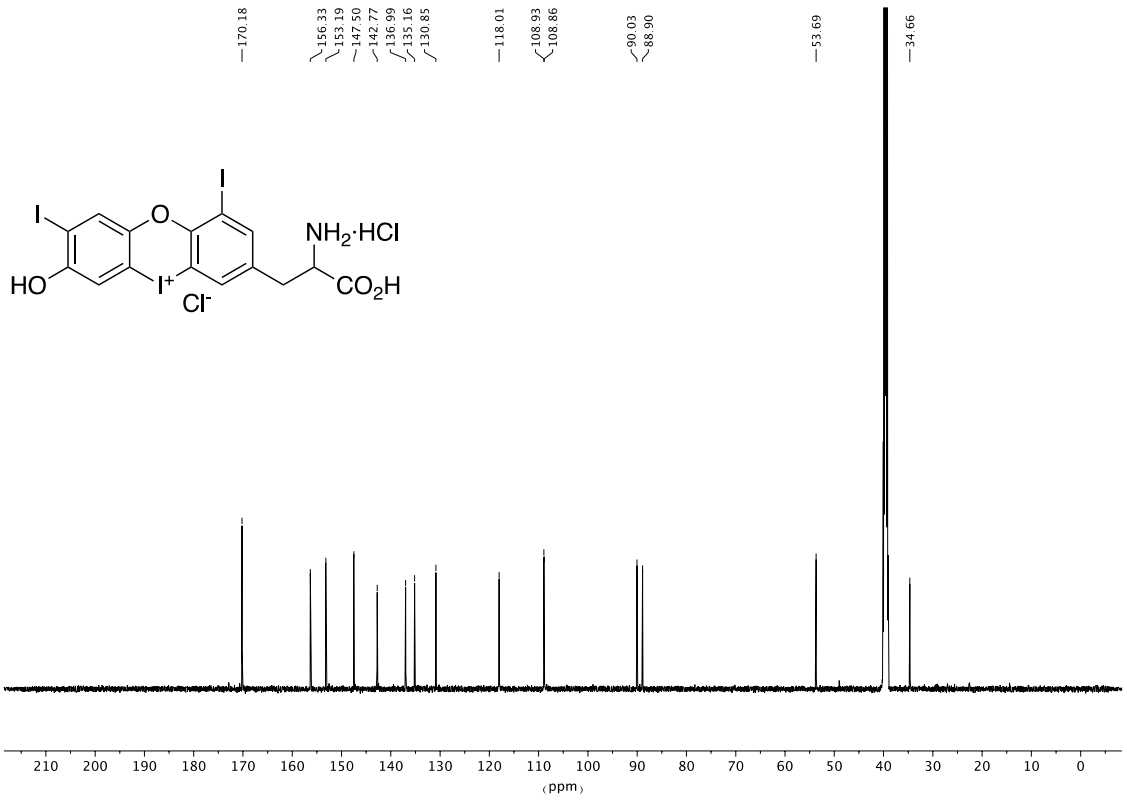

*Figure S52: 151 MHz ^{13}C-NMR spectrum of compound **1b** in DMSO-d_6 + 10% D_2O.*

7 Literature

1. Wilfred L.F. Armarego, C. C. *Purification of Laboratory Chemicals*; Butterworth-Heinemann: 2013.
2. Duggan, B. M.; Craik, D. J. *J. Med. Chem.* **1996**, *39*, 4007-4016.
3. Sheldrick, G. M. *Acta Crystallogr., Sect. A: Found. Adv.* **2015**, *71*, 3-8.
4. Dolomanov, O. V.; Bourhis, L. J.; Gildea, R. J.; Howard, J. A. K.; Puschmann, H. *J. Appl. Crystallogr.* **2009**, *42*, 339-341.
5. Sheldrick, G. M. *Acta Crystallogr., Sect. C: Struct. Chem.* **2015**, *71*, 3-8.
6. Macrae, C. F.; Sovago, I.; Cottrell, S. J.; Galek, P. T. A.; McCabe, P.; Pidcock, E.; Platings, M.; Shields, G. P.; Stevens, J. S.; Towler, M.; Wood, P. A. *J. Appl. Crystallogr.* **2020**, *53*, 226-235.
7. Mazzocchi, P. H.; Ammon, H. L.; Liu, L.; Colicelli, E.; Ravi, P.; Burrows, E. *The Journal of Organic Chemistry* **1981**, *46*, 4530-4536.
8. Neese, F. *WIREs Computational Molecular Science* **2022**, *12*.
9. Adamo, C.; Barone, V. *The Journal of Chemical Physics* **1999**, *110*, 6158-6170.
10. Grimme, S.; Antony, J.; Ehrlich, S.; Krieg, H. *J. Chem. Phys.* **2010**, *132*, 154104.
11. Grimme, S.; Ehrlich, S.; Goerigk, L. *J. Comput. Chem.* **2011**, *32*, 1456-1465.
12. Weigend, F.; Ahlrichs, R. *Phys. Chem. Chem. Phys.* **2005**, *7*, 3297-3305.
13. Helmich-Paris, B.; de Souza, B.; Neese, F.; Izsak, R. *J. Chem. Phys.* **2021**, *155*, 104109.
14. Barone, V.; Cossi, M. *The Journal of Physical Chemistry A* **1998**, *102*, 1995-2001.
15. Maeda, S.; Harabuchi, Y.; Ono, Y.; Taketsugu, T.; Morokuma, K. *Int. J. Quantum Chem* **2014**, *115*, 258-269.

8 Bibliography

[1] B. Courtois, *Ann. Chim.* **1813**, *88*, 304–310.

[2] H. Davy, *Philos. Trans. R. Soc. London* **1814**, *104*, 74–93.

[3] J. L. Gay-Lussac, *Ann. Chim.* **1813**, *88*, 319–321.

[4] B. Nachtsheim, P. Finkbeiner, *Synthesis* **2013**, *45*, 979–999.

[5] H. Togo, S. Iida, *Synlett* **2006**, *2006*, 2159–2175.

[6] S. Stavber, M. Jereb, M. Zupan, *Synthesis* **2008**, *2008*, 1487–1513.

[7] *Hypervalent Iodine Chemistry*, (Ed.: T. Wirth), Springer Berlin Heidelberg, Berlin, Heidelberg, **2003**.

[8] A. Parra, *Chem. Rev.* **2019**, *119*, 12033–12088.

[9] X. Peng, A. Rahim, W. Peng, F. Jiang, Z. Gu, S. Wen, *Chem. Rev.* **2023**, *123*, 1364–1416.

[10] R. Robidas, D. L. Reinhard, C. Y. Legault, S. M. Huber, *Chemical Record* **2021**, *21*, 1912–1927.

[11] F. V. Singh, S. E. Shetgaonkar, M. Krishnan, T. Wirth, *Chem. Soc. Rev.* **2022**, *51*, 8102–8139.

[12] B. Winterson, D. Bhattacherjee, T. Wirth, *Adv. Synth. Catal.* **2023**, *365*, 2676–2689.

[13] A. Yoshimura, A. Saito, V. V. Zhdankin, *Chem. - Eur. J.* **2018**, *24*, 15156–15166.

[14] A. Yoshimura, V. V. Zhdankin, *Chem. Rev.* **2016**, *116*, 3328–3435.

[15] V. V. Zhdankin, P. J. Stang, *Chem. Rev.* **2008**, *108*, 5299–5358.

[16] V. V. Zhdankin, *Hypervalent Iodine Chemistry: Preparation, Structure and Synthetic Applications of Polyvalent Iodine Compounds*, John Wiley & Sons, **2013**.

[17] J. C. Martin, *Science* **1983**, *221*, 509–514.

[18] J. I. Musher, *Angew. Chem. Int. Ed.* **2003**, *8*, 54–68.

[19] M. Ochiai in *Reactivities, Properties and Structures* (Ed.: T. Wirth), Springer Berlin Heidelberg, Berlin, Heidelberg, **2003**, pp. 5–68.

[20] V. V. Zhdankin in *Introduction and General Overview of Polyvalent Iodine Compounds*, John Wiley & Sons, **2013**, pp. 1–20.

[21] X. Li, W. Wang, C. Zhang, *Adv. Synth. Catal.* **2009**, *351*, 2342–2350.

[22] L. Liu, D. Zhang-Negrerie, Y. Du, K. Zhao, *Org. Lett.* **2014**, *16*, 436–439.

[23] D. Sharma, P. Ranjan, O. Prakash, *Synth. Commun.* **2009**, *39*, 596–603.

[24] C. Zhang, J. Yu, *Synthesis* **2009**, *2009*, 2324–2328.

[25] Z. X. Wang, K. Livingstone, C. Humpel, C. G. Daniliuc, C. Muck-Lichtenfeld, R. Gilmour, *Nature Chemistry* **2023**, *15*, 1515–1522.

[26] B. Winterson, T. Rennigholtz, T. Wirth, *Chem. Sci.* **2021**, *12*, 9053–9059.

[27] Z. Zhao, A. J. To, G. K. Murphy, *Chem. Commun.* **2019**, *55*, 14821–14824.

[28] T. Dohi, N. Takenaga, A. Goto, H. Fujioka, Y. Kita, *J. Org. Chem.* **2008**, *73*, 7365–7368.

[29] C. Willgerodt, *Ber. Dtsch. Chem. Ges.* **1892**, *25*, 3494–3502.

[30] Y. Ye, H. Wang, R. Fan, *Org. Lett.* **2010**, *12*, 2802–2805.

[31] Y. Ye, L. Wang, R. Fan, *J. Org. Chem.* **2010**, *75*, 1760–1763.

[32] Y. Ye, C. Zheng, R. Fan, *Org. Lett.* **2009**, *11*, 3156–3159.

[33] J. A. Jordan-Hore, C. C. Johansson, E. M. Beck, M. J. Gaunt, *J. Am. Chem. Soc.* **2008**, *130*, 16184–16186.

[34] K. Kiyokawa, T. Watanabe, L. Fra, T. Kojima, S. Minakata, *J. Org. Chem.* **2017**, *82*, 11711–11720.

[35] K. Kiyokawa, S. Yahata, T. Kojima, S. Minakata, *Org. Lett.* **2014**, *16*, 4646–4649.

[36] G. Q. Liu, Y. M. Li, *J. Org. Chem.* **2014**, *79*, 10094–10109.
[37] S. Minakata, K. Kiyokawa, K. Takemoto, S. Yahata, T. Kojima, *Synthesis* **2017**, *49*, 2907–2912.
[38] V. Telvekar, K. Sasane, *Synlett* **2010**, *2010*, 2778–2780.
[39] J.-M. Vatèle, *Synlett* **2014**, *25*, 1275–1278.
[40] L. Fra, A. Millan, J. A. Souto, K. Muniz, *Angew. Chem. Int. Ed.* **2014**, *53*, 7349–7353.
[41] M. J. Raihan, V. Kavala, P. M. Habib, Q. Z. Guan, C. W. Kuo, C. F. Yao, *J. Org. Chem.* **2011**, *76*, 424–434.
[42] M. Ueno, T. Nabana, H. Togo, *J. Org. Chem.* **2003**, *68*, 6424–6426.
[43] H. Cheng, J. Ma, P. Guo, *Adv. Synth. Catal.* **2023**, *365*, 1112–1139.
[44] E. A. Merritt, B. Olofsson, *Angew. Chem. Int. Ed.* **2009**, *48*, 9052–9070.
[45] E. Le Du, J. Waser, *Chem. Commun.* **2023**, *59*, 1589–1604.
[46] J.-Y. Chen, J. Huang, K. Sun, W.-M. He, *Org. Chem. Front.* **2022**, *9*, 1152–1164.
[47] X. Mi, C. Pi, W. Feng, X. Cui, *Org. Chem. Front.* **2022**, *9*, 6999–7015.
[48] V. V. Zhdankin, *J. Org. Chem.* **2011**, *76*, 1185–1197.
[49] C. Hartmann, V. Meyer, *Ber. Dtsch. Chem. Ges.* **1894**, *27*, 502–509.
[50] C. Hartmann, V. Meyer, *Ber. Dtsch. Chem. Ges.* **1894**, *27*, 426–432.
[51] G. Laudadio, H. P. L. Gemoets, V. Hessel, T. Noel, *J. Org. Chem.* **2017**, *82*, 11735–11741.
[52] B. Olofsson in *Arylation with Diaryliodonium Salts* (Ed.: T. Wirth), Springer International Publishing, Cham, 2015th ed., **2016**, pp. 135–166.
[53] F. Dumur, *Eur. Polym. J.* **2023**, *195*, 112193.
[54] M. Topa, J. Ortyl, *Materials* **2020**, *13*, 4093.
[55] R. J. Mayer, A. R. Ofial, H. Mayr, C. Y. Legault, *J. Am. Chem. Soc.* **2020**, *142*, 5221–5233.
[56] R. Robidas, D. L. Reinhard, S. M. Huber, C. Y. Legault, *ChemPhysChem* **2023**, *24*, e202200634.
[57] E. Linde, S. Mondal, B. Olofsson, *Adv. Synth. Catal.* **2023**, *365*, 2751–2756.
[58] N. S. Soldatova, P. S. Postnikov, M. S. Yusubov, T. Wirth, *Eur. J. Org. Chem.* **2019**, *2019*, 2081–2088.
[59] C. Arakawa, K. Kanemoto, K. Nakai, C. Wang, S. Morohashi, E. Kwon, S. Ito, N. Yoshikai, *J. Am. Chem. Soc.* **2024**, *146*, 3910–3919.
[60] K. Kanemoto, K. Yoshimura, K. Ono, W. Ding, S. Ito, N. Yoshikai, *ChemRXiv* **2024**.
[61] J. Malmgren, S. Santoro, N. Jalalian, F. Himo, B. Olofsson, *Chem. - Eur. J.* **2013**, *19*, 10334–10342.
[62] Y. An, X. M. Zhang, Z. Y. Li, W. H. Xiong, R. D. Yu, F. M. Zhang, *Chem. Commun.* **2018**, *55*, 119–122.
[63] A. Monastyrskyi, N. K. Namelikonda, R. Manetsch, *J. Org. Chem.* **2015**, *80*, 2513–2520.
[64] C. H. Oh, J. S. Kim, H. H. Jung, *J. Org. Chem.* **1999**, *64*, 1338–1340.
[65] X. Qian, J. Han, L. Wang, *Adv. Synth. Catal.* **2016**, *358*, 940–946.
[66] M. K. Zaheer, N. K. Vaishanv, R. Kant, K. Mohanan, *Chem. - Asian J.* **2020**, *15*, 4297–4301.
[67] M. A. Carroll, R. A. Wood, *Tetrahedron* **2007**, *63*, 11349–11354.
[68] P. Li, Y. Weng, X. Xu, X. Cui, *J. Org. Chem.* **2016**, *81*, 3994–4001.
[69] E. Linde, D. Bulfield, G. Kervefors, N. Purkait, B. Olofsson, *Chem* **2022**, *8*, 850–865.
[70] N. Purkait, G. Kervefors, E. Linde, B. Olofsson, *Angew. Chem. Int. Ed.* **2018**, *57*, 11427–11431.
[71] G. Kervefors, L. Kersting, B. Olofsson, *Chem. - Eur. J.* **2021**, *27*, 5790–5795.
[72] E. Linde, B. Olofsson, *Angew. Chem. Int. Ed.* **2023**, *62*, e202310921.
[73] B. Nachtsheim, S. Riedmüller, *Synlett* **2015**, *26*, 651–655.

[74] L. Chan, A. McNally, Q. Y. Toh, A. Mendoza, M. J. Gaunt, *Chem. Sci.* **2015**, *6*, 1277–1281.

[75] N. Jalalian, T. B. Petersen, B. Olofsson, *Chem. - Eur. J.* **2012**, *18*, 14140–14149.

[76] G. Kervefors, A. Becker, C. Dey, B. Olofsson, *Beilstein J. Org. Chem.* **2018**, *14*, 1491–1497.

[77] K. Kikushima, N. Miyamoto, K. Watanabe, D. Koseki, Y. Kita, T. Dohi, *Org. Lett.* **2022**, *24*, 1924–1928.

[78] E. Lindstedt, R. Ghosh, B. Olofsson, *Org. Lett.* **2013**, *15*, 6070–6073.

[79] R. Ghosh, E. Lindstedt, N. Jalalian, B. Olofsson, *ChemistryOpen* **2014**, *3*, 54–57.

[80] E. Lindstedt, E. Stridfeldt, B. Olofsson, *Org. Lett.* **2016**, *18*, 4234–4237.

[81] S. K. Sundalam, D. R. Stuart, *J. Org. Chem.* **2015**, *80*, 6456–6466.

[82] V. Arun, M. Pilania, D. Kumar, *Chem. - Asian J.* **2016**, *11*, 3345–3349.

[83] T. B. Petersen, R. Khan, B. Olofsson, *Org. Lett.* **2011**, *13*, 3462–3465.

[84] X. Xu, D. Wang, C. Ge, X. Yu, H. Wan, *Synlett* **2016**, *27*, 2616–2620.

[85] B. Hu, W. H. Miller, K. D. Neumann, E. J. Linstad, S. G. DiMagno, *Chem. - Eur. J.* **2015**, *21*, 6394–6398.

[86] J. Ke, B. Zu, Y. Guo, Y. Li, C. He, *Org. Lett.* **2021**, *23*, 329–333.

[87] K. M. Lancer, G. H. Wiegand, *J. Org. Chem.* **2002**, *41*, 3360–3364.

[88] Y. Yamada, K. Kashima, M. Okawara, *Bull. Chem. Soc. Jpn.* **1974**, *47*, 3179–3180.

[89] Y. D. Kwon, J. Son, J. H. Chun, *J. Org. Chem.* **2019**, *84*, 3678–3686.

[90] A. Maisonial-Besset, A. Serre, A. Ouadi, S. Schmitt, D. Canitrot, F. Léal, E. Miot-Noirault, D. Brasse, P. Marchand, J. Chezal, *Eur. J. Org. Chem.* **2018**, *2018*, 7058–7065.

[91] A. V. Ozerskaya, M. S. Larkina, E. V. Podrezova, D. Y. Svitich, R. Y. Yusubova, V. V. Zhdankin, M. S. Yusubov, *ARKIVOC* **2022**, *2022*, 108–125.

[92] A. Yamaguchi, H. Hanaoka, T. Higuchi, Y. Tsushima, *J. Labelled Compd. Radiopharm.* **2020**, *63*, 368–375.

[93] D. Del Mazza, M. G. Reinecke, *J. Org. Chem.* **1988**, *53*, 5799–5806.

[94] R. D. Miller, L. Franz, G. N. Fickes, *J. Org. Chem.* **1985**, *50*, 3200–3203.

[95] B. E. Metze, R. A. Roberts, A. Nilova, D. R. Stuart, *Chem. Sci.* **2023**, *14*, 13885–13892.

[96] E. Stridfeldt, E. Lindstedt, M. Reitti, J. Blid, P. O. Norrby, B. Olofsson, *Chem. - Eur. J.* **2017**, *23*, 13249–13258.

[97] M. Wang, Z. Huang, *Org. Biomol. Chem.* **2016**, *14*, 10185–10188.

[98] T. Kitamura, K. Gondo, J. Oyamada, *J. Am. Chem. Soc.* **2017**, *139*, 8416–8419.

[99] T. Kitamura, M. Yamane, *J. Chem. Soc. Chem. Commun.* **1995**, 983–984.

[100] A. Yoshimura, J. M. Fuchs, K. R. Middleton, A. V. Maskaev, G. T. Rohde, A. Saito, P. S. Postnikov, M. S. Yusubov, V. N. Nemykin, V. V. Zhdankin, *Chem. - Eur. J.* **2017**, *23*, 16738–16742.

[101] R. Robidas, V. Guerin, L. Provencal, M. Echeverria, C. Y. Legault, *Org. Lett.* **2017**, *19*, 6420–6423.

[102] Z. Chen, W. F. Wang, H. Yang, X. F. Wu, *Org. Lett.* **2020**, *22*, 1980–1984.

[103] N. Chatterjee, A. Goswami, *Eur. J. Org. Chem.* **2017**, *2017*, 3023–3032.

[104] G. Grelier, B. Darses, P. Dauban, *Beilstein J. Org. Chem.* **2018**, *14*, 1508–1528.

[105] V. V. Grushin, *Chem. Soc. Rev.* **2000**, *29*, 315–324.

[106] S. Altenhofer, K. A. Radermacher, P. W. Kleikers, K. Wingler, H. H. Schmidt, *Antioxid. Redox Signaling* **2015**, *23*, 406–427.

[107] M. M. Konate, S. Antony, J. H. Doroshow, *Antioxid. Redox Signaling* **2020**, *33*, 435–454.

[108] J. Reis, M. Massari, S. Marchese, M. Ceccon, F. S. Aalbers, F. Corana, S. Valente, A. Mai, F. Magnani, A. Mattevi, *Redox Biol.* **2020**, *32*, 101466.

[109] Y. Zhang, B. Deng, Z. Li, *Ecotoxicol. Environ. Saf.* **2018**, *158*, 187–192.

[110] M. Liu, H. Jiang, J. Tang, Z. Ye, F. Zhang, Y. Wu, *Org. Lett.* **2023**, *25*, 2777–2781.

[111] N. S. Antonkin, Y. A. Vlasenko, A. Yoshimura, V. I. Smirnov, T. N. Borodina, V. V. Zhdankin, M. S. Yusubov, A. Shafir, P. S. Postnikov, *J. Org. Chem.* **2021**, *86*, 7163–7178.

[112] Y. Wu, S. Izquierdo, P. Vidossich, A. Lledos, A. Shafir, *Angew. Chem. Int. Ed.* **2016**, *55*, 7152–7156.

[113] M. Elsherbini, W. J. Moran, *Org. Biomol. Chem.* **2021**, *19*, 4706–4711.

[114] M. J. Peacock, D. Pletcher, *J. Electrochem. Soc.* **2001**, *148*, D37–D42.

[115] K. Watts, W. Gattrell, T. Wirth, *Beilstein J. Org. Chem.* **2011**, *7*, 1108–1114.

[116] B. Zu, J. Ke, Y. H. Guo, C. He, *Chin. J. Chem .* **2021**, *39*, 627–632.

[117] T. Dohi, N. Yamaoka, Y. Kita, *Tetrahedron* **2010**, *66*, 5775–5785.

[118] L. Eberson, M. P. Hartshorn, O. Persson, F. Radner, *Chem. Commun.* **1996**, 2105–2112.

[119] L. D. Caspers, J. Spils, M. Damrath, E. Lork, B. J. Nachtsheim, *J. Org. Chem.* **2020**, *85*, 9161–9178.

[120] M. Damrath, L. D. Caspers, D. Duvinage, B. J. Nachtsheim, *Org. Lett.* **2022**, *24*, 2562–2566.

[121] M. Wang, Q. Fan, X. Jiang, *Org. Lett.* **2016**, *18*, 5756–5759.

[122] K. Zhu, K. Xu, Q. Fang, Y. Wang, B. Tang, F. Zhang, *ACS Catal.* **2019**, *9*, 4951–4957.

[123] F. Heinen, D. L. Reinhard, E. Engelage, S. M. Huber, *Angew. Chem. Int. Ed.* **2021**, *60*, 5069–5073.

[124] M. V. Il'in, Y. V. Safinskaya, D. A. Polonnikov, A. S. Novikov, D. S. Bolotin, *J. Org. Chem.* **2024**, *89*, 2916–2925.

[125] V. Carreras, A. H. Sandtorv, D. R. Stuart, *J. Org. Chem.* **2017**, *82*, 1279–1284.

[126] K. Kikushima, N. Miyamoto, K. Watanabe, D. Koseki, Y. Kita, T. Dohi, *Org. Lett.* **2022**, *24*, 1924–1928.

[127] H. Peng, Q. Liu, Y. Sun, B. Luo, T. Yu, P. Huang, D. Zhu, S. Wen, *Org. Chem. Front.* **2022**, *9*, 1137–1142.

[128] T. M. Milzarek, T. A. M. Gulder, *Org. Lett.* **2021**, *23*, 102–106.

[129] A. J. Canty, J. Patel, T. Rodemann, J. H. Ryan, B. W. Skelton, A. H. White, *Organometallics* **2004**, *23*, 3466–3473.

[130] T. Cui, J. Qin, K. Harms, E. Meggers, *Eur. J. Inorg. Chem.* **2018**, *2019*, 195–198.

[131] F. Li, A. Thevenon, A. Rosas-Hernandez, Z. Wang, Y. Li, C. M. Gabardo, A. Ozden, C. T. Dinh, J. Li, Y. Wang, J. P. Edwards, Y. Xu, C. McCallum, L. Tao, Z. Q. Liang, M. Luo, X. Wang, H. Li, C. P. O'Brien, C. S. Tan, D. H. Nam, R. Quintero-Bermudez, T. T. Zhuang, Y. C. Li, Z. Han, R. D. Britt, D. Sinton, T. Agapie, J. C. Peters, E. H. Sargent, *Nature* **2020**, *577*, 509–513.

[132] C. Willgerodt, G. Hilgenberg, *Ber. Dtsch. Chem. Ges.* **1909**, *42*, 3826–3833.

[133] G. A. Olah, Y. K. Mo, E. G. Melby, H. C. Lin, *J. Org. Chem.* **1973**, *38*, 367–372.

[134] G. A. Olah, P. W. Westerman, E. G. Melby, Y. K. Mo, *J. Am. Chem. Soc.* **1974**, *96*, 3565–3573.

[135] Y. Yamada, K. Kashima, M. Okawara, *J. Polym. Sci. Part B: Polym. Lett.* **1976**, *14*, 65–71.

[136] T. Kitamura, R. Furuki, H. Taniguchi, P. J. Stang, *Mendeleev Commun.* **1991**, *1*, 148–149.

[137] T. Kitamura, D. Inoue, I. Wakimoto, T. Nakamura, R. Katsuno, Y. Fujiwara, *Tetrahedron* **2004**, *60*, 8855–8860.

[138] T. Kitamura, R. Furuki, K. Nagata, H. Taniguchi, P. J. Stang, *J. Org. Chem.* **2002**, *57*, 6810–6814.

[139] T. Kitamura, R. Furuki, L. Zheng, T. Fujimoto, H. Taniguchi, *Chem. Lett.* **1992**, *21*, 2241–2244.

[140] T. Kitamura, R. Furuki, L. Zheng, K. Nagata, T. Fukuoka, Y. Fujiwara, H. Taniguchi, *Bull. Chem. Soc. Jpn.* **1995**, *68*, 3637–3641.

[141] T. Kitamura, L. Zheng, H. Taniguchi, M. Sakurai, R. Tanaka, *Tetrahedron Lett.* **1993**, *34*, 4055–4058.

[142] T. Kitamura, T. Fukuoka, L. Zheng, T. Fujimoto, H. Taniguchi, Y. Fujiwara, *Bull. Chem. Soc. Jpn.* **1996**, *69*, 2649–2654.

[143] M. Ochiai, Y. Kitagawa, N. Takayama, Y. Takaoka, M. Shiro, *J. Am. Chem. Soc.* **1999**, *121*, 9233–9234.

[144] S. Companys, P. A. Peixoto, C. Bosset, S. Chassaing, K. Miqueu, J. M. Sotiropoulos, L. Pouysegu, S. Quideau, *Chem. - Eur. J.* **2017**, *23*, 13309–13313.

[145] Q. Tan, D. Zhou, T. Zhang, B. Liu, B. Xu, *Chem. Commun.* **2017**, *53*, 10279–10282.

[146] A. Boelke, T. J. Kuczmera, E. Lork, B. J. Nachtsheim, *Chem. - Eur. J.* **2021**, *27*, 13128–13134.

[147] B. Wu, N. Yoshikai, *Angew. Chem. Int. Ed.* **2015**, *54*, 8736–8739.

[148] U. Radhakrishnan, P. J. Stang, *J. Org. Chem.* **2003**, *68*, 9209–9213.

[149] P. J. Stang, V. V. Zhdankin, *J. Am. Chem. Soc.* **1993**, *115*, 9808–9809.

[150] W. W. Chen, M. Artigues, M. Font-Bardia, A. B. Cuenca, A. Shafir, *J. Am. Chem. Soc.* **2023**, *145*, 13796–13804.

[151] J. Spils, *Masterthesis*, **2019**.

[152] B. R. Kaafarani, H. Gu, A. Alan Pinkerton, D. C. Neckers, *J. Chem. Soc. Dalton Trans.* **2002**, 2318–2321.

[153] A. Bondi, *The Journal of Physical Chemistry* **2002**, *68*, 441–451.

[154] H. Bock, M. Sievert, Z. Havlas, *Chem. - Eur. J.* **1998**, *4*, 677–685.

[155] T. Wirth, M. Brown, M. Delorme, F. Malmedy, J. Malmgren, B. Olofsson, *Synlett* **2015**, *26*, 1573–1577.

[156] T. S. Alexander, T. J. Clay, B. Maldonado, J. M. Nguyen, D. B. C. Martin, *Tetrahedron* **2019**, *75*, 2229–2238.

[157] V. N. Nemykin, A. V. Maskaev, M. R. Geraskina, M. S. Yusubov, V. V. Zhdankin, *Inorg. Chem.* **2011**, *50*, 11263–11272.

[158] D. Seyferth, S. C. Vick, *J. Organomet. Chem.* **1977**, *141*, 173–187.

[159] A. Boelke, B. J. Nachtsheim, *Adv. Synth. Catal.* **2019**, *362*, 184–191.

[160] B. M. Duggan, D. J. Craik, *J. Med. Chem.* **1996**, *39*, 4007–4016.

[161] C. C. Wilfred L.F. Armarego, *Purification of Laboratory Chemicals*, Butterworth-Heinemann, **2013**.

[162] O. V. Dolomanov, L. J. Bourhis, R. J. Gildea, J. A. K. Howard, H. Puschmann, *J. Appl. Crystallogr.* **2009**, *42*, 339–341.

[163] G. M. Sheldrick, *Acta Crystallogr. Sect. A: Found. Adv.* **2015**, *71*, 3–8.

[164] G. M. Sheldrick, *Acta Crystallogr. Sect. C: Struct. Chem.* **2015**, *71*, 3–8.

[165] C. F. Macrae, I. Sovago, S. J. Cottrell, P. T. A. Galek, P. McCabe, E. Pidcock, M. Platings, G. P. Shields, J. S. Stevens, M. Towler, P. A. Wood, *J. Appl. Crystallogr.* **2020**, *53*, 226–235.

[166] J. R. Suresh, G. Whitener, G. Theumer, D. J. Brocher, I. Bauer, W. Massa, H. J. Knolker, *Chem. - Eur. J.* **2019**, *25*, 13759–13765.

[167] H. E. Katz, *Organometallics* **2002**, *5*, 2308–2311.

A List of Abbreviations

AcOH / AcO^-	acetic acid / acetate
Ar	Aryl
$BArF_4^-$	Tetrakis(3,5-bis(trifluoromethyl)phenyl)borate
Cy	Cyclohexane
DFT	Density functional theory
DIPEA	Diisopropylethylamine
eq.	equivalents
HFIP	1,1,1,3,3,3-Hexafluoroisopropanol
HRMS	High-resolution mass spectrometry
LA	Lewis acid
*m*CPBA	*meta*-Chloroperoxybenzoic acid
NADH	Nicotinamide adenine dinucleotide
NADPH	Nicotinamide adenine dinucleotide phosphate
NMR	Nuclear magnetic resonance
Nu	Nucleophile
Oxone	$2\,KHSO_5 \cdot KHSO_4 \cdot K_2SO_4$
PE	Petroleum ether
PIDA	Phenyliodine(III)diacetate or (diacetoxyiodo)benzene
*p*TsOH	*para*-Toluenesulfonic acid
Selectfluor	1-(Chloromethyl)-4-fluoro-1,4-diazabicyclo[2.2.2]octane-1,4-diium ditetrafluoroborate
T3	Triiodthyronine / (*S*)-2-amino-3-(4-(4-hydroxy-3-iodophenoxy)-3,5-diiodophenyl)propanoic acid
T4 / Thx	Levothyroxine / (*S*)-2-amino-3-(4-(4-hydroxy-3,5-diiodophenoxy)-3,5-diiodophenyl)propanoic acid
TBS	*tert*-Butyldimethylsilyl
TFE	2,2,2-Trifluoroethanol
THF	Tetrahydrofurane
TMS	Trimethylsilyl
TfOH / TfO^-	Trifluoromethanesulfonic acid (triflic acid) / trifluoromethanesulfonate (triflate)
TBAF	Tetrabutylammonium fluoride